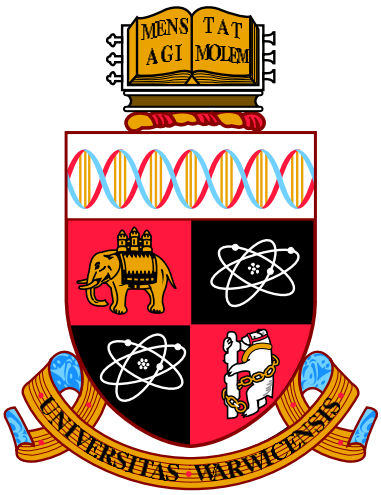

Meiosis associated Argonautes in male reproductive development

Robert Maple

Thesis submitted to the University of Warwick

for the degree of

Doctor of Philosophy

Department of Life Sciences

August 2019

Table of Contents

List of figures

List of figures

List of Tables

Acknowledgements

Firstly, I would like to express my sincere gratitude to my supervisor Dr Jose Gutierrez-Marcos for giving me the opportunity to join the lab and for the continuous patience, support and encouragement throughout my research.

I would also like to thank Dr Jacques Rouster and Biogemma for funding the project, in addition to their assistance generating transgenic lines and constructs for research use. I would also like to thank the BBSRC for their funding contribution in this research.

I would like to thank past and present members of the Marcos lab for their support, encouragement, and research expertise, but also for encouraging social 'activities' usually involving copious amounts of beer, with special thanks to Yang-Seok for his infinite patience, help and dedication to research, in addition to his excellent taste in Korean pot noodles.

I would also like to thank friends and family including the Maple clan, Laura and Craig for their encouragement and support with thanks to Rachel for her assistance.

Finally, I would like to give thanks to Sarah who sparked my initial love of science. She has imparted me with a strong sense of determination and perseverance for which I will always be grateful and for which this thesis has heavily relied upon.

Declaration

This thesis is submitted to the University of Warwick in support of my application for the degree of Doctor of Philosophy. It has been composed by myself and has not been submitted in any previous application for any degree. The work presented (including data generated and data analysis) was carried out by the author except in the cases outlined below:

Dr Yang-Seok Lee (University of Warwick) assisting with slide preparation for protein immunolocalization, RNA *in situ* hybridization experiments and tobacco infiltrations.

Alex Dawson (University of Warwick) assisting with transcriptome data analysis (Chapter 6.0)

Jacques Rouster (Biogemma) Generating RNAi transgenic maize lines

Abstract

Unlike animals, plants do not specify their germline until late in development from adult somatic cells. During the specification of the germline, dynamic epigenetic reprogramming events take place, necessary to reset somatic epigenetic marks. During this stage, the plant germline is especially susceptible to transposable element activation and transposition events. Therefore, plants must deploy diverse mechanisms to tightly control the transcription and translation of these repetitive elements. Argonaute proteins are thought to be critical components of the RNA mediated epigenetic silencing involved in these processes. However, their precise mechanisms in reproductive development are not known. We identified two meiosis associated Argonautes that accumulate in developing anthers and bind to a discrete class of sRNA. Genetic analysis revealed that these proteins are necessary for male reproductive development and plants defective in MAGO proteins display male fertility defects, especially when exposed to heat stress. Genomic analysis revealed that MAGO proteins regulate the transcriptional activation of LTR retrotransposons after heat stress. Collectively, our data indicates that MAGO and associated small RNAs are required to maintain the male germline under stress.

List of Abbreviations

5’tRF	5' tRNA derived fragment
5mC	5-methylcytosine
Ad	*Arundo donax*
AGO	Arogonaute
AMP1	Altered Meristem Program 1
ARF	Auxin Response Factors
At	*Arabidopsis thaliana*
BCIP	5-bromo-4-chloro-3-indolylphosphate
Bd	*Brachypodium distachyon*
bp	basepair
CaMV 35S	35S Cucumber mosaic virus 35S promotor
CC	Central cell
cm	Centimetres
CMT1/2/3	Chromomethylase 1/2/3
DCL-1/3/4/5	Dicer-Like 1/3/4/5
DDM1	Decrease in DNA Methylation 1
DEG	Differentially Expressed Gene
DEX	Dexamethasone
DME	Demeter
DMR	Differentially Methylated Region
DNA	Deoxyribonucleic Acid
DNMT1	DNA Methyltransferase1
dNTPs	deoxynucleotide Triphosphates
DRM1/2	Domains Rearanged Methyltransferase 1/2
dsRNA	double stranded RNA
DTT	Dithiothreitol
E(z)	Enhancer of Zeste
EAT1	Eternal Tapetum 1
EC	Egg cell
EDTA	Ethylenediaminetetra-acetic Acid
EN	Endothecium
EP	Epidermis
eYFP	enhanced Yellow Fluorescent Protein
FDR	False Discovery rate adjusted
fiLUC	Firefly Luciferase

FITC	Fluorescein isothiocyanate
FPKM	Fragments Per Kilobase of transcript per Million mapped reads
g	grams
GFP	Green fluorescent protein
GO	Gene Ontology
GUS	β-glucuronidase
H1	Histone 1
H2A	Histone 2A
H2B	Histone 2B
H3	Histone 3
H3K9me2	Histone 3 dimethylation of lysine 9 dimethylation
H4	Histone 4
HAT	Histone Acetyltransferases
HCPro	Helper Component Proteinase
HDAC	Histone Deacetylase
HDZIP III/VI	Homeodomain-leucine Zip III/IV
HphasiRNA	Heat -induced phasiRNA
HSP	Heat Shock Protein
Hv	*Hordeum vulgare*
HYL1	HYPONASTY LEAVES1
kDA	Kilo Daltons
KYP	Kryptonite
L	Letre
lncRNA	long non-coding RNA
LTR	Long Terminal Repeat
MAGO	Meiosis-associated Argonaute
MEL1	Meiosis Arrested at Leptotene 1
MET1	DNA Methyltransferase 1
mg	milligram
MID	Middle domain
MIL1	MICROSPORELESS1
miRNAs	micro Ribonucleic Acid
MITE	Miniature Inverted-repeat TE
ML	Middle layer
mL	millilitre
mM	millimolar
mm	millimetre

mRNA	messenger RNA
MSCA1	Male Sterile Converted Anther 1
NAT-siRNAs	natural antisense transcript small interfering Ribonucleic Acid
NBT,	nitroblue tetrazolium
ncRNA	non-coding Ribonucleic Acid
nm	nanometre
NOS	Nopaline Synthase
nt	nucleotide
ºC	degrees Centigrade
OCL4	Outer cell layer 4
OCS	octopine synthase
Os	*Oryza sativa*
PAGE	Polyacrylamide gel electrophoresis
PAZ	Piwi/Argonaute/Zwille
PBS	Phosphate Buffered Saline
PCR	Polymerase Chain Reaction
PD	Plasmodesmata
piRNA	PIWI-interacting RNA
PIWI	P ELEMENT-INDUCED WIMPY TESTIS
PMC	Pollen mother cell
Pol II/IV/V	RNA polymerase II/IV/V
pri-miRNA	precursor micro RNA
PTGS	Post-transcriptional Gene Silencing
RCI3	Rare Cold Inducible 3
RdDM	RNA-directed DNA methylation
RDR2/6	RNA-dependent RNA polymerase2/6
RdRP	RNA-dependent RNA polymerase
RISC	RNA Acid induced silencing complex
RNA	Ribonucleic Acid
RNAi	RNA interference
ROS	Reactive Oxygen species
ROS1	Repressor of Silencing 1
rpm	revolutions per minute
SAM	Shoot Apical Meristem
Sb	*Sorghum bicolor*
SC	Sperm cell
SDS	Sodium dodecyl sulphate

SGS3	Suppressor of gene silencing
Si	*Setaria italica*
siRNA	small interfering Ribonucleic Acid
SRE	Stress-responsive regulatory element
sRNA	small Ribonucleic Acid
sRNA-IP	small RNA immunoprecipitation
ssRNA	single stranded RNA
TA	Tapetum
ta-siRNA	trans-acting small interfering RNAs
TE	Transposable element
TF	Transcription factors
TGS	Transcriptional Gene Silencing
tRNA	transfer RNA
VC	vegetative cell
viRNA	virus-induced siRNAs
WSMV	wheat streak mosaic virus
WT	Wild Type
Zm	*Zea mays*
µl	microliter
µm	micrometre
µmol	micromolar

1.0 General Introduction

1.1 General overview

The term epigenetics was first coined in 1942, defined as the complex developmental processes that link phenotype with genotype (Waddington 2012). Over the years this definition has been redefined to include meiotically and mitotically heritable changes in gene expression, not attributed to changes in the genome (Wolffe and Guschin 2000). These changes include both DNA and histone modifications and RNA silencing mechanisms that can alter the transcriptional state of a cell or organism in plants and animals. Unlike animals, which specify most organs and tissues during embryo development, plants continually lay down new organs post embryonically from their meristems, a population of self-renewing stem cells. Additionally, this stem cell population is continually influenced by external environmental stimuli which shape and influence the epigenetic state. As plants are sessile organisms, they cannot escape adverse environmental conditions. Consequently epigenetic mechanisms can facilitate changes to gene expression helping plants adapt to unfavourable growth conditions (Goldberg, Allis et al. 2007).

While epigenetic mechanisms are common to both plants and animals, many epigenetic phenomena were first identified in plants, classically in maize (*Zea mays*) and the model organism *Arabidopsis*. Paramutation, results from interactions between different alleles in *trans* leading to stable changes to gene expression. It was first described in maize and has since been identified in other plants, fungi and animals (Brink 1958, Arteaga-Vazquez and Chandler 2010). Genomic imprinting, results from genes that are differentially expressed based on their parent of origin, were first described in maize and later found in animals and are likely the result of competition for resources during embryogenesis (Kermicle 1970, Alleman and Doctor 2000). Transposable elements (TEs), are stretches of DNA which

have the propensity to move from place-to-place throughout the genome. They were first discovered in maize in the 1940s due to their ability to cause chromosomal breaks and disrupt host genes (McClintock 1946). TEs are controlled by epigenetic mechanisms and lead to epigenetic changes in or around neighbouring genes in which they integrate (Lisch 2009). Finally, co-suppression was first identified in petunia after overexpression of the pigment controlling gene chalcone synthase (*CHS*) resulted in white or variegated flowers. Although it is not strictly epigenetic, the silencing of the *CHS* gene occurs through epigenetic pathways (Napoli, Lemieux et al. 1990). All of these phenomena are largely controlled by epigenetic mechanisms and are to some degree heritable and reversible. As knowledge of these mechanisms has developed, they are now routinely exploited for the targeted disruption of gene expression (Aigner 2006). Epigenetic mechanisms are additionally vital for development, especially in the germline, which is specified post embryonically in plants (Berger and Twell 2011). Mechanisms impacting the epigenome of the plant must be maintained in the meristem and germ cells to prevent adverse epigenetic changes from being passed on to the next generation of cells or organisms.
This introduction will cover the fundamental epigenetic mechanisms of plants and animals and discuss their impact on gene expression. This thesis will focus on how these mechanisms may impact the early stages of maize male reproductive development and their necessity for pollen production.

1.2 Small RNA biogenesis

Small RNAs (sRNA) are fragments of non-coding RNA (ncRNA) ranging from 20-24 nucleotides in length, which regulate the transcriptional (TGS) or post-transcriptional gene silencing (PTGS) of genes (Axtell 2013). Various types of sRNA have been discovered and are classified by their mode of biogenesis

and function (Chen 2009). A major distinction can be made between the sRNAs originating from a single stranded imperfect hairpin structure such as microRNAs (miRNAs), and the small interfering RNAs (siRNAs), which are derived from a perfectly complimentary double stranded RNA precursor (Axtell 2013). The siRNAs can be broadly subdivided into the heterochromatic siRNAs, secondary siRNAs and natural antisense transcript siRNAs (NAT-siRNAs). The biogenesis of miRNAs begins with the transcription of miRNA genes by DNA-dependent RNA Pol II to generate the stem loop precursor miRNA (pri-miRNA)(Xie, Allen et al. 2005). The pri-miRNA forms a double stranded hairpin that is a substrate for DICER-LIKE1 (DCL1) processing aided by HYPONASTY LEAVES1 (HYL1) and SERRATE (SE) to generate 21-nt miRNA/miRNA* duplex (Kurihara and Watanabe 2004, Vazquez, Gasciolli et al. 2004, Dong, Han et al. 2008). HUA ENHANCER1 methylates the 2' hydroxyl group of 3' miRNA ends to increase stability and one of the miRNA duplex is selectively incorporated into ARGONAUTE1 (AGO1) to form the RNA induced silencing complex (miRNA-RISC) (Baumberger and Baulcombe 2005, Yu, Yang et al. 2005). AGO1 has endonucleolytic activity and can carry out cleavage of complimentary target mRNAs silencing them post transcriptionally (Fig 1.1A)(Qi, Denli et al. 2005). In addition to target mRNA slicing, AGO1 can silence genes through translational inhibition through interacting with ALTERED MERISTEM PROGRAM1 (AMP1) on the endoplasmic reticulum (Li, Liu et al. 2013). These miRNAs primarily play a role in plant development, with mutations in miRNAs or their biogenesis often displaying severe developmental abnormalities. Approximately half of all known miRNA targets in plants are transcription factors (Laufs, Peaucelle et al. 2004, Vaucheret, Vazquez et al. 2004, Wu, Zhang et al. 2009, Axtell 2013).

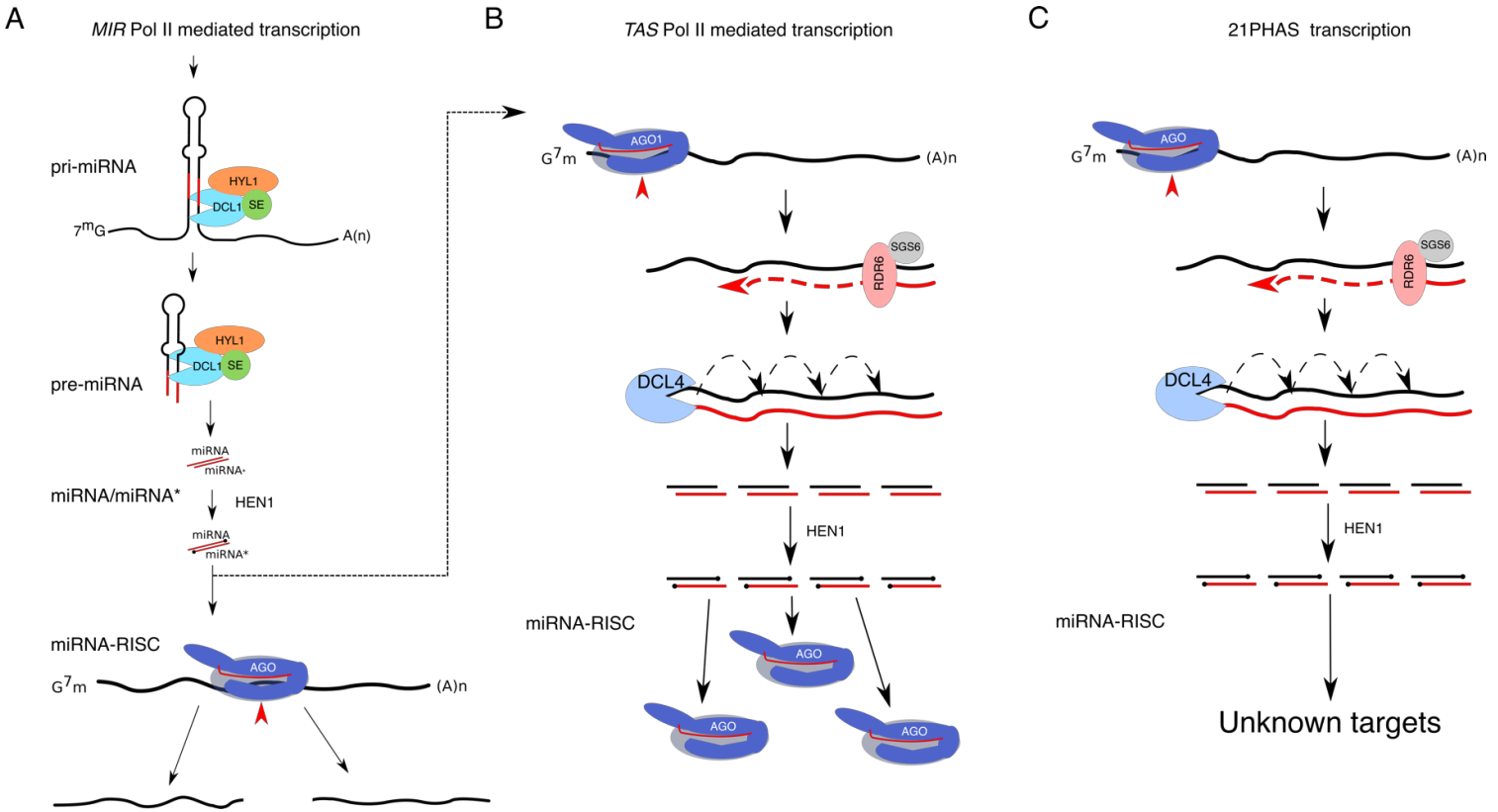

Figure 1.1: The biogenesis of miRNAs secondary siRNAs. (A) miRNAs are processed from long non-coding Pol II transcripts that fold to form a hairpin structure. Two rounds of DCL1 cleavage result in the formation of the miRNA/miRNA* duplex. The miRNA is exported from the nucleus and methylated by HEN1 to form the mature miRNA and incorporated into AGO, while the miRNA* is degraded. (B) TAS 1/2/4 are transcribed by Pol II and targeted by miRNA-AGO1. The 5' fragment is degraded while the 3' fragment is a substrate for RDR6, which forms dsRNA. The dsRNA is acted on by DCL4 which sequentially cleaves the dsRNA into tasiRNA/tasiRNA* which are loaded into respective AGOs and target genes (C) 21-nt phasiRNA transcripts transcribed from 21PHAS loci are cleaved by miR2118-RISC complexes. The dsRNA is acted on by DCL4 which sequentially cleaves the dsRNA into phased phasiRNA/phasiRNA* duplexes. Their molecular targets are unknown. (Borges and Martienssen 2015)

With miRNA, the dsRNA substrate of DCL1 is formed from the imperfectly hybridised stem of the hairpin, but this is not the case with siRNAs. Instead, the dsRNA can be generated from the hybridisation of complementary antisense transcripts, as is the case with NAT-siRNA (Zhang, Xia et al. 2012). Additionally, the RNA transcripts can be a substrate for RNA-dependent RNA polymerase (RdRP) enzymes, which generate the complementary RNA strand. The trans-acting small interfering RNAs (ta-siRNAs) are a class of secondary siRNAs generated from such a pathway after a precursor 'TAS' long non-coding RNA (lncRNA) transcript is cleaved by miRNA-RISC. Four TAS gene families (TAS1-4) have been identified in *Arabidopsis* that originate from 8 loci (Allen, Xie et al. 2005). TAS loci can be broadly grouped based on the number of miRNA target cut sites (one/two hit) and the identity of the triggering miRNA (Yoshikawa 2013). TAS1 and TAS2 harbour a single miRNA target site for 22-nt miR173-AGO1, and the derived tasiRNAs target penta-tricopeptide repeats (Montgomery, Yoo et al. 2008, Felippes and Weigel 2009). TAS3 loci are targeted twice by 21-nt miR390-AGO7 with derived taisRNAs targeting the AUXIN RESPONSE FACTORs (ARF) ARF2, ARF3, ARF4 regulating various developmental aspects (Fahlgren, Montgomery et al. 2006, Garcia, Collier et al. 2006, Marin, Jouannet et al. 2010). Finally TAS4 is targeted once by 22-nt miR828 with derived tasiRNAs targeting MYB transcription factors PRODUCTION OF ANTHOCYANIN PIGMENT1 (PAP1), PAP2, and MYB113 impacting anthocyanin production (Luo, Mittal et al. 2012).

Targeting by miRNA-RISC triggers the conversion of the ssRNA to dsRNA by DEPENDENT RNA POLYMERASE6 (RDR6) and SUPPRESSOR OF GENE SILENCING3 (SGS3) with the subsequent dsRNA becoming a substrate for DICER like proteins (Peragine, Yoshikawa et al. 2004, Yoshikawa, Peragine et al. 2005). The primary DICER component of tasiRNA biogenesis is DCL4 which

generates 21-nt phased tasiRNAs which can be loaded into AGO1 to target downstream genes (Figure 1.1B) (Gasciolli, Mallory et al. 2005, Yoshikawa 2013).

1.3 Plant DNA methylation

DNA methylation is an important epigenetic mark in plants and animals, it is vital for many epigenetic phenomena and, it is associated with gene silencing and heterochromatin formation. This epigenetic mark is heritable and formed almost exclusively by the direct covalent modification at the 5 position of cytosine forming 5-methylcytosine (5mC). In mammals, 70%–80% of all cytosines are methylated in this way which occurs primarily at CG dinucleotide clusters (termed CpG islands) (Li and Zhang 2014). In plants, methylation occurs in three different sequence contexts. In *Arabidopsis*, DNA methylation is found in: 24% of CG, 6.7% of CHG, and 1.7% of CHH sequence contexts (where H indicates A C or T) (Cokus, Feng et al. 2008). However, this is highly variable between species, for example, in maize, which is known to possess large numbers of TEs and repetitive regions in the genome, much higher levels of CG methylation are detected and general increases in all three sequence contexts are observed (65% for CG, 50% for CHG, and 5% for CHH) (Regulski, Lu et al. 2013). This cytosine methylation in plants is nonrandomly distributed and accumulates in TEs and repetitive elements in addition to the promotors and gene body of differentially expressed genes (Zilberman, Gehring et al. 2007). In *Arabidopsis*, the vast majority of TEs and a large proportion of pseudogenes are methylated (91% and 58% respectively) contrasting with 20% meC at non-TE associated gene sequences (Zilberman, Gehring et al. 2007). Gene associated methylation is evolutionarily conserved across eukaryotes and its function in plants is still debated but appears to be associated with open chromatin conformation

the histone variant H3.3 and moderate gene expression (Feng, Cokus et al. 2010, Bewick, Ji et al. 2016, Wollmann, Stroud et al. 2017).

1.4 Maintenance of plant DNA methylation in plants

DNA methyltransferases maintain pre-existing DNA methylation marks at symmetrical CG and CHG contexts (Cokus, Feng et al. 2008). It is this symmetry which permits the faithful maintenance of these marks during replication from the mother strand to the daughter strand. Prior to replication, both DNA strands are fully methylated and contributes one strand of hemimethylated DNA to the daughter strand. As these marks are symmetric, the hemimethylated DNA serves as a template for the deposition of methylation to the newly synthesised DNA strand (Cokus, Feng et al. 2008). The plant homologue of the mammalian DNA methyltransferase DNMT1, DNA METHYLTRANSFERASE 1 (MET1) and the plant specific CHROMOMETHYLASE 3 (CMT3) are responsible for maintenance of CG and CHG contexts respectively (Vongs, Kakutani et al. 1993, Bartee, Malagnac et al. 2001, Lindroth, Cao et al. 2001). In mammals, as is likely the case in plants, DNMT1 is known to associate with the replication foci and facilitates the maintenance of DNA methylation using the hemimethylated strand of newly synthesized DNA as a template (Fig 1.2A) (Leonhardt, Page et al. 1992, Pradhan, Bacolla et al. 1999, Takebayashi, Tamura et al. 2007). UHRF1/ NP95, the mammalian homologue of the VARIANT IN METHYLATION (VIM1) in *Arabidopsis* has also been found to specifically target DNMT1 to hemimethylated CG dinucleotides during replication (Bostick, Kim et al. 2007, Arita, Ariyoshi et al. 2008). However, it is not yet certain whether CG maintenance in plants occurs in a mechanistically similar fashion (Law and Jacobsen 2010). To maintain CHG methylation, the chromodomain of CMT3 must bind to the repressive histone 3 dimethylation of lysine 9

(H3K9me2)(Du, Zhong et al. 2012). Methylation of CHG contexts additionally recruits the SET- AND RING-ASSOCIATED (SRA) of the histone methyltransferase SU(VAR) HOMOLOGUE 4 (SUVH4)/KRYPTONITE (KYP), which results in a feedback loop reinforcing CHG methylation (Figure 1.2B)(Stroud, Greenberg et al. 2013).

1.5 Establishment of DNA methylation in plants

DOMAINS REARRANGED METHYLTRANSFERASE 2 (DRM2) homologue of the mammalian DNMT3 is responsible for the *de novo* methylation of asymmetric CHH contexts and is directed by siRNAs in the RNA-directed DNA methylation (RdDM) pathway (or facilitated by CMT3 at some select loci) (Cao and Jacobsen 2002). RdDM is a complex process relying on key proteins from the RNAi machinery such as argonaute and dicer-like proteins, as well as chromatin remodellers and RNA polymerases (Pol IV, Pol V)(Pikaard, Haag et al. 2008, Matzke, Kanno et al. 2009). The canonical RdDM pathway begins with Pol IV dependent biogenesis of 24-nucleotide siRNAs. Pol IV is recruited by SAWADEE HOMEODOMAIN HOMOLOGUE 1 (SHH1) to a subset of its target loci where it transcribes single stranded RNA (ssRNA) (Law, Du et al. 2013). The ssRNA is copied by RNA-dependent RNA polymerase (RDR2) into dsRNA which is cleaved by DICER-LIKE 3 (DCL3) into 24-nt siRNAs that are further stabilised by 3' methylation by HUA ENHANCER 1 (HEN1) and loaded into Argonaute 4 (AGO4)(Figure 1.3B)(Haag, Ream et al. 2012, Ji and Chen 2012). It is thought that transcription of intergenic non-coding loci by Pol V produces a scaffold that works with AGO4 bound siRNAs to bring the RdDM silencing complex (Wierzbicki, Haag et al. 2008). Once recruited, AGO4 can recruit DRM2 through interactions with RNA-DIRECTED DNA METHYLATION 1 (RDM1) to bring *de novo* methylation to the region (Figure 1.3B)(Law, Ausin et al. 2010).

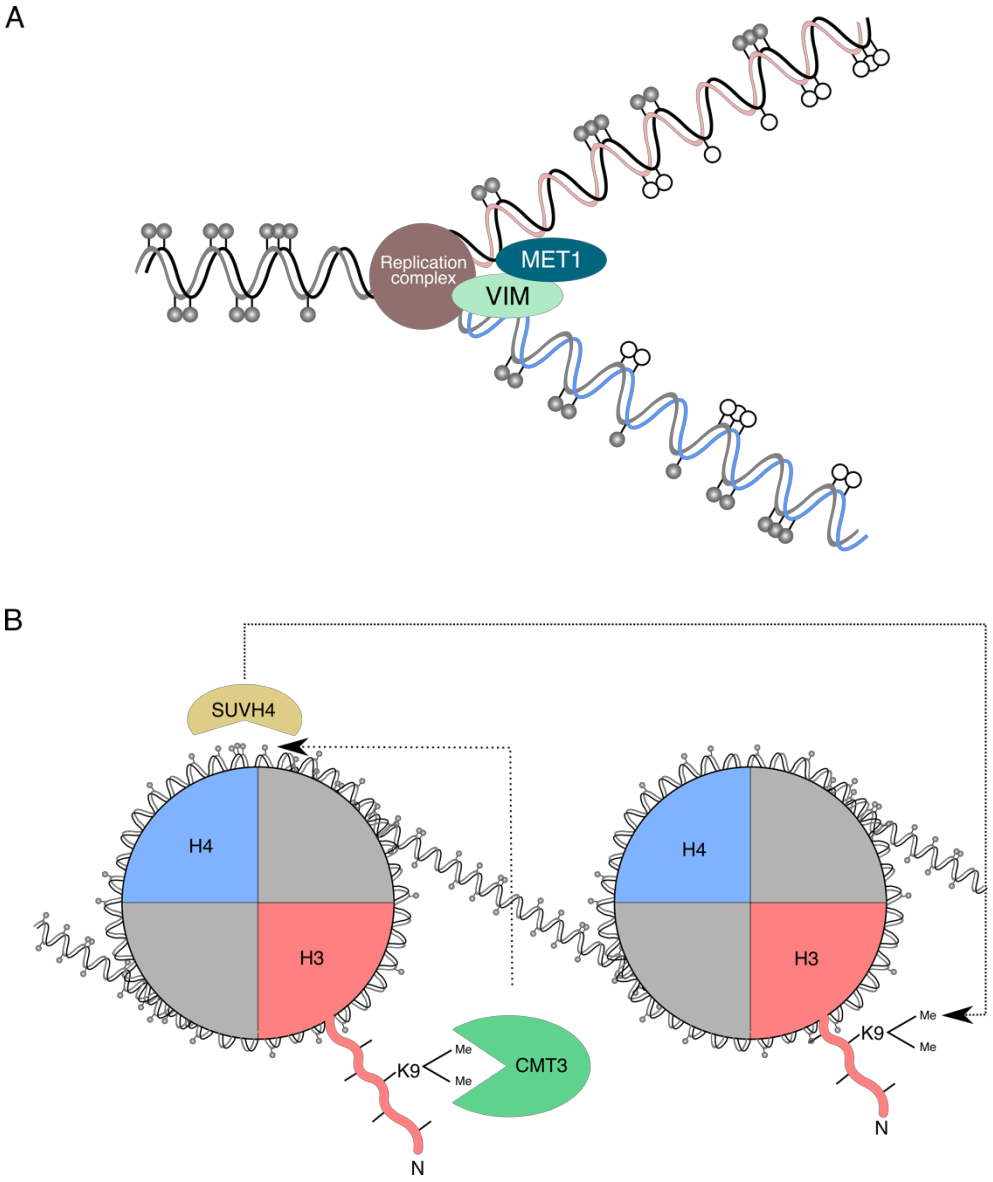

Figure 1.2: Maintenance of DNA methylation in plants. (A) maintenance of CG methylation at the replication fork. Met1 is thought to localize to the replication fork with assistance from VIM proteins to methylate hemimethlated daughter strands. (B) CMT3 is recruited by H3K9Me2 histone marks bringing methylation to the DNA in CHG contexts. CHG methylation brings SUVH4 which methylates H3K9. (Law and Jacobsen 2010)

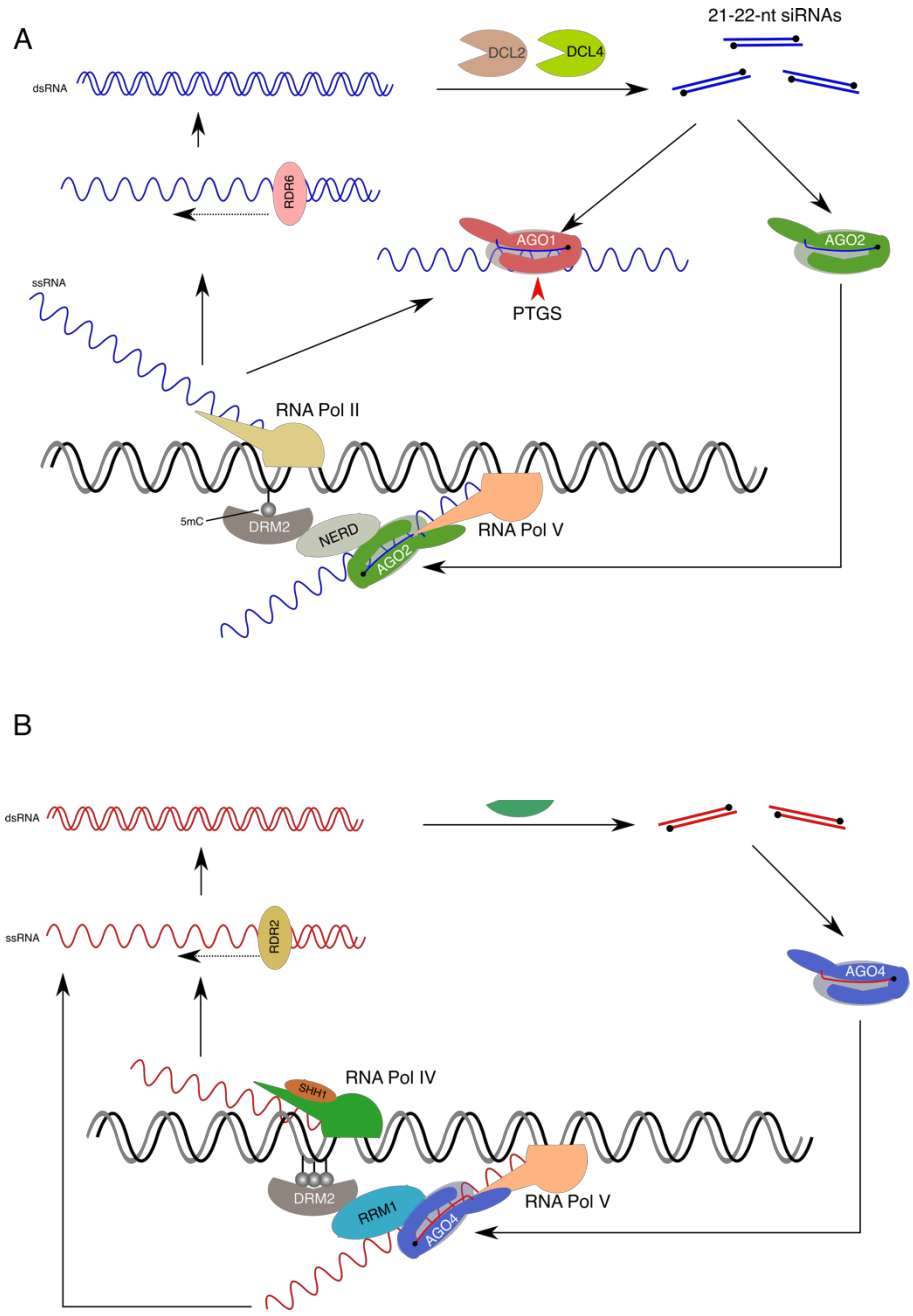

Figure 1.3: The non-canonical and canonical RdDM pathways in plants. (A) A new transposable element for example is transcribed by RNA polymerase II (Pol II). Some transcripts are made double stranded by RNADEPENDENT RNA POLYMERASE 6 (RDR6) and processed by Dicer like 2 (DCL2) and DCL4 into 21-22nt siRNAs. These are loaded into AGO1 and guide cleavage of TE transcripts post transcriptionally. Additionally, these siRNAs can trigger low levels of DNA methylation by loading into AGO2 and directing DRM2 by interacting with nascent Pol V transcripts and NEEDED FOR RDR2-INDEPENDENT DNA METHYLATION (NERD). (B) Small RNA directed DNA Methylation. siRNAs are generated from Pol IV transcripts processed by the RDR2 and DCL3 into AGO4 RISC factors. AGO4 with bound siRNA interacts with homologous Pol V nascent transcripts and recruits the DNA methylation machinery. (Law and Jacobsen 2010)

In addition to the canonical RdDM pathway, the non-canonical pathway generates 21nt sRNAs by DICER-like 1 (DCL1) cleavage of Pol II transcripts that are exported to the cytoplasm and loaded into AGO1 where they guide the cleavage of complimentary target mRNA transcripts (Figure 1.3A)(Nuthikattu, McCue et al. 2013). Additionally, these Pol II transcripts can be processed by DCL2 and DCL4 to produce 21-22-nt siRNAs, which are loaded into AGO2 and leads to *de novo* DNA methylation by DRM2 and aided by NEEDED FOR RDR2-INDEPENDENT DNA METHYLATION (NERD). This generates low levels of DNA methylation that can then trigger the canonical RdDM pathway enhancing the silencing signal (Marí-Ordóñez, Marchais et al. 2013, Nuthikattu, McCue et al. 2013). These RDdM pathways likely work together to carry out many biological roles in transcriptional gene silencing (TGS) ranging from the silencing of transposons, regulating the plant stress response and plant development (Mosher, Schwach et al. 2008, Garcia-Aguilar, Michaud et al. 2010, Lee, Gurazada et al. 2012, Popova, Dinh et al. 2013).

1.6 Removal of DNA cytosine demethylation in plants

Although DNA methylation is stable, loss of DNA methylation does occur throughout development in plants and animals. This demethylation process can be passive demethylation through inactivity of the methylation maintenance pathway or active demethylation through the removal of methylated cytosines. Active demethylation in plants is mediated by DNA glycosylase in conjunction with the DNA excision repair pathway (Ikeda and Kinoshita 2009, Zhu 2009). In *Arabidopsis*, demethyation is carried out by the glycosylase enzymes DEMETER (DME), REPRESSOR OF SILENCING 1 (ROS1) in addition to DEMETER-LIKE 2 (DML2) and DML3 (Choi, Gehring et al. 2002, Gong, Morales-Ruiz et al. 2002, Ortega-Galisteo, Morales-Ruiz et al.

2008). The ROS1/DME glycosylases are bifunctional, first cleaving the N-glycosidic bond, generating an abasic site followed by nicking of the phosphodiester link generating a single nucleotide gap (Agius, Kapoor et al. 2006, Baute and Depicker 2008, Gehring, Reik et al. 2009). This cytosine can then be replaced by the base excision pathway (Gehring, Reik et al. 2009).

Despite their biochemical similarities, both ROS1 and DME have distinct biological functions. While ROS1 is broadly expressed in vegetative tissues, DME is vital during gametogenesis where it removes 5mC necessary for imprinting and seed viability (Choi, Gehring et al. 2002, Huh, Bauer et al. 2008, Schoft, Chumak et al. 2011). Plants have exquisite control of the deposition and removal of transcriptional silencing and use these marks to control expression throughout development.

1.7 The interplay between histone modifications and DNA methylation I plants

Chromatin compaction represents a further avenue for modulation of gene expression. In Eukaryots, ~146bp of genomic DNA is associated with the histone octamer (H2A H2B H3 H4) forming the nucleosome, which can form a barrier to processes such as transcription and replication (Luger, Mäder et al. 1997, Berger 2007). These histone proteins are each post-translationally modified at their N-terminal tails which extend from the DNA-histone core. Acetylation, methylation, phosphorylation and ubiquitination marks work together with DNA methylation to control the expression state of the cell via the accessibility of DNA (Fuchs, Demidov et al. 2006, Tan, Luo et al. 2011). Each specific modification is associated with active or silenced chromatin, whereby histone modifications on one or more tails act cumulatively to produce unique chromatin architecture associated with distinctive transcriptional states.

Histone acetylation is generally associated with active transcription and open chromatin while transcriptionally silent regions typically lack acetylation (Marmorstein and Zhou 2014). Histone acetylation is reversible, deposited by histone acetyltransferases (HAT) and removed by histone deacetylase (HDAC) enzymes (Chen and Tian 2007). These HATs can be divided into five subfamilies based on homology and each with specific substrates and distinct biological functions (Earley, Shook et al. 2007). For example, the *Arabidopsis* AtGCN5/HAG1 acetylates H3 lysine 9 (H3K9), H3K14 and H4K27 and is essential for meristem function, cell differentiation, and environmental stress response (Servet, e Silva et al. 2010). Four classes of HDACs have been identified in plants and are responsible for the reversible removal of histone acetylation: Class I, class II, class III and plant-specific HD2-like histone deacetylase (Lusser, Brosch et al. 1997, Lusser, Kölle et al. 2001). HDA6 for example is generally associated with repressive chromatin and maintains CG and CHG methylation in conjunction with MET1 (Aufsatz, Stoiber et al. 2007). Although many HDACs show redundant function, HDA6 is necessary for seed maturation, controls flowering time and the stress response (Kim, To et al. 2012).

Histone methylation is also a reversible mark affecting chromatin. Histone lysine methyltransferases (HKMTs) are categorised into four groups of SET domain proteins; E(Z), ASH1, TRX, and the SU(VAR)3-9-related proteins (Pontvianne, Blevins et al. 2010). As mentioned, SUVH4/KYP binds to 5mC through the SRA domain to bring H3K9me2 and repressive chromatin that recruits CMT3 to maintain CHG DNA methylation (Figure 1.2) (Stroud, Greenberg et al. 2013). There are two groups of proteins which catalyse the demethylation of histones and do so via two alternative pathways (Liu, Lu et al. 2010). The lysine-specific histone demethylase-LIKE (LDL) proteins remove methylation via amine oxidation while the JUMONJI-C-DOMAIN

(JmjC) proteins act via hydroxylation (Cheng 2014). Histone modifications are just one of many mechanisms for plants to modulate their transcriptomic profile.

1.8 Epigenetic reprogramming during sexual reproduction in plants

Many epigenetic marks have been described such as DNA methylation and histone marks in plants that regulate the activity of the genome throughout development and in response to external stimuli. However, unlike mammals, which specify their germline early in embryogenesis, plants do not specify their germline until late in adult development (Hajkova 2011, Kawashima and Berger 2014). Additionally plant germ cells are specified from differentiated adult somatic cells in a position dependent manor (Berger and Twell 2011). Epigenetic reprogramming is known to occur in both male and female germline development, and this reprogramming is essential for plants reproduction (Crevillén, Yang et al. 2014).

Before meiosis takes place, major proliferation and patterning events must occur. The anther epidermis in maize arises from the L1 derived layer of the anther primordia while the other 3 layers and the meiocytes arise from the multipotent sub-epidermal L2 derived layer of the anther primordia (Dawe and Freeling 1990, Dawe and Freeling 1992). Anther development is first initiated by the specification of the archesporial cells in the anther primordia from the L2 derived cells in the inflorescence meristem (Figure 1.4). Archesporial cell identity is acquired in central cells from a field of equivalent L2 derived cells (Kelliher and Walbot 2011). Archesporial cell specification is initiated by a redox potential mediated by *Male Sterile Converted Anther 1* (MSCA1) (Kelliher and Walbot 2012). During anther growth, hypoxic conditions in the centre of anther primordia triggers MSCA1-mediated

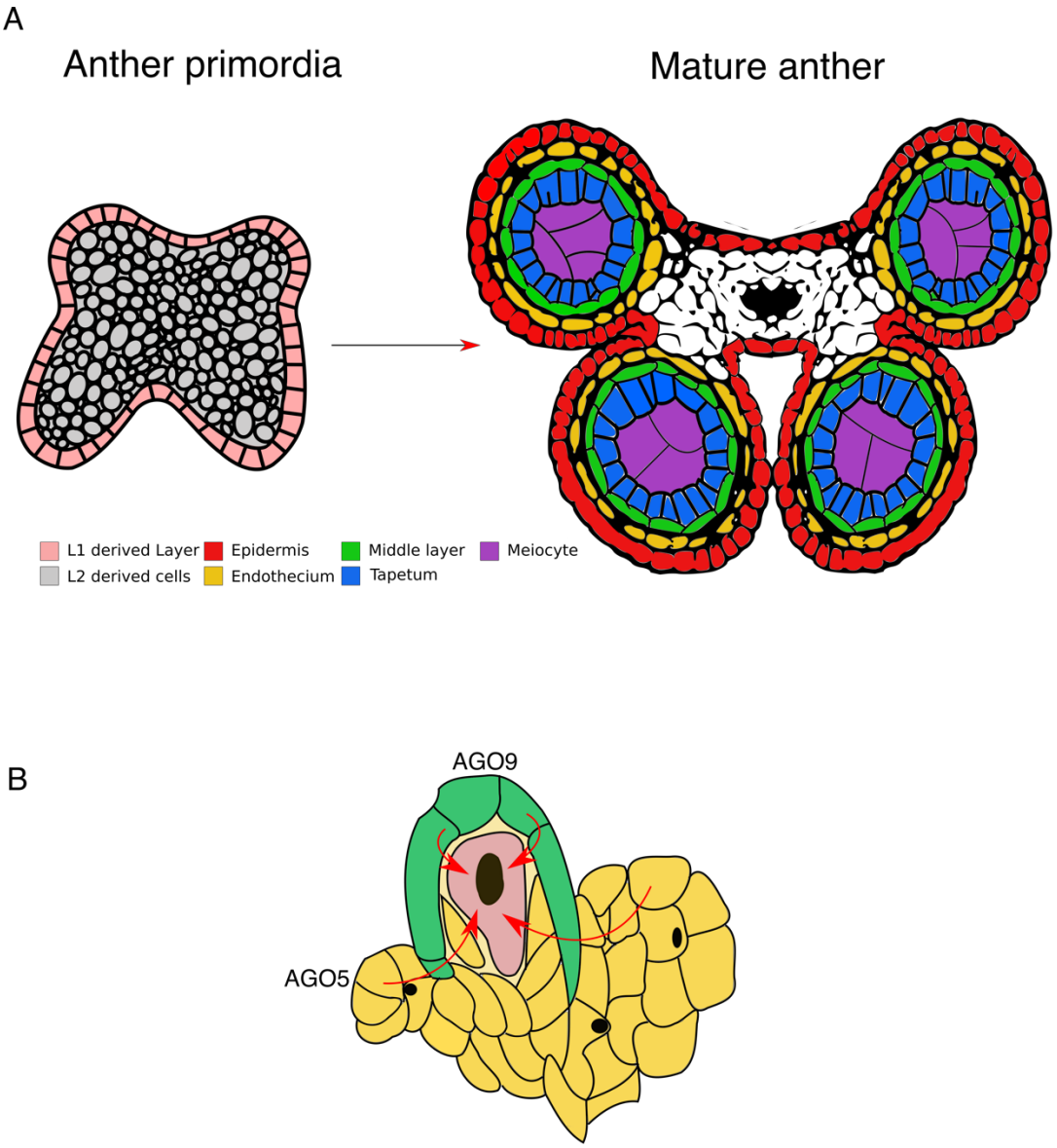

Figure 1.4: Cell specification during maize anther development. (A) Anther primordia can be divided into L1 and L2 derived cells. The L1 layer generates the anther epidermis, while the internal layers are derived from the multipotent sub-epidermal L2 derived cells of the anther primordia. A transverse section through a mature anther reveals the concentric somatic cell layers –the Epidermis and internal Endothecium, Middle, and Tapetum layers which support the growth and development of the meiocytes. (B) The action of AGO9 (green) and AGO5 (yellow) in sporophytic tissues restrict megaspore initiation and promote megasporogenesis, respectively in the developing ovule (red). (Adapted from (Gutierrez-Marcos and Dickinson 2012).

Responses resulting in the formation of a column of archesporial cells in the centre of each lobe. The archesporial cells secrete MAC1 which suppresses archesporial proliferation and triggers the periclinal division of neighbouring subepidermal L2 derived cells to form the secondary parietal cell layer and the endothecium (Wang, Nan et al. 2012). The final anther cell specification event occurs when the secondary parietal cell layer divides periclinaly to produce the middle layer and the tapetum cell layer, which is responsible for nourishing developing microspores. The tapetum is vital for the production of viable pollen, and many male-sterile mutants are defective in tapetum development (Aarts, Hodge et al. 1997, Niu, Liang et al. 2013, Fernández Gómez and Wilson 2014). Once the male pollen mother cells have been specified, each PMC undergoes meiosis to generate haploid microspore tetrads that separate into individual microspores (Bedinger and Fowler 2009). During microgamatogenesis, the microspores enlarge and undergo an asymmetric cell division to a small generative cell which is engulphed by the larger vegetative cell (Borg, Brownfield et al. 2009, Twell 2011).

Formation of the female gametophyte begins with the specification of the megaspore mother cell by AGO5 and AGO9 from a single subepidermal cell, at the distal tip of the premature ovule (Olmedo-Monfil, Durán-Figueroa et al. 2010, Tucker, Okada et al. 2012). The female megaspore mother cell undergoes meiosis to form a single megaspore which undergoes 3 rounds of nuclear division to generate the syncytial female gametophyte. After cytokinesis partitioning of the nuclei the female gametophyte consists of the egg cell, central cell and accessory synergid and antipodal cells (Berger and Twell 2011). Fertilization of the female gametophyte gives rise to the diploid zygote and a second fertilization event in the central cell gives rise to the endosperm (Li and Berger 2012). Overall, gametogenesis is associated with

a global reduction in DNA methylation attributed to the activity ad expression of DME/ROS1 and after fertilization takes place, the zygote re-establishes DNA methylation levels through the RdDM pathway (Gehring, Huh et al. 2006, Jullien, Susaki et al. 2012).

Dynamic epigenetic reprogramming is known to takes place during male gametogenesis. During sporogenesis, epigenetic silencing is briefly released, resulting in the expression of many normally silenced TEs (Chen, Farmer et al. 2010, Yang, Lu et al. 2011). However, this appears to be short-lived as TE transcripts are not over represented in the resulting microspore presumably resilenced by the RdDM pathway (Honys and Twell 2004). Additionally the microspore stage is associated with the upregulation of many microspore specific miRNAs and siRNAs, which are essential for development (Le Trionnaire, Grant-Downton et al. 2010, Wei, Yan et al. 2011). During sperm cell development, CG methylation remains at a comparable level to the microspore while CHH methylation is depleted, consistent with the expression of MET1 and loss of DRM2 (Calarco, Borges et al. 2012, Jullien, Susaki et al. 2012). Furthermore H3K9me2 levels are maintained, which presumably maintains TE silencing (Schoft, Chumak et al. 2009).

The vegetative cell loses CG methylation relative to the microspore, likely a result of a decrease in MET1 expression and active DNA demethylation by DME (Schoft, Chumak et al. 2011, Jullien, Susaki et al. 2012). As a result of the loss in CG methylation and loss of H3K9me2 histone marks, genes and TEs are normally silenced by these marks become hypomethylated and actively expressed (Schoft, Chumak et al. 2009, Slotkin, Vaughn et al. 2009). CHG methylation is unchanged in these cells and CHH methylation is increased relative to the microspore in TE-rich pericentromeric regions. However TEs are actively expressed in the vegetative cell indicating that they are not silenced by the canonical RdDM pathway (Calarco, Borges et al.

2012, Ibarra, Feng et al. 2012). Active transcription of TEs in the vegetative cells and the discovery of TE derived siRNAs in the sperm cells has lead to the proposal that TE derived 21-nt siRNAs are generated in the vegetative cell and move to the sperm cells to reinforce TE silencing by RdDM (Figure 1.5)(Slotkin, Vaughn et al. 2009). This is supported by evidence of artificial silencing signals moving between these cells and evidence of vegetative cell projections which link these two cell types (Slotkin, Vaughn et al. 2009, McCue, Cresti et al. 2011, Grant-Downton, Kourmpetli et al. 2013).

Female meiocytes are also specified from precursor somatic cells and undergo epigenetic reprogramming. AGO5 and AGO9 are expressed in the somatic companion cells surrounding the early female meiocytes, along with components of the RNA silencing pathway and control cell fate acquisition and support gametogenesis (Figure 1.4) (Singh, Goel et al. 2011, Tucker, Okada et al. 2012). Based on observations of siRNA mobility and the outcome of AGO9/5 disruption, it has been proposed that these pathways act non-cell autonomously to impact germ cell identity (Singh, Goel et al. 2011, Tucker, Okada et al. 2012). In parallel to the male gametogenesis, female meiocytes also express silenced TEs to reinforce silencing in the germline, likely as a result of MET1 silencing and expression of DME, resulting in the loss of DNA methylation in all sequence contexts (Figure 1.5)(Kubo, Fujita et al. 2013). DME expression is necessary for regulation of maternally imprinted genes in the endosperm such as FWA (Kinoshita, Miura et al. 2004, Hsieh, Shin et al. 2011). Maternal genes are demethylated by DME in the endosperm, however, the methylation of the paternal genome is maintained in the sperm cell resulting in a methylation imbalance contributing to imprinting (Gehring, Bubb et al. 2009). The egg cell does not express MET1 and CMT3 and in contrast to central cells, though the egg cell does not express DME

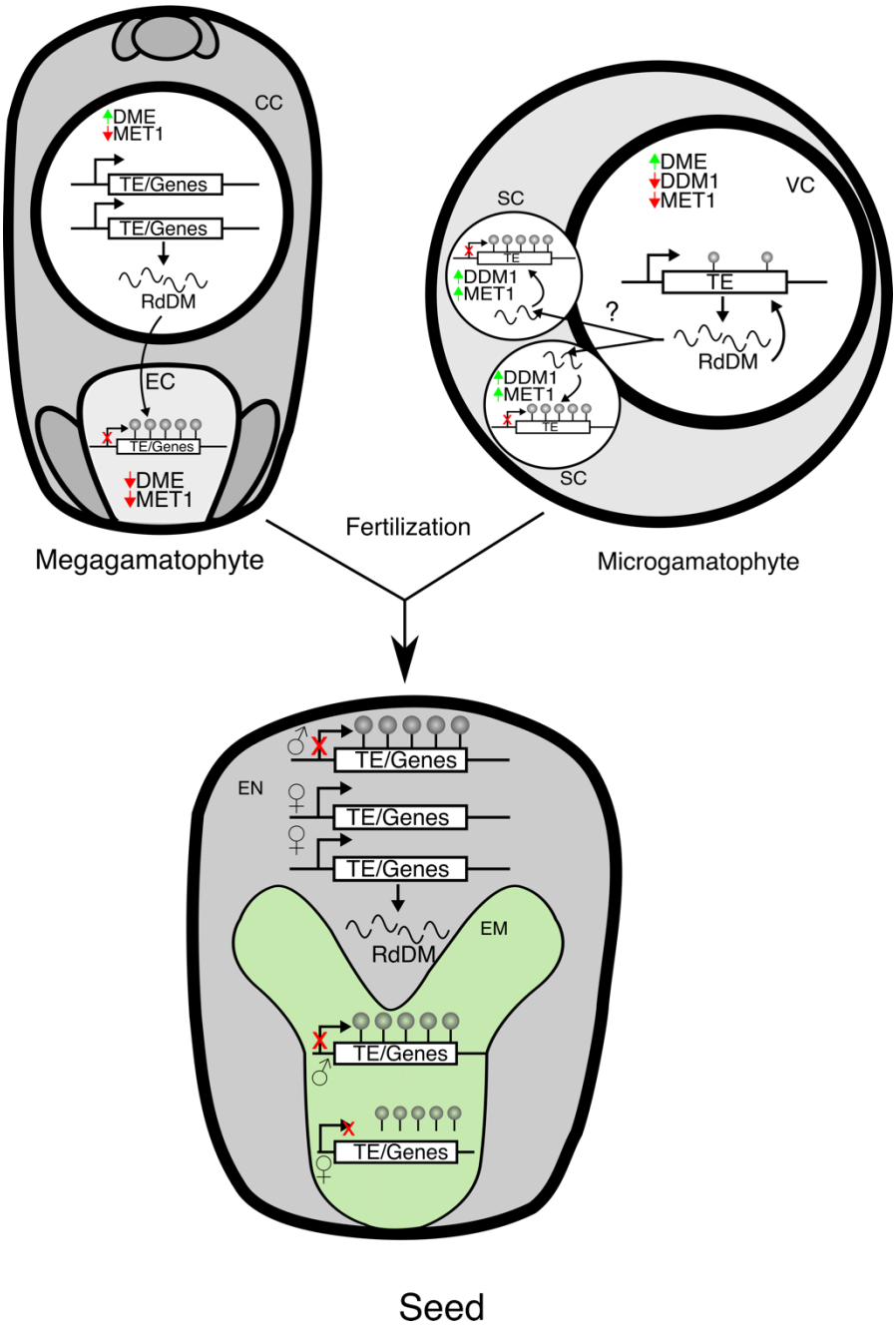

Figure 1.5: Reprogramming of epigenetic marks at TEs and imprinted genes during gametogenesis and fertilization in plants. CH methylation in the vegetative cell (VC) is depleted relative to microspore expression and correlated with down regulation of MET1 and expression of DME. Despite active RdDM and increased CHH methylation in the VCs, transposons are actively expressed resulting in the generation of predominantly 21-nt siRNAs. These are hypothesized to migrate to the sperm cells (SC) and promote DNA methylation through the non-canonical RdDM pathway. Expression of DME and decreased expression of MET1 in the central cell (CC) leads to global demethylation of the genome including TEs and imprinted genes. Like in pollen, siRNAs derived from these TEs may move to the egg cell (EC) and direct methylation to these transposons. After fertilization, the endosperm is comprised of maternal demethylated and paternal methylated DNA and this methylation imbalance could be the basis of genomic imprinting (Law and Jacobsen 2010).

(Jullien, Susaki et al. 2012). Instead, DNA methylation is maintained by de novo RdDM pathways mediated by DRM1 and DRM2 (Gehring, Bubb et al. 2009, Ibarra, Feng et al. 2012, Jullien, Susaki et al. 2012). TE derived siRNAs are thought to be generated in the central cell as a result of TE activation, which then migrate to the egg cell to reinforce RdDM silencing (Ibarra, Feng et al. 2012). Following fertilization, genes involved in DNA methylation are activated and remain so throughout early embryogenesis, likely compensating for the net loss of methylation in the various cell types during gametogenesis (Jullien, Susaki et al. 2012, Belmonte, Kirkbride et al. 2013). CG methylation is returned to adult levels by the globular stage embryo, however due to the incorporation of the CHH depleted paternal germline, CHH levels initially drop but return to adult levels by the heart-shaped embryo stage (Jullien, Susaki et al. 2012).

Epigenetic reprogramming is vital for development, gametogenesis and to regulate imprinted genes. A common strategy to both plants and animals appears to be the relaxation of epigenetic silencing in somatic tissues, so that sRNA silencing signals can be generated and pass to the germ cells. However, this relaxation may also lead the release of transposable elements. Without their tight control, transposons can wreak havoc on the genome, generating chromosomal rearrangements, gene duplications and generate DNA double strand breaks (Gasior, Wakeman et al. 2006), the majority of which are detrimental to host fitness (Svoboda, Robson et al. 1995, Durdevic, Pillai et al. 2018).

Transposition in the germline can have catastrophic impacts on fertility and may have drastic consequences for the offspring (Aarts, Dirkse et al. 1993, Batista, Ruby et al. 2008). Uncontrolled transposon activation in germ cell lineages frequently leads to DNA double strand breaks, sometime resulting in sterility or genetic lesions that are transmitted to the offspring (Aarts,

Dirkse et al. 1993, Walsh, Chaillet et al. 1998, Carlson, Dupuy et al. 2003, Keng, Yae et al. 2005, Carmell, Girard et al. 2007). Furthermore, transposon insertions within or near genes can alter their expression, resulting in dominant effects in the haploid genome (Szövényi, Devos et al. 2014). In order to protect the germline from transposable elements, Eukaryotic organisms must deploy silencing mechanisms to tightly control their transcription and translation during germ cell reprogramming.

Argonaute proteins are the frontline of defence to protect against TE damage (Zhang, Xia et al. 2015). Transposon silencing is mediated by the generation of TE- derived siRNAs, which sometimes affect homologous sequences and also endogenous genes (McCue and Slotkin 2012). In unicellular organisms, such as Neurospora fungi and algae, transposons in their gametes are controlled through RNA silencing (Cogoni, Irelan et al. 1996, Wu-Scharf, Jeong et al. 2000). However, in multicellular organisms, the silencing of transposons in the germline could be mediated by the somatic companion cells that encapsulate them. In animals silencing of transposons in the germline is directed by PIWI, a discrete group of argonaute proteins (Cox, Chao et al. 1998, Carmell, Girard et al. 2007). PIWI proteins are predominantly expressed in the germline in vertebrates but in surrounding somatic cells in arthropods, and they bind to noncoding, repeat-associated siRNAs that silence transposons (Lewis, Quarles et al. 2018). These factors regulate germline development and are absolutely essential for maintaining silencing of TEs and some genes during spermatogenesis (Brennecke, Aravin et al. 2007, Carmell, Girard et al. 2007, Houwing, Kamminga et al. 2007). Similarly in plants, AGO9 is expressed in the somatic companion cells surrounding the ovule primordia and restricts the specification of gametophyte precursors (Olmedo-Monfil, Durán-Figueroa et al. 2010). AGO9 also interacts with TE derived siRNAs in the soma and like

the piRNAs, directs RNA silencing of transposons in pericentromeric regions in the ovule (Durán-Figueroa and Vielle-Calzada 2010).

A novel class of secondary siRNAs termed the phased small interfering RNAs (phasiRNAs) has been recently identified in the male germline of monocots. These phasiRNAs accumulate during reproductive development in somatic companion cells and are divided into two classes: the 21nt reproductive phasiRNAs triggered by miR2118-RISC and processed by DCL4, and the 24-nt reproductive phasiRNAs triggered by miR2275-RISC and processed by DCL5 (formerly DCL3b) (Margis, Fusaro et al. 2006, Johnson, Kasprzewska et al. 2009, Song, Li et al. 2012). Both classes originate predominantly from nonrepeat associated lncRNA with 705 21PHAS loci and 27 24PHAS identified in rice and 463 21PHAS loci and 176 24PHAS loci identified in maize (Figure 1.1C) (Johnson, Kasprzewska et al. 2009, Zhai, Zhang et al. 2015). Additionally, disruption of the phasiRNA biogenesis pathway demonstrates their functional importance during male reproductive development (Nonomura, Morohoshi et al. 2007, Song, Li et al. 2012, Kakrana, Mathioni et al. 2018). Despite the functional importance of the reproductive phasiRNAs, molecular targets remain elusive and their molecular function remains unknown.

1.9 Project aim

The reproductive phasiRNAs are a class of secondary siRNAs co-ordinately expressed during male reproductive development with unknown function. As a class of siRNA, the phasiRNAs likely take part in RNA silencing and thus almost certainly interact with an argonaute protein. In rice a phasiRNA interacting argonaute has been identified that is important for male meiosis, however the precise function of these factors remains elusive. Maize, like rice accumulate reproductive phasiRNAs and rice argonaute homologues have been identified in maize. The aim of this thesis is to identify maize Argonaute proteins that interact with reproductive phasiRNAs

2.0 Materials and methods

2.1 General plant Materials and Methods

2.1.1 Maize growth conditions

Plants were grown in compost containing 1-part Sphagnum moss peat, 1-part John Innes No.3, 1-part course grade horticultural sand and 3 $g \cdot L^{-1}$ Osmocote slow release fertilizer. Plants grown in glasshouse conditions (16-hour day/ 8-hour night photoperiod) were germinated in 9 cm pots and transferred to 23 cm pots after 3-4 weeks of growth and grown to maturity. For heat stress experiments, plants were transferred to Growth chambers for 3 days (16-hour day, 35°C/ 8-hour night, 22°C photoperiod, light intensity 500 $\mu mol \cdot m^{-2} \cdot s^{-1}$, humidity 75%).

2.1.2 *Tjuntiwari* growth conditions

N. benthamiana seeds were germinated on M2 soil (Levington Advance, UK) (200 $\mu mol \cdot m^{-2} \cdot s^{-1}$for 16-hour day/ 8-hour night photoperiod; 22°C/ 22°C) and maintained for 2 weeks. Plantlets were then picked into individual 9 cm pots with F2 soil (Levington Advance, UK) and grown to adult stage.

2.1.3 Plant stocks

MAGO1/2 RNAi lines were generated and supplied by Biogemma. Dexamethasone inducible *wmvHCPro* maize lines were generated in collaboration with Prof. James Birchler (University of Missouri) and the two-component HDZIV6 driver lines were supplied by Prof. Anne Sylvester (University of Wyoming) and Prof. David Jackson (CSHL). GFP *N. benthamiana* were provided by the Prof. David Baulcombe (University of Cambridge) (Table 2.1)

2.0 Materials and methods

Table 2.1: Plant materials

Plant stocks	Abbreviations	Source	Accession
B73 Wild Type (WT)	B73	-	-
A188 Wild type (WT)	A188	Biogemma	-
MAGO1/MAGO2 RNAi (A188 background)	*MAGO* RNAi	Biogemma	GRMZM2G059033, GRMZM2G123063
indWMVHCPRro	HCPro	J.Birchler (University of Missouri)	
pZmHDZIV6::LhG4 (maize optimized)	HDZIV6	A.Sylvester (University of Wyoming)	GRMZM2G001289
N. benthamiana p35S::GFP5	GFP	D.Baulcombe (University of Cambridge)	mGFP5

2.2 General Cloning methods

2.2.1 Generation of maize RNAi transgenic lines

A 250bp fragment of *MAGO1* and *MAGO2* were chemically synthesised as a tandem inverted repeat separated by the *StLS1* intron and cloned into a simple plasmid p*UC57* (Genscript). One plasmid for the promoter fragment, another for the *MAGO* RNAi fragment, one for the terminator, and the destination vector which contained the reporter and marker cassettes. Then Golden Gate cloning using SapI as type II restriction enzyme with different overhangs. SapI1 – promoter – SapI2 + SapI2 -*MAGO*_RNAi fragment – SapI3 + SapI3 – terminator – SapI4 + SapI1/SapI4 destination vector. The *Agrobactirium tumefaciens* strain LB4404 was transformed with this binary vector and used to transform the Maize cultivar A188 as previously described (Ishida, Saito et al. 1996).

2.2.2 *pZmHDZIV6-LhG4* driver construct design

pZmHDZIV6-LhG4 driver vector was constructed using the MultiSite Gateway method (Invitrogen). The native 3164 bp promoter of *ZmHDZIV6* (GRMZM2G001289) was amplified with primers ZmHDZIV6_ACTp1 and ZmHDZIV6_ACTp4 and the 945 bp native terminator of *ZmHDZIV6* was amplified with primers ZmHDZIV6_ACTp3 and ZmHDZIV6_ACTp2 and cloned into MultiSite Gateway donor vectors, p*DONR221* P1-P4 and p*DONR221* P3-P2, respectively. The maize codon-optimized LhG4 was cloned into MultiSite Gateway donor vector p*DONR221* P4r-P3r. The resulting three entry vectors were then recombined into the binary vector p*AL010* (a derivative of p*TF101.1* carrying the Gateway Cassette and a *GUS<< pOp >>NLS-TagRFP-T* reporter cassette) yielding *pZmHDZIV6-LhG4*. It was introduced into *Agrobacterium tumefaciens* EHA101 and transformed into maize Hi II at

Table 2.2: Primer table

ID	Primer name	Sequence (5' - 3')	Gene
RM01	HcPRO1_RTF1	AACACAGACGGCTAAGAACC	*HCRPO*
RM02	HcPRO1_RTR1	CCACTGTATGATGCGTGTTT	*HCRPO*
RM03	pWUS1F1	CCCGGCGCCAACCTATATC	*pWUS::LhG4*
RM04	LhG4-183R	GCTTTGTTTACCAGCCAGCTGCT	*pWUS::LhG4*
RM05	pHDZIV6 197F3	AGACGACGTCCAATAAATCCA	*pHDVIV6::LhG4*
RM06	LhG4-183R	GCTTTGTTTACCAGCCAGCTGCT	*pHDVIV6::LhG4*
RM07	GFP_F3(Biogema)	CCACATGAAGCAGCACGACT	*DRM1/2 RNAi*
RM08	GFP_R3(Biogema)	TGTCGGCGGTGATATAGACG	*DRM1/2 RNAi*
RM09	ZsGreen_F3	TTAACCTGTGCGTGGTCGAG	*MAGO RNAi*
RM10	ZsGreen_R3	CTGGGAAGTTCACCCCGTAG	*MAGO RNAi*
RM11	pNOS F1	TGAACCGCAACGTTGAAGGAG	*FiLUC-phasiRNA sensor*
RM12	pNOS R1	TGGCGTCTTCCATGGTAATTGGATACCGAGGGGAATTTATG	*FiLUC-phasiRNA sensor*
RM13	fiLUC F1	CGGTATCCAATTACCATGGAAGACGCCAAAAACATAAAGAAAGG	*FiLUC-phasiRNA sensor*
RM14	fiLUC R1	ATTCGTTGCGGCCGCTTACACGGCGATCTTTCCG	*FiLUC-phasiRNA sensor*
RM15	NOStF1	AAGATCGCCGTGTAAGCGGCCGCAACGAATG	*FiLUC-phasiRNA sensor*
RM16	NOStR1	CGATCTAGTAACATAGATGACACCG	*FiLUC-phasiRNA sensor*
RM17	5' res site	TGTAAAACGACGGCCAGTAAGCTTGAACCGCAACGTTGAAGGAG	*FiLUC-phasiRNA sensor*
RM18	3'res site	GGAAACCTATGACCATGGGATCCGATCTAGTAACATAGATGACACCG	*FiLUC-phasiRNA sensor*
RM19	3' del res site	GGAAACCTATGACCATGGGATCC	*FiLUC-phasiRNA sensor*
RM20	MAGO1_F3_12attB1	AAAAAGCAGGCTGGATGGCGAGCAGGGGGAG	*MAGO* Gateway cloning
RM21	MAGO1_R2_12attB2	AGAAAGCTGGGTGGCAGAAGAACATAACCTCCT	*MAGO* Gateway cloning
RM22	MAGO2_F2_12attB1	AAAAAGCAGGCTGGATGGCTTACAGGGGCGG	*MAGO* Gateway cloning
RM23	MAGO2_R2_12attB2	AGAAAGCTGGGTGGCAGTAGAACATCACATCCTT	*MAGO* Gateway cloning
RM24	attB1_adapter	GGGGACAAGTTTGTACAAAAAAGCAGGCT	*MAGO* Gateway cloning
RM25	attB2_adapter	GGGGACCACTTTGTACAAGAAAGCTGGGT	*MAGO* Gateway cloning
RM26	T7 promoter forward	TAATACGACTCACTATAGGG	-
RM27	SP6 promoter forward	ATTTAGGTGACACTATAG	-
RM28	M13 forward	TGTAAAACGACGGCCAGT	-
RM29	M13 Reverse	CAGGAAACAGCTATGAC	-
RM30	ZmHDZIV6_ACTp1	GGGGACAAGTTTGTACAAAAAAGCAGGCTTTTGGCATAAGAGCACCGCT	*pZmHDZIV6* Gateway cloning
RM31	ZmHDZIV6_ACTp4	GGGGACAACTTTGTATAGAAAAGTTGGGTGTTCTCCTCTCGCGGAACCTC	*ZmHDZIV6ter* Gateway cloning
RM32	ZmHDZIV6_ACTp3	GGGGACAACTTTGTATAATAAAGTTGAGCTAGCTTAGTCGAATCAGAC	*ZmHDZIV6ter* Gateway cloning
RM33	ZmHDZIV6_ACTp2	GGGGACCACTTTGTACAAGAAAGCTGGGTAAGAACTTTGACTTGCTTAGG	*pZmHDZIV6* Gateway cloning

Iowa State University Plant Transformation Facility. The positive transgenic lines were crossed to B73 at least twice for analysis.

2.2.3 *indHCPRO* construct design

To generate a chemical inducible Wheat Mosaic Virus HCPRO construct (*indHCPRO*) we synthetized a gene fragment flanked by the *attB1* and *attB2* recombination sites (IDT, Leuven, BE). The synthetic gene was subcloned into p*DONR207* by BP recombination and the positive clones were selected in media supplemented with Gentamycin. After selection, this was cloned by LR reaction into the binary vector (*pZZ-TOP*, unpublished) which contains the *Bar* for transgene selection, a *LhG4:GR* gene fusion (Samalova, Brzobohaty et al. 2005) that is constitutively expressed from a maize Ubiquitin promoter, and a bi-directional *pOp6* promoter (Craft, Samalova et al. 2005) which enables the inducible expression of a beta-glucuronidase (GUS)(see 2.5.6) reporter and the gene of interest after exposure to dexamethasone (DEX)(see 2.4.8).

2.2.4 FiLUC-sensor construct design

The *nopaline synthase* (*NOS*) promoter region and *miR2118-target::truncated-GFP::NOSt* region were synthesized (IDT, Leuven, BE). The miRNA2118 target region was designed manually using predicted RNA hybridization energies between amiR2118 and the target sequences. Four such sequences were designed in tandem with a 4bp linker sequence. Both gBlock pieces were amplified by extension proof-reading PCR using specific primers (RM12,13 RM15,16; Table 2.2) and Phusion polymerase (NEB, UK). The full-length firefly luciferase gene was amplified by extension PCR from purified p*LUC+* plasmid vector (PROMEGA) using specific primers (RM14,15; Table 2.2). The three extension PCR amplicons were run on a 1% TAE agarose

gel, visualized using a UV light transilluminator and purified by gel extraction (Qiagen). The full construct was assembled by overlap PCR of the three purified PCR products using the Q5 polymerase (NEB, UK). To purify the full-length product, end primers were added to the reaction mix and the reaction allowed to continue for a further 15 cycles (RM17,18). The reaction was run on a 0.8% TAE agarose gel until the 2.7 kb product was resolved and the desired band was cut and gel purified. A-tailing was carried out by adding dNTPs (10 mM), 10X KAPA Taq Buffer A (KAPA Biosystems) and KAPA Taq DNA Polymerase (5 units·μL^{-1}; KAPA Biosystems) and incubating the reaction at 72°C for 30 minutes. The A-tailed product could then be ligated into the pGEM®-T Easy cloning vector and transformed into *E. coli*. The amiR2118 sequence was chemically synthesised as a gBlock (IDT, Leuven, BE) A-tailed and cloned into pGEM®-T Easy Vector (Figure 2.1) (See 2.2.8).

2.2.6 FiLUC-sensor binary vector cloning

The *FiLUC*-sensor sensor construct (See 2.2.4) and the p*BIN*+ binary vector were digested with *Bam*HI and *Hind*III and fragments were resolved on a 1% agarose TAE Gel with bands isolated by gel purification kit (Qiagen). The *FiLUC*-sensor construct was ligated into the p*BIN*+ vector by combining the fragments with T4 DNA ligase in T4 ligase buffer (NEB) and incubating overnight at 4°C before transforming into Top10 chemically competent *E. coli* (Invitrogen) (van Engelen, Molthoff et al. 1995). The p*35S*::*GUS* reporter gene was cut from the pSLJ4J8 plasmid vector by restriction digest with *Hind*III (Jones, Shlumukov et al. 1992). The fragment was blunt ended by combining the fragment with T4 DNA polymerase and 1X reaction buffer supplemented with 100 µM dNTPs (NEB) and incubated at 12°C for 15 mins. The reaction was stopped by the addition of 10 mM EDTA and incubating at 72°C for 20 mins. The fragment was additionally cut with *Eco*RI, resolved on

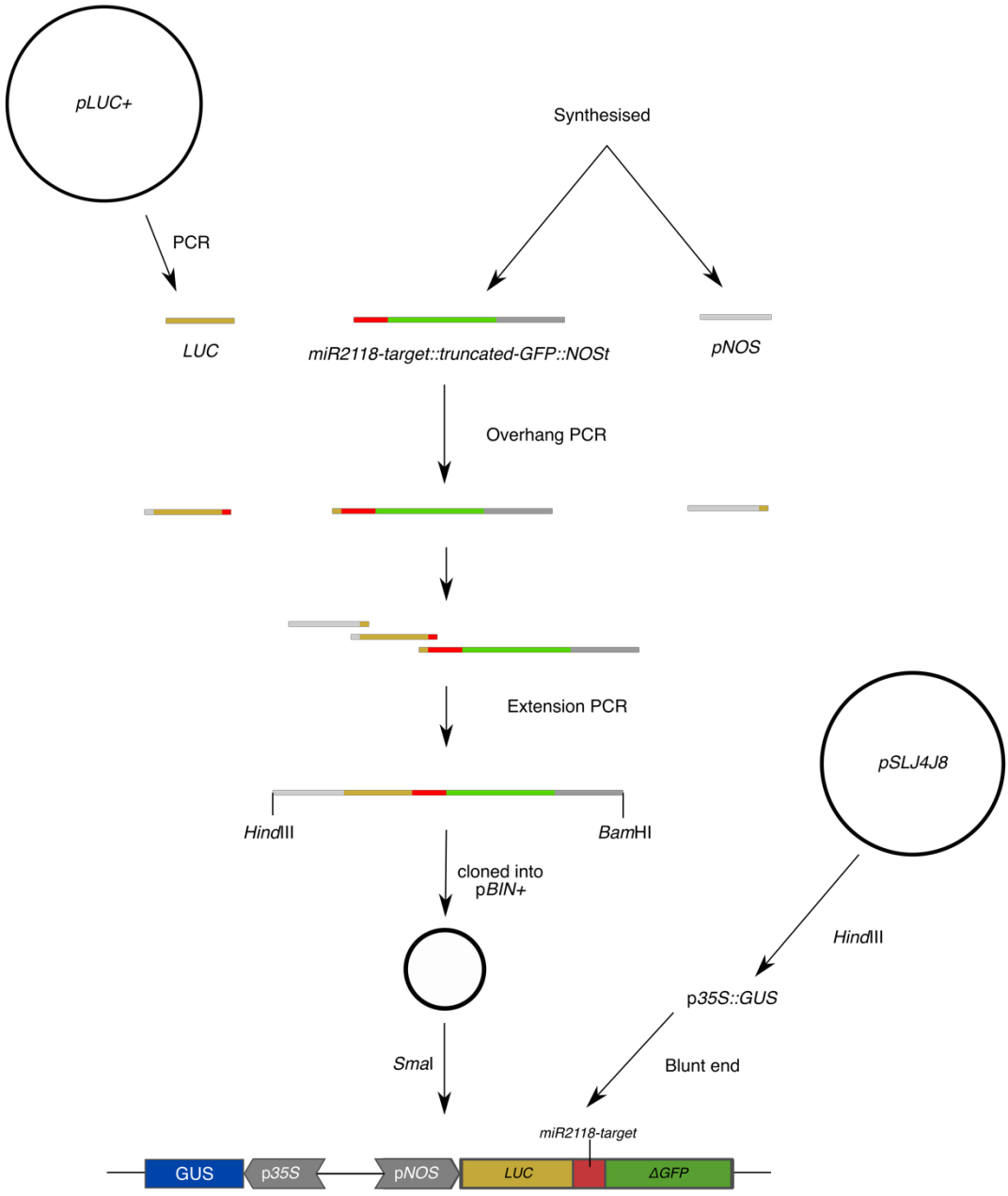

Figure 2.1: Cloning strategy to generate p*BIN-p35S::GUS-pNOS::FiLUC-PHAS-ΔGF-nosT. LUC* was amplified from the p*LUC+* vector and the *nopaline synthase* (*NOS*) promoter region and *miR2118-target::truncated-GFP::NOSt* region were chemically synthesized. These were assembled by extension-overlap PCR and blonde into the pBIN+ binory vector. P35S::GUS was cut from the pSLJ4J8 plasmid vector and cloned into p*BIN-pNOS::FiLUC-PHAS-ΔGF-nosT.*

a 1% agarose TAE Gel and bands were isolated by gel purification kit (Qiagen). p*BIN-pNOS::FiLUC-PHAS-ΔGF-nosT* was also cut with *Sma*I and *Eco*RI into which the p*35S*::*GUS* was ligated by combining the fragments with T4 DNA ligase and T4 DNA ligase buffer (NEB) and incubating over night at 4°C before transforming into Top10 chemically competent E. coli (Invitrogen) (Figure 2.1).

2.2.7 p*BIOS* cloning and gateway cloning

For expressing artificial miRNA2118 (amiR2118), we designed a construct containing an *octopine synthase* (*OCS*) enhancer, amiR2118 sequence and *nopaline synthase* (*NOS*) terminator. This fragment including flanking *Asc*I sites was chemically synthesized (IDT). The synthesized DNA fragment was amplified using M13_F and M13_R primers (RM28,29) and cloned into a pGEM®-T Easy vector (See 2.2.8) (Promega, WI, USA).

To generate vectors that simultaneously expressed MAGO and amiR2118, the *N. benthamiana* codon-optimized *ZmMAGO1* (GRMZM2G059033) and *ZmMAGO2* (GRMZM2G123063) were synthesized and cloned p*UC57* (Genscript). One plasmid for the promoter fragment, another for the *MAGO* codon optimised gene, one for the terminator, and the destination vector which contained the reporter and marker cassettes. Golden gate cloning using SapI as type II restriction enzyme with different overhangs. SapI1 – promoter – *Sap*I2 + *Sap*I2 -*MAGO* genes – *Sap*I3 + *Sap*I3 – terminator – *Sap*I4 + *Sap*I1/*Sap*I4 destination vector to generate the binary vectors p*BIOS11743* and p*BIOS11746*. The amiR2118 fragment was cut by *Asc*I and sub-cloned into the p*BIOS11743* and p*BIOS11746* to generate the final vector (Appendix).

To detect subcellular localization of MAGO proteins, *MAGO1* and *MAGO2* coding regions were amplified from cdsBGA_11372 and cdsBGA_11372 high

copy number plasmid vectors by PCR using gene specific primers pairs (RM20-23). Amplicons were cloned into a pDONR207 via BP recombination reaction followed by LR recombination reaction into a pGWB441, to generate c-terminal EYFP protein fusion.

2.2.8 pGEM®-T Easy cloning

A-tailed PCR products were ligated into the pGEM®-T Easy Vector by adding 2X Rapid Ligation Buffer (Promega, UK), pGEM®-T or pGEM®-T Easy Vector (50ng) (Promega, UK), T4 DNA Ligase and incubating the reaction overnight at 4°C.

2.2.9 pET29a cloning

Constructs were first cloned into the pGEM-T Easy cloning vector (See 2.2.8). Positive transformants were isolated by cutting with *Nde*I and *Hind*III, run on a 1% TAE agarose gel and Gel purified with purified by gel extraction (Qiagen). Purified insert was ligated into pET29a cut with *Nde*I and *Hind*III, by incubating overnight with T4 DNA ligase at 4°C (NEB). This vector was then transformed into chemically competent *E. coli* strain BL21(DE3) (See 2.2.7).

2.2.10 Transformation of chemically competent *E. coli*

Chemically competent *E. coli* were thawed on ice. Ligation reaction was added directly to the cells, mixed gently and incubated on ice for 30 min. The cells were then heat shocked at 42°C for 30 sec and placed immediately on ice with 250µl of S.O.C media (2% tryptone, 0.5% yeast extract, 10 mM NaCl, 2.5 mM KCl, 10 mM $MgCl_2$, 10 mM $MgSO_4$, and 20 mM glucose). After 2 min the cells were transferred to a 37°C shaking incubator (225 rpm) for 1hr. The transformation reaction was plated on an LB agar plate

supplemented with Ampicillin (50 mg·mL^{-1}), 100 mM IPTG (Isopropyl ß-D-1-thiogalactopyranoside)) and X-gal (5-bromo-4-chloro-indolyl-β-D-galactopyranoside)(20 mg·mL^{-1}) Plates were incubated overnight at 37°C. Positive blue/white colonies were picked and confirmed by colony PCR.

2.2.11 *Agrobacterium tumefaciens* transformation

The electrocompetent *Agrobacterium tumefaciens* GV3101 was thawed on ice. Binary vector was directly added to the cells and mixed gently. The cells were transferred into an electrophoresis cuvette, put into MicroPulser^{TM} Electroporator (Bio-Rad, UK) and pulse applied using the Agr setting (2.20 kV). LB low salt (1 mL) was added to the cells and the resulting mixture incubated in a 28°C shaking incubator (225 rpm) for 1 hr. The cells were spread onto an LBA plate supplemented with rifampicin (10 mg·L^{-1}), spectinomycin (50 mg·L^{-1}), streptomycin (50 mg·L^{-1}) and gentamycin (10 mg·L^{-1}) grown for 48 hrs 28°C and positive transformants were confirmed by colony PCR.

2.2.12 *Nicotiana benthamiana* leaf transient transformation

Transformed *A. tumefaciens* was cultured overnight in MGL media (0.25% Yeast extract [w/v], 0.5% Tryptone [w/v], 0.5% NaCl [w/v], 0.5% Mannitol [w/v], 0.116% Monosodium Glutamate [w/v], 0.25 g·L^{-1} KH_2PO_4, 0.1 g·L^{-1} $MgSO_4 \cdot 7H_2O$, 1 μg·L^{-1} Biotin, pH 7.0) at 28°C. The culture was pelleted at 5000g at room temperature and resuspended in infiltration buffer (10 mM MES (2-(*N*-morpholino) ethanesulfonic acid, pH5.7), 10 mM $MgCl_2$). *N. benthamiana* leaves were infiltrated with *Agrobacterium* and incubated under normal growth conditions for 2-3 days.

2.2.13 DNA Sanger sequencing

Bacterial cultures were inoculated with positive colonies selected on antibiotic media and grown overnight at 37°C. Plasmid minipreps were carried out on the overnight cultures (Qiagen). The isolated plasmid (500ng) was combined with sequencing primers or internal oligos and sequenced using Sanger sequencing (Eurofins-GATC).

2.3 General molecular methods

2.3.1 Plant DNA extraction

Leaf samples (~1 cm^2) were collected into 1.5 mL Eppendorf tubes along with glass (2 mm diameter) and ceramic (1 mm diameter) beads and flash frozen in liquid nitrogen. Samples were ground (approx. 4500 rpm) individually using a Silamat S6 mixer for 1 minute and centrifuged briefly 3000g. Leaf samples were homogenised in 300 µL of extraction buffer (100 mM Tris-Cl, pH 8.0; 50 mM EDTA, pH 8.0; 500 mM NaCl; 10 mM β-Mercaptoethanol) 40 µL of 10% SDS was added and vortexed followed by incubation at 65°C for 20 min. After 10 mins incubation on ice, 100 µL of 5 M KOAc was added and incubated for an additional 20 mins. Samples were centrifuged at max speed for 20 min and 125 µL of supernatant transferred to 200 µL of isopropanol and mixed. Samples were incubated at -20°C for a minimum of 30 mins to precipitate the DNA. Samples were then centrifuged at max speed for 30 mins, the isopropanol removed, and the pellet washed with 70% cold Ethanol. The Ethanol was removed and the pellet allowed to dry before being resuspended in 100 µL of TE buffer (10 mM Tris-HCL, 1 mM EDTA, pH 8.0 with 20 $\mu g \cdot mL^{-1}$ RNaseA (Invitrogen, UK)), or ddH_20. The DNA concentration was assessed by Nanodrop (Thermo Scientific).

2.3.2 PCR Genotyping

For the genotyping of transgenic plants, gDNA was extracted and PCR was performed using gene specific primers. A mastermix was prepared for a 20 µL final volume reaction consisting of; 0.5 µL gene specific primers(0.2uM), 0.5 µL dNTPs (10mM), 2 µL 10X KAPA Taq Buffer A (KAPA Biosystems), 0.1 µL KAPA Taq DNA Polymerase (5 units·µL^{-1}; KAPA Biosystems), H_2O (13.7 µL). 17 µL of mastermix was combined with 3 µL of template DNA. PCR amplicons were resolved by (1-2%) agarose (Sigma, St. Louis, MO) gel electrophoresis.

2.3.3 Colony PCR

A mastermix was prepared for a 20 µL final volume reaction consisting of; 0.5 µL insert/backbone specific primers (0.2 µM), 0.5 µL dNTPs (10 mM), 2 µL 10X KAPA Taq Buffer A (KAPA Biosystems), 0.1 µL KAPA Taq DNA Polymerase (5 units·µL^{-1}; KAPA Biosystems), H_2O (16.7 µL). Overnight colonies were picked resuspended in water and added directly to the PCR reaction. The PCR reaction was run using standard conditions and PCR amplicons were resolved on agarose (Sigma, St. Louis, MO) (1-2%) gel electrophoresis.

2.3.4 RNA extraction

Total sRNA was extracted using TRIzol® Reagent (Invitrogen, UK). Tissue was ground in liquid nitrogen and 1 mL TRIzol reagent added. The sample was vortexed and then incubated for 5 mins at room temperature before adding 0.2 vol. of chloroform and a further 5 mins incubation at room temperature. The mixture was centrifuged for 10 mins at 10,000g 4°C. The upper aqueous phase was removed and mixed with 1 µL of GlycoBlue™ Coprecipitant (15 mg·mL^{-1})(Ambion, UK) and precipitated overnight at -20°C with an equal volume of Isopropanol. After centrifuging the sample for 10 minutes 10,000g

4°C, the pellet was washed with 80% cold ethanol and resuspended in 10 µL of diethyl pyrocarbonate (DEPC)-treated water and stored at -80°C. RNA quantity was briefly checked by NanoDrop (Thermo Scientific) before quality was determined using and Agilent Bioanalyzer 2100 (Agilent, USA).

2.3.5 sRNA isolation

Total RNA (See2.3.4) was resuspended in 1 volume denaturing loading dye (NEB, UK) and run on a 15% polyacrylamide TBU gel (Novex, UK). The gel was stained with ethidium bromide and the gel pieces that contained sRNA (15-40 bp) were excised. The gel pieces were macerated and incubated with 300 mM NaCl overnight to elute the sRNA. The gel slurry was filtered by 0.45 µm cellulose acetate Corning Costar Spin-X centrifuge tube filters (Sigma-Aldrich, UK). Precipitation of RNA was carried out by combining with 0.1 vol 3M CH_3COONa (pH 5.2), and 2 volumes 100% isopropanol and incubate for 1 hr -80°C. sRNA was centrifuged for 10 mins at max speed at 4°C, washed using ice cold 70% ethanol and centrifuged again for 10 mins at 4°C The supernatant was discarded, the pellet air dried and dissolved in DEPC-treated water.

2.3.6 Degradome Anther RNA extraction

Anther RNA for degradome analysis was extracted using Direct-zol RNA miniprep kit (ZYMO). Anthers were ground (approx. 4500 rpm) individually using a Silamat S6 mixer for 3x 15 secs, centrifuged briefly (3000g) and homogenized with TRI reagent before carrying out the miniprep. DNase treatment was carried out on column. Eluted RNA quantity was briefly checked by NanoDrop before quality checking by Agilent Bioanalyzer 2100. RNA with RQN/RIN >7.5 were considered for library preparation.

2.3.7 cDNA synthesis

To remove DNA contamination, 10 μg of total RNA was combined with 10X TURBO DNase buffer and TURBO DNase (Invitrogen, UK)(2U) and incubated for 30 minutes at 37°C. DNase treatment was stopped by the addition of DNase Inactivation Reagent (Invitrogen, UK) incubated at room temperature for 5 minutes followed by centrifugation (10,000 g for 1.5 mins). The supernatant was transferred to a 1.5 ml RNase free tube.

1 μg of DNase treated total RNA was combined with 500 ng of oligo(dT)18 (Thermo Scientific), dNTP mix 10 mM and dH_2O to 13 μL and denatured at 65°C for 5 minutes before chilling on ice for 1 min. 5X First Strand Buffer, 100 mM DTT (Invitrogen, UK), RNase inhibitor and SuperScript III RT (200 $U \cdot \mu L^{-1}$) were added and incubated at 50°C for 1 hr. The reaction was inactivated at 70°C for 15 mins and RNA removed by incubating at 37°C for 20 mins with RNase H.

2.3.8 RT-PCR amplification

A mastermix was prepared for a 20 μL final volume reaction consisting of; 0.5 μL gene specific RT-PCR primers (0.2 μM), 0.5 μL dNTPs (10mM), 2 μL 10X KAPA Taq Buffer A (KAPA Biosystems), 0.1 μL KAPA Taq DNA Polymerase (5 $units \cdot \mu L^{-1}$; KAPA Biosystems), H_2O (13.7 μL). 17 μL of mastermix was combined with 2 μL of template cDNA. The PCR amplicons were resolved on a 2% agarose TAE gel and images taken on gel documentation system (SYNGENE).

2.3.9 Preparation of RNA probes for in situ hybridisation

RNA probes for 21-nt phasiRNA, miR2118 and scrambled RNA were provided by the Blake Meyers' laboratory. To generate RNA probes for heat-induced

phasiRNAs, ten tandem heat-induced 21-nt phasiRNAs were chemically synthesized, including flanking T3 and T7 polymerase binding sequences. RNA was generated by transcription with T3 or T7 RNA polymerase (Roche) for 2 hrs at 37°C, labelled by DIG-UTP (Roche). The reaction was treated with stop solution (0.1 Units·µL-1 DNase (Ambion, USA), 10 mM Tris-Cl, 10 mM $MgCl_2$, 50 mM NaCl, pH 7.5) for 30 mins at 37°C. The synthesized RNA probes were precipitated using a precipitation solution (0.8 M LiCl, 0.3 M NaOAc, 200 µg·mL-1 tRNA (Sigma, St. Louis, MO), 66.7% (v/v) ethanol, pH 5.2) overnight at -20°C, centrifuged for 10 mins at 16000g at 4°C, washed using 70% ethanol, centrifuged for 10 mins at 16000g at 4°C, and precipitate was air dried before resuspension in DEPC-treated water. The dissolved RNA probes were hydrolysed in carbonate buffer (40 mM $NaHCO_3$, 60 mM Na_2HCO_3, pH 10.2) for 60 mins at 60°C, precipitated in precipitation solution (10% (v/v) acetic acid, 90 mM NaOAc, 66.7% ethanol, pH 5.2) for 2 hours at -80°C, centrifuged for 10 mins at 16000g at 4°C, washed using 70% ethanol, centrifuged for 10 mins at 16000g at 4°C, discarded supernatant, air dried and dissolved in DEPC-treated distilled water.

2.4 General biochemical Methods

2.4.1 Luciferase assay in N.benthamiana leaves

A Luciferin solution (1 mM D-luciferin potassium salt, 0.1% Triton X-100) was sprayed onto *N. benthamiana* leaves and incubated in the dark for 10 minutes. Whole leaves were isolated and luciferase activity measured and quantified using a High Resolution Photon Counting System (HRPCS218; Photek)

2.4.2 Expressing recombinant HCPro protein

For generating recombinant WSMV (wheat streak mosaic virus) HCPro, a partial DNA fragment of *WSMVHCPro* was synthesized (Appendix)(IDT) and

the DNA fragment was cloned into the pGEM-T Easy vector (See 2.2.8) (Promega, WI, USA). To express a protein in *E. coli*, the synthetic *HCPro* coding sequence was sub-cloned into the pET29a expression vector and transformed into the *E. coli* strain BL21(DE3) (See 2.2.9). Positive transformants were grown at 28°C and induced by the addition of IPTG to the growth media at OD_{600} 0.6 and incubated for 12 hours. The cells were centrifuged for 10 mins at 16000g and the cell pellet was resuspended in extraction buffer (50mM $NaPO_4$, 300 nM NaCl, pH 8.0) followed by sonication (70% amplitude) to lyse the cells. The lysate was cleared by centrifuging for 10 mins at 16000g and soluble HC-Pro was His-tag purified using Immobilized metal affinity chromatography (IMAC; See 2.4.3).

2.4.3 IMAC protein purification

Clarified protein extract was passed through the nickel-nitroacetic acid (Ni-NTA) charged IMAC column equilibrated with His-binding buffer (50 mM Tris-HCl (pH8.0), 5mM Imidazole, 100mM NaCL, 0.1 mM EDTA). Column was washed with 25 ml of His-binding buffer, followed by 50ml of His-wash buffer (50 mM Tris-HCl (pH8.0), 20 mM Imidazole, 300 mM NaCl, 0.1mM EDTA) to remove weakly bound proteins. Finally, proteins were eluted with 15ml of His Elution buffer (50 mM Tris-HCl (pH8.0), 300 mM Imidazole, 50 mM NaCl, 0.1 mM EDTA) and 1.5 ml fractions collected. Each fraction was checked by SDS-PAGE with Coomassie stain to determine protein purity, and Bradford staining was used to measure protein concentration. Selected fractions were pooled for PD10 column clean up (GE Healthcare) and eluted in elution buffer (10 mM Tris-HCl pH8.0).

2.4.4 Antisera production

Polyclonal antisera were raised in rabbit against synthetic peptides for MAGO1 (VETEHQQGKRSIYRI) or MAGO2 (IIEGQKYPRKLSDTQV) (Eurogentec, liege, BE). Both peptide antisera were affinity purified with an immobilized peptide using a Sulpholink coupling gel system (Pierce, Rockford, IL). For generating an antiserum of WSMV (wheat streak mosaic virus) HCPro (Helper component-proteinase), polyclonal antiserum was raised in rabbit against purified HC-Pro protein (See 2.4.3) (Eurogentec, Liege, BE). HC-Pro antiserum was affinity purified with immobilized HC-Pro protein using a Sulpholink coupling gel system (Pierce, Rockford, IL).

2.4.5 MAGO small RNA immunoprecipitation

Immunoprecipitation was preformed using maize immature male inflorescence protein extract (Extraction buffer: 20 mM Tris-Cl pH 7.5, 300 mM NaCl, 5 mM $MgCl_2$, 5 mM DTT, 1% (v/v) protease inhibitor cocktail). Lysates were pre-cleared with 40 μl of protein-A agarose beads (Sigma-Aldrich, UK) and incubated with anti-MAGO antibodies (1:200) for 2 hours at 4°C. Following this, 40 μl of protein-A agarose beads were added to the sample and incubated for a further 2 hours. The beads were washed 4-5 times with extraction buffer supplemented with 0.5% NP-40 (Sigma, St. Louis, MO). For western blot analysis, beads were suspended directly in 1x SDS loading buffer and heated 70°C before electrophoresis. For isolation of small RNA, the bead slurry was digested with proteinase K (100 $\mu g \cdot mL^{-1}$) and incubated 1 hr at 37°C prior to RNA extraction using TRIZOL® Reagent (Invitrogen, UK) (See 2.3.4).

2.4.6 Plant Protein Isolation

Plant tissues was flash frozen in liquid nitrogen and ground into fine powder using a mortar and pestle. 1 g of ground tissue was homogenised in 2 mL of QB buffer (100 mM KPO_4 (pH 7.8), 1 mM EDTA, 1% Triton X-100, 10% Glycerol, 1 mM DTT, 1X Protease Inhibitor Cocktail (Roche)) and placed on ice. Extracts were centrifuged at max speed for 15 minutes at 4°C. the supernatant was transferred to a new tube and the centrifugation was repeated if necessary. Protein concentration was quantified using Quick Start Bradford Protein Assay (Bio-Rad, UK).

2.4.7 SDS-Page and Western blot

Protein extracts were mixed with 6X SDS Sample Buffer (0.375 M Tris pH 6.8, 12% SDS, 60% glycerol, 0.6 M DTT, 0.06% bromophenol blue) and heated at 95°C for 10 minutes. 5 μg of total protein extract was loaded into a 12% polyacrylamide SDS-PAGE gel In and electrophoresis chamber filled with running buffer (25 mM Tris-Cl, 190 mM Glycine, 0.1% SDS, pH 8.3) (Bio-Rad, UK). The Gel was run until the dye front reached the bottom of the gel. The gel was removed and equilibrated in transfer buffer (48 mM Tris-Cl, 39 mM Glycine, 20% Methanol, 0.04% SDS) and transferred to an activated Polyvinylidene difluoride PVDF membrane (Thermo Scientific, UK) using the semidry transfer method (25 volts for 30 minutes) (Bio-Rad, UK). The blot was removed from the semidry transfer cassette and briefly washed with PBS before blocking with Blocking solution (5% skimmed milk/PBS-tween 0.1%) on a shaker for 1 hour at room temperature. The blot was washed 3 times 15 minutes with PBS-T before adding primary antibody solution (primary antibody diluted in 1% BSA/PBS-T) and incubating overnight at 4°C. The blot was washed 3 times 15 minutes with PBS-T and incubated in secondary antibody solution (horseradish peroxidase (HRP) conjugated

secondary antibody diluted in 1% BSA in PBS-T) for 1 hr at room temperature. The blot was washed 3 times for 15 mins each and stored in 1x PBS until Enhanced Chemoluminescence (ECL) detection (GE). Excess liquid was removed and the blot incubated for 1 min in equal volumes of the ECL reagent A and B after which the blot was drained and covered in saranwrap for detection. Protein bands were detected using an ImageQuant gel documentation instrument (GE Healthcare).

2.4.8 Anther *HcPRO* Induction by Dexamethasone

Dexamethasone (DEX) inducible *HcPRO* maize were grown to adult stage 13 leaf stage. At the appropriate stage the whorl was cut open to reveal the developing tassel. The floret tips were cut using fine scissors and the floret cavity filled with DEX solution (50 µM DEX, 0.1% Silwet-77 (De Sangosse, Cambridge, UK)). Plants were incubated for 3 days under normal growth conditions before anthers were isolated for biochemical and molecular analysis. Additionally, plants were grown to flowering to assess pollen viability (Figure 2.2).

2.5 Histological methods

2.5.1 Alexander's staining of pollen

Alexander's staining was carried out as previously described (Peterson, Slovin et al. 2010). Flower buds were collected and the anthers extracted before being fixed in Carnoy's fixative (60% ethanol, 30% chloroform, 10% acetic acid) for a minimum of 2 hours. Fixed anthers were blotted dry and placed on a microscope slide along with 2-4 drops of Alexander's stain (10

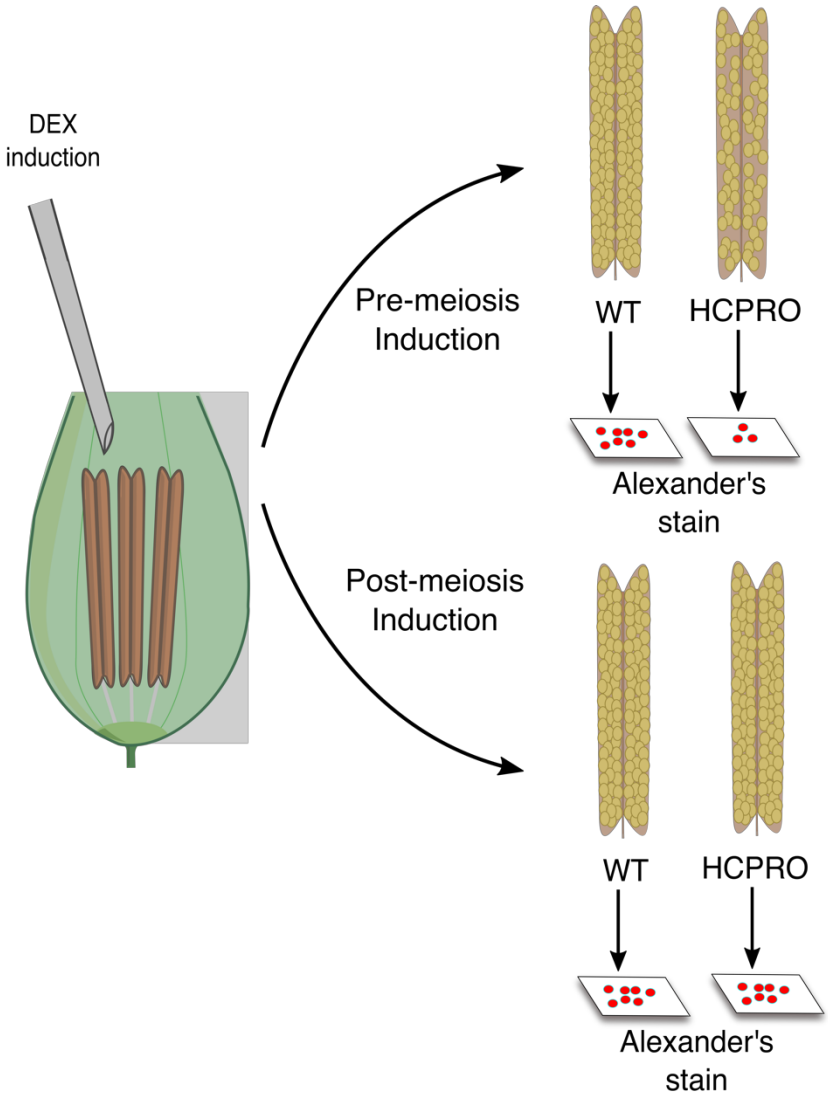

Figure 2.2: Dexamethasone induction of *ind*HcPro in maize anthers. Suitably staged maize were dissected to reveal the developing tassel. Florets were cut at the tip and DEX solution was infiltrated into the floret cavity. The plants were allowed to recover and mature anther viability was assessed by Alexanders stain.

mL 95% ethanol, 1 mL Malachite green (1% solution in 95% ethanol), 50 mL distilled water, 25 mL glycerol, 5 mL acid fuchsin (1% solution in water), 0.5 mL orange G (1% solution in water), 4 mL glacial acetic acid and distilled water (4.5 mL to a total of 100 mL). Anthers were dissected to release the pollen into the stain solution and plant debris were removed. Slides were slowly heated until near boiling to allow penetration of the dye into the pollen. A cover slip was placed over the sample and sealed with paraffin before imaging.

2.5.2 Acetocarmine staining of maize meiocytes

Acetocarmine staining was performed as described (Dukowic-Schulze, Sundararajan et al. 2014). Maize plants at approximately 6-8 weeks old were tested for meiotic stage. An incision was made midway up the stalk to expose the developing male inflorescence. Flower buds were extracted, opened and the anthers inside were fixed in Farmer's fixative (3:1 ethanol : acetic acid) for at least 10 mins. Fixed anthers were dissected on a microscope slide and stained with acetocarmine solution (0.5% w/v carmine dissolved in 45% (v/v) acetic acid). The sample slide was heated at 65°C for 10 mins while mixing with an iron oxide rod. the anther was then squashed with a cover slip to release the stained meiocytes for imaging.

2.5.3 Anther Immunolocalisation

For anther immunolocalisation, male florets were submerged in 4% paraformaldehyde (PFA) and vacuum infiltrated three times for 10 minutes. The fixative was then replaced and the sample incubated over night at 4°C. After fixation, the samples were washed using phosphate buffered saline (PBS; 10 mM sodium phosphate and 150 mM NaCl, pH 7.4), dehydrated via a graded ethanol series and embedded in Paraplast Plus (Sigma, St. Louis,

MO). Sections were cut at 10 micrometre and mounted on Superfrost Plus slides (Thermo Scientific, UK). The mounted samples were deparaffinised using Histoclear (National Diagnostics, Hull, UK), rehydrated through an ethanol series and blocked in 0.1% bovine serum albumin (BSA) in PBS for 30 mins at room temperature. The blocked slides were washed using 0.1% BSA in PBS for 15 mins at room temperature and incubated overnight at 4˚C with purified anti-MAGO1 (diluted 1:200), anti-MAGO2 (diluted 1:200) or anti-HC-Pro (diluted 1:100) antibodies in a humid chamber. The immunodetections were performed using goat anti-rabbit alkaline phosphatase-conjugated secondary antibody (Sigma, St. Louis, USA; diluted 1:100) and nitroblue tetrazolium/5-bromo-4-chloro-3-indolylphosphate (NBT/BCIP; Sigma, Pooler, UK) was used as detection substrate. The stained slides by NBT/BCIP was mounted in Entellan (Merck, UK) and cover slipped. For immunofluorescence, goat anti-rabbit Alexa Fluor 680-conjugated secondary antibody (Sigma, St. Louis, USA; diluted 1:100) was incubated for 1 hour at room temperature and the slides were mounted in VECTASHIELD® mounting medium (Vector Laboratories, CA, USA).

2.5.4 Meiocyte immunolocalisation

Meiocyte immunolocalisation was carried out as previously reported (Higgins 2013). Ten staged anthers were transferred to 2 µL of extraction buffer (6 mM citrate buffer) to release mieocytes. Meiocytes were transferred to 6 µL digestion media (0.375 g sucrose and 0.25 g polyvinylpyrrolidone (MW 40,000) in 25 mL distilled water) and incubated for 2 minutes at 37°C. 2 µL of the cell suspension was mixed with 10 µL of 0.1% Lipsol® on a treated Superfrost Plus slide (Thermo Scientific, UK). 10 µL of fixative (4% PFA, pH 8.0) was added and the slide dried.

Slides were washed twice for 5 minutes in wash buffer (PBS with 0.1% Triton X-100) and blocked with 100 µL blocking buffer (1% BSA in PBS) for 45 minutes. For immunolocalisation, anti-MAGO1, anti-MAGO2, anti-ASY1 or anti-ZYP1 were used as primary antibodies. Anti-ASY1 and anti-ZYP1 antisera were used as previously reported (Armstrong et al. 2002; Higgins et al. 2005). 100 µL of primary antibody diluted in blocking solution (0.1% Triton X-100 and 1% BSA in PBS) was applied to the slide and incubated at 4°C for 30 mins. Slides were washed twice for 5 mins in wash buffer before applying secondary antibody diluted in blocking solution and incubating for 90 minutes at room temperature. For immunofluorescence, Alexa Fluor 594-conjugated (Sigma, UK), Alexa Fluor 680-conjugated (Abcam, UK) and FITC-conjugated (Sigma, UK) secondary antibodies were used. Slides were washed twice for 5 mins and mounted with DAPI (10 $\mu g \cdot mL^{-1}$) in VECTASHIELD® mounting medium (Vector Laboratories, CA, USA).

2.5.5 RNA in situ hybridization in developing anthers

To avoid contaminations of RNase, glassware was baked at 180°C for 8 hours, plasticware was treated by 0.1 M NaOH (Sigma, St. Louis, MO) overnight at 37°C and solutions were treated by 0.1% diethyl pyrocarbonate (DEPC, Sigma, St. Louis, MO). For RNA in situ hybridization in developing anthers, male florets were submerged in 4% paraformaldehyde (PFA, Agar Scientific, Essex, UK) and vacuum infiltrated three times 10 minutes. The fixative was then replaced and the sample incubated over night at 4°C. After fixation, the samples were washed using phosphate buffered saline (PBS; 10 mM sodium phosphate and 150 mM NaCl, pH 7.4) with 0.1% DEPC, dehydrated via a graded ethanol series and embedded in Paraplast Plus (Sigma, St. Louis, MO). Sections were cut at 10 µm and mounted on Superfrost Plus slides (Thermo Scientific, UK). The mounted samples were

deparaffinized using Histoclear (National Diagnostics, Hull, UK), rehydrated through an ethanol series, treated by Pronase (Merck, Darmstadt, Germany) for 10 mins at 37°C, fixed by 4% PFA for 10 mins at room temperature, acetylated by acetic anhydride (Sigma, St. Louis, MO) in 100 mM triethanolamine (Sigma, St. Louis, MO) for 10 mins at room temperature and re-dehydrated by an ethanol series. To prepare RNA probe hybridization solution, hybridization buffer (10 mM Tris-Cl, 300 mM NaCl, 10 mM $NaPO_4$, 5 mM EDTA, 1.25 $mg \cdot mL^{-1}$ tRNA (Sigma, St. Louis, MO), 1.25x Denhardt's (Sigma, St. Louis, MO), 12.5% dextran sulphate (AP Biotech), 50% deionized formamide (Sigma, St. Louis, MO), pH 6.8) was mixed by vortexing, spun down and left at room temperature. RNA probe solution was prepared with mixing RNA probes and deionized formamide in 1:1 ratio the solution was heated for 2 mins at 80°C, spun down and kept on ice. The probe solution was mixed with the hybridization buffer in a 4:1 buffer : probe ratio, vortexed, spun down and left at room temperature. To prevent RNA probes from adhering to the coverslip, they were first treated by Sigmacote (Sigma, St. Louis, MO) for 10 secs at room temperature, washed with absolute ethanol and dried in fume hood before starting hybridization procedures. 50-100 µL of RNA probe hybridization solution was added to the slide, covered with a Sigmacote-treated coverslip and incubated in humid chamber overnight at 45°C. The slides were dipped in 2 x SSC buffer (150 mM NaCl, 15 mM NaOAc), agitated gently until the coverslips were fell off, moved to a new 2 x SSC buffer, incubated for 30 mins at 45°C, moved once more to a new 2 x SSC buffer, incubated for 90 mins at 45°C, washed twice using NTE buffer (10 mM Tric-Cl, 500 mM NaCl, 1 mM EDTA, pH 7.5) for 5 mins at 37°C, treated by RNase buffer (20 $\mu g \cdot mL^{-1}$ RNase A (Sigma, St. Louis, MO) in NTE buffer) for 30 mins at 37°C, washed three times using NTE buffer for 5 mins at 37°C, incubated in 0.5 x SSC buffer for 1 hr at 45°C and washed

using PBS for 5 mins at room temperature. The washed slides were incubated for 5 mins in DIG Buffer I (100 mM Tris-Cl, 150 mM NaCl, pH 7.5) at room temperature, blocked for 30 mins in DIG Buffer II (0.5% (w/v) blocking reagent (Boehringer) in DIG buffer I) at room temperature, transferred to DIG Buffer III (0.1% (w/v) BSA, 0.3% (v/v) Triton X-100 (Sigma, St. Louis, MO) in DIG Buffer I), incubated for 30 mins in DIG Buffer III at room temperature, transferred to DIG Buffer IV (1:3000 anti-digoxigenin-AP (Roche) in DIG Buffer III), incubated for 90 mins in DIG Buffer IV at room temperature, washed four times using DIG Buffer III for 20 mins at room temperature, washed using DIG Buffer I for 5 mins at room temperature, washed using DIG Buffer V (100 mM Tris-Cl, 100 mM NaCl, 50 mM $MgCl_2$, pH 9.5) for 5 mins at room temperature and incubated for 6 to 36 hours in Buffer VI (75 $mg \cdot mL^{-1}$ nitroblue tetrazolium (NBT, Sigma, Poole, UK), 50 $mg \cdot mL^{-1}$ 5-bromo-4-chloro-3-indolylphosphate (BCIP, Sigma, Poole, UK), 24 $mg \cdot mL^{-1}$ Levamisole (Sigma, Pooler, UK) in DIG Buffer V) under dark conditions at room temperature, incubated in TE buffer (10 mM Tris-Cl, 1 mM EDTA, pH 7.5) for 10 mins at room temperature, washed for 2 mins in distilled water, dehydrated through an ethanol series, dried completely, mounted in Entellan (Merck, UK) and covered by coverslip.

2.5.6 Histochemical staining of GUS expression

Plant material was were submerged in GUS staining solution (50 mM sodium phosphate, 1 mM potassium ferricyanide, 1 mM potassium ferrocyanide, 0.1% Triton X-100, 10 mM EDTA, 1.0 $mg \cdot mL^{-1}$ 5-Bromo-4-chloro-3-indolyl-β-d-glucuronic acid, 1% DMSO) and incubated at 37°C overnight. To remove chlorophyll, samples were incubated at 65°C with 70% and 100% Ethanol. GUS staining was observed using a Leica MZ FLIII stereomicroscope and images captured using a nikon digital sight ds-fi2 camera.

2.5.7 tdTomato detection in anther sections

Tissue was isolated and fixed in SR2200 solution (4% PFA in PBS (pH7.4), 0.1% SR2200 (Renaissance Chemicals)) and vacuum infiltrated, three times 5 minutes. Samples were incubated overnight 4°C. Samples were washed with PBS and submerged in Clearsee solution (Xylotol [10% (w/v)], Sodium deoxycholate [15% (w/v)], Urea [25% (w/v)])(Kurihara, Mizuta et al. 2015). Samples were again vacuum infiltrated 3 times 5 minutes and incubated for at least 12 hours or until tissue was cleared. Finally samples can be washed and stored in PBS. Cleared tissue was embedded in 4% agarose, were trimmed and mounted onto vibratome blocks. 150 μm sections were cut by Lancer Vibratome Series 1000 Sectioning System and mounted on a slide with water and coverslips attached.

2.5.8 Toluene Blue staining of anther sections

Maize anther sections were stained with a 0.05% solution of Toluidine Blue (Sigma) for 1 minute. Stain was removed and the slide was washed for 1 minute with dH_2O for a further 1 minutes. Slides were then air dried and mounted with Entellan (Merck, UK).

2.5.9 Confocal microscopy

Confocal microscopy was carried out using Carl Zeiss LSM 710 confocal laser scanning microscope with fluorescence detected using the following excitation and emission parameters with pinhole set to 1AU. DAPI (4',6-diamidino-2-phenylindole) and SR2200 was excited by the 405nm line and detected between 410-476nm, FITC (Fluorescein isothiocyanate) was excited by the 488nm line and detected between 515-545, Alexafluor594 was excited by the 561/594nm lines and detected between 590-630nm,

Alexafluor680 was excited by the 633nm line and detected between 640-680nm, tdTomato was excited by the 532nm line and detected between 574-606nm)

2.6 Illumina sequencing methods

2.6.1 RNA library preparation

RNA sequencing libraries were prepared from total maize anther RNA extrancts (See 2.3.4). All mRNA libraries were prepared with a TruSeq Stranded mRNA Library Preperation kit (Illumina, UK). Sequencing was performed on an Illumina Nextseq550 system at the University of Warwick Genomics Facility.

2.6.2 sRNA library preparation

All small RNA libraries were prepared using the TruSeq Small RNA Sample Preparation Kit using immunopurified (See 2.4.5) or total isolated sRNA (2.3.5)(Illumina, UK). Sequencing was performed on an Illumina Miseq instrument at the University of Warwick and an Illumina Hiseq2500 at the University of Delaware (DBI).

2.7 Computational analysis

2.7.1 Phylogenetic analysis

Maize AGO protein sequences along with AGO5 sequences from barley (*Hordeum vulgare*), sorghum (*Sorghum bicolor*), wheat (*Triticum aestivum*), foxtail millet (*Setaria italica*), rice (*Oryza sativa*), purple false brome (*Brachypodium distachyon*), giant cane (*Arundo donax*) and Arabidopsis (*Arabidopsis thaliana*) were aligned using MEGA7 and a phylogenetic tree constructed using the neighbor-joining method, with bootstrapping to

providing confidence to each node (Kumar, Stecher et al. 2016). The tree was configured using FigTree (Rambaut 2018)

2.7.2 Argonaute conserved domain analysis

Protein sequences were obtained for AtAGO1, AtAGO5, OsMEL1, ZmMAGO1 and ZmMAGO2 and analysed using the conserved domain database (NCBI). Schematic diagrams of each protein along with protein domain structures and essential catalytic residues were compiled using DOG (Domain Graph, version 2.0) (Ren, Wen et al. 2009)

2.7.3 RNA Sequencing analysis

Reads from mRNA sequencing were trimmed with Trimmomatic (v0.36) to remove adapter content and low quality reads (Bolger, Lohse et al. 2014). Reads were aligned to the B73 version 4 reference genome (Jiao, Peluso et al. 2017) using the TopHat alignment tool (Trapnell, Pachter et al. 2009). Read mapping was conducted with TEtranscripts (Jin, Tam et al. 2015) to include TEs in the differential expression analysis. Differential expression analysis was performed using DESeq2 (FDR adjusted cutoff $p < 0.01$, fold change cut-off of log2(4)) (Love, Huber et al. 2014).

2.7.4 sRNA sequencing analysis pipeline

Reads from sRNA sequencing were trimmed with cutadapt (-n 3 -q 24,24 -m 18 -M 35)(Martin 2011) to remove adapter content and low quality reads. Reads were aligned to the B73 version 4 reference genome (Jiao, Peluso et al. 2017) using the Shortstack alignment tool to generate sRNA clusters (--nohp) (Johnson, Yeoh et al. 2016). Reads were also mapped to the known PHAS loci (Zhai, Zhang et al. 2015) in maize using featurecounts (-M -O -T 4 -M)(Liao, Smyth et al. 2013) and differential expression analysis of sRNA

clusters and PHAS loci was performed using DESeq2 (FDR adjusted cutoff p < 0.01)(Love, Huber et al. 2014). Target sRNA prediction was performed using psRNAtarget with Schema V2 (Dai, Zhuang et al. 2018). Gene Ontology enrichment analysis of sRNA gene targets was performed with AgriGO (Tian, Liu et al. 2017).

2.8 Statistical analysis

2.8.1 Welch's unequal variances t-test

Welch's unequal variances t-test was used to test the hypothesis that two populations have equal means when unequal variance is assumed. The test was carried out using the statistical software package - R using the following equation:

$$t = \frac{\bar{X}_1 - \bar{X}_2}{\sqrt{\frac{s_1^2}{N_1} + \frac{s_2^2}{N_2}}}$$

Where $\bar{X}_i$ = sample mean, s_i^2 = sample varience, and N_i = sample size.

2.8.2 ANOVA multiple comparisons test

One- way Analysis of variance (ANOVA) with Tukey's honestly significant difference (HSD) post hoc test using the statistical software package - R to compare the means of two or more samples.

2.8.3 Chi-squared goodness of fit test

The Chi-squared goodness of fit test was used to compare the observed distribution of predicted transposon target sites with the expected probability distribution. The test was carried out in Microsoft Excel using the following formula:

$$x^2 = \sum \frac{(Observed - Expected)^2}{Expected}$$

3.0 Functional characterisation of meiosis-associated Argonautes MAGO in maize

3.0 Functional characterisation of meiosis-associated Argonautes MAGO in maize

3.1 Introduction

Plants and animals have developed a plethora of mechanisms to control and regulate gene expression, from individual cells and throughout development. One of such mechanisms includes the formation of small regulatory RNAs (sRNAs), which when bound to an Argonaute protein, part of the RNA induced silencing complex (RISC), can regulate gene expression. Small RNAs guide RISC to their mRNA targets through sequence dependent complementarity with the target transcript. Once RISC has found its target, expression changes are brought about by their ability to slice target mRNA transcripts, inhibit translation, destabilise RNA or by bringing DNA methylation or histone modifications to a precise region of the genome (Zilberman, Cao et al. 2003, Vazquez, Vaucheret et al. 2004, Yang, Wu et al. 2012, Li, Liu et al. 2013).

Argonautes are the major effector components of many epigenetic pathways, they are essential and thus highly conserved in both plants and animals (Hutvagner and Simard 2008, Vaucheret 2008). Generally, Argonautes can broadly be split into three groups based on their preference for different sRNAs and their phylogenetic relationships. These are: the Argonaute-like proteins which bind to miRNAs and siRNAs, the PIWI-like proteins which bind to the piRNAs and the *C. elegans* group 3 proteins (only been described in worms) which bind to secondary siRNAs (Baumberger and Baulcombe 2005, Yigit, Batista et al. 2006). As a consequence of multiple duplication and divergence events, the number of Argonautes between organisms varies considerably, in plants the PIWI group has been lost entirely (Hutvagner and Simard 2008). Presumably to compensate, the number of Argonaute-like genes within plant lineages has duplicated and diversified substantially with: 10 genes identified in *Arabidopsis*, 17 in maize

and 19 in rice (Morel, Godon et al. 2002, Nonomura, Morohoshi et al. 2007, Kapoor, Arora et al. 2008, Zhai, Sun et al. 2014).

3.1.1 Protein domain structure and function of Argonautes

All Argonautes harbour a variable N-terminal domain, in addition to three conserved domains: a C-terminal PAZ (Piwi/Argonaute/Zwille) , PIWI (P ELEMENT-INDUCED WIMPY TESTIS) and MID (middle) domain (Hutvagner and Simard 2008). The PAZ domain can also be found in DICER-like proteins, and biochemical analysis suggests that this domain is responsible for single stranded RNA (ssRNA) binding due to its resemblance to OB-fold (oligonucleotide/oligosaccharide-binding) proteins known to bind ssRNA and for its affinity for 3' overhang sRNA in vitro (Song, Liu et al. 2003, Lingel, Simon et al. 2004, Ma, Ye et al. 2004). The MID domain binds to the sRNA 5' residue, a process dependent on the 5' phosphorylation of miRNAs and siRNAs (Nykänen, Haley et al. 2001)(Fig 3.1). The PIWI domain RNase H like fold was discovered from solving the crystal structure and its target mRNA nuclease activity is absolutely dependent on the Asp-Asp-[Glu/Asp] catalytic residues in the PIWI like group or the Asp-Asp-[Asp/Glu/His/Lys] catalytic residues in the Argonaute-like group (Song, Smith et al. 2004, Nowotny, Gaidamakov et al. 2005, Rivas, Tolia et al. 2005, Yuan, Pei et al. 2005, Tolia and Joshua-Tor 2007). Presence of these catalytic residues does not however guarantee slicer activity as there are examples of Argonautes which possess these residues but have not been found to have nuclease activity (Meister, Landthaler et al. 2004). Additionally, many new argonatute functions are being discovered such as DNA repair and splicing (Ameyar-Zazoua, Rachez et al. 2012, Wei, Ba et al. 2012).

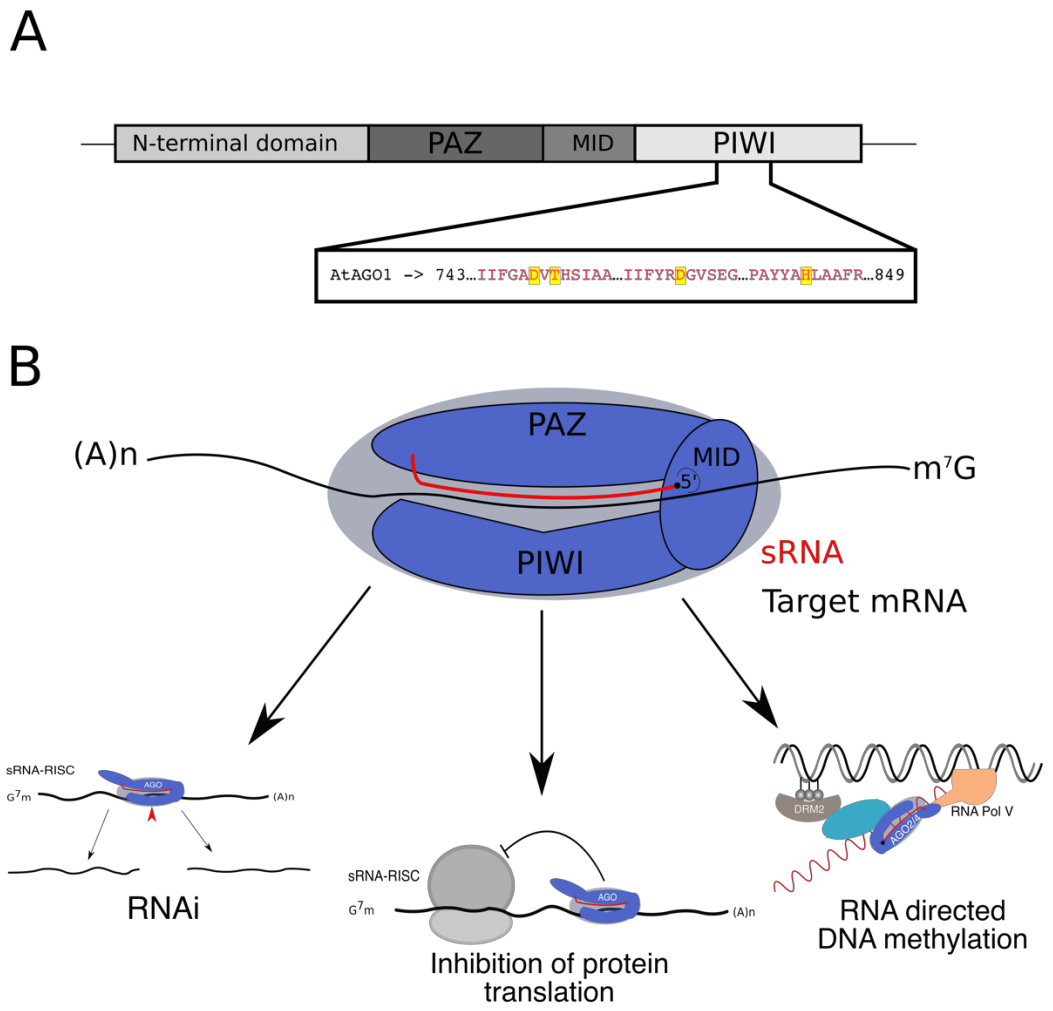

Figure 3.1: Structural conservation of Argonaute proteins. (A) Domain architecture of AtAGO1 with variable N-terminal domain, conserved sRNA binding PAZ (Piwi/Argonaute/Zwille), MID (middle) and PIWI (P ELEMENT-INDUCED WIMPY TESTIS) RNA cleavage domains with conserved catalytic residues necessary for RNase activity (Highlighted yellow). (B) Schematic of sRNA targeted mRNA silencing by argonaute proteins. Argonautes can regulate expression at the transcriptional (Right), post-transcriptional (left) and translational (middle) level.

3.1.2 Clade I Argonautes in plants

In all flowering plants, the Argonaute group can be sub categorised into three clades: clade I (AGO1/5/10), clade II (AGO2/3/7), and clade III (AGO4/6/8/9)(Vaucheret 2008, Zhang, Xia et al. 2015). Additionally, rice and maize have acquired AGO18, which forms a subclade with clade I. Clade I group AGO1/5/10 has expanded greatly in the grasses, with many of the *Arabidopsis* Argonaute homologs duplicated at least once (Zhang, Xia et al. 2015). AtAGO1 ,the founding Argonaute member, preferentially binds to 21-nt miRNAs with a preference for 5'uridine (5'U) and regulates genes and development through mRNA target slicing and translational inhibition (Bohmert, Camus et al. 1998, Mi, Cai et al. 2008, Yang, Wu et al. 2012, Li, Liu et al. 2013). AGO1 has duplicated in the grasses with rice and maize having 4 homologues each ZmAGOa/b/c/d and OsAGO1a/b/c/d (Zhang, Xia et al. 2015). The miRNA loading of OsAGO1a/b/c has been found to be non-discriminant in rice in all but a subset of miRNAs. This subset of sRNAs is specifically incorporated or excluded from specific Argonautes and these loaded Argonautes mostly target transcription factors affecting developmental and physiological processes (Wu, Zhang et al. 2009). This demonstrates the redundancy present in these Argonaute proteins though they have already begun to develop specialised functions since this family duplicated.

AtAGO5 binds siRNAs with preference for 5' cytosine (5'C) and it is specifically expressed in the megaspore mother cell and surrounding cells (Mi, Cai et al. 2008). However, functional studies in the *AtAGO5 null* plants do not show developmental phenotypes, with only a mild defect in the initiation of megagametogenesis identified in a semi-dominant mutant recovered from T-DNA mutagenesis (Tucker, Okada et al. 2012). *MEIOSIS ARRESTED AT LEPTOTENE1, OsAGO5c* (*MEL1),* one of five AGO5 homologues

in rice display early meiotic arrest in addition to various pollen defects including multinucleated pollen, vacuolated pollen mother cells and irregular pollen size (Nonomura, Morohoshi et al. 2007). MEL1 has been shown to bind preferentially to 21-nt siRNAs with preference for 5'C in addition to the 21-nt phased small RNAs (phasiRNAs). However, the mechanism by which MEL1 affects meiosis and the role of the associated phasiRNAs is not yet clear.

Similarly AtAGO10 is phylogenetically most similar to AtAGO1 and regulates shoot apical meristem (SAM) development. Despite being highly similar to AGO1, AGO10 almost completely and exclusively sequesters miR165/166 from AGO1 mediated RNA silencing during embryogenesis. The miR165/166-RISC typically targets AGO1 leading to the silencing of homeodomain-leucine Zip III (HD-ZIP III) transcription factors which regulate leaf polarity, vasculature development, meristem initiation and embryogenesis (Otsuga, DeGuzman et al. 2001, Emery, Floyd et al. 2003, Prigge, Otsuga et al. 2005).

The AGO18 subclade is only found in grasses and is most similar to clade I. *AGO18* expression is usually undetectable but is induced upon viral infection and overexpression lines confer broad range antiviral response with mutants becoming more sensitive in rice. AGO18 does not directly suppress viral infection and does not bind to virus-derived siRNAs (vsiRNAs), instead it is thought to compete with AGO1 (Wu, Yang et al. 2015). Interestingly, AGO18b in maize has been found highly enriched in tapetum and germ cells in meiotic anthers. Additionally, expression is highly correlated both temporally and specially with the accumulation of the 24-nt phasiRNAs, yet the role of AGO18 in reproductive development is currently unknown (Zhai, Sun et al. 2014).

3.1.3 Clade II Argonautes in plants

The clade II group includes AGO2/3/7. AtAGO2 binds primarily to 21-nt miRNA preferentially with 5' adenosine (s'A) and it is thought to be involved in plant immunity (Mi, Cai et al. 2008, Takeda, Iwasaki et al. 2008, Harvey, Lewsey et al. 2011). Expression of AGO2 is induced upon infection with *Pseudomonas syringae* pv. tomato (Pst) DC3000. AGO2 binds strongly to miR393b∗ promoting effective secretion of antimicrobial pathogenesis related proteins (Zhang, Zhao et al. 2011). Consequently AGO2 mutants are hypersensitive to infection by RNA viruses especially in *ago1ago2* (Harvey, Lewsey et al. 2011, Wang, Jovel et al. 2011).

AtAGO3 is highly similar to AtAGO2 (70% identity) and is located only 3kb apart leading to speculation they may be functionally redundant (Vaucheret 2008, Zhang, Liu et al. 2016). However, it is now known that they have already diverged quite significantly with AtAGO3 unable to complement AtAGO2 null mutants. Additionally AtAGO3 binds predominantly 24-nt siRNAs with preference for (5'A) with its sRNA selection resembling AGO4 over AGO2 and is even capable of complementing the DNA methylation defect in AGO4 mutants (Zhang, Liu et al. 2016). Rice and maize do not have an AGO3 homolog which possibly highlights to its recent acquisition in *Arabidopsis.* However, they do have two AGO2 homologues *AGO2a and AGO2b*. The final member of clade II is AGO7, which is known to be highly specific for miR340, and it is necessary for the initiation of TAS3 derived tasiRNAs (Adenot, Elmayan et al. 2006, Montgomery, Yoo et al. 2008, Marin, Jouannet et al. 2010). The TAS3 tasiRNAs go on to target the AUXIN RESPONSE FACTORs ARF3 and ARF4 which regulate developmental timing and patterning in plants (Fahlgren, Montgomery et al. 2006).

3.1.4 Clade III Argonautes in plants

The Clade III group includes AGO4/6/8/9. With the exception of AtAGO8, which is considered to be a pseudogene duplicated from AtAGO9, all members of this clade are known to direct DNA methylation through the RNA-directed DNA methylation (RdDM) pathway (Mallory and Vaucheret 2010). These Argonautes bind predominantly to 24-nt sRNAs with 5'A but discriminate between siRNA originating from different loci (Havecker, Wallbridge et al. 2010). The different loading preferences has been attributed to the differential expression of these Argonautes and their component sRNAs (Havecker, Wallbridge et al. 2010). Once associated, these Argonautes bind nascent polV transcripts and recruit DNA methylation machinery (Pikaard, Haag et al. 2008, Matzke, Kanno et al. 2009).

AtAGO9 is a reproductive Argonaute expressed in somatic cells and controls female gamete formation by restricting the specification of the precursor gametophyte. AtAGO9 preferentially binds to 24-nt transposable element (TE) -derived siRNAs to silence TEs in the gametes (Olmedo-Monfil, Durán-Figueroa et al. 2010). The process of TE-derived sRNA silencing of TEs in the germline is remarkable similar to the piRNAs in animals, which are crucial for zebrafish and Drosophila germline development. (Carmell, Girard et al. 2007, Chen, Pane et al. 2007, Houwing, Kamminga et al. 2007).

The maize *AGO9* homologue *ZmAGO9* (formerly *ZmAGO104*) is also expressed in the somatic cells surrounding the female gametophyte, however in this case it acts to repress somatic fate in germ cells (Singh, Goel et al. 2011).

Meiosis in *Arabidopsis* is associated with the expression of many Argonautes from various clades (Olmedo-Monfil, Durán-Figueroa et al. 2010, Tucker, Okada et al. 2012). During meiosis and reproductive development, extensive epigenetic reprogramming takes place. It is now accepted that Argonautes

have multiple functions that cannot be defined through homology alone, though, the molecular function of Argonautes can be inferred from a collection of biochemical and genetic analyses.

3.1.5 Subcellular localisation of Argonautes

The subcellular localisation of Argonautes is an important characteristic to consider when inferring their function. While it does not offer conclusive evidence, it may suggest which RNA silencing pathways the Argonaute of interest primarily belongs. AGO4 for example, is a well-documented component of the RdDM pathway which occurs in the nucleus (Zilberman, Cao et al. 2003). AGO4 accumulates in the nucleus and it is found associated with mRNA processing in Cajal foci in the nucleus (Li, Pontes et al. 2006, Li, Henderson et al. 2008). AGO1 in contrast, is primarily known for its role in RNAi. As expected, studies have indeed shown AGO1 binding to membrane bound polysomes on the cytoplasmic side of the ER in an RNA dependent manner (Li, Le et al. 2016). AGO1 localisation is not exclusive to the nucleus and in *Arabidopsis* it is known to shuttle between the cellular compartments. Argonaute loading of miRNA appears to take place in the nucleus and is only then exported to the cytosol as a complex (Bologna, Iselin et al. 2018). Additionally, in *Arabidopsis*, AGO1 is found to bind to chromatin under stress conditions leading to gene activation (Liu, Xin et al. 2018). While subcellular localisation of Argonautes may provide clues about their function, this localisation is clearly dynamic and responds to different external stimuli and developmental stages, with particular emphasis on reproductive development (Kapoor, Arora et al. 2008, Zhang, Xia et al. 2015, Liu, Xin et al. 2018).

3.1.6 Chapter Aim

It is clear from established evidence that determining the function of Argonaute proteins requires complex experimental evidence. While plant Argonautes share highly conserved functional domains, they have expanded and specialised to take on many diverse roles. It is becoming clear that these roles are often dynamic, responding to developmental or environmental cues. The aim of this chapter is to determine the function of meiosis-associated Argonautes in maize by conducting genetic, biochemical and phylogenetic analyses.

3.2 Results

3.2.1 Meiosis-Associated Argonautes (MAGO1 and MAGO2) in maize

Anther development and male microgametogenesis are developmental events, rich in epigenetic reprogramming. These timepoints are also associated with fluctuations in both the sRNA repertoire and elevated expression of associated Argonaute proteins (Nonomura, Morohoshi et al. 2007, Creasey, Zhai et al. 2014, Fei, Yang et al. 2016). These reprogramming events are not limited to plants and are also well documented in animals (Aravin, Naumova et al. 2001, Conine, Sun et al. 2018). Of particular interest are the 21-nt and 24-nt phased small interfering RNAs(phasiRNAs); a class of secondary small RNAs associated with the male germline in plants, but with as of yet unknown function.

To understand the potential function of the small RNA accumulating during meiosis, we identified two maize meiosis-associated Argonaute proteins *MAGO1* (Zm0001d007786) and *MAGO2* (Zm0001d035747), that are predicted to be expressed in developing inflorescences at the time of meiosis (Walley, Sartor et al. 2016). These Argonautes are highly expressed in immature tassels and meiotic tassels (with 13 and 18 emerged leaves respectively) (Figure 3.2) (Stelpflug, Sekhon et al. 2016, Walley, Sartor et al. 2016). Both genes are expressed at various stages of female reproductive development, albeit at much lower levels than in male reproductive development.

Few meiosis associated proteins have been identified in plants. Understanding the conservation of these meiosis-associated Argonautes between different species and their comparison with other Argonautes within and between different clades may be informative. Using phylogenetic

3.0 Functional characterisation of meiosis-associated Argonautes MAGO in maize

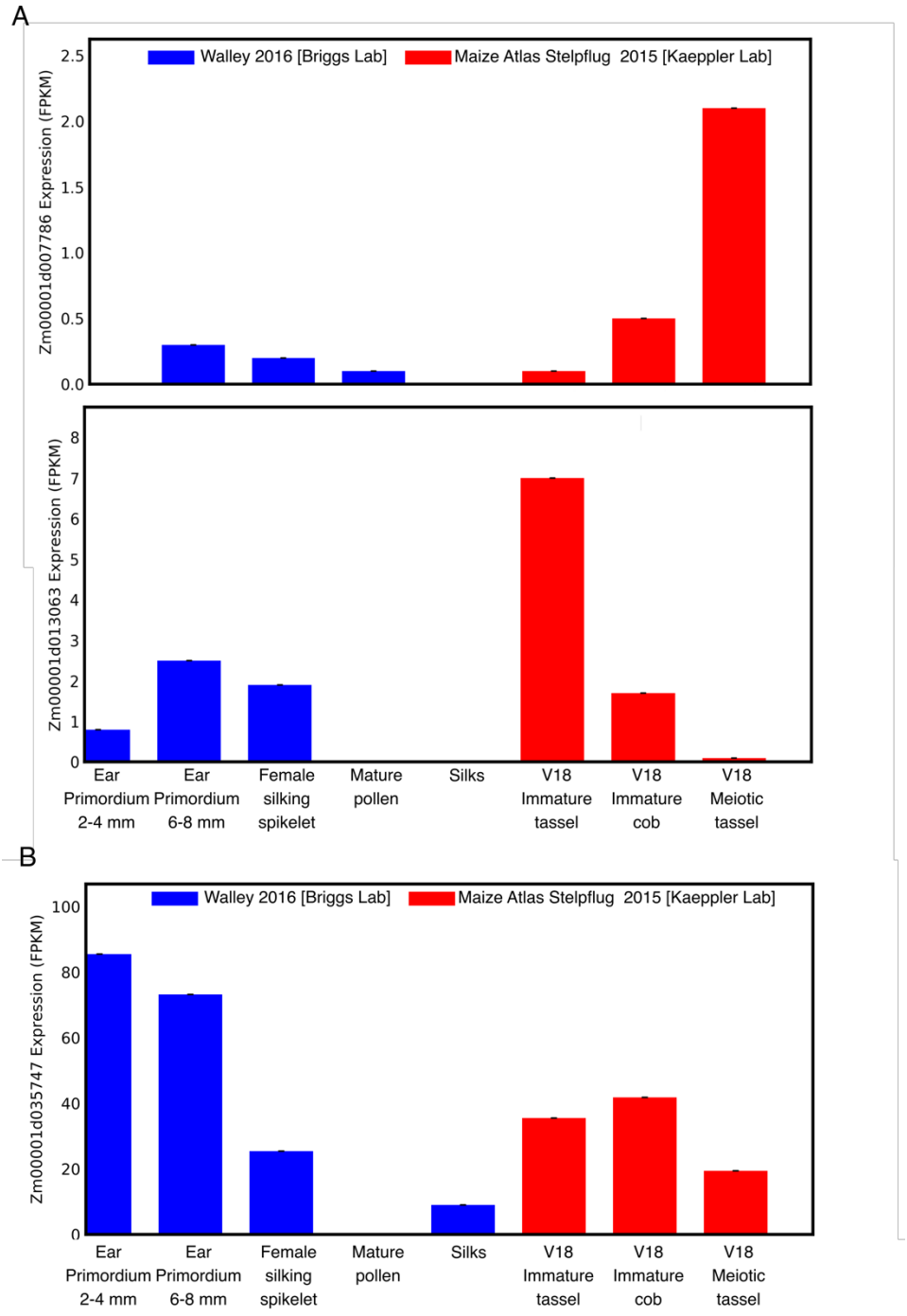

Figure 3.2: Expression profile of two meiosis-associated Argonaute proteins in maize (Stelpflug, Sekhon et al. 2016, Walley, Sartor et al. 2016). (A) RNAseq data shows *MAGO1* (Zm0001d007786) is expressed primarily in meiotic tassels with low expression levels detected in immature cobs and the various stages of female reproductive development while *MAGO2* (Zm0001d035747) is expressed primarily in the V13 immature tassel in the early stages of male reproductive development and also harbors low levels of expression in female reproductive development. (B) *AGO1a* (Zm0001d035747) is expressed highly in female reproductive tissues and expressed moderately in male reproductive tissues. Fragments Per Kilobase of transcript per Million mapped reads (FPKM).

analysis we found that MAGO1 and MAGO2 are highly similar to rice MEL1 (70.3% and 80.5% similarity), which is known to interact with phasiRNAs and their miRNA trigger miR2118 in rice. *MEL1* is also expressed in developing rice anthers, however the role of MEL1 and the phasiRNAs remain elusive (Komiya, Ohyanagi et al. 2014). MAGO proteins belong to the AGO5 clade that appears to have undergone a duplication event in the monocots. Two MAGO like genes could be found in many of the major crop cereals including wheat, rice, sorghum, but not in barley (Figure 3.3). Yet, this duplication could not be found in the dicots, which may suggest a specialised function for these Argonautes in the grass lineages. Only one AGO5 could be found for *Arabidopsis*, though this protein appears to group away from MAGO and more closely resembles ZmAGO5a. Moreover, *Arabidopsis* AGO5 is not thought to be involved in male reproductive development, though it is involved in female development (Tucker, Okada et al. 2012).

3.2.2 MAGO1 and MAGO2 have conserved catalytic DDH residues

Argonautes have many characterised functions, which in some cases require the presence of specific functional domains. MAGO1, MAGO2 and MEL1 have highly conserved PIWI, PAZ and MID domains typical of Argonaute proteins (Figure 3.4). Additionally, all three are predicted to have the necessary residues to facilitate 5’ RNA guide strand anchoring (data not shown). MEL1 and MAGO1/2 are also predicted to have the 3 DDH residues constituting the RNase H active site suggesting nuclease activity (Figure 3.4). The variable N-terminal region is less similar between this family of Argonautes, though they all share some form of G/A rich region though this region does not resemble any already characterised functional domains.

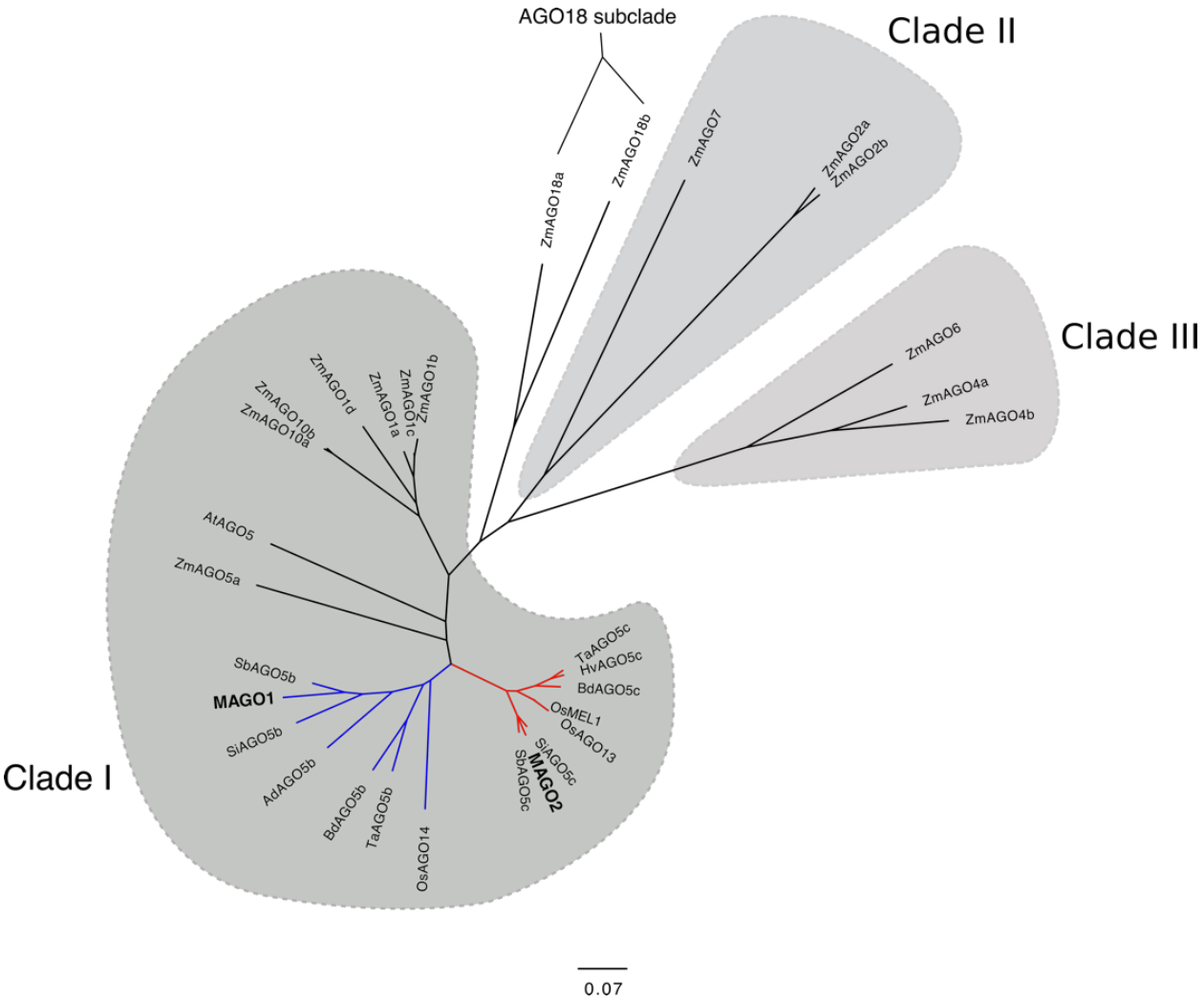

Figure 3.3: Evolutionary conservation of the grass AGO5b/c family. An unrooted phylogenetic tree of argonaute full length protein sequence to show homology of meiosis associated proteins across the grass lineages with AGO5b/MAGO1 branch (Blue) and AGO5c/MAGO2 branch (Red). Species: *Zea mays* (Zm), *Oryza sativa* (Os), *Arabidopsis thaliana* (At), *Sorgum biccolor* (Sb), *Triticum aestivum* (Ta), *Hordeum vulgare* (Hv), *Setaria italica* (Si), *Arundo donax* (Ad), *Brachypodium distachyon* (Bd).

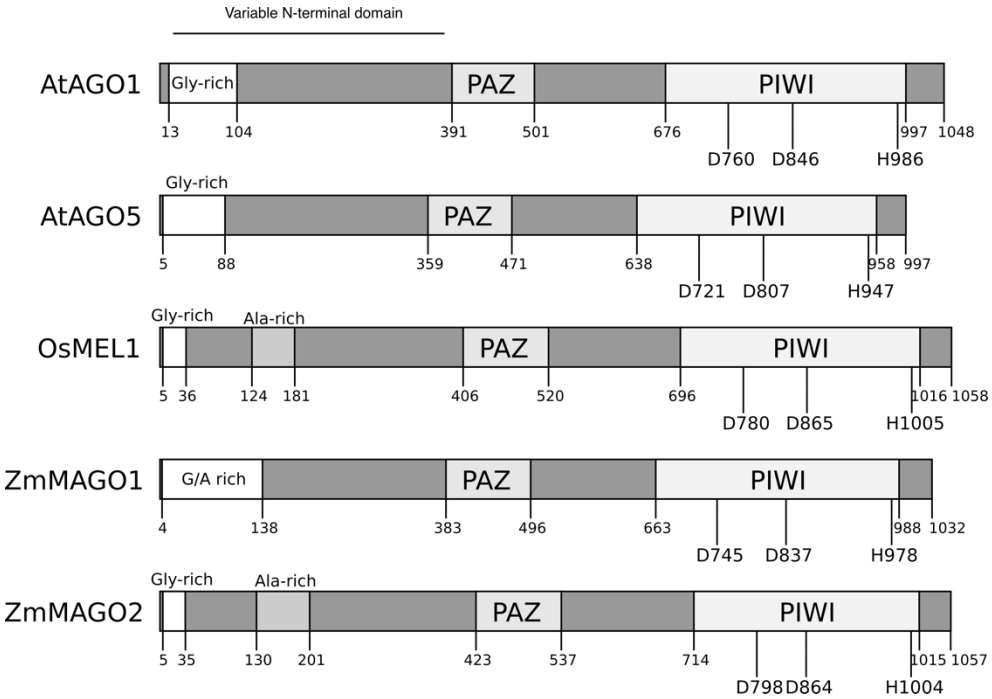

Figure 3.4: Annotated conserved domains and catalytic residues between members of the AGO5 family. All analysed AGO5 members have the conserved DDH (Asp, Asp, His) catalytic residues. Gly-rich, glycine rich region; Ala-rich, Alanine rich region; G/A-rich, Glycine Alanine rich region; PAZ, PAZ domain; PIWI, PIWI domain.

3.2.3 Distinct temporal and spatial expression of MAGO1 and MAGO2 during maize anther development

MAGO 1 and 2 are associated with male reproductive organs undergoing meiosis. To better understand the dynamics of MAGO accumulation in maize anthers, we generated antibodies (see 2.4.4) to target each protein by immunolocalization in developing anthers (Figure 3.5) (Figure 8.3). MAGO proteins are expected to accumulate during specific stages of anther development and evidence from homologous proteins suggests they may be associated with meiosis (Nonomura, Morohoshi et al. 2007). We found that MAGO1 and MAGO2 accumulate early in anther development with distinct localisation patterns. MAGO1 accumulates in the anther epidermis before meiosis and its localisation appears largely cytoplasmic (Figure 3.5). This coincides the reported accumulation of miR2118, a known trigger of the 21-nt phasiRNA pathway in pre-meiotic anthers (Figure 3.5 ; (Zhai, Zhang et al. 2015)). Later in development, MAGO1 accumulates in the cytosol of tapetum cells and meiocytes. On the other hand, MAGO2 accumulates in anthers undergoing meiosis and appears to localise as discrete nuclear foci in the meiotic pollen mother cells (PMCs) and meiocytes (Figure 3.5).

To further investigate the cellular localisation of MAGO1 and MAGO2, we first analysed MAGO1 and MAGO2 sequences using *in silico* prediction tools. Both MAGO1 and MAGO2 returned predicted nuclear localisation signal (NLS) signals (MAGO1:Score = 0.86, MAGO2:Score = 0.89)(Lin and Hu 2013)(Appendix). To validate these findings, both MAGO1 and MAGO2 were fused to eYFP and expressed transiently in *N. benthamiana* (Appendix). proteins were found to localise both in the nucleus and the cytoplasm of epidermal cells (Figure 3.6) suggesting that these proteins may shuttle between the both compartments as it has been shown for other argonaute proteins in *Arabidopsis* (Bologna, Iselin et al. 2018).

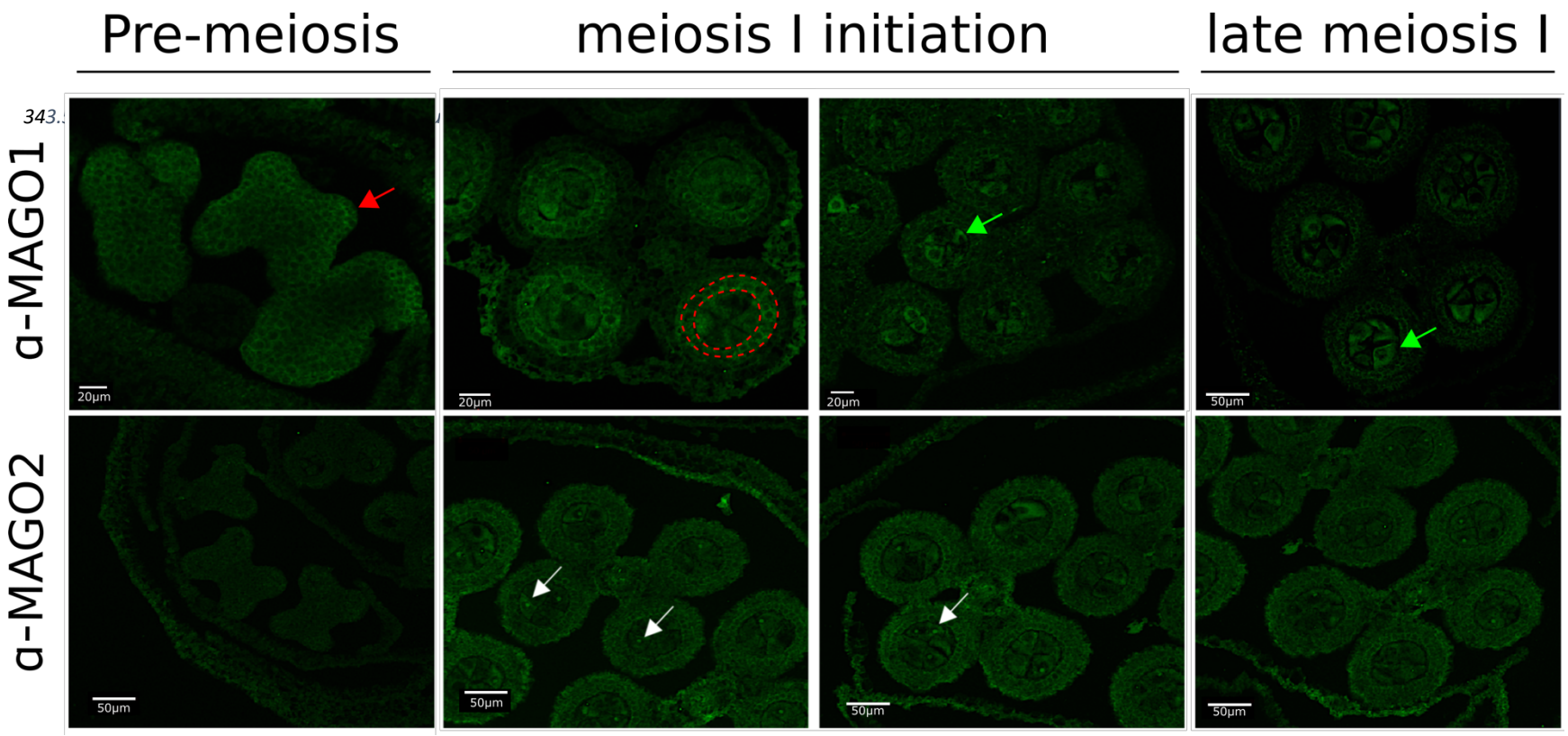

Figure 3.5: Immunolocalisaton of MAGO proteins during maize anther development. MAGO1 is expressed in the premeiotic anther epidermis (red arrow) and moves to the tapetum (red circle) and meiocytes (green arrow) during meiosis. MAGO2 can be detected in the meiocyte nucleus (white arrow) and meiocyte cytosol until late meiosis.

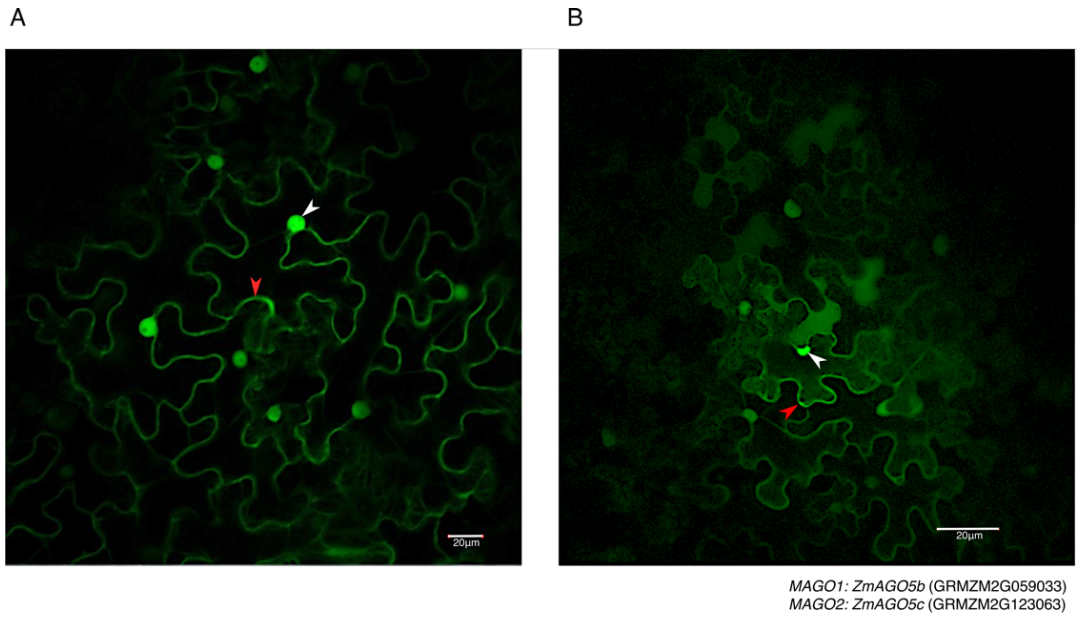

Figure 3.6: Transient expression of MAGO-eYFP in *N. benthamiana* leaves. (A) MAGO1-YFP and (B) MAGO2-YFP localizes primarily to the nucleus (white arrow) and cytosol (red arrow) 3 days after infiltration.

3.2.4 MAGO proteins bind the 21-nt and 24-nt phasiRNAs

Both the spatial and temporal localisation of the MAGO proteins, overlap with the accumulation of phasiRNAs in early anther development. The 21-nt phasiRNA trigger miR2118, and the precursor PHAS transcripts are known to be expressed in the pre-meiotic anther epidermis/endothecium (Zhai, Zhang et al. 2015). In order to assess the role that MAGO proteins may have, we assessed the binding capacity of both proteins in 1.3mm and 1.5mm anthers by immunoprecipitation with an antibody targeting both proteins (figure 8.3), followed by sRNA sequencing. The small RNA immunoprecipitation (sRNA-IP) sequencing data was mapped to the maize genome to determine the abundances of the bound sRNA, in particular 21- and 24-nts which map to the previously identified PHAS loci (See Table 8.2) (Zhai, Zhang et al. 2015). MAGO proteins appear to bind to 21-nt phasiRNAs, accounting for a small fraction of the library (2.4% ,1.3mm anthers; 1%, 1.5mm anthers). Surprisingly, we also found that these proteins also bind to 24-nt phasiRNAs which represented a significant proportion of the library (34.3% ;1.3mm, 24.4%; 1.5mm) (Figure 3.7). MAGO bound siRNAs were unexpectedly enriched for 5'G, not commonly found in 21-nt siRNAs (40.1% and 54.2% for 1.3mm and 1.5mm anthers respectively). Additionally, enrichment for small RNAs 22-nt in length was also found (19.3% and 33.8% for 1.3mm and 1.5mm anthers respectively). This enrichment was found to be attributed to small RNAs originating from a single tRNA gene (Figure 3.8) (Gramene ID: Zm00001d045542), which represents 16.3% and 31.2% of the MAGO-IP libraries respectively. This suggests that MAGO proteins bind to different classes of sRNAs in early developing anthers.

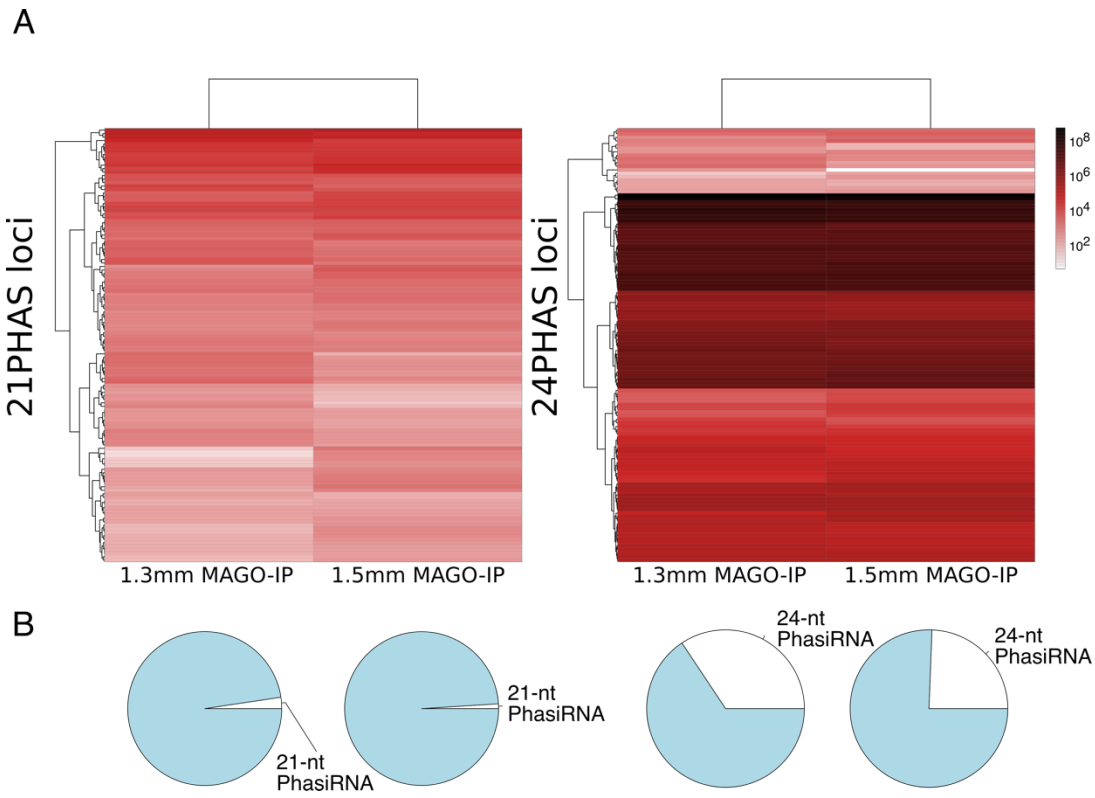

Figure 3.7: MAGO proteins bind to the previously identified phasiRNAs. (A) Normalized (DeSeq2) abundance of small RNAs mapping to the previously identified 21- (left) and 24-PHAS (right) loci in 1.3mm and 1.5mm anthers. (B) Percentage of the sRNA library mapping to the 21- (left) and 24-PHAS (right) loci.

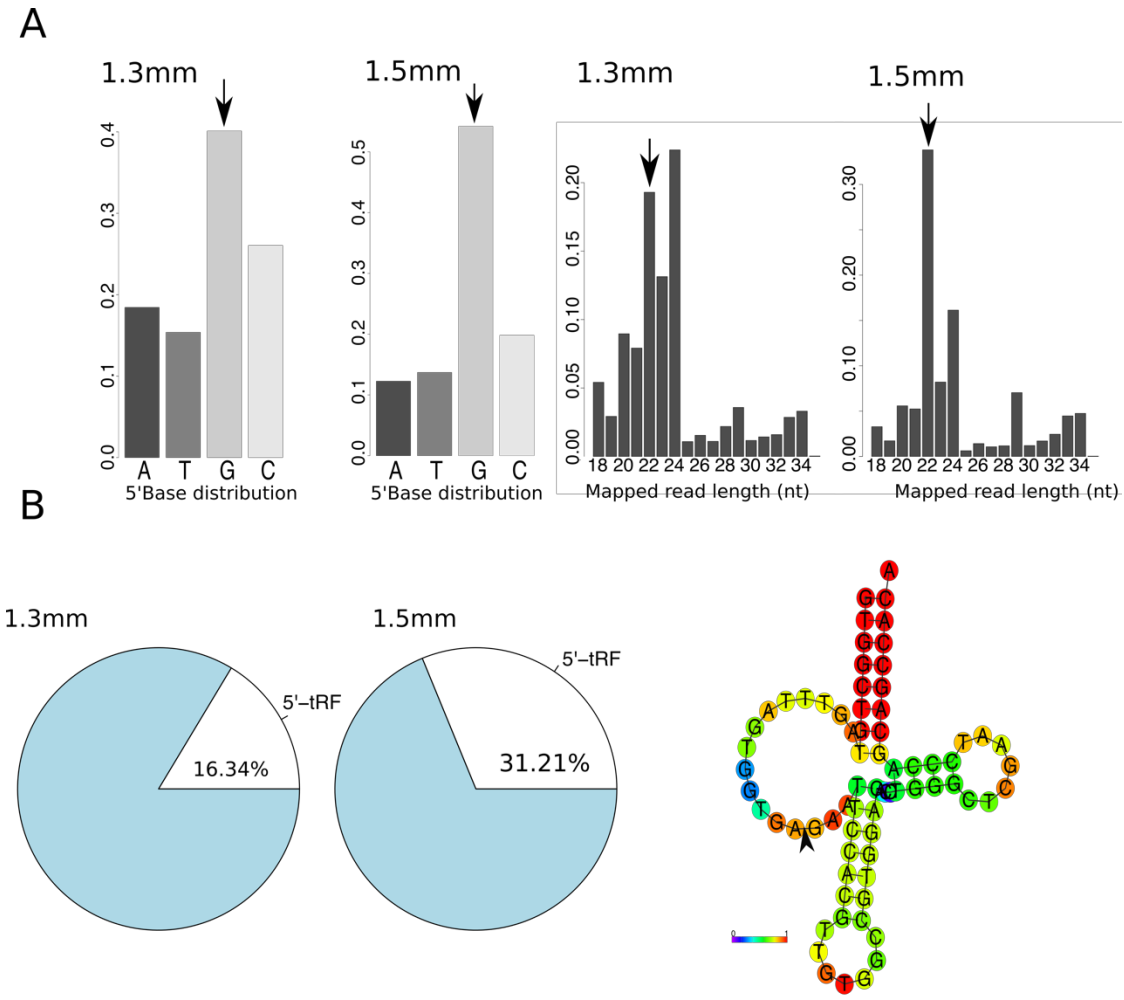

Figure 3.8: MAGO proteins bind to 22-nt tRNA fragments (tRFs). (A) 5'base distribution (left) and size distribution (right) of MGO-IP sRNA sequencing libraries. MAGO-IP shows a sRNA preference for 5'Guanine and is enriched for small RNAs 22-nt in length. (B) Proportion of the sRNA-IP libraries corresponding to a single tRF. Proportion contribution of the library attributed to the 5'tRF(left). RNA secondary structure (RNAfold) (right). Scale indicates base-pair probabilities.

3.2.5 MAGO proteins have slicing activity

The evidence thus far suggests that MAGO proteins are capable of binding to the mature phasiRNAs, however their importance in phasiRNA biogenesis and whether or not they actively slice RNA is not known. To understand the precise role of MAGO proteins, we designed a synthetic Luciferase reporter to measure MAGO RNA slicing activity (See Figure 3.9 for hypothetical working model). When infiltrated alone, the fiLUC-phasiRNA sensor effectively expressed the luciferase reporter gene, as determined by luminescence, when exposed to the luciferin substrate. Additionally, when infiltrated with the artificial miRNA2118, luminescence was not significantly affected. However, when we infiltrated both components along with MAGO proteins, luminescence (photon intensity) was found to be significantly lower when compared with the control lacking MAGO proteins and sensor control lacking MAGO proteins and the amiR2118 ($p>0.001$) (Figure 3.10). Furthermore, MAGO1 and MAGO2 appear to be equally efficient in reducing the luciferase reporter signal. Collectively, this data suggests that these proteins can bind to the mature mR2118 and initiate RNA slicing.

We hypothesised that slicing of the fiLUC-phasiRNA sensor by MAGO proteins could trigger the production of secondary sRNAs. If this occurs, we expect them to originate from the region downstream of the miRNA slice site (Figure 3.11). To detect if secondary sRNAs are formed, we used our fiLUC-phasiRNA reporter system in a transgenic N. benthamiana line expressing constitutively the GFP reported (Figure 3.11). In untreated GFP plants, we could clearly detect GFP signals in the leaves. This signal is maintained when we infiltrate with our fiLUC-phasiRNA sensor and when we infiltrate along with the amiR2118. However, we do not see an indication of GFP down regulation in these lines when we co-infiltrate leaves with *MAGO* genes (Figure 3.11).

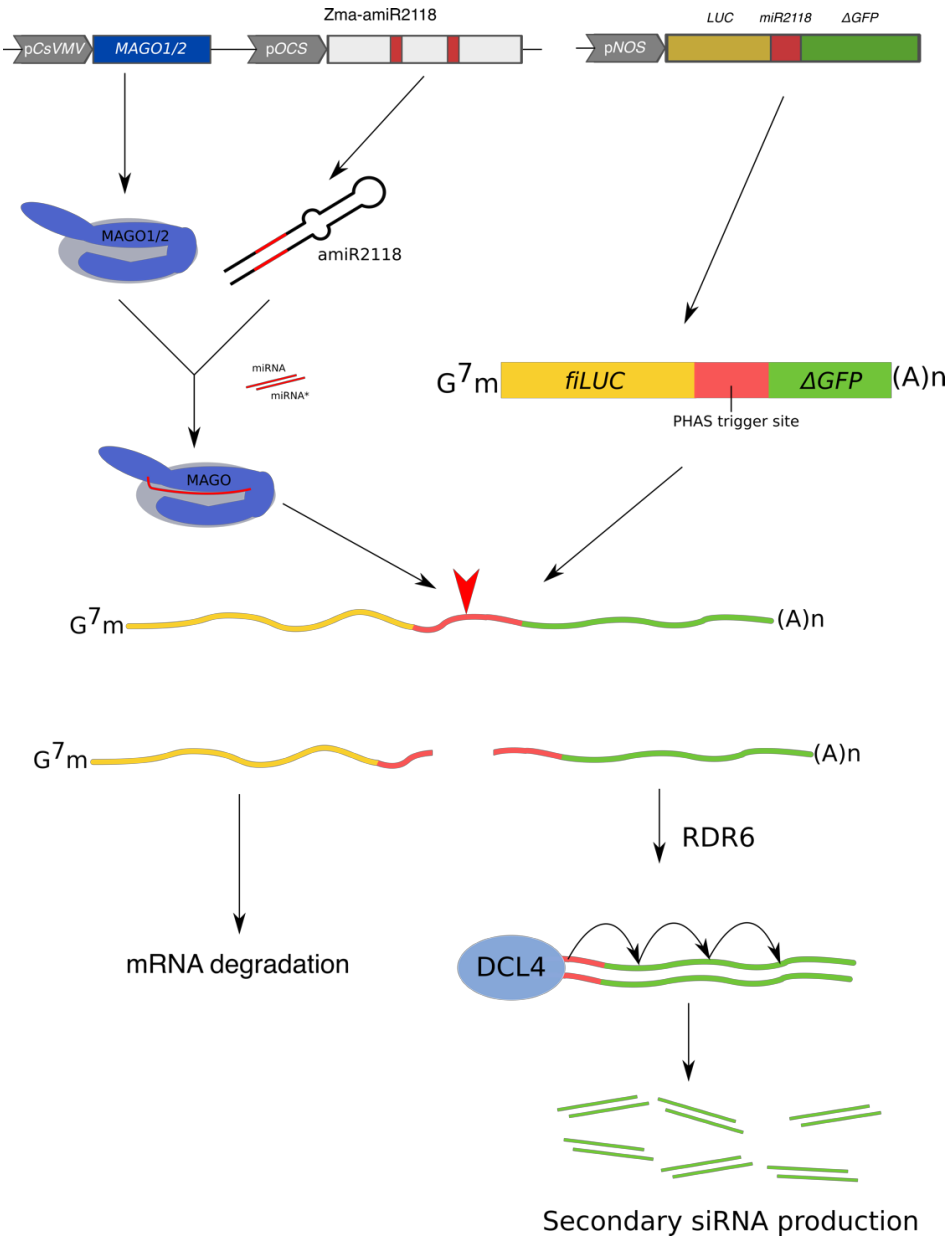

Figure 3.9: Design of a reporter system to detect Argonaute slicing activity. MAGO genes, artificial miRNA 2118 (amiR2118) and fiLUC-PHAS-ΔGFP sensor are coinfiltrated into *N. benthamiana* leaves. If amiR2118/MAGO can target the fiLUC-PHAS-ΔGFP sensor, the 5' luciferase mRNA is degraded. Slicing activity can be measured by luciferase assay. If slicing takes place, we hypothesis that the 3' mRNA will become a substrate for RDR6 and DCL4, generating secondary sRNAs from this region. Should this take place, secondary sRNAs will be generated from the engineered ΔGFP sequence down-stream of the slice site and silencing GFP siRNAs will be generated. When infiltrated into an *N. benthamiana* transgenic line expressing GFP constitutively, we expect to detect the downregulation of the GFP signal.

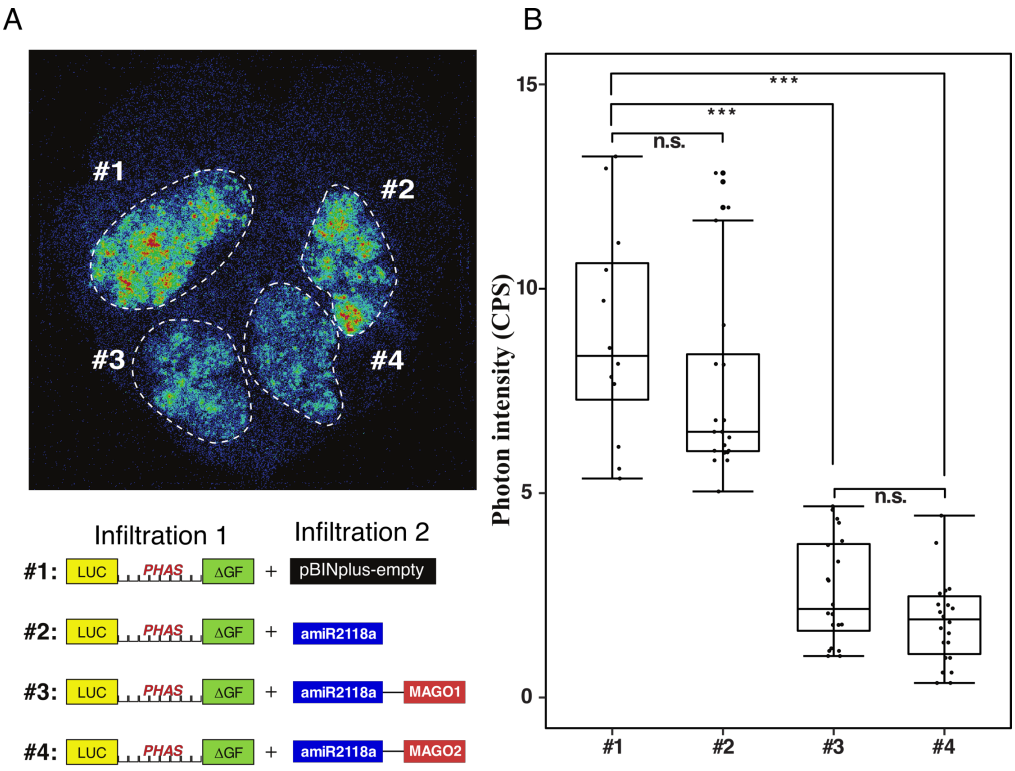

Figure 3.10: MAGO proteins display RNA slicing activity. (A) (1) Luciferase reporter co-infiltrated with empty binary, (2) Luciferase reporter co-infiltrated with amiR2118 only, (3) Luciferase reporter co-infiltrated with amiR2118 and MAGO1, (4) Luciferase reporter co-infiltrated with amiR2118 and MAGO2. (B) Photon intensity was recorded 3 days after infiltration and recorded in counts per second (CPS). Significant differences between groups were determined one-way ANOVA ($p<0.001$)

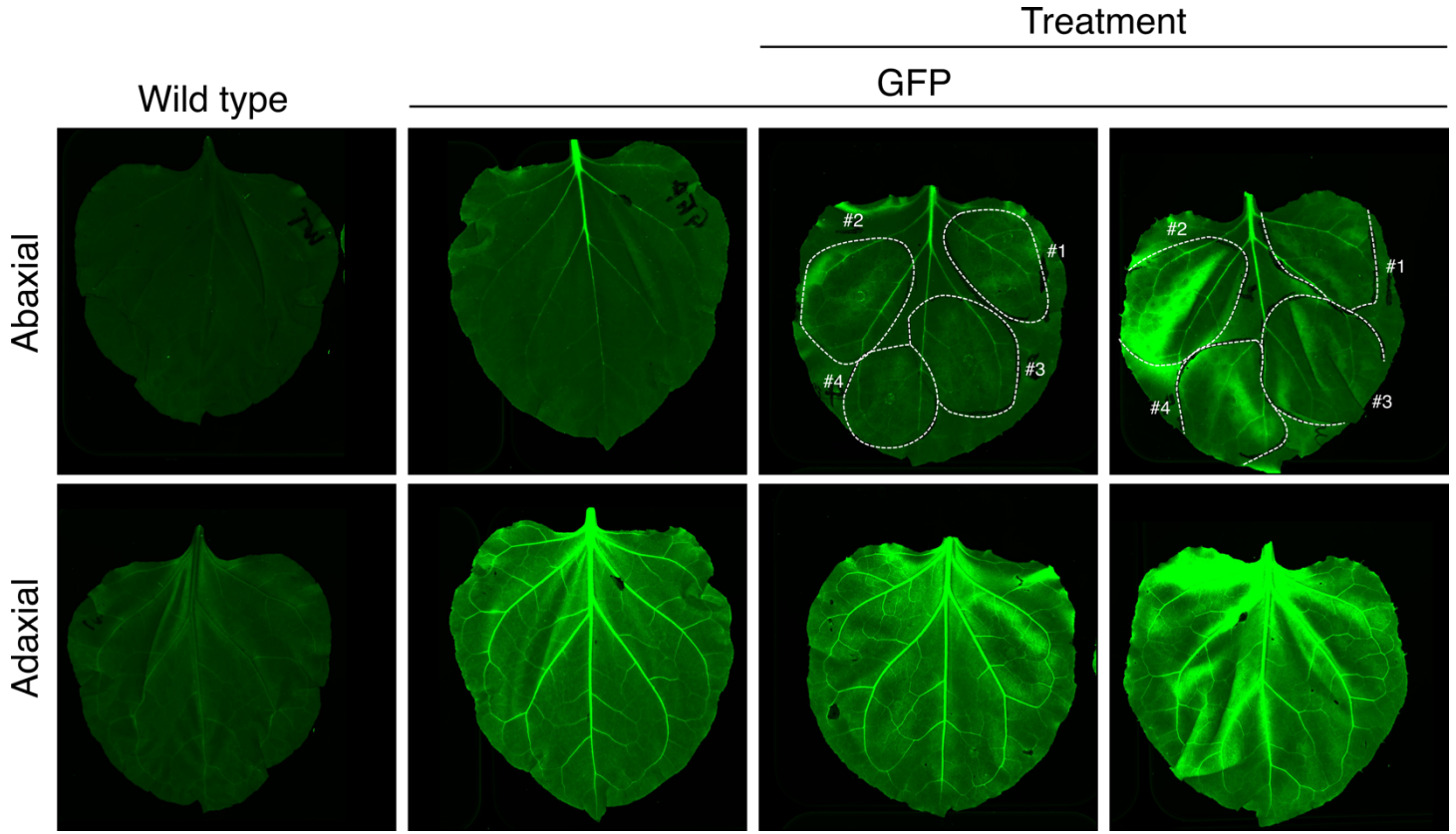

Figure 3.11: Silencing of GFP in *N. benthamiana* lines. Adaxial and abaxial leaf surface of wild type and GFP *N. benthamiana* before and after infiltration. (1) Luciferase reporter co-infiltrated with empty binary, (2) Luciferase reporter co-infiltrated with *amiR2118* only, (3) Luciferase reporter co-infiltrated with *amiR2118* and *MAGO1*, (4) Luciferase reporter co-infiltrated with *amiR2118* and *MAGO2*.

3.0 Functional characterisation of meiosis-associated Argonautes MAGO in maize

Summary

MAGO proteins have distinct spatial and temporal accumulation patterns during reproductive development. Additionally, these proteins bind to the epidermally accumulating 21-nt phasiRNAs and are able to direct mRNA target slicing.

3.3 Discussion

Much is known about argonaute proteins in various organisms. Although they are well conserved across kingdoms of life, they have developed diverse molecular functions. To begin to understand the roles of meiosis associated argonautes we first draw on knowledge of characterised argonautes to build our hypothesis and elude to their possible functions.

MAGO proteins belong to Clade I of the AGO-like plant genes (Figure 3.3). This clade is heavily duplicated and diversified in grass species and includes the founder Argonaute AGO1, which is well known for its role in PTGS by target mRNA slicing and translational inhibition (Baumberger and Baulcombe 2005, Li, Liu et al. 2013, Zhang, Xia et al. 2015). MAGO proteins are related to AGO5, a family already implicated in reproductive development. In *Arabidopsis*, AGO5 is expressed in the megaspore mother cell and surrounding cells and acts to promote the initiation of megagametogenesis and specifically binds to 21-nt 5'C siRNAs (Tucker, Okada et al. 2012). Rice possesses five AGO5 genes, of which, only *mel1/OsAGO5c* is well characterised and displays fertility defects (Zhang, Xia et al. 2015). Contrary to *Arabidopsis*, MEL1 is expressed in the developing anther and predominantly binds to the 21-nt phasiRNAs with a preference for 5'C (Nonomura, Morohoshi et al. 2007, Komiya, Ohyanagi et al. 2014). While these meiosis associated Argonautes have been characterised, little is known of their molecular function.

MAGO genes were identified as being highly expressed in the developing maize anther with lower expression also detected in the developing ear (Stelpflug, Sekhon et al. 2016, Walley, Sartor et al. 2016) (Figure 3.2). Phylogenetically, these argonautes have high similarity to MEL1 and to a lesser extent AtAGO5 and therefore were expected to also bind to 21-nt 5'C phasiRNAs as Argonautes are highly selective in their sRNA binding

preference (Mi, Cai et al. 2008, Wu, Zhang et al. 2009, Komiya, Ohyanagi et al. 2014) (Figure 3.2 & 3.3).

The grasses have expanded the AGO5 family between the last common ancestor with *Arabidopsis,* with all but one grass member analysed having 2 conserved MAGO-like proteins. This points to a functional conservation of a MAGO pathway across the grasses hinting at its importance in reproduction. Coincidentally, the reproductive phasiRNAs have also been largely conserved in grass species, they are expressed in the developing anther and are predicted to be associate with MAGO based on its homology to rice MEL1 (Kakrana, Mathioni et al. 2018).

MAGO, like all plant Argonaute genes, harbour a variable N-terminal domain and conserved PAZ, PIWI and mid domains. Both the PAZ domains of these proteins have the required residues for sRNA guide strand binding. MAGO proteins are additionally predicted to have the conserved DDH residues for slicer activity which may be required for miR2118 mediated 21PHAS triggering, in addition to a role in down-stream 21nt-phasiRNA mediated silencing.

MAGO proteins bind to diverse classes of sRNAs

Rice MEL1 is known to bind preferentially to 21-nt phasiRNAs with a preference for 5'C (Komiya, Ohyanagi et al. 2014). To determine MAGO binding preferences, MAGO bound siRNAs were isolated followed by sRNA sequencing. To capture both classes of reproductive phasiRNAs, we selected a developmental stage in which both classes are known to be simultaneously expressed in maize (Zhai, Zhang et al. 2015). To target these stages we used Anther length, which is known to strongly correlate with anther development, as a guide (Ma, Skibbe et al. 2008). Both 21-nt and 24-nt phasiRNAs were detected in our data which suggests that MAGO proteins

are capable of binding both phasiRNA classes and consistent with MEL1 data (Komiya, Ohyanagi et al. 2014) (Figure 3.7). However, a substantial proportion of the RNA library mapped to 24-nt PHAS loci (19.7% of assigned reads (Table 8.1). While unexpected, sampling may have taken place too late to substantially sample the 21-nt phasiRNAs, which are short-lived and rapidly downregulated shortly before meiosis takes place (Zhai, Zhang et al. 2015). Therefore, in future, to enrich for MAGO bound 21-nt phasiRNA, anthers must be collected earlier in development.

The MAGO sRNA immunoprecipitation data also showed a large proportion of tRNA derived fragments (tRFs), which are enriched during meiosis (Figure 3.8). These tRFs are known to be associated with the silencing of transposons and the stress response (Alves, Vicentini et al. 2017, Schorn, Gutbrod et al. 2017). The tRFs are additionally highly selective, binding only with specific Argonaute proteins and binding is enhanced under certain stress conditions (Cognat, Morelle et al. 2016). The tRFs identified are 22-nt in length with 5'G and appear to have formed from the cleavage of the D arm of a precursor tRNA (Zm00001d045542). The timing would suggest that this tRF is associated with meiosis and MAGO proteins and might suggest MAGO proteins are involved in transposable element regulation or the stress response during meiosis, as has been shown in animals and other plants species (Molla-Herman, Vallés et al. 2015, Alves, Vicentini et al. 2017).

Spaciotemporal localisation of MAGO proteins

Expression data shows that MAGO proteins are associated with inflorescences undergoing meiosis. However, while MAGO proteins are associated temporally with meiosis in developing tassels, the cellular and subcellular localisation was unknown. Immunolocalisation assays using MAGO specific antibodies allowed better resolution of MAGO expression

(Figure 3.5). MAGO1 localisation appears predominantly to be cytoplasmic, consistent with presumed location of PTGS. Additionally, It appears to originate in the anther epidermis, consistent with documented miR2118 expression pattern in both rice and maize (Komiya, Ohyanagi et al. 2014, Zhai, Zhang et al. 2015).

MAGO2 is predominantly expressed during meiosis and appears to exclusively localise to discrete foci in the male meiocyte nucleus. This is supported by transient expression of MAGO YFP fusion proteins in *N. benthamiana* (Figure 3.6). However, it is not clear whether over expression of MAGO YFP fusion proteins may overwhelm protein transport systems leading to the observed localisations. Our investigation into the targeting of MAGO to the nucleus by its NLS signal is ongoing and would be supported by the inclusion of several controls including NLS-GFP controls and MAGO lacking an NLS.

AGO1, a member of the same clade as MAGO, has also been found to localise in the nucleus when bound to 24-nt sRNAs (Zhang, Yazaki et al. 2006, Wang, Zhang et al. 2011). Under salinity stress, nuclear AGO1 was found to transcriptionally regulate the expression of MIR161 and MIR173 precursors and interact with RNA pol II resulting in premature disassembly from the DNA template (Dolata, Bajczyk et al. 2016). Other studies have linked nuclear AGO1 localisation to regulation of stress responses in plants whereby AGO1 can bind to chromatin and recruit remodelling complexes to activate genes (Liu, Xin et al. 2018). It is therefore likely MAGO proteins share this dynamic functionality with AGO1 (Zhang, Xia et al. 2015).

Molecular function of MAGO proteins

To verify the RNA slicer activity of MAGO1 and MAGO2 we engineered a slicing, luciferase sensor. Both MAGO proteins were able to modulate the

expression of the luciferase sensor when in the presence of a miR2118 trigger (Figure 3.10). This suggests that MAGO proteins can slice RNA in *N. benthamiana* and may be sufficient to generate the phasiRNAs in maize anthers. However, the slicing of the phasiRNA sensor did not result in detectable silencing of the GFP transgene in *N. benthamiana*. The biogenesis of 21-nt phasiRNAs is thought to require DCL4 and RDR6, which are also required for the biogenesis of tasiRNAs in plant leaves (Komiya 2017). There may be significant protein sequence divergence in these biogenesis components between maize and *N. benthamiana* that may disrupt the necessary protein-protein interactions necessary for phasiRNA production. Sequencing the small RNA of transformed leaves would determine if MAGO is generating phased siRNAs from the luciferase-sensor. Furthermore, GFP is a highly stable protein with a slow turnover, therefore RNA silencing by GFP siRNAs may have a limited impact on GFP protein levels and subsequent fluorescence (Ward 2005). A positive GFP silencing control would allow us to determine the impact of sRNA silencing on the expression levels of GFP in transformed *N. benthamiana* leaves.

4.0 The role of MAGO proteins in anther development

4.1 Introduction

4.1.1 Anther development

Unlike animals, in which germline differentiation occurs during embryogenesis, plants specify their germline late in development (Boavida, Becker et al. 2005). In flowering plants, the male reproductive processes occur in the stamen. It is here where diploid cells undergo meiosis to produce haploid microspores which go on to develop into pollen grains containing the mature sperm cells. Stamen development is a highly coordinated process which requires the communication of many cell types and the coordinated expression of multiple genes (Boavida, Becker et al. 2005). This precisely choreographed developmental plan is highly sensitive to external stimuli, more so than vegetative plant growth (Hall 2018). To ensure the reliable progression of male reproduction, plants have evolved diverse mechanisms to regulate gene expression and ensure genome stability in the germline. There are many plant mutants in which this developmental process is disrupted, impacting pollen viability to varying degrees of severity (Dawson, Wilson et al. 1993).

The stamen can be divided into two morphologically distinct tissues, the anther and the filament. The filament is a vasculature tissue which provides water and nutrients to the developing anther and connects the anther to the flower. The anther is made up of both reproductive and somatic tissue responsible for the development and release of the pollen grains so that fertilisation can occur (Walbot and Evans 2003). Unlike typical flowers which contain both male stamen and female carpel reproductive organs, maize has separate female inflorescences which contain many carpels and a branched terminal tassel which contains thousands of stamens. These stamens are organised within the tassel flower (spikelet) and each individual spikelet contains a pair of floral compartments (florets) each with 3 stamens (Figure

4.1). Carpels within the tassel spikelets and stamens within the ear abort early in development ensuring that there is complete separation of the male and female reproductive organs in maize (Cheng, Greyson et al. 1983, Boavida, Becker et al. 2005, Kellogg 2007).

Before meiosis takes place, major proliferation and patterning events must occur within the developing anther. A transverse cross-section through an anther undergoing meiosis will reveal 4 equal anther lobes (locules) each consisting of 4 differentiated somatic cell layers - the epidermis (EP), endothecium (EN), middle layer (ML) and tapetum (TA) arranged in concentric rings surrounding the globular meiotic cells (meiocytes)(Figure 4.1) (Bedinger and Fowler 2009, Kelliher and Walbot 2011). The 4 cell layers serve to coordinate development and provide the meiocytes with nutrients and coatings required for pollen maturation (Canales, Bhatt et al. 2002, Wilson and Zhang 2009). The proper specification of all cell types is required for normal pollen development and many male-sterile mutants exist which lack one or more of these somatic cell layers (Sheridan, Golubeva et al. 1999, Vernoud, Laigle et al. 2009, Wang, Nan et al. 2012, Nan, Zhai et al. 2016).

The anther epidermis arises from the L1 derived layer of the anther primordia while the other 3 layers and the meiocytes arise from the multipotent sub-epidermal L2 derived layer of the anther primordia (Dawe and Freeling 1990, Dawe and Freeling 1992). The multi-layered anther structure is initiated by the specification of the archesporial cells in the anther primordia from the L2 derived cells. Historically this was thought to occur by the periclinal division of hypodermal cells to form a single primary parietal cell adjacent to the epidermis and an archesporial cell which is internal (Wilson and Zhang 2009). New evidence now suggests that archesporial cell identity is acquired in central cells from a field of equivalent L2 derived cells (Kelliher and Walbot 2011).

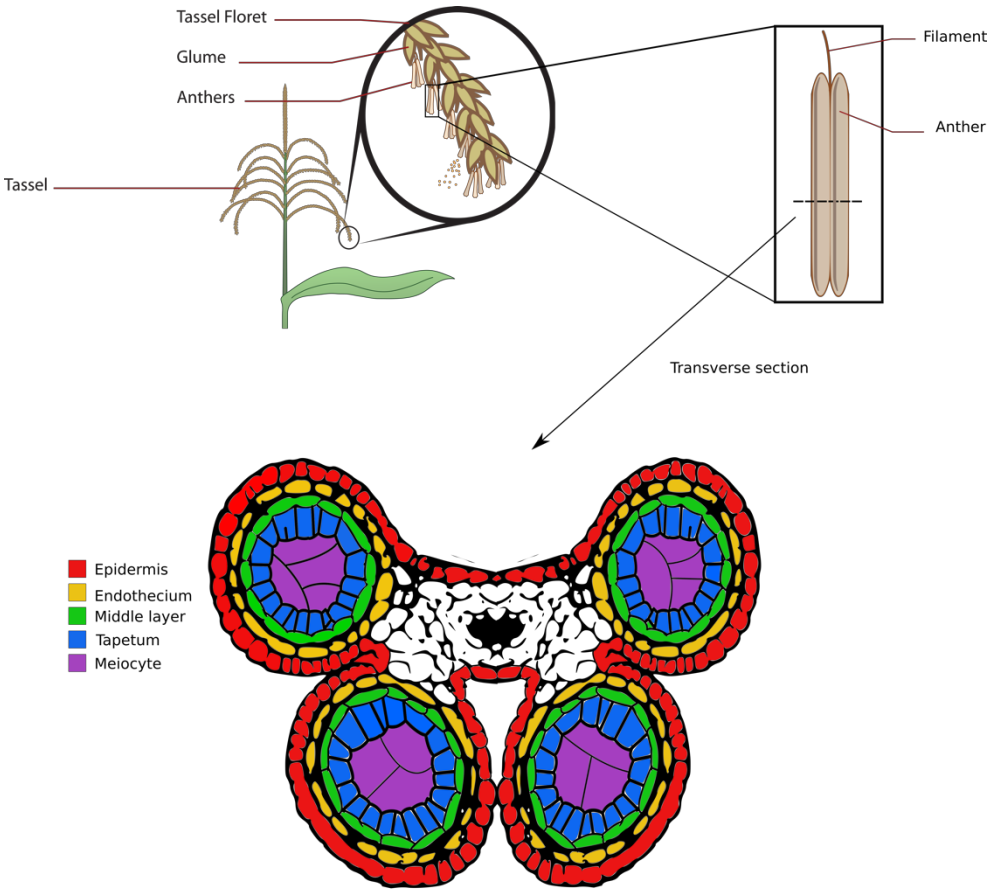

Figure 4.1: Maize stamen morphology. The maize male reproductive organs are satiated on a terminal tassel. The tassel contains many stamen with 2 florets each. Each floret contains two stamen pairs which are each of which can be divided into two morphologically distinct tissues – the filament and anther. A transverse section through a 1.3mm anther prior to meiosis reveals the concentric somatic cell layers –the Epidermis, Endothecium, Middle layer, and Tapetum which support the growth and development of the meiocytes.

Archesporial cell specification is initiated by a naturally arising redox gradient in the developing anther and mediated by *Male Sterile Converted Anther 1* (MSCA1) (Kelliher and Walbot 2012). During anther growth, hypoxic conditions in the centre of anther primordia triggers MSCA1-mediated responses resulting in the formation of a column of archesporial cells in the centre of each lobe. The archesporial cells secrete MULTIPLE ARCHISPORIAL CELLS 1 (MAC1) which suppresses archesporial proliferation and triggers the periclinal division of neighbouring subepidermal L2 derived cells to form the secondary parietal cell layer and the endothecium (Wang, Nan et al. 2012). Mutations in both genes therefore give rise to catastrophic developmental and fertility defects.

MSCA1 is a Glutaredoxin which initiates archesporial cell specialisation by targeting disulphide bonds on transcription factors (Hong, Tang et al. 2012, Kelliher and Walbot 2012). Maize *msca1* and rice homologue *MICROSPORELESS1 (MIL1)* mutants are male sterile as the central archesporial cell fails to differentiate and instead resembles leaf tissue (Chaubal, Anderson et al. 2003). Consequently, somatic cell architecture is also disrupted in the *mil1* resulting in locules filled with somatic cells. Initially anther development appears normal in *mac1* mutants. However shortly after archesporial cell specification, the subepidermal L2-derived cell layer fails to divide periclinally and by meiosis, *mac1* anthers contain 3 times the number of archesporial cells (Golubovskaya, Grebennikova et al. 1993, Sheridan, Golubeva et al. 1999). The archesporial cells appear to have the correct cell identity but meiosis fails in prophase I due to the absence of a functional tapetum resulting in complete male sterility in maize (Wang, Nan et al. 2012). *Outer cell layer 4* (OCL4) is a member of the HDZIP IV class of transcription factors and controls the differentiation and maintenance of the epidermal cell layer. In addition to defects in trichome development, *ocl4*

mutants display partial male fertility defects due to an additional endothecium-like subepidermal cell layer (Vernoud, Laigle et al. 2009).

The final anther cell specification event occurs when the secondary parietal cell layer divides periclinaly to produce the middle layer and the tapetum cell layer, which is responsible for nourishing developing microspores. Microspore maturation is dependent on a healthy tapetum to supply nutrients and later pollen wall coating, therefore there are many male sterile mutants defective in tapetal development (Jung, Han et al. 2005, Wang, Nan et al. 2012, Fernández Gómez and Wilson 2014, Nan, Zhai et al. 2016). *Male Sterile23* (Ms23) is required for tapetum development and codes for a basic Helix-loop-helix (bHLH) transcription factor, a master regulator of tapetum development. The secondary parietal cell in *ms23* divides normally, however there are additional abnormal periclinal divisions resulting in five somatic cell layers and myocytes that arrest during meiosis (Nan, Zhai et al. 2016). *Male Sterile32* (Ms32) is a bHLH transcription factor required for tapetum specification, though functioning downstream of *ms23* to repress abnormal extra periclinal divisions (Moon, Skibbe et al. 2013). ETERNAL TAPETUM1 (EAT1) is also a member of the bHLH family of transcription factors that is necessary for tapetal programmed cell death in addition to promoting the expression of the 24-nt phasiRNAs (Niu, Liang et al. 2013, Ono, Liu et al. 2018). EAT1 meiocytes are able to pass meiosis but abort due to tapetal defects. Therefore, for normal pollen, development, the tapetum must be specified and degenerate correctly.

OsAGO5c designated *mel1 (MEIOSIS ARRESTED at LEPTOTENE1)* is expressed in developing rice anthers and binds to the 21-nt and 24-nt phasiRNAs. Their function is currently unknown, however *mel1* mutants are male-sterile and meiosis arrests in early prophase (Nonomura, Morohoshi et al. 2007, Komiya, Ohyanagi et al. 2014). Surprisingly, the *Arabidopsis* homologue of

AGO5 is expressed in the somatic cells surrounding the megaspore mother cell and likely binds 24-nt sRNAs to promote the transition to megagametogenesis. AtAGO5 mutants induce female sterility along with ovule and seed defects (Tucker, Okada et al. 2012). Furthermore, AtAGO9 is implicated in female gametogenesis and also binds 24-nt siRNAs to prevent subepidermal cells from differentiating as megaspore cells. AGO9 mutants show signs of seed abortion and sub-epidermal cells were unusually large (Olmedo-Monfil, Durán-Figueroa et al. 2010). Clearly argonautes have vital and highly specialised functions during both male and female gamete development.

The plant meiosis-associated Argonautes bare remarkable similarity to the animal PIWI proteins and PIWI interacting RNAs that are expressed almost exclusively in the gonads. PIWIs have been reported to silence retrotransposons in the germline of Drosophila, zebrafish and mice, thereby protecting germline integrity (Kalmykova, Klenov et al. 2005, Houwing, Kamminga et al. 2007, Nishida, Saito et al. 2007, Kuramochi-Miyagawa, Watanabe et al. 2008). PIWIs are expressed in the soma follicular cells and deficiencies in the mouse PIWI proteins results in expression of LINE and LTR retrotransposons in the germline (Cox, Chao et al. 1998, Malone, Brennecke et al. 2009). This leads to arrest of gametogenesis and male sterility, likely due to excessive double strand breaks caused by transposition (Aravin, Sachidanandam et al. 2007, Carmell, Girard et al. 2007, Klattenhoff, Bratu et al. 2007).

4.1.2 Male meiocyte development

Provided that anthers develop normally with the correct number of cellular layers, meiocytes will enter meiosis. Meiosis is a specialised cell division in which one round of DNA replication is followed by two rounds of nuclear

division to form 4 haploid cells. In the anther all four cells go on to produce mature pollen grains, whereas only one of the female spores develops into the gametophyte (Bowman 2012). Many plant meiosis mutants exist, which affect both male and female meiosis equally. However a relatively small number do appear to be male or female specific (Caryl, Jones et al. 2003).

During meiotic S-phase, cohesin complex is loaded onto sister chromatids during DNA replication. After G2, prophase I of meiosis I begins with the elaboration of the cohesion complex and joining of the sister chromatids in so called axial elements, looped arrays which are maintained until anaphase II (Zickler and Kleckner 1999, Kleckner 2006) (Figure 4.2). Mutants that affect cohesion of sister chromatids display greater impact on female gametogenesis. *SWITCH1(SWI1)/DYAD* is expressed specifically in meiocytes and is required for sister chromatin cohesion (Agashe, Prasad et al. 2002). Mutants fail to form bivalents and instead form univalent which undergo aberrant chromosome segregation and eventual degeneration (Mercier, Vezon et al. 2001).

Progressing into zygotene, homologous chromosomes are brought into close proximity. During zygotene, lateral elements form between homologues and a central element forms running parallel in the zone in which they meet. By the end of the zygotene, homologues are fully synapsed, with the synaptonemal complex running the full length of the chromosomes (Heyting 1996). Proteins that comprise the synaptonemal complex are structurally conserved in most eukaryotes, however the protein sequence conservation is limited. *Arabidopsis ZYP1a/ZYP1b* are structurally similar to synaptonemal transverse filament components of other species (Higgins, Sanchez-Moran et al. 2005). ZYP1a/ZYP1b localizes to the central region of the synaptonemal complex during prophase I and is required for normal chromosome synapsis. ZYP1a/ZYP1b first appears as punctate foci

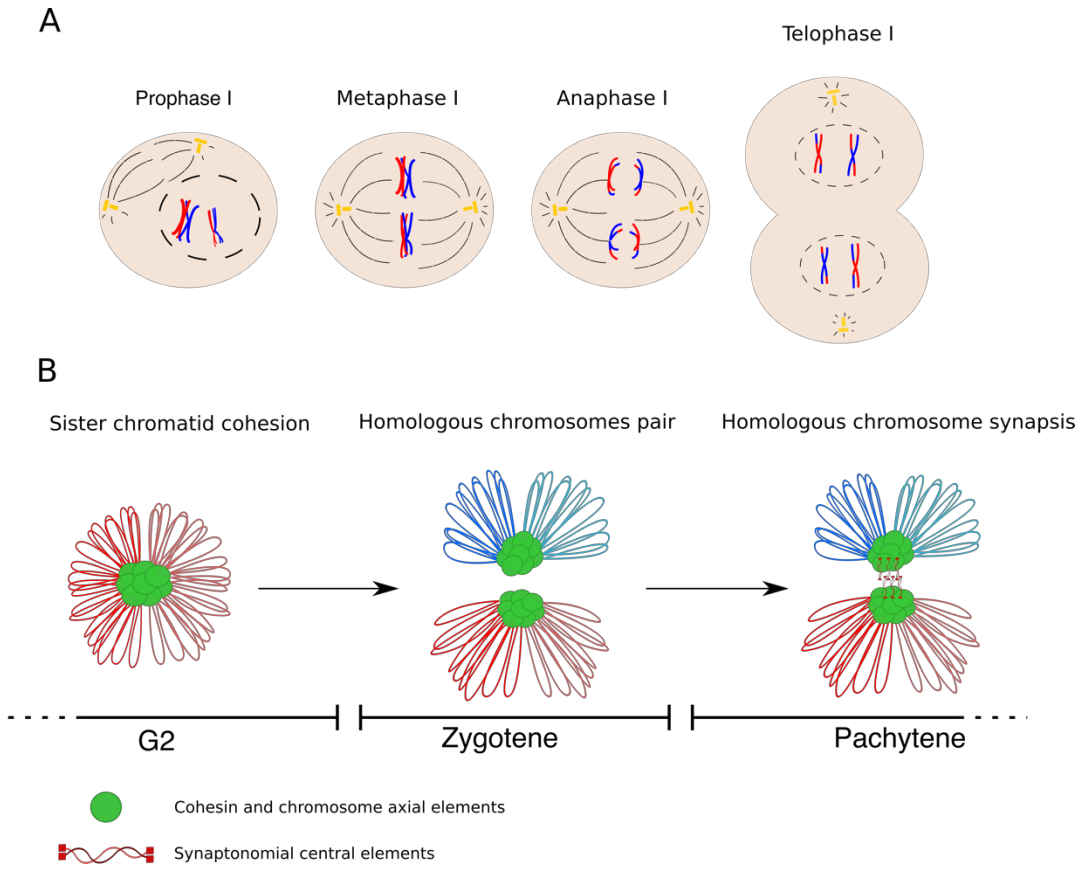

Figure 4.2: Key landmarks in meiosis. (A) stages of meiosis I. Prophase I is subdivided into 5 stages – Leptotene, Zygotene, Pachytene, Diplotene and Diakanesis where chromosomes condense, pair and recombine. Metaphase I, the synapsed chromosomes align along the cell equator. Anaphase I, homologous chromosomes are puled to opposite polls of the cell. Telophase I, Chromosomes gather at the cell polls while the cytoplasm divides. (B) During S-phase, the replicating DNA is loaded with cohesin complex proteins. By G2 the cohesion complex is elaborated and the sister chromatids join. During Zygotene, homologous chromosomes pair and by Pachytene, the synaptonomial complex is formed along their length.

during leptotene which extend to form single linear signals extending the full length of the synapsed chromosomes by pachytene. The progression of prophase I is severely delayed in ZYP1a/ZYP1b mutants, in addition to a reduction in seed set and recombination events between non-homologous chromosomes (Higgins, Sanchez-Moran et al. 2005). *Arabidopsis ASY1* is an axis-associated protein that is essential for homologous chromosome synapsis (Armstrong, Caryl et al. 2002). ASY1 localises during G2/leptotene as discrete foci, prior to ZYP1 localisation, which expand to form a continuous signal along the length of the synapsed homologous with the exception of the telomeric regions. *Arabidopsis asy1* mutants are severely defective in both male and female meiosis and homologues are unable to establish the synaptonemal complex following telomere pairing (Caryl, Armstrong et al. 2000, Armstrong, Franklin et al. 2001).

Both ZYP1 and ASY1 are well conserved plant synaptonemal components with distinct spaciotemporal localisation during the early stages of prophase I (Caryl, Armstrong et al. 2000, Higgins, Sanchez-Moran et al. 2005). ASY1 and ZYP1 are therefore routinely used to assess the formation of the synaptonemal complex in mutants affecting meiosis (Golubovskaya, Hamant et al. 2006, Wang, Carlton et al. 2009).

Spo11 is a eukaryotic homologue of a type II topoisomerase VI first found in Archeabacteria and is responsible for forming a large number of double strand breaks (DSB) during meiosis (Keeney 2001, Villeneuve and Hillers 2001). These DSBs are then repaired through recombination resulting in the physical exchange between chromosomes (Villeneuve and Hillers 2001, Hamant, Ma et al. 2006). *Arabidopsis* possesses 3 homologues of SPO11, only 2 of which are necessary for recombination. A drastic reduction in recombination along with random chromosomal segregation and a large proportion of non-functional gametes has been observed in AtSPO11

mutants (Grelon, Vezon et al. 2001, Hartung and Puchta 2001). Repair of DSBs requires the AtRAD51/AtDMC1 mediated removal of SPO11 which remains covalently attached to the 5' strand and strand resection allowing strand exchange to take place (Neale, Pan et al. 2005). Homozygous *Atdmc1* are severely affected in fertility and chromosomes appear to randomly segregate in male and female meiocytes (Couteau, Belzile et al. 1999).

At diplotene/diakinesis the homologous chromosomes condense and desynapse and the synaptonemal complex disassembles leaving bivalents attached at chiasmata signalling the end of prophase I (Ross, Fransz et al. 1996). In metaphase I the homologues align at the cell equator with the centromeres aligned to the poles before migrating in anaphase I. at telophase the chromosomes partially decondense but do not reach interphase conditions before the second meiotic division (Ross, Fransz et al. 1996).

Most, but not all meiosis specific mutants affect male and female meiosis equally (Caryl, Jones et al. 2003). The *mie1/ mcd1* mutant in *Arabidopsis* is reported to affect meiosis and is male-sterile female-fertile (He, Tirlapur et al. 1996). Meiocytes appear relatively normal in early prophase, however chromatin fragmentation is apparent around diplotene indicating disruption of DSB repair. Mutants display tetrad defects in which up to eight cells can be visualised instead of the usual four (He, Tirlapur et al. 1996, Ross, Fransz et al. 1997). Other male meiosis specific mutants include *KATA/ATK1* in which chromosomes fail to align at metaphase I, affecting chromatid segregation (Chen, Marcus et al. 2002).

Many mutants have been identified which disrupt reproductive development and meiosis. The severity and mechanism of these mutants in addition to the time and place are important considerations when characterising MAGO defects.

4.1.3 Chapter aim

MAGO proteins have been found to be expressed specifically in reproductive tissues during development though the purpose of MAGO in these tissues remains elusive. In this chapter, we aim to identify MAGO function during reproduction using maize MAGO knockdown lines. Using these tools, we aim to uncover the roles of MAGO in meiosis and reproductive development.

4.2 Results

4.2.1 *MAGO* RNAi results in pollen viability defects

MAGO1 and MAGO2 protein sequences show high levels of similarity (59.5%). While both proteins are expressed during meiosis in developing anthers (Figure 3.2), their temporal and subcellular accumulation is distinct (Figure 3.5). We first obtained *MAGO* single UniformMu transposon insertion lines (MaizeGDB; (McCarty, Mark Settles et al. 2005). However, although MAGO proteins appear to have functionally diverged, single *MAGO* mutants do not display a fertility phenotype (data not shown). This may indicate that MAGO proteins have retained redundant functions despite their differences in amino acid sequence. Since both MAGO proteins are preferentially expressed in early anther development (Figure 3.5), disruption of MAGO expression may lead to defects in reproductive development and male specific flower phenotypes. It is suspected that MAGO, like MEL1, is required for the normal progression of meiosis in maize anthers. To determine the function of MAGO proteins in maize we generated RNAi lines to simultaneously downregulate both *MAGO1* and *MAGO2* (GRMZM2G059033 and GRMZM2G123063). This was achieved by expressing a hairpin RNA containing 250bp of each *MAGO* coding sequence driven by the proVirCsVMV (see 2.1.3). We identified 19 lines carrying a single copy of the transgene (Appendix). To investigate the effect of downregulating *MAGO* expression, WT and RNAi lines were tested for pollen defects by Alexander's staining (Figure. 4.3). Among the 19 MAGO RNAi lines tested, significant pollen viability defects were observed in seven lines, which were selected for further analysis. Three lines (CM-08901O-2, CM-08902H-2, CM-08904E-2) were selected based on the significance of the pollen viability phenotype ($P < 0.01$) (Appendix)(R04,R08,R09 Figure 4.3). The selected RNAi lines

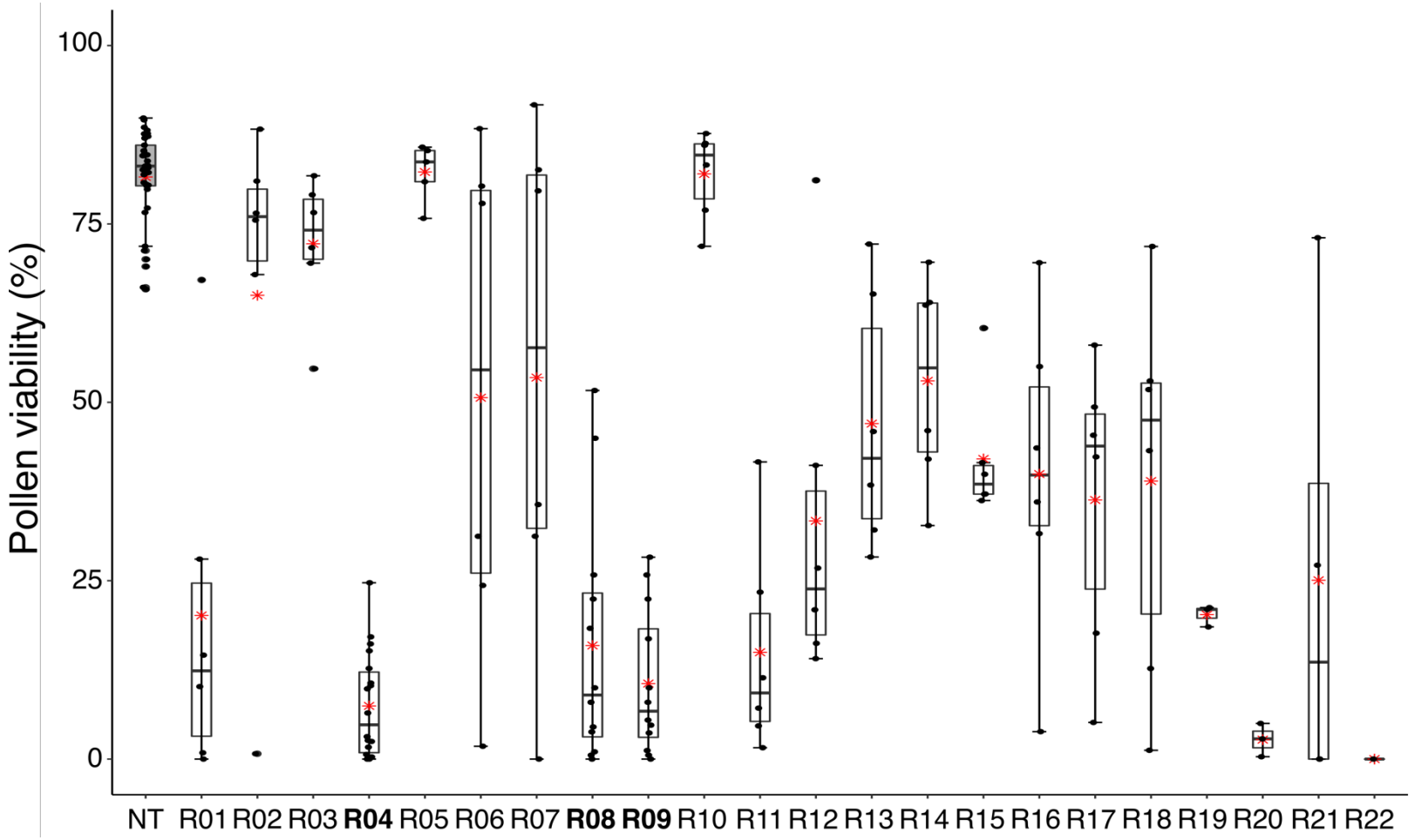

Figure 4.3: *MAGO RNAi* T3 lines show variable levels of male fertility. Pollen viability distribution determined by Alexander's staining of mature pollen in *MAGO RNAi* (lines R1-R22) compared to non-transgenic plants.

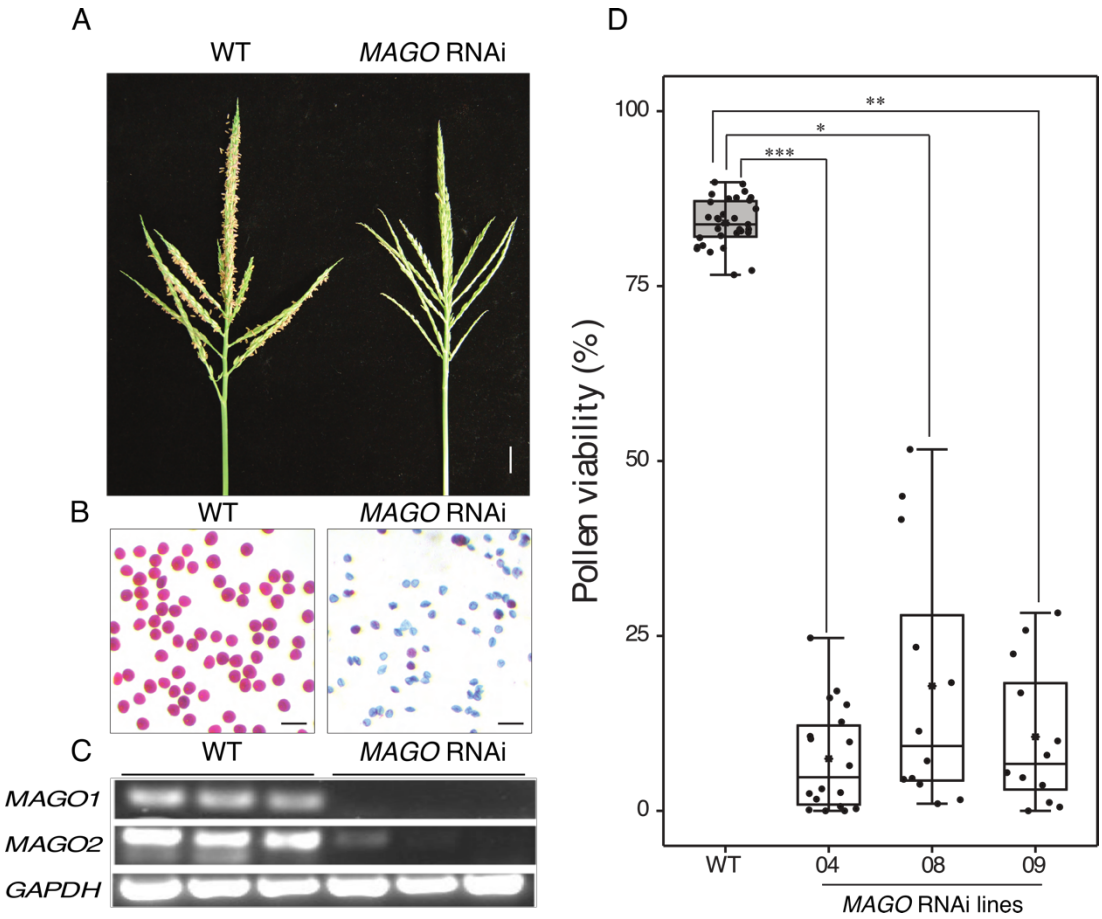

Figure 4.4: *MAGO* RNAi lines show reduced male fertility. (A) Representative tassel phenotype whereby *MAGO RNAi* anthers fail to emerge from florets (line R04) (bar = 5 cm).(B) Comparison between wild-type and *MAGO RNAi* pollen viability by Alexander's staining (line R04) (bar = 500 µm). (C) Expression level of *MAGO1* and *MAGO2* in RNAi lines compared to wild type expression (line R04). *GAPDH* was used as an RNA loading control. (D) Pollen viability (%) in 3 independent *MAGO RNAi* lines (R04, R08 & R09) compared with wild type (WT). Significant differences between groups were determined one-way ANOVA (*$P < 0.01$; **$P < 0.001$; ***$P < 0.0001$).

showed additional male flowering (tassel) defects such as failure to release anthers (Figure 4.4A) and a significant difference in male fertility when compared with WT (Figure 4.4D). Notably, these RNAi lines did not show defects in the female flower (ear), which were fully fertile after downregulated lines were backcrossed (data not shown). In order to evaluate the efficiency of the RNAi construct, wild type and selected *MAGO* RNAi lines were grown to maturity and the expression of *MAGO* genes was assessed by semi-quantitative RT-PCR in developing anthers. We found that the expression of *MAGO1* and *MAGO2* was below detection in the selected RNAi lines compared to wild type, indicating both genes were effectively downregulated (Figure 4.4C).

4.2.2 MAGO downregulation leads to a delay in male meiosis

Meiosis is divided into several distinct stages, prophase, metaphase, anaphase and telophase with prophase further divided into leptotene, zygotene, pachytene, diplotene and diakinesis. Since *MEL1* mutants are known to arrest early in leptotene of prophase I (Nonomura, Morohoshi et al. 2007), we monitored anther development, staining meiocytes with acetocarmine to assess whether *MAGO* RNAi lines showed similar meiotic defects. First, we mapped meiotic progression across wild type anthers of varying length. It has been reported that anther length strongly correlates with anther meiosis and development in the maize cultivar W23 and B73, and thus anther length is frequently used as a guide in maize meiotic studies (Figure 4.5A) (Ma, Skibbe et al. 2008, Zhai, Zhang et al. 2015). Consistent with reported data, anther length in the wild type A188 cultivar, which was used to generate *MAGO* RNAi lines, is also a good predictor of meiotic progression. Although, in this cultivar, meiosis appears to initiate at around

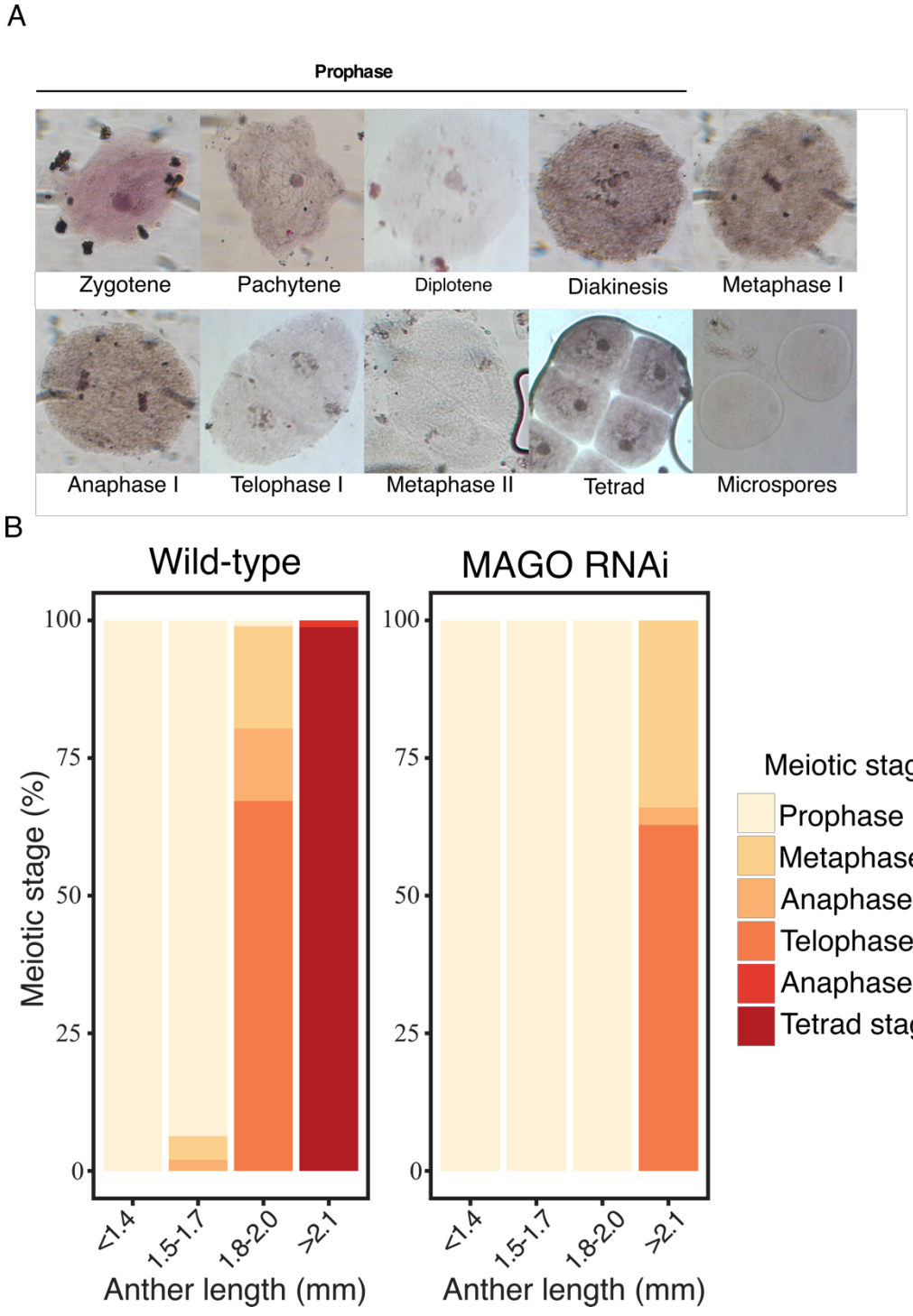

Figure 4.5 Meiotic development is delayed in MAGO downregulated lines. (A) Carmine red staining of meiotic chromosomes verified the relationship between anther length and meiotic stage. (B) Meiocytes were delayed in progressing from early prophase I in *MAGO* RNAi lines compared with wild type anthers.

1.3mm and concludes ~2.1mm, earlier than is reported for B73 (~1.5-2.5mm) (Appendix). We found that by 2.0 mm, almost all meiocytes had passed prophase I in wild type A188 anthers with 67% already in telophase (Figure 4.5B). Additionally, 98.7% of meiocytes had reached the tetrad stage by 2.1 mm (Figure 4.5B). In contrast, in RNAi lines meiocytes remained in prophase I even until 2.0 mm and had only entered telophase at 2.1 mm (Figure 4.5B). These results are consistent with the developmental delay observed in *mel1* rice mutants (Nonomura, Morohoshi et al. 2007).

Prophase I is subdivided into 5 stages, leptotene, zygotene, pachatene diplotene and diakinesis. A common defect observed in male sterile mutants is a delay of meiotic progression and this can be attributed to either early developmental defects such as in tapetal development or defects in meiosis. *MAGO* silencing clearly results in a delay in meiotic development that appears to originate in early prophase I around zygotene/pachytene (Figure 4.5B, Appendix). Additionally, we have shown MAGO2 localising to the meiocyte nucleus during meiosis (Figure 3.5). During these stages, double strand break repair, chromosomal structural organisational changes and the pairing of homologous chromosomes is thought to occur (Hamant, Ma et al. 2006).

In order to detect meiotic defects, meiocyte immunolocalisation was performed with antibodies specific to MAGO2 along with synaptonemal complex components ASY1 and ZYP1 to precisely determine the meiotic stage (Figure 4.6). We found that MAGO2 is strongly detected in association with meiotic chromosomes (Figure 4.6). However, we could not detect MAGO2 in meiocytes from RNAi lines indicating the efficiency of the RNAi construct (Figure 4.6). Meiocytes at zygotene stage allow us to detect components of the synaptonemal complex ASY1 and ZYP1. In the MAGO RNAi lines, in addition to loss of MAGO2 localisation, we found a disruption

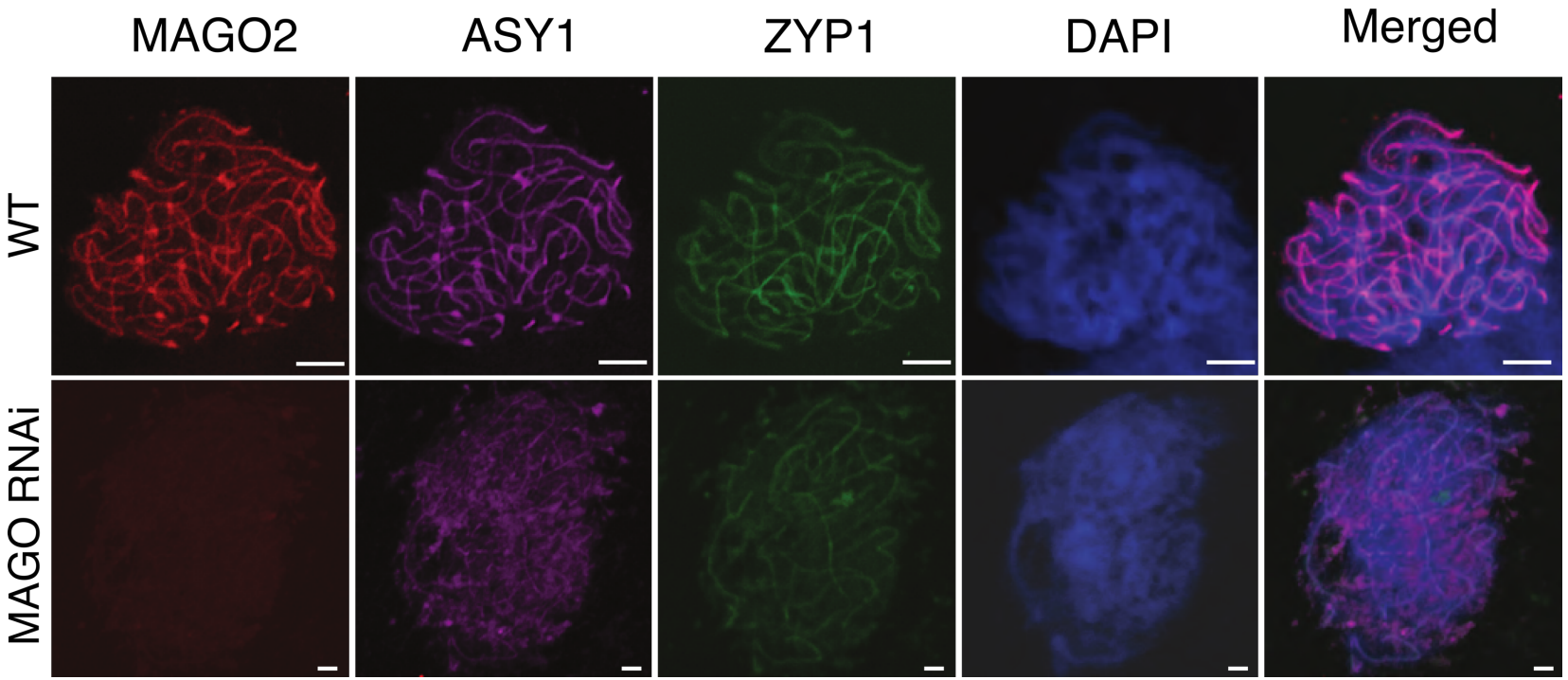

Figure 4.6: MAGO 2 associates with the meiotic chromatin during synapsis. Immunolocalisation for MAGO2 (red), ASY1 (magenta), ZYP1 (green) and chromosomes (blue) in male meiocytes of WT and RNAi. MAGO2 is labelled with Alexa Fluor 680; ASY1 is labelled with Alexa Fluor 594; ZYP1 is labelled with FITC and chromosomes are stained by DAPI (line R04) (bars = 5 µm).

in ASY1 localisation (Figure 4.6). Rather than associating with the axial elements, ASY1 accumulation appeared diffused and did not appear to associate with the synapsing chromosomes in meiocytes from RNAi lines. ASY1 is a synaptonemal complex component required for homologous chromosome synapsis in early prophase I which could account for the MAGO dependent meiotic defects we have observed (Armstrong, Caryl et al. 2002).

Summary

MAGO1 and MAGO2 are necessary for male reproductive development and downregulation of these genes causes, delays in meiotic progression and ultimately severe pollen viability defects in some cases, while female reproductive development appears unaffected. Furthermore, MAGO2 localises to the male meiocyte nucleus indicating possible roles in chromatin compaction, assembly of the synaptonomial complex and maintaining genome integrity during meiosis.

4.3 Discussion

Argonaute proteins are known regulators of developmental transition, maintaining transposon silencing and regulate gene expression through various small RNA mediated pathways (Baumberger and Baulcombe 2005, Olmedo-Monfil, Durán-Figueroa et al. 2010, Zhai, Zhang et al. 2015). The maize MAGO1 and MAGO2 proteins are expressed during male and female reproductive development and are associated with meiosis. MAGO proteins are similar in protein sequence but distinct in their temporal and spatial expression. Because of their sequence similarity, and the lack of single mutant phenotypes, MAGO proteins are thought to be at some level functionally redundant.

MAGO proteins are crucial for pollen development

A crucial step in dissecting their function was the generation of *MAGO* RNAi lines that simultaneously target both proteins. *MAGO* downregulation resulted in a marked reduction in male fertility in a number of independent RNAi lines, consistent with its expression in these organs (Figure 4.3 & 4.4). However, the fertility defects appear to be exclusive to the male germline as all lines could be successfully backcrossed with wild type pollen, with no apparent defects in female fertility nor impacts on seed set. While male infertility is consistent with MEL1 data, the expression data for MAGO proteins would suggest that the female should also display fertility defects (Nonomura, Morohoshi et al. 2007). We hypothesise that MAGO knockdown in the female inflorescence is compensated by other female specific, meiosis-associated Argonautes. AGO9 and AGO5 are both female meiosis-associated Argonautes known to control female gamete formation in *Arabidopsis* (Olmedo-Monfil, Durán-Figueroa et al. 2010, Tucker, Okada et al. 2012). Perhaps ZmAGO5a, a member of the same family as MAGO

proteins is able to compensate for MAGO downregulation in female reproductive development (Figure 3.3).

Tapetum development is another avenue for explaining the male specific fertility defect observed in *MAGO* RNAi lines. The tapetum is an anther specific tissue which is critical to nourish the developing meiocytes and must be specified, and degenerate in a timely manner (Twell 2011). Furthermore, because of its importance in male, but not female, reproductive development, many tapetal mutants have been identified from male sterility screens (Jung, Han et al. 2005, Kawanabe, Ariizumi et al. 2006, Nan, Zhai et al. 2016, Yi, Moon et al. 2016). In the case of *MAGO* RNAi, meiocytes appear normal, as do the somatic subepidermal anther cell layers (Figure 6.3). While the tapetum appears to develop normally, MAGO may be controlling tapetal gene expression or cell identity which could have profound impacts on pollen development.

MAGO2 localises to meiotic chromatin in male meiocytes

MAGO proteins accumulate in meiocytes during meiosis (Figure 3.5). Consequently, *MAGO* RNAi lines were severely delayed in early prophase I at zygotene/pachytene. This observation is sometimes seen in developmental mutants such as *eat1*. EAT1 accumulates in the tapetum and is responsible for inducing expression of the 24-nt reproductive phasiRNAs (Niu, Liang et al. 2013, Ono, Liu et al. 2018). Interestingly MAGO is known to bind the 24-nt phasiRNAs and the EAT1 pollen defects further support the MAGO/24-nt phasiRNA interaction. EAT1 meiocytes are delayed in early prophase I, but ultimately complete meiosis (Ono, Liu et al. 2018). EAT1 pollen viability defects are expected to be caused by tapetal defects, though

whether *MAGO* RNAi defects are a result of similar tapetal defects or by downstream 24-nt phasiRNA mediate processes is not known.

At zygotene/pachytene chromosome pairing has occurred and the synptonomial complex is forming (Hamant, Ma et al. 2006). Mutants affecting synapsis are known, for example loss of ZPY1 is known to lead to a severe delay in early prophase in addition to reduced seed set, however this affects both male and female fertility (Higgins, Sanchez-Moran et al. 2005). It is possible that MAGO plays a role in the formation of this complex in male meiocytes. Meiocyte immunolocalization shows that MAGO2 is associated with chromatin during pachytene and appears to colocalise with the components of the synaptonemal complex (Figure 4.6). Specifically, it appears alongside the axis associated ASY1. However, in RNAi lines this localisation could no longer be detected coinciding with mislocalisation of ASY1, thus suggesting that MAGO2 could be implicated in chromosome pairing during meiosis.

Leading up to meiosis, chromosomes must condense and pair, and this process requires the deposition of repressive histone marks (Prieto, Shaw et al. 2004). Recent work in with MEL1 has shown evidence of large-scale chromosome reprogramming in MEL1 mutants during meiosis, which could also be the case for MAGO (Liu and Nonomura 2016). However, it is not clear if chromatin remodelling is directly linked to MEL1 activity. Furthermore, it is not clear whether meiotic defects in *MAGO* RNAi lines is specific to meiosis or whether they also impact on mitosis. Further meiocyte immunolocalisations should therefore be carried out on anther mitoses in order to rule out a role for MAGO in general chromatin condensation.

Argonautes are additionally required for the effective silencing of transposable elements, such as the role of AGO5 in Arabidopsis ovule development. Animal PIWI proteins are also well known for their role in

silencing of transposable elements in the germ line (Kalmykova, Klenov et al. 2005, Houwing, Kamminga et al. 2007, Kuramochi-Miyagawa, Watanabe et al. 2008). During plant and animal germline development, dynamic epigenetic reprogramming takes place, though opportunistic transposable elements remain silent. It is possible MAGO proteins could regulate TE expression in the germ cells during meiosis, much like PIWI RNAs in some animals. Unregulated TEs in in the absence of MAGO function might lead to increased transposition, dsDNA breaks and genomic instability. Furthermore, these disruptions would activate cell cycle checkpoints leading to disruption or delay in meiosis such as we have observed in *MAGO* RNAi meiocytes.

5.0 The role of epidermal premeiotic sRNAs in male fertility

5.1 Introduction

5.1.1 Small RNAs as small mobile signalling molecules

Cellular processes such as development, the response to stress and disease resistance are all regulated by small mobile signalling molecules such as hormones and transcription factors. Small RNA is now regarded as also being a mobile signal with several reported examples (Hamilton and Baulcombe 1989, Voinnet and Baulcombe 1997, Voinnet, Vain et al. 1998). Small RNAs are able to move both locally from cell-to-cell or systemically over much greater distances. Once inside a target cell these small RNAs can be loaded into argonaute proteins before they are guided to their target mRNAs. The AGO-sRNA complex can then regulate target expression via various mechanisms, directing epigenetic changes by RdDM, RNA interference and translational repression of target transcripts (Hamilton and Baulcombe 1999, Baumberger and Baulcombe 2005, Li, Liu et al. 2013).

5.1.2 Local mobility of small RNA

sRNA-mediated silencing signals in plants are non-cell autonomous and so can spread locally cell-to-cell or systemically over long distances (Figure 5.1) (Dunoyer, Himber et al. 2005). Short distance mobile sRNA are predominantly 21-nt in length and can affect target expression up to 15 cells away (Himber, Dunoyer et al. 2003, Parizotto, Dunoyer et al. 2004, Martínez, Panda et al. 2016). These small RNAs can be critical for development or defence against pathogens. For example, tasiRNAs are known to form an adaxial to abaxial small RNA gradient in leaves (Fahlgren, Montgomery et al. 2006, Chitwood, Nogueira et al. 2009). This gradient is necessary to pattern the AUXIN RESPONSE FACTOR3 (ARF3) required for adaxial leaf determination. The *Arabidopsis* miR394 produces a developmentally critical

5.0 The role of epidermal premeiotic sRNAs in male fertility

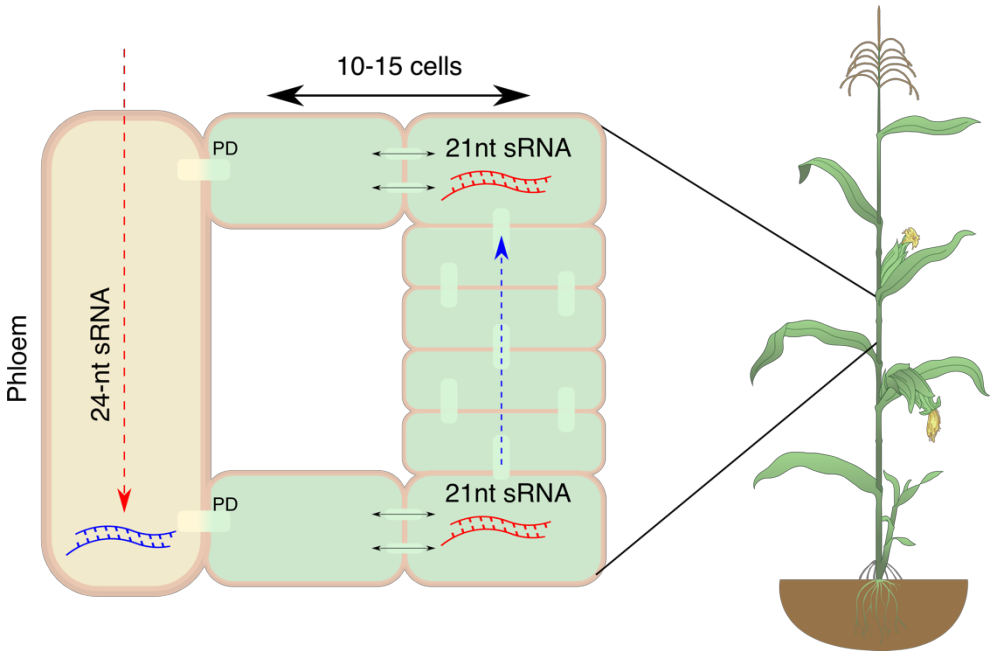

Figure 5.1: Schematic diagram illustrating the movement of sRNAs in plants. Various mechanisms allow for the movement of small RNAs in plants. 21-nt sRNAs can move locally cell-to-cell through the plasmodesmata (PD) over 10-15 cells. Long range root-to-shoot movement is also thought to take place through the PD (blue arrow). Additionally, long range shoot-to-root movement occurs through the phloem and directs DNA methylation to recipient cells. Additional local cell-to-cell movement through recipient cells also occurs.

inwardly decreasing gradient over three cell layers in the shoot apical meristem. This miRNA is expressed in the L1 layer and contributes to meristem cell maintenance by repressing the F box protein LEAF CURLING RESPONSIVENESS (LCR) in the subepidermal cells, which activates the WUSCHEL transcription factor (Knauer, Holt et al. 2013). In plant roots, endodermal microRNA165/6 acts non-cell autonomously by moving to the stele and regulating xylem patterning by targeting HD-ZIP III (Carlsbecker, Lee et al. 2010). Additionally, plant viral RNA and viral induced small RNAs are able to move locally and systemically, and contribute to naïve cell immunity (Nelson and Citovsky 2005, Voinnet 2005, Melnyk, Molnar et al. 2011). Therefore, the ability to move does not appear to be an exclusive characteristic of a distinct class of small RNAs.

The local sRNA signal is thought to spread via the plasmodesmata, a membrane lined channel which connects the endoplasmic reticulum and cytoplasm of adjacent cells (Maule 2008). This cytoplasmic continuum, called the symplast, allows for the exchange for small regulatory molecules and transcription factors between neighbouring cells and gradually declines as cells differentiate (Kim and Zambryski 2005). This is exemplified by the lack of cell-to-cell silencing observed in stomatal guard cells, provided they developed before the spread of the silencing signal (Voinnet, Vain et al. 1998).

The local RNA signal could be dsRNA or ssRNA. Micro bombardment of cells with both ds- and ss- RNA clearly demonstrate the movement of the dsRNA but not ssRNA (Dunoyer, Brosnan et al. 2010). However, similar microinjection studies failed to detect the movement of small dsRNAs (Yoo, Kragler et al. 2004). Whether or not the dsRNAs require accessory proteins is also not known, although many viruses are known to produce movement proteins that aid the cell-to-cell movement and transmission of viral RNA

through the plasmodesmata (Hong and Ju 2017). The size limit of plasmodesmata is dynamic and it is regulated throughout plant development. The upper size limit was once thought to be relatively small (~27 kDa) though it is now established that molecules up to 70kDa can be transported between neighbouring cells, which may permit the movement of larger protein/RNA complexes (Imlau, Truernit et al. 1999, Brunkard and Zambryski 2017).

Although no mutants have been identified that lack plasmodesmata, some mutants do impact their formation or function. The *Arabidopsis* mobile sRNA root-to-shoot signal appears to be regulated by reactive oxygen species (ROS), which are thought to control plasmodesmata permeability through cell wall remodelling (Liang, White et al. 2014). In *RCI3* (*Rare Cold Inducible 3*) mutants, ROS homeostasis is compromised, leading to the disruption of plasmodesmata and impaired RNA silencing transduction from the root to the shoot. Other genes have been identified in *Arabidopsis* that enhance or reduce the silencing signal but they often belong to RNAi silencing pathway (Himber, Dunoyer et al. 2003, Smith, Pontes et al. 2007, Melnyk, Molnar et al. 2011). However, it is not clear whether these genes are required to generate the silencing signal and/or for its movement.

5.1.3 Systemic small RNA movement

The local movement of RNA silencing signals can only cover 10-15 cells, though some small RNAs have targets in distal tissues of the plant (Figure 5.1) (Himber, Dunoyer et al. 2003). For such long-distance transport of the RNA silencing signal, the small RNAs must be transported to the phloem, in order to access the rest of the organism. Grafting experiments have clearly identified small RNAs as a mobile signal which can alter the epigenetic of their distal recipient cells (Yoo, Kragler et al. 2004, Buhtz, Springer et al.

2008, Molnar, Melnyk et al. 2010, Lewsey, Hardcastle et al. 2016). However, it is not yet clear whether this signal is ssRNA or dsRNA. Analysis of phloem sap suggests the mobile signal is single stranded, however both miRNA and miRNA* were found in equal abundance. The miRNA* is usually degraded upon miRNA incorporation into RISC, therefore systemic movement is expected to be AGO independent (Yoo, Kragler et al. 2004, Buhtz, Springer et al. 2008). *Arabidopsis* grafting experiments have shown that the systemic sRNAs are predominantly of the 24-nt class and that these mobile signals tend to move from shoot to root (Molnar, Melnyk et al. 2010). This is supported by the finding of 24-nt sRNAs in the phloem sap of *Brassica napus* while the xylem is completely devoid of detectable sRNA (Buhtz, Springer et al. 2008). Systemic movement is additionally not exclusive to 24-nt sRNAs as other RNA species including miRNAs, 21-nt siRNAs mRNAs and virus induced RNAs (viRNAs) have been detected in phloem sap and are also known to act systemically (Yoo, Kragler et al. 2004, Haywood, Yu et al. 2005, Pant, Buhtz et al. 2008, Dunoyer, Brosnan et al. 2010).

The phloem sap environment is nuclease free and known to stably harbour single stranded mRNA molecules for systemic transport (Doering-Saad, Newbury et al. 2002). Therefore, the free, phloem transport of a systemic single stranded RNA silencing signal is possible. Equally though, the RNA silencing signal could be transported in association with RNA binding proteins. Indeed, many plant RNA binding proteins have been identified. Though a role for these proteins is not clear, they are likely important for post-transcriptional gene regulation, development and the response to stress (Voinnet and Baulcombe 1997, Yoo, Kragler et al. 2004, Lin, Lee et al. 2009). Analysis of pumpkin (*Cucurbita maxima*) phloem sap for example led to the identification of Phloem Small RNA Binding Protein1 (PSRP1). This sRNA binding protein binds selectively to 25-nt ssRNA but not to dsRNA. This

lead to the conclusion that PSRP1 is involved in the local and systemic control over developmental processes in plants and equivalent RNA binding proteins have been identified in cucumber (*Cucumis sativus*) and lupin (*Lupinus albus*) (Yoo, Kragler et al. 2004).

5.1.4 Suppressors of silencing as tools to analyse sRNA mobility

RNA mobility is difficult to analyse as it is not often possible to uncouple sRNA biogenesis with mobility. Very few mutants exist that are defective only in sRNA movement and such mutants likely impact all sRNA species in addition to other important mobile signals (Liang, White et al. 2014). Grafting of plants deficient in RNA silencing is traditionally employed to investigate systemic movement of sRNAs but this is not feasible when trying to understand local cell-to-cell movements of sRNA silencing signals (Palauqui, Elmayan et al. 1997, Voinnet and Baulcombe 1997).

To dissect the local movements of sRNAs, viral suppressors of silencing are frequently used to disrupt these processes (Voinnet, Pinto et al. 1999, Dunoyer, Schott et al. 2010). During viral infection, dsRNA and imperfect dsRNA hairpins are produced, which are recognised by DCL proteins resulting in the production of viRNAs. These viRNAs are incorporated into RISC not only to silence viral mRNAs but they can also move locally and systemically to provide viral immunity to distal naïve cells (Voinnet 2005). Viruses have evolved many mechanisms to overcome viral induced RNA silencing and to promote infection, and these mechanisms have been discovered in almost all plant viruses (Voinnet 2005).

The tombusviral P19 protein promotes the movement and pathogenicity of the virus (Voinnet, Pinto et al. 1999). This is a result of the P19 proteins affinity to bind to and sequester 21-nt small RNA duplexes and preventing their incorporation into the RISC (Silhavy, Molnár et al. 2002, Chapman,

Prokhnevsky et al. 2004, Lakatos, Szittya et al. 2004). In addition to sequestering sRNAs, the Cucumber mosaic virus suppressor 2b can also bind to and disrupt argonaute activity. The 2b protein has been shown to directly interact with AGO1 and AGO4 through the PIWI and PAZ domains and reduce both slicer activity and their ability to methylate target loci (Zhang, Yuan et al. 2006, Hamera, Song et al. 2012).

Viral suppressors of silencing can additionally impact host transcription to promote infection. For example the Geminiviral Transcriptional activator protein (TrAP) C2 is essential for pathogenesis and post-transcriptional gene silencing suppression (van Wezel, Dong et al. 2002). Mungbean yellow mosaic virus (MYMV) AC2 protein is a strong activator of viral transcription and affects the expression of around 30 host transcripts including *WERNER EXONUCLEASE-LIKE 1* (WEL1), a known negative regulator of host RNA silencing (Trinks, Rajeswaran et al. 2005).

Finally the potyvirus Helper Component Proteinase (HCPro), is a multifunctional protein with several known activities including promoting aphid transmission, genome amplification and long distance movement of viral mRNAs (Atreya and Pirone 1993, Kasschau, Cronin et al. 1997, Anandalakshmi, Pruss et al. 1998, Brigneti, Voinnet et al. 1998). HCPro is also known interact with DCL1 and to specifically sequester 21-nt dsRNAs (Kasschau, Xie et al. 2003). Sequestering sRNAs appears to be a common strategy for viral suppressors of silencing in order to prevent the silencing of viral mRNAs by the host (Dunoyer, Lecellier et al. 2004, Mérai, Kerényi et al. 2006). The ability of HCPro proteins to specifically target 21-nt sRNAs RNAs make perfectly suitable for dissecting the role of the 21-nt phasiRNAs in maize.

3.1.5 Chapter aim

By targeting the expression of the viral *HCPro* to the anther epidermis and thus sequestering 21-nt dsRNA, we aim to demonstrate the importance of the epidermally derived sRNAs in male gamete development.

5.2 Results

5.2.1 Ectopic expression of viral *HCPro* in maize anthers leads to male infertility

The helper component proteinase (HCPro) can bind to and sequester 21nt-dsRNA and has been routinely used as a tool to sequester small RNAs and to uncover their roles in development (Anandalakshmi, Pruss et al. 1998, Dunoyer, Lecellier et al. 2004). Constitutive expression of HcPro is known to cause developmental defects in *Arabidopsis* due to the disruption of developmentally important miRNAs (Kasschau, Xie et al. 2003). Therefore, a chemically (Dexamethasone) inducible *HcPro1* (*indHCPro*) expression construct was generated and stably transformed in maize (Figure 5.2A) (see 2.2.3). Eight lines were assessed by northern blot analysis to detect the expression of the expression of LhGR and *HcPro* in leaves and by western blot to detect the accumulation of HCPro protein after Dex treatment (data not shown). Three independent lines with good levels of induction were selected by monitoring the expression of a GUS reporter in leaves after exposure to a chemical inducer Dex. The developing tassel is embedded deep within the leaf whorl and so is not easily accessible. Thus, to test whether *HCPro* could be chemically induced in developing anthers, seven-week-old *indHCPRO* maize plants were dissected to reveal the tassel, and a 50μM DEX solution was introduced into the floret cavity encapsulating the developing anthers (see 2.4.8) (Figure 2.2). Three days after treatment, the GUS reporter could be detected along the length of the anther locules in three independent lines (Figure 5.2B), thus confirming the transgene could be efficiently induced. To confirm that *HCPro* was induced after DEX treatment, antibodies were raised against the full length recombinant HCPro protein (See 2.4.4) (Appendix). Antibodies were purified against isolated

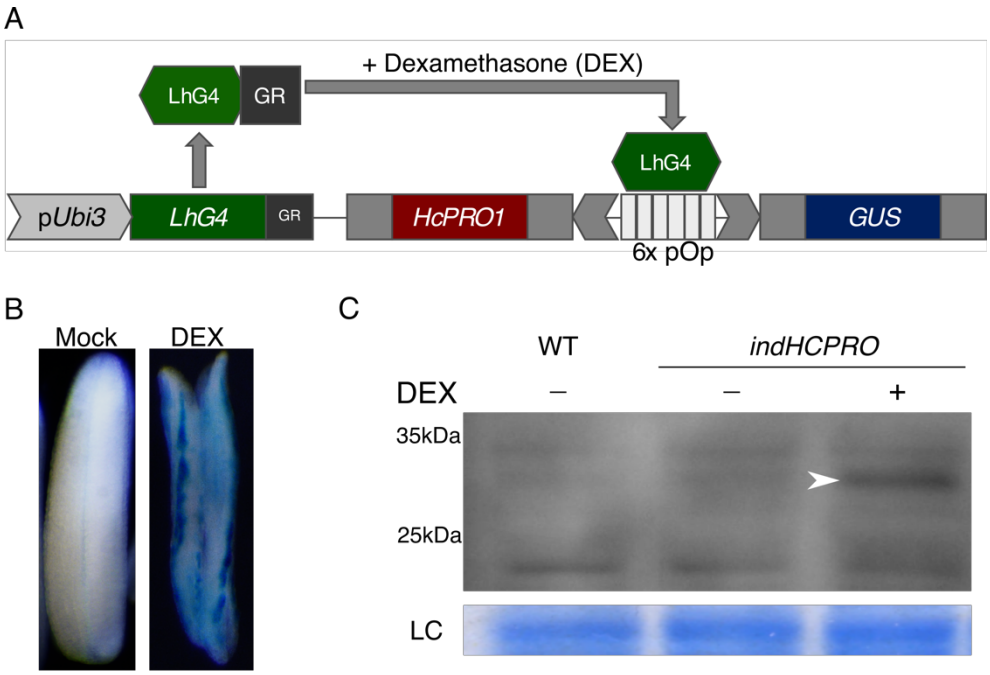

Figure 5.2: A chemically-induced two-component transcriptional activation system used to ectopically express *HCPro* in developing anthers. (A) A Schematic diagram of DEX-inducible pOp transactivation vector transformed in maize. Ubi3, ubiquitin 3 promoter; LhG4, synthetic transcription factor LhG4; GR, Glucocorticoid receptor; 6x pOp, minimal lac operator; GUS, β-glucuronidase. (B) GUS staining of anthers in the HC-Pro inducible lines after mock (left) or DEX (right) treatments after 3 days. (C) HCPro protein expression can be detected by western blot only after DEX induction (white arrow) (3 days post treatment). (LC, loading control).

recombinant HCPro and used in immunoblotting detection using protein extracts from induced leaf tissues. We found that we could detect the accumulation of HCPro (28.2 kDa) only in leaves of plants treated with the chemical inducer (Figure 5.2C). To further investigate the impact of *HCPro* induction in male fertility, we chemically induced the expression of *HCPro* in developing anthers. After induction plants were grown for five days and pollen viability was assessed in treated mature anthers by staining the pollen grains with Alexander staining solution. We induced *HCPro* expression both before and after meiosis to ascertain whether sequestering sRNAs at a defined developmental stage had an effect on male fertility. The viability of pollen inside of stained anthers was quantified by counting viable and nonviable pollen grains with empty anthers scoring 0. Pollen staining in mock induced *indHCPro* anthers indicated that viable pollen is produced (Figure 5.3A) and this is comparable to wild type pollen viability levels observed in A188 (~75% viability ratio) (Figure 4.4D). We found that pre-meiotic induction led to a significant decrease in pollen viability compared to mock induced plants indicated by a lack of pollen staining in anthers (Figure 5.3A). Staining pollen of mature anthers indicated the production of non-viable pollen after meiotic induction of *HCPro*. Additionally, meiotic induction of *HCPro* resulted in a significant reduction in pollen viability with many pollen staining blue, though not as strong as that seen with pre-meiotic induction of *HCPro*. (Pre-meiotic induction, ~30% viability ratio $p < 0.01$; meiotic induction, ~55% viability ratio $p < 0.05$) (Figure 5.3B).

HCPro is known to bind 21-nt sRNAs to help RNA viruses to evade the plant RNA silencing defence mechanisms (Kasschau, Xie et al. 2003). To determine if HCPro is binding to sRNAs in anthers, we collected chemically induced anthers at pre-meiotic and meiotic stages and immunoprecipitated HCPro, thus allowing us to sequence bound sRNAs. We found that, as expected, 21-

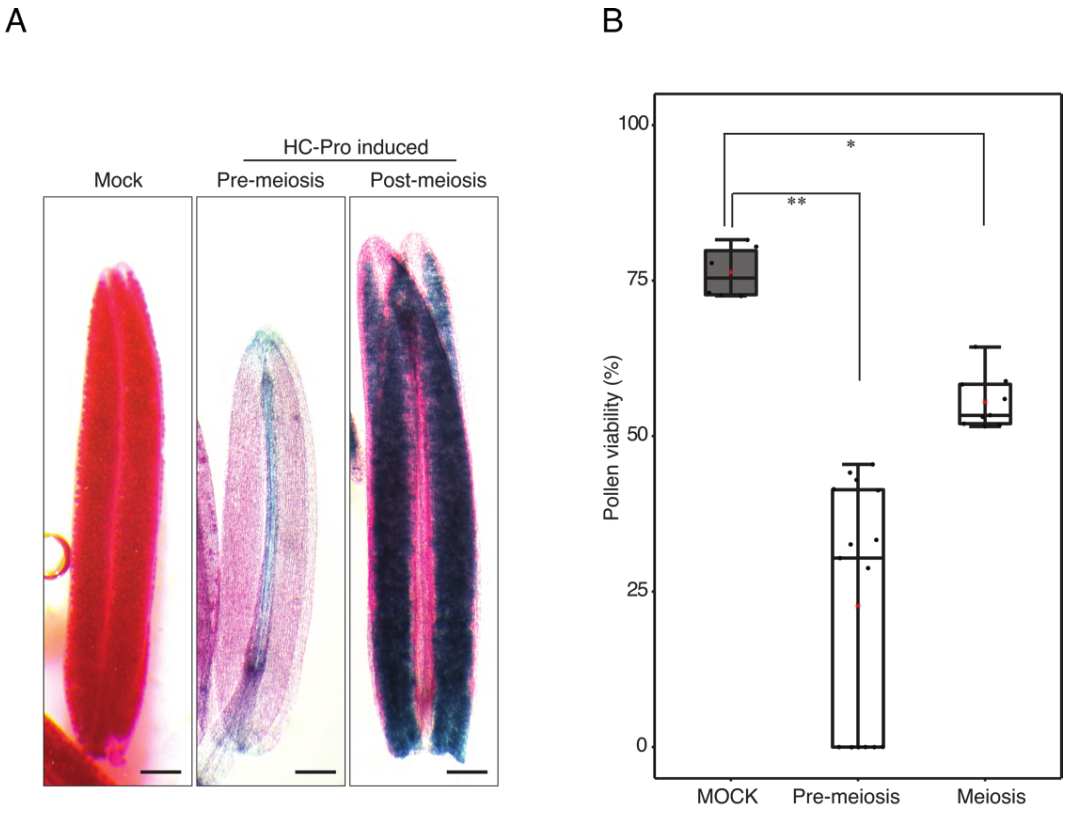

Figure 5.3: Male fertility is impaired after HCPro is ectopically expressed in developing anthers. (A) Comparison of pollen viability among mock premeiotic induction (left), pre-meiotic induction of HC-Pro (middle) and post-meiotic induction of HC-Pro (right) via Alexander's staining. Viable pollen stains red (left), non-viable pollen stains blue (right) and empty anthers stain clear (middle) Scale bars, 100 µm. (B) Pollen viability distribution in mock (left) and HC-Pro lines after pre-meiosis induction (middle) and meiotic induction (right) (A significant p-value resulting from a one-way ANOVA test indicates *$P < 0.01$; **$P < 0.001$).

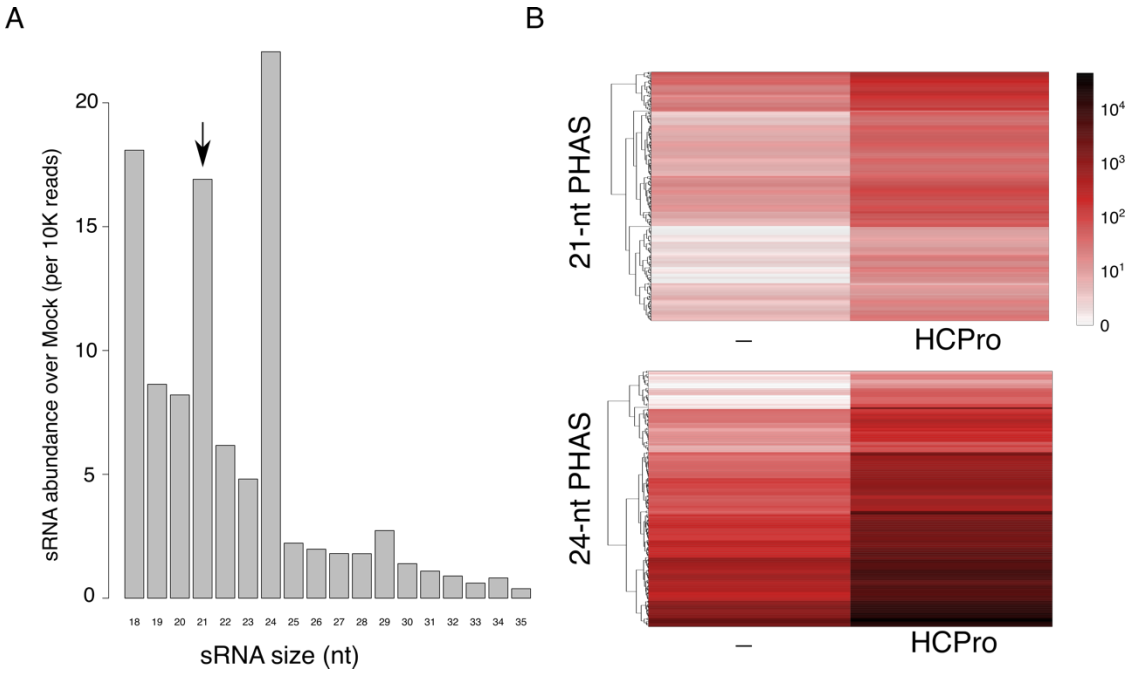

Figure 5.4: Ectopic induction of HCPro sequesters sRNAs in anthers. (A) Relative sRNA abundance of sRNAs bound to HcPro in premeiotic anthers. 21-nt sRNAs (arrow) and 24-nt sRNAs are enriched in the HCPro fraction (Mock values subtracted). (B) Abundance (log10 normalised hits) of 21-nt and 24-nt phasiRNAs bound to HCPro compared to mock induced anthers.

nt sRNAs were bound to HCPro but we also detected 24-nt and 18-nt sRNAs (Figure 5.4A). Additionally, we found the 21-nt and 24-nt phasiRNAs were highly abundant in the HCPro fraction (see Table 8.1) (Figure 5.4B). The ectopic induction of *HCPRO* in developing anthers led to male infertility (due to the production of non-viable pollen) especially when HCPro was expressed in premeiotic anthers, however, these defects could be caused by the capture of sRNAs that may be essential to the development of the different anther cell types (Figure 4.1). To specifically express HCPro in the anther epidermis, the source of 21-nt phasiRNAs, we crossed our *indHCPro* line with 3 independent epidermal trans-activation lines (*pHDZIV6:LhG4*). We determined the epidermal expression of these transgenic lines by monitoring the expression of a tdTomato reporter (Figure 5.5). The reporter was found to accumulate in the anther epidermis throughout anther development, which is consistent with expression of *HDZIV6* (Vernoud, Laigle et al. 2009) (Figure 5.5). We found that the reporter was also detected in the anther endothecium, but expression was not detected in any other cell layer nor in the developing meiocytes. To determine if the p*HDZIV6:LhG4* could drive the expression of *HCPro* in the anther epidermis, we collected developing p*HDZIV6>>HCPro* anthers and used them for Immunolocalization assays using our immunopurified HCPro antisera (See 2.4.4). We found that HCPro proteins were predominantly detected in the anther epidermis and endothecium in p*HDZIV6>>HCPro* and absent in non-transgenic lines, in agreement with the reporter expression (Figure 5.5C).

If the movement of the 21-nt phasiRNAs from the anther epidermis is necessary for male fertility, the ectopic expression of *HCPro* in these cells should affect male fertility. Moreover, it is expected that the p*HDZIV6>>HCPro* lines would have a pollen viability defect consistent with

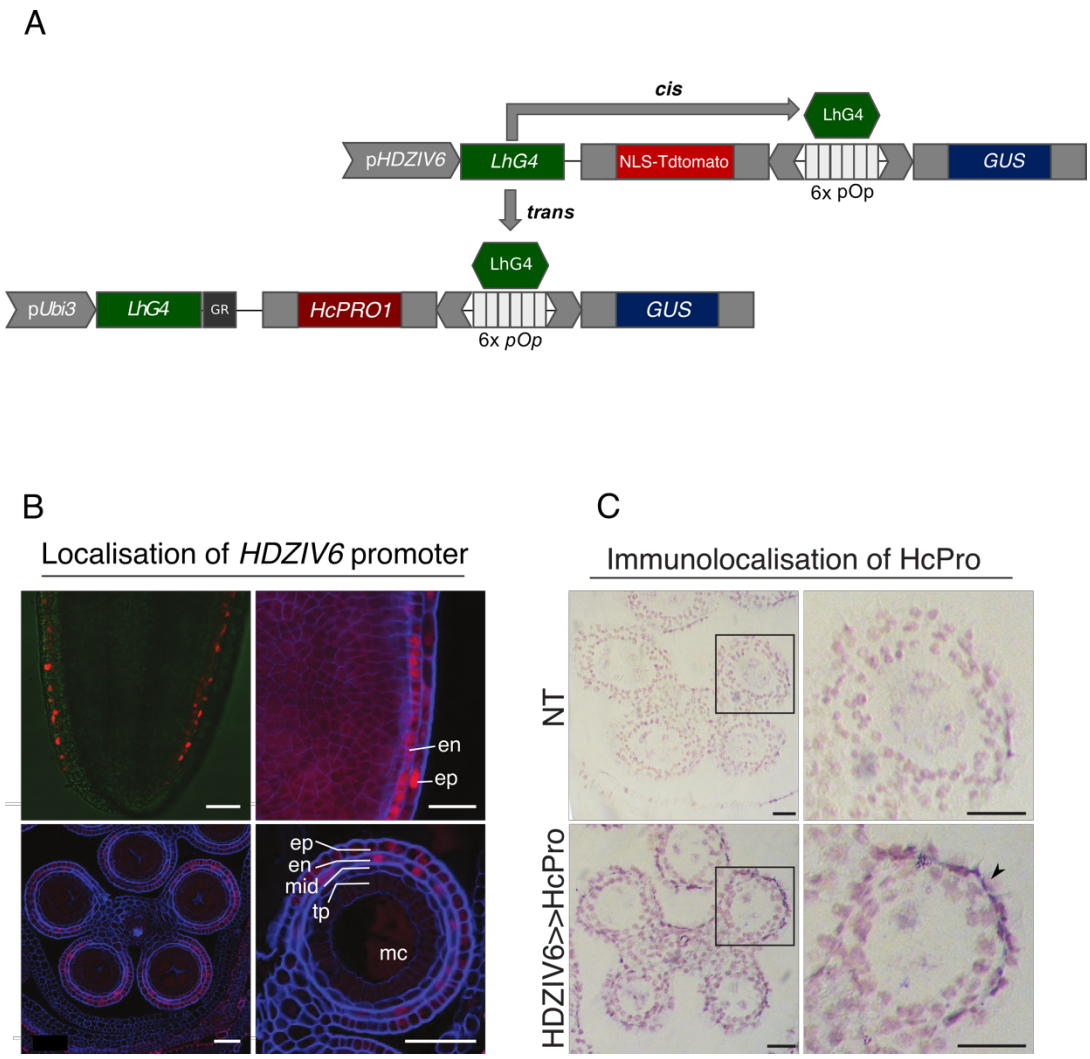

Figure 5.5: Epidermal expression of *HCPro* using a two-component transactivation system. (A) Schematic diagram of trans-activated HC-Pro induction system. pHDZIV6, promoter of the Homeodomain leucine zipper IV 6; NLS-Tdtomato, RFP reporter; Ubi3, ubiquitin 3 promoter; LhG4, synthetic transcription factor LhG4; GR, Glucocorticoid receptor; 6x pOp, minimal lac operator; GUS, β-glucuronidase. (B) Promoter activity of homeodomain leucine zipper IV 6 (HDZIV6) in developing anthers of maize. Scale bars, 50 µm. (C) Immunolocalisation of HC-Pro in anthers of non-transgenic (NT) and HDZIV6 transactivated HC-Pro (pHDZIV6>>HC-Pro) lines. Scale bars, 50 µm.

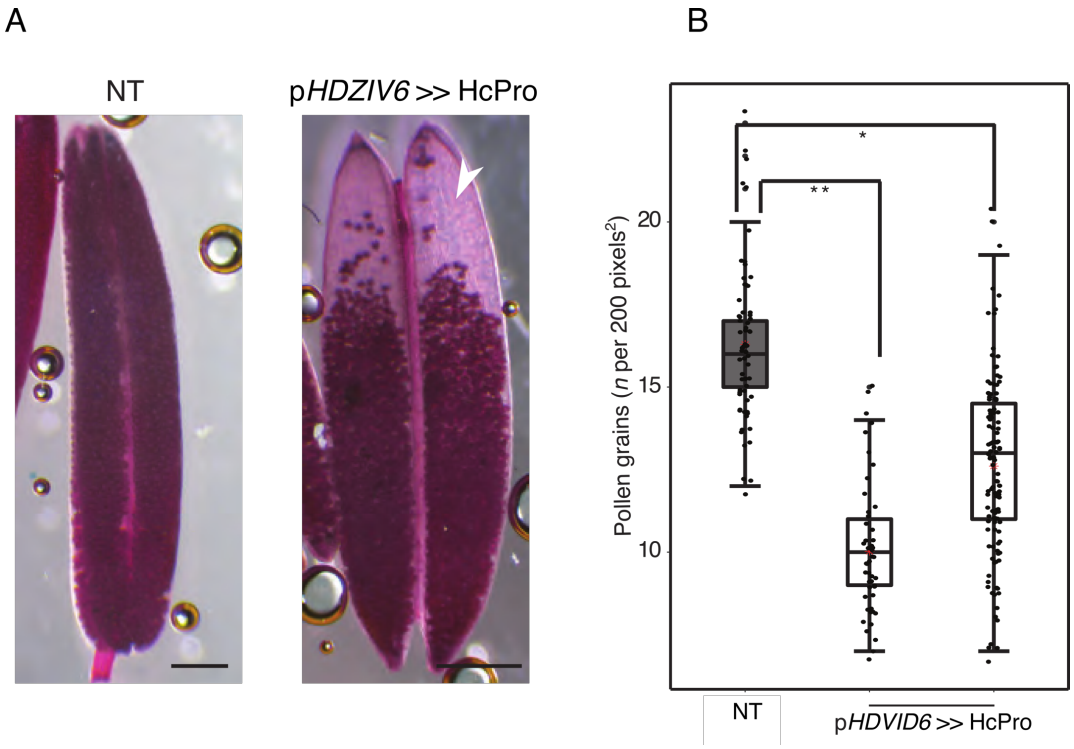

Figure 5.6: Pollen production is reduced in *pHDZIV6 >> HcPro* transactivated lines. (A) Comparison between anthers of non-transgenic (left) and HC-Pro trans-activated by the *HDZIV6* promoter (right). Anthers frequently presented empty locules (white arrow). Scale bars, 100 µm. (B) Pollen density (pollen grains per 200 pixels^2) in non-transgenic (NT) and two independent *HDZIV6>>HCPRO* trans-activated lines (A significant p-value resulting from a one-way ANOVA test indicates*$P < 0.01$; **$P < 0.001$).

the downregulation of *MAGO*. We assessed male fertility in p*HDZIV6>>HCPro* lines by staining mature anthers by Alexander's staining and found these anthers to be depleted of pollen grains (Figure 5.6A). Additionally, we measured pollen density in these anthers and found a significant decrease in both p*HDZIV6>>HCPro* lines tested when compared with the non-transgenic control lines (n=2; *P < 0.01; **P < 0.001) (figure 5.6B)

Summary

We have used a two-component transactivation system to regulate temporally and spatially the expression of the viral suppressor of silencing HCPro in maize anthers. Expression of *HCPro* in anther epidermis results in reduced fertility only when induced before meiosis. Furthermore, fertility defects were maintained when *HCPro* expression was restricted to the outer anther soma. These findings suggest that small RNAs accumulating in anther epidermis are strictly necessary for the development of the male gametes in maize.

5.3 Discussion

The biogenesis of phasiRNAs in maize is thought to take place in the developing anther epidermis. Before meiosis the anther epidermis accumulates the mature miR2118, the long non coding RNAs that act as precursors of PHAS, and MAGO1 (Figure 3.5) (Zhai, Zhang et al. 2015). We have already established that MAGO 1 and 2 are necessary for meiosis. However, the need for the 21-nt phasiRNAs, which bind to MAGO proteins was unexplored. For phasiRNAs to directly impact on meiocyte development, they would need to move from the anther epidermis in-ward towards the tapetum or the developing meiocytes.

Generating PHAS mutants to disrupt the production of the phasiRNAs is not feasible as there are approximately 463 21-nt PHAS loci and at least 7 miR2118 triggers. Lines expressing a short tandem target mimic (STTM) could be generated to disrupt the phasiRNA biogenesis pathway in maize anthers by sequestering miR2118. Such lines are routinely used and have already been demonstrated in both animals and plants but would require the generation of new maize transgenics (Tang, Yan et al. 2012, Yan, Gu et al. 2012, Canto-Pastor, Santos et al. 2019). To dissect the molecular function of the phasiRNAs, we ectopically expressed *HCPro* in developing anthers taking advantage of maize *ind*HCPro lines we already generated and characterised.

The ectopic expression of *HCPro* in pre-meiotic anthers resulted in severe pollen defects, while *HCPro* expression in anthers undergoing meiosis caused a mild reduction in pollen viability (Figure 5.3). The results suggest that the 21-nt sRNAs sequestered by HCPro are vital for male gamete development in maize. Moreover, the function of these sRNAs are especially critical before meiosis. These results are consistent with maize male sterile mutants defective in 21-nt phasiRNA. Mutants defective in OCL4, an HD-ZIP

IV family of plant-specific transcription factors involved in epidermal patterning, are partially male sterile (Vernoud, Laigle et al. 2009). These mutants display defects in the production of phasiRNAs, causing male sterility phenotype similar to those found in *MAGO* RNAi (Zhai, Zhang et al. 2015). However, these results would be strengthened by the addition of mock treatments post meiosis anthers and by the addition of non-transgenic treatment controls. This would determine the impact Dex treatment has on anther development both pre- and post-meiosis.

HCPro is expected to specifically and non-discriminately sequester 21-nt double stranded sRNAs of any class. Many different 21-nt sRNAs are produced during reproductive development with diverse roles such as timing developmental transition and epigenetic reprogramming in the germline (Peragine, Yoshikawa et al. 2004, Slotkin, Vaughn et al. 2009, Zhang, Xia et al. 2012). Indeed, sequencing of the HCPro bound sRNAs revealed that, although HCPro can bind 21-nt phasiRNAs, many other classes of 21-nt and 24-nt sRNAs were sequestered (Table 8.1). Of note is the enrichment of the 24-nt phasiRNAs in the HCPro IP fraction. 24-nt phasiRNAs are primarily localised to the tapetum and meiocytes (Zhai, Zhang et al. 2015). It appears then that HCPro is not just binding the 21-nt dsRNAs but many classes of sRNAs. Furthermore, DEX may be inducing HCPro in internal cell layers such as the tapetum, maybe even the developing meiocytes.

Epidermal expression of *HCPro* is sufficient to disrupt male fertility

To specifically target epidermal sRNAs including the phasiRNA pathway we controlled the expression of *HCPro* using the epidermal two-component transactivation system (Figure 5.5). Using this technique, we were able to precisely target the expression of *HCPro* to the anther epidermis before meiosis. Furthermore, *HCPro* expression in these cells should sequester the

21-nt sRNAs including the 21-nt phasiRNAs and prevent them from moving to the meiocytes. As expected, we discovered a significant fertility defect in the transactivated lines, though this fertility defect was less severe than that observed in *ind*HCPro anthers (Figure 5.6). It is likely the reduced severity is caused by reduced HCPro dosage. HDZIV6 is an epidermal transcription factor and thus the *proHDZIV6* we use to drive *HCPro* expression is certainly weaker than direct *HCPro* induction by DEX.

HDZIV>>HCPro anthers produced fertile pollen, though the pollen density in these lines was significantly decreased. Additionally, large gaps with no pollen grains were observed in some anther locules. Interestingly this phenotype resembles *ROXY1* and *ROXY2* mutants in *Arabidopsis*, in which abaxial pollen mother cells degenerate early in development resulting in empty locules (Xing and Zachgo 2008). ROXY1 and ROXY2 are both redundant glutaredoxins thought to control male gamete development through cellular redox regulation. It is now well established that cellular redox state heavily impacts intercellular transport through the plasmodesmata, including sRNAs (Stonebloom, Brunkard et al. 2011, Liang, White et al. 2014). This therefore supports our work to disrupt phasiRNA movement in developing maize anthers. Several maize male sterile lines are also known to affect the redox potential (Kelliher and Walbot 2012, Wang, Nan et al. 2012). It would therefore be interesting to test the pollen viability in maize lines which are disrupted in their plasmodesmata transport (such as mutants with disrupted redox homeostasis) to determine their impact on sRNA mobility. Furthermore, the plasmodesmata could be disrupted by treating anthers with H_20_2 (Kelliher and Walbot 2012). Alternatively, the phenotype observed for *pHDZIV6>>HCPro* could be a due to disruptions in somatic cell layer development in early anthers, a common feature in several male sterility mutants (Walbot and Egger 2016). While anthers appeared

normal, histological analysis of these lines should be carried out to ensure that cell pattering in pre-meiotic anthers is normal.

6.0 The role of MAGO proteins in male fertility under heat stress

6.0 The role of MAGO proteins in male fertility under heat stress

6.1 Introduction

6.1.1 Stress response during anther and pollen development

As sessile organisms, plants are highly sensitive to environmental stresses such as extreme temperature, drought, and salinity stress. Stress is critical during reproductive development, particularly anther (Peet, Sato et al. 1998, Erickson and Markhart 2002, Mesihovic, Iannacone et al. 2016, Ma, Min et al. 2018). This is especially important for cereal crop production, which are known fail to set fruit under elevated temperatures due do male infertility (Rudich, Zamski et al. 1977, Prasad, Craufurd et al. 2001, Dewan, Vander Mijnsbrugge et al. 2018). With climate change resulting in more extreme weather conditions, understanding how plants respond to temperature stress during reproduction could aid the development of crops with improved heat tolerance (Blum, Klueva et al. 2001, Benlloch-González, Sánchez-Lucas et al. 2018).

A critical step in the development of male reproductive lineages is the formation of archesporial cells, which must be correctly specified in the early anther (Results 4.1) (Bedinger and Fowler 2009, Kelliher and Walbot 2011). Archesporial cells must then complete microsporogenesis and microgamatogenesis to successfully produce pollen. During microsporogenesis, the meiotic cell division leads to the production of haploid microspore tetrads and ends with the separation of the microspores by tapetal secreted enzymes (Bedinger and Fowler 2009). During microgamatogenesis, the microspores enlarge and undergo an asymmetric cell division Pollen Mitosis I (PMI) resulting in a small generative cell which is engulphed by the larger vegetative cell (Borg, Brownfield et al. 2009). The generative cell finally undergoes Pollen Mitosis II (PMII) to produce twin sperm cells.

The process of anther and pollen development requires the coordinated expression of many genes both temporally and spatially (Boavida, Becker et al. 2005). This precisely choreographed developmental plan is highly sensitive to external stresses, which can affect early soma development, cell pattering, meiosis, pollen germination , pollen tube growth and fertilisation (Peet, Sato et al. 1998, Rang, Jagadish et al. 2011). Specific processes within development and between species are more sensitive to heat stress than others. In *Arabidopsis* short premeiotic heat stress (40°C 4 hrs) led to male specific meiotic defects and later stages failed release from the pollen sac indicating the stage specific sensitivity (Kim, Hong et al. 2001). In Tomato, plants grown under moderately elevated temperature, whole vegetative growth appeared normal and only anthers were effected (Sato, Kamiyama et al. 2006).

Tapetal defects and premature programmed cell death of the tapetum is a common theme in male-sterile mutants and it appears to also be the case in many cases heat sensitivity (Ahmed, Hall et al. 1992, Jung, Han et al. 2005, Nan, Zhai et al. 2016, Walbot and Egger 2016). In cowpea, male sterility induced by heat stress (30°C night) results from defects in endothecium development and a premature degeneration of the tapetum (Ahmed, Hall et al. 1992). In wheat, heat stress (30°C 3d) results in premature degeneration of the tapetum, leading to complete male sterility. Additionally, in some anthers, microspores completed meiosis successfully, however microspores became disorientated from the tapetum and undergo cell cycle arrest(Sakata and Higashitani 2008). Heat stress (30°C day/25°C night 5d) during barley reproductive development results in male sterility, however this is highly dependent on the timing of stress induction. Early heat stress at the 4 leaf stage leads to premature degradation of tapetum cells and premature synapsis of meiotic prophase (Sakata and Higashitani 2008). The

tapetum is clearly important for male development. Successful male reproductive development is dependent on correct tapetum differentiation and degeneration. When tapetum degeneration is inhibited or delayed, pollen development is affected resulting in male sterility (Kawanabe, Ariizumi et al. 2006). It has been suggested that the very involvement of programmed cell death in anther development may be the reason male fertility is more sensitive to environmental stresses (Sakata and Higashitani 2008).

6.1.2 Transcriptional changes associated with heat stress in male reproductive development

Developing anthers undergo the same general and specific transcriptional changes in response to temperature stress as vegetative tissue (Bita, Zenoni et al. 2011). These transcriptional changes include, the silencing of DNA polymerases, replication licencing factors and histones, and upregulation of lipid transfer proteins (LTPs), meiosis specific genes such as *Asy1* , Heat Shock Proteins (HSPs) and abiotic stress factors in rice (Zhang, Li et al. 2012). When rice panicles are heat stressed, they appear to transcriptionally resemble older panicles, which could account for the premature degradation of the tapetum. Additionally, LTP has been shown to be pro-apoptotic and accumulate in tapetum cells prior to degeneration, which could also contribute to male-sterility phenotype (Crimi, Astegno et al. 2006). Silencing of replication factors and DNA polymerases could account for the arrest of anther development which is often observed in heat stressed rice (Zhang, Li et al. 2012).

Heat stress transcription factors (Hsfs) and HSPs are inherently involved in the heat shock response (Kotak, Larkindale et al. 2007, Keller and Simm 2018). HSPs are molecular chaperones that refold denatured, misfolded and

aggregated proteins, one of the main damaging effects of high temperature (Bukau, Weissman et al. 2006). There are several classes of HSPs including Hsp100, Hsp90, Hsp70, Hsp60 and the small HSPs and their expression is controlled by Hsf transcription factors (Scharf, Berberich et al. 2012). Many studies have shown the upregulation of HSP and Hsf after heat stress in male reproductive development in many different species (Oshino, Abiko et al. 2007, Frank, Pressman et al. 2009, Zhang, Li et al. 2012, Li, Lawas et al. 2015). In addition to maintaining protein homeostasis in the cytosol, chaperones such as Hsp70/DnaJ and Hsp90 along with the ER folding machinery are necessary for the unfolded protein response that is also activated by heat stress (Rieu, Twell et al. 2017). The unfolded protein response mitigates stress induced damage by increasing the ERs capacity for protein folding and is essential for pollen development, germination and fertilisation (Fragkostefanakis, Mesihovic et al. 2016). The proteins bZIP60, bZIP28 and bZIP17 are known to elicit the unfolded protein response and bZIP60 is highly expressed in microspore and tapetal cells (Iwata, Fedoroff et al. 2008). Moreover *bZIP28* null mutants are temperature sensitive and the *ire1a ire1b* double knockout mutant required for *bZIP60* splicing, is male sterile at elevated temperatures (Deng, Srivastava et al. 2016). Additionally, tapetal defects were detected in the double mutant at high temperatures, likely a result of the tapetal requirement of the unfolder protein response to maintain active secretion during heat stress.

6.1.3 Reactive oxygen species scavenging during heat stress

Reactive oxygen species (ROS) are well known to be rapidly generated during stress in plants, and they induce transcriptional changes to maintain homeostasis and prevent oxidative cell damage (Volkov, Panchuk et al. 2006, Cheng, Yun et al. 2007, Veal, Day et al. 2007). In addition to their cellular

toxicity, ROS also acts as a signalling molecule regulating many stress responses such as biotic and abiotic stress and in developmental processes (Baxter, Mittler et al. 2013). The steady state of ROS must therefore be tightly controlled and plants encode many ROS-scavenging and ROS-producing enzymes (Mittler, Vanderauwera et al. 2004). Under heat stress, ROS-scavenging enzymes are upregulated to suppress ROS accumulation which would otherwise result in oxidative cell damage (Mittler, Vanderauwera et al. 2004, Driedonks, Xu et al. 2015).

ROS and ROS scavenging enzymes are important factors for male reproductive development. During early anther development, hypoxic conditions are known to trigger archesporial cell differentiation by MSCA1 and *Arabidopsis* ROXY1 and ROXY2 are known to regulate development through the cellular redox state (Xing and Zachgo 2008, Kelliher and Walbot 2012). Additionally ROS is shown to be involved in tapetal programmed cell death in both *Arabidopsis* and rice (Hu, Liang et al. 2011, Xie, Wan et al. 2014, Yi, Moon et al. 2016). Furthermore, a reduction of ROS in rice and *Arabidopsis* mutants leads to delay in tapetal programmed cell death resulting in male sterility. Consequently high levels of ROS in rice leads to premature tapetum programmed cell and pollen defects among other oxidative stress phenotypes (Hu, Liang et al. 2011, Luo, Xu et al. 2013). Tight control of ROS is clearly vital for pollen development and the involvement of ROS signals in male reproductive development, particularly tapetum development, are the likely cause of male temperature sensitivity.

6.1.4 Stress induced Transposable element activity

Stress-responsive regulatory elements (SREs) are frequently present in LTR retrotransposon and MITE transposons that are responsive to external stress both biotic and abiotic (Yasuda, Ito et al. 2013). These TE SREs result

in the stress-induced transcription of transposons and consequently neighbouring genes (Cavrak, Lettner et al. 2014). Additionally, heat stress is known to release epigenetic regulation such as DNA methylation from many genes and repetitive elements (Pecinka, Dinh et al. 2010, Tittel-Elmer, Bucher et al. 2010). *Arabidopsis ONSEN*, a Ty1/copia LTR retrotransposon, is activated by heat stress (Ito, Gaubert et al. 2011, Ito, Yoshida et al. 2013). During heat shock *ONSEN* is demethylated and transcription is activated upon binding of HSFA2, a native plant heat induced transcription factor and has been shown to generate novel ONSEN insertions in mutants defective in epigenetic silencing (Cavrak, Lettner et al. 2014). Interestingly, activity of ONSEN is higher in dividing tissue where the heat shock response is more pronounced but is not activated in non-stressed plants deficient in DNA methylation pathways (Cavrak, Lettner et al. 2014). Similarly, rice Miniature *Ping* (*mPing*) is an active miniature inverted-repeat TE that can also be induced by stress (Yasuda, Ito et al. 2013). Both *mPing* and *ONSEN* insertions into gene promoters sometimes act as stress-induced cis regulatory elements (Yasuda, Ito et al. 2013, Cavrak, Lettner et al. 2014). It is now generally accepted that TEs might function to drive rapid genome evolution to adverse conditions and stress, conferring novel gene functions (Dubin, Scheid et al. 2018).

While TEs might represent a source of genomic variation for plants, they must be controlled to prevent unregulated transposition events that are often detrimental to plant health and fitness due to mutations and genomic rearrangements (Lisch and Bennetzen 2011). TEs are controlled by epigenetic silencing pathways including DNA methylation, chromatin modifications and small RNAs (Feschotte 2008, Ito, Gaubert et al. 2011). TE silencing is especially important in the germline, where transposition events could be heritable.

In addition to siRNAs, tRNA derived fragments are also generated during the plant stress response and are linked to the silencing of TEs (Raina and Ibba 2014). tRNA-derived fragments are 18-26-nt sRNA fragments originating from the targeted cleavage of tRNA transcripts in eukaryotes (Honda, Loher et al. 2015, Chen, Yan et al. 2016, Sharma, Conine et al. 2016, Schorn, Gutbrod et al. 2017) (Figure 6.1A). 5'tRFs are the most abundant form of tRNA derived fragment, generated from the DCL1 dependent cleavage of the tRNA D-loop while 3'tRNAs are generated from T-loop cleavage (Cole, Sobala et al. 2009, Martinez, Choudury et al. 2017). Additionally tRNA-halves (tRHs) are generated by the anticodon cleavage by DCL1 resulting in the production of 5'tRH and 3'tRHs (Thompson, Lu et al. 2008). Several studies have linked tRFs to TE suppression, specifically the LTR retrotransposons (Martinez, Choudury et al. 2017, Schorn, Gutbrod et al. 2017). LTR retrotransposons exploit tRNAs for their replication. During reverse transcription of an LTR RNA molecule, tRNAs are used prime reverse transcription by binding to the primer binding site (PBS) (Figure 6.1B) (SanMiguel and Vitte 2009). Furthermore, both TEs and tRFs have been shown upregulated by stress and mutations in processors of tRNAs such as RNaseP cause sterility in *Drosophila* (Hsieh, Lin et al. 2009, Thompson and Parker 2009, Hackenberg, Huang et al. 2012, McCue, Nuthikattu et al. 2012, Molla-Herman, Vallés et al. 2015). This sterility is caused by derepression of TEs and activation of DNA damage checkpoints in germ cells. Due to their expression in the male reproductive program, tRFs silence stress-induced TEs such as LTR retrotransposons to prevent transposition events in the developing gametes (Schorn, Gutbrod et al. 2017).

In animals, PIWI Argonaute proteins and piRNAs regulate germline development (Brennecke, Aravin et al. 2007). Both PIWI proteins and piRNAs are absolutely essential for maintaining silencing of TEs during

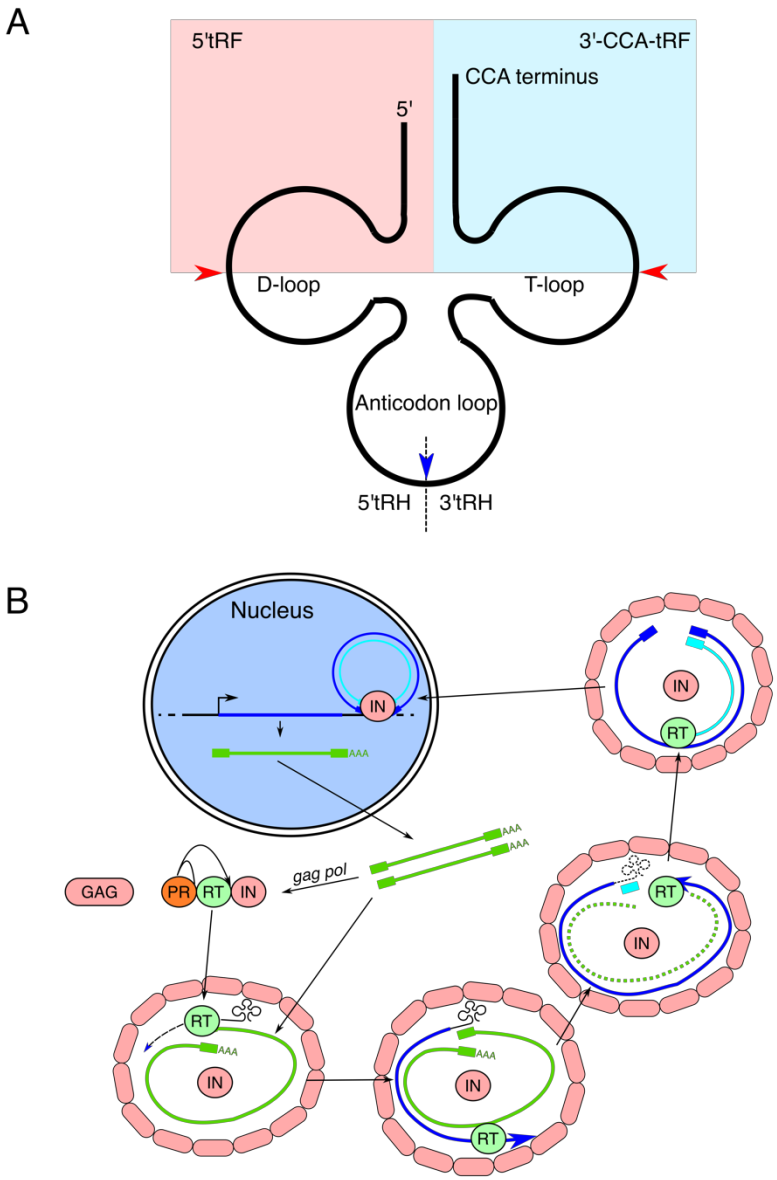

Figure 6.1: tRNAs and tRNA derived fragments are associated with LTR retrotransposon activity. (A) Cleavage of a tRNA molecule in the D-loop or T-loop (red arrows) generates 18-26-nt 5'tRFs and 3'tRFs respectively. If the cleavage event takes place in the anticodon loop (blue arrow), tRNA halves are generated. (B) Transcription of an LTR retrotransposon generates RNA (green) that is exported to the cytoplasm. Here, the LTR derived *gag* and *pol* mRNAs are translated. GAG assembles into the Virus-Like Particle. Reverse transcription is initiated by the annealing of the tRNA to the primer binding site (PBS) (clover shape). Plus strand synthesis occurs and once the PBS has been synthesized, the tRNA is degraded followed by integration of the nascent retrotransposon at a new genomic location by IN. IN: integrase, RT: reverse-transcriptase, GAG: structural protein. (SanMiguel and Vitte 2009)

spermatogenesis (Carmell, Girard et al. 2007, Houwing, Kamminga et al. 2007). Disruption of the PIWI pathway leads to activation of LINE1 and IAP retrotransposon TE families and results in meiotic arrest at zygotene to pachytene stage, enhanced double strand breaks and altered histone and transcriptome profiles, and ultimately male sterility which is enhanced by stress (Carmell, Girard et al. 2007, Kuramochi-Miyagawa, Watanabe et al. 2008, Manakov, Pezic et al. 2015).

6.1.5 Chapter aim

To determine the role of MAGO proteins in male fertility under heat stress by performing whole-genome transcriptome analyses.

6.2 Results

6.2.1 MAGO RNAi male infertility is enhanced by temperature stress

Heat stress negatively affects plant development and leads to disruption of gene expression, the altered timing of development and the activation of silenced transposons (Qu, Ding et al. 2013). Reproductive development is particularly sensitive to heat stress, especially the development of the male reproductive lineages (Kim, Hong et al. 2001). Additionally, specific developmental stages within male gamete development are more sensitive to heat stress than others, particularly before meiosis (Ahmed, Hall et al. 1992, Sakata and Higashitani 2008, Walbot and Egger 2016). We have found that MAGO proteins preferentially bind to a specific 5'tRf during anther development (Results 3.2.5). TRfs are reported to play essential roles in regulating the plant stress response and silence transposable elements (Thompson and Parker 2009, Martinez, Choudury et al. 2017). To understand if MAGO proteins are involved in the heat stress during male gamete development, lines that downregulate *MAGO1* and *MAGO2* were stressed at different stages of anther development. We assessed male fertility defects by staining mature anthers with Alexander's staining solution after heat stress. Pollen staining of wild type pollen indicated the production of viable pollen after pre-meiotic heat stress. However, RNAi fertility was significantly affected by heat stress before meiosis, and staining indicated the production of non-viable, abnormal pollen (Figure 6.2A). When we induced heat stress during meiosis, both wild type and *MAGO1/2* RNAi plants did not show defects in male fertility and pollen development (Figure 6.2). Heat treatment appears to be catastrophic for pre-meiotic development in RNAi lines (13% viability ratio) compared to wild type (91%

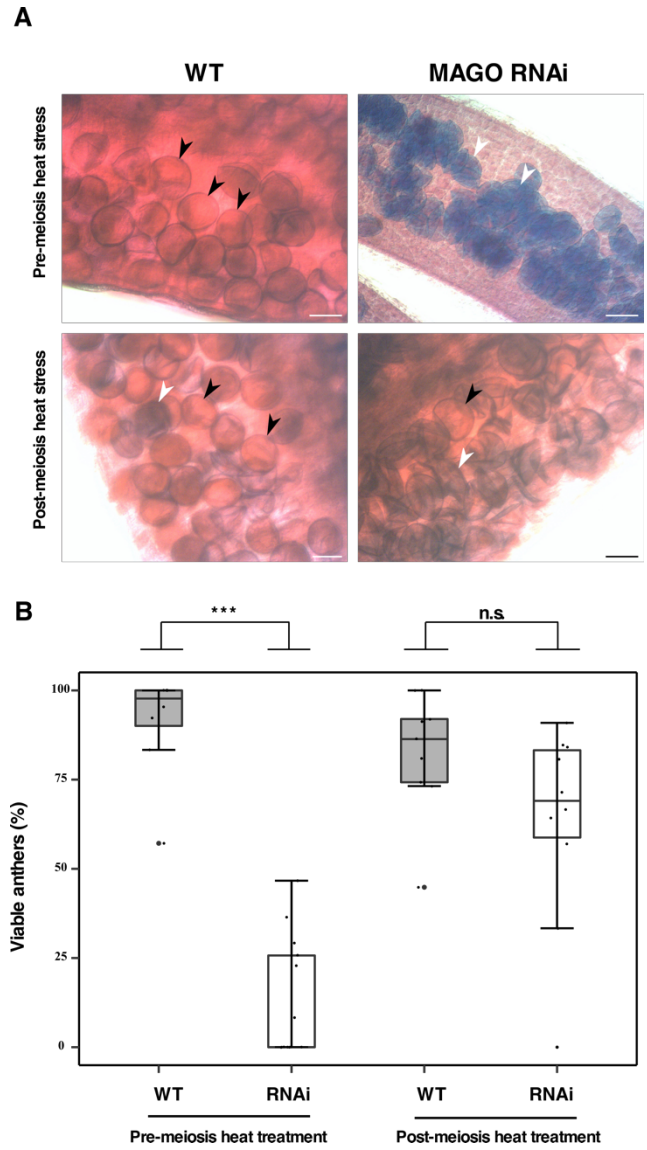

Figure 6.2: MAGO1/2 are required before meiosis for heat stress responses. (A) Observation of anther viabilities between WT (top left panel) and RNAi (top right panel) after pre-meiosis heat treatment 35ºC for 3 days via Alexander's staining of anthers (top panels). Comparison between anthers between WT (bottom left panel) and RNAi (bottom right panel) after post-meiosis heat treatment (bottom panels). Scale bars, 100 µm. Black arrow heads, viable pollen; white arrow heads, non-viable pollen. (B) boxplot of pollen viability in WT and RNAi plants under control and heat conditions. Error bars indicate standard deviations; WT pre-meiotic heat (n = 131), RNAi pre-meiotic heat (n = 84), WT post-meiotic heat (n = 166), RNAi post-meiotic heat (n = 63). A significant p-value resulting from a one-way ANOVA test indicates ***$P < 0.0001$; ns, not significant.

viability ratio). These results suggest that MAGO proteins are necessary before meiosis protect against stress and to confer heat stress response in maize anthers. To test this hypothesis, we compared pollen viability of *MAGO* knockdown lines grown under control (28°C day/25°C night) and heat stress (35°C day/25°C night) conditions. Under control conditions, wild type plants were fully fertile with the majority of pollen appearing viable, while *MAGO1/2* RNAi plants displayed a mild reduction in fertility, with a mixture of viable and non-viable pollen (Figure 6.3). Furthermore, when these lines were exposed to heat stress before meiosis, wild type pollen viability was unaffected. However, *MAGO1/2* RNAi male fertility was reduced and pollen viability was significantly altered (Figure 6.3).

6.2.2 *MAGO* RNAi lines display morphological defects after heat stress

Male sterility phenotypes are frequently the result of defects in somatic subepidermal anther development (Walbot and Egger 2016). Additionally, it is these cell layers that are particularly sensitive to heat stress (Ahmed, Hall et al. 1992, Walbot and Egger 2016). To determine if *MAGO1/2* RNAi impacts anther wall patterning, we investigated the impacts of heat stress on anther morphology in RNAi lines after pre-meiotic heat stress (35/25°C). Under control conditions, all five anther cell types appeared normal in wild type anthers. Additionally, no observable defects could be observed in *MAGO* RNAi anthers (Figure 6.4). The somatic cell layers of wild type plants after pre-meiotic heat stress appeared relatively normal, but with some mild disorder to the somatic cell layer boundaries. Despite these defects, wild type plants ultimately produce viable pollen, comparable to control

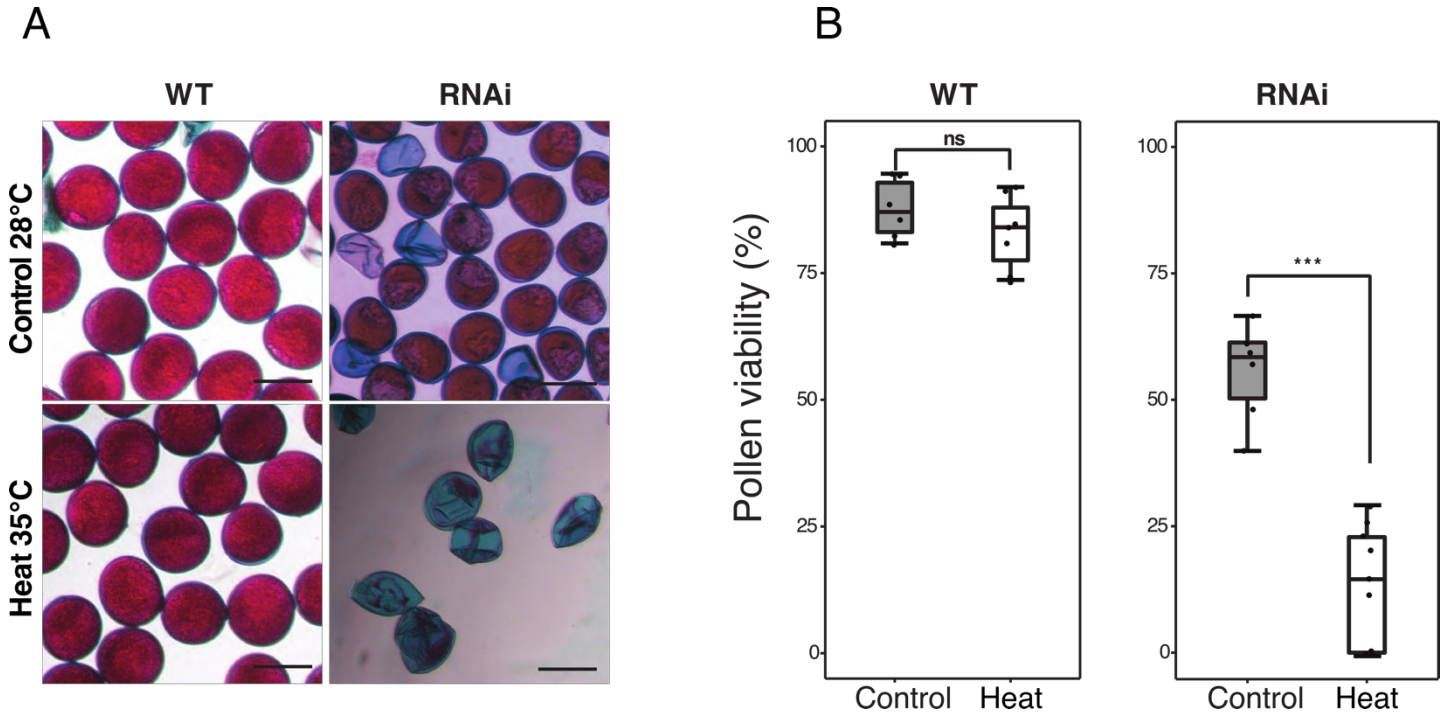

Figure 6.3: MAGO1/2 are required for male fertility under heat stress. (A) Comparison of pollen viabilities between WT and *MAGO* RNAi plants under control conditions (28°C) (top left and right panels) and heat treatment (35°C)(bottom left and right panels). Scale bars, 50 µm. (B) Comparison of pollen viability distribution in WT between control and heat conditions (left). Pollen viability distribution in WT (left graphs) and RNAi plants (right graphs) under control and heat conditions (A significant p-value resulting from a one-way ANOVA test indicates ***$P < 0.0001$; ns, not significant).

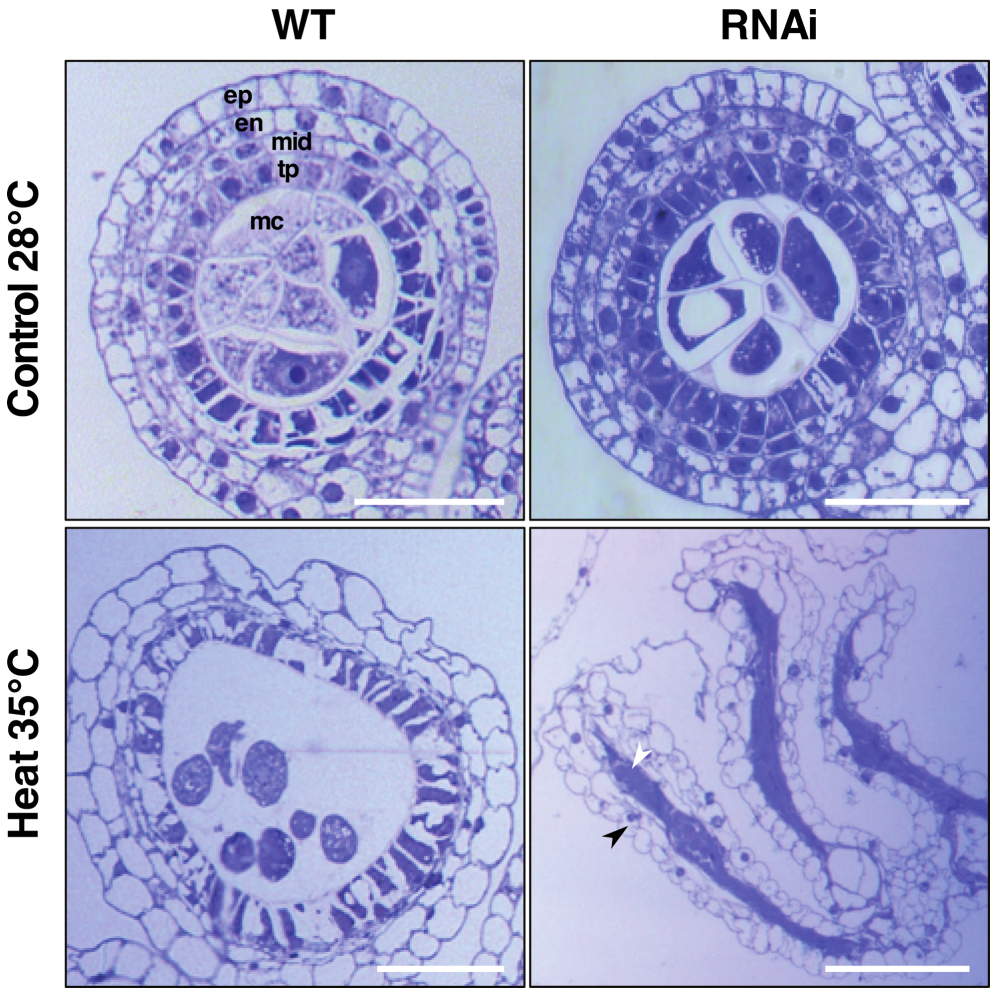

Figure 6.4: Heat stress negatively impacts anther morphology in *MAGO* RNAi. Transverse sectional comparison between WT (left two panels) and RNAi (right two panels) anthers under control (top two panels) and heat (bottom two panels) conditions. RNAi lines are highly sensitive to heat stress. Anthers have highly disorganized epidermal and endothecial like cell layers (black arrow) and degenerated middle, tapetal and meiocyte cells (white arrow). Scale bars, 50 µm. ep, epidermis; en, endothecium; mid, middle layer; tp, tapetum; mc, meiocyte.

conditions (Figure 6.3). RNAi anthers display catastrophic morphological defects after pre-meiotic heat stress. The meiocytes, tapetum, middle layer and endothecium appear to have degenerated completely with only an epidermal like layer and occasional endothecium cells remaining (Figure 6.4).

6.2.3 Transcriptome analysis of anthers under heat stress

Upon exposure to stress, plants must harness complex regulatory networks and alter gene expression to adapt and overcome this physiological burden. Plants can use hormonal signalling and transcription factors to alter the expression of genes in response to stress or alternatively they can use diverse epigenetic mechanisms to regulate the stress response (Abe, Urao et al. 2003, Boyko and Kovalchuk 2008). Argonaute proteins are essential components of the epigenetic silencing machinery and are required to direct repressive epigenetic marks (Zhang, Xia et al. 2015). Consequently, Argonaute proteins and sRNAs are essential for plant stress responses (Jones-Rhoades and Bartel 2004, Sunkar and Zhu 2004). *MAGO* downregulation results in a male fertility defects that are temperature dependent. To identify the transcriptional changes taking place in *MAGO* knockdown lines, we sequenced RNAs from the anthers of wild type and *MAGO* RNAi lines under control and heat stress conditions. We conducted pairwise comparisons between all groups and we detected 2721 differentially expressed transcripts, the majority of which were detected when comparing wild type plants grown in control and heat stress conditions (Figure 6.5) (FDR < 0.01 and fold change cut-off of 2). We found 1209 differentially expressed transcripts belonging to genes that were affected by heat treatment and 119 differentially expressed transcripts belong to genes affected by genotype indicating that heat stress

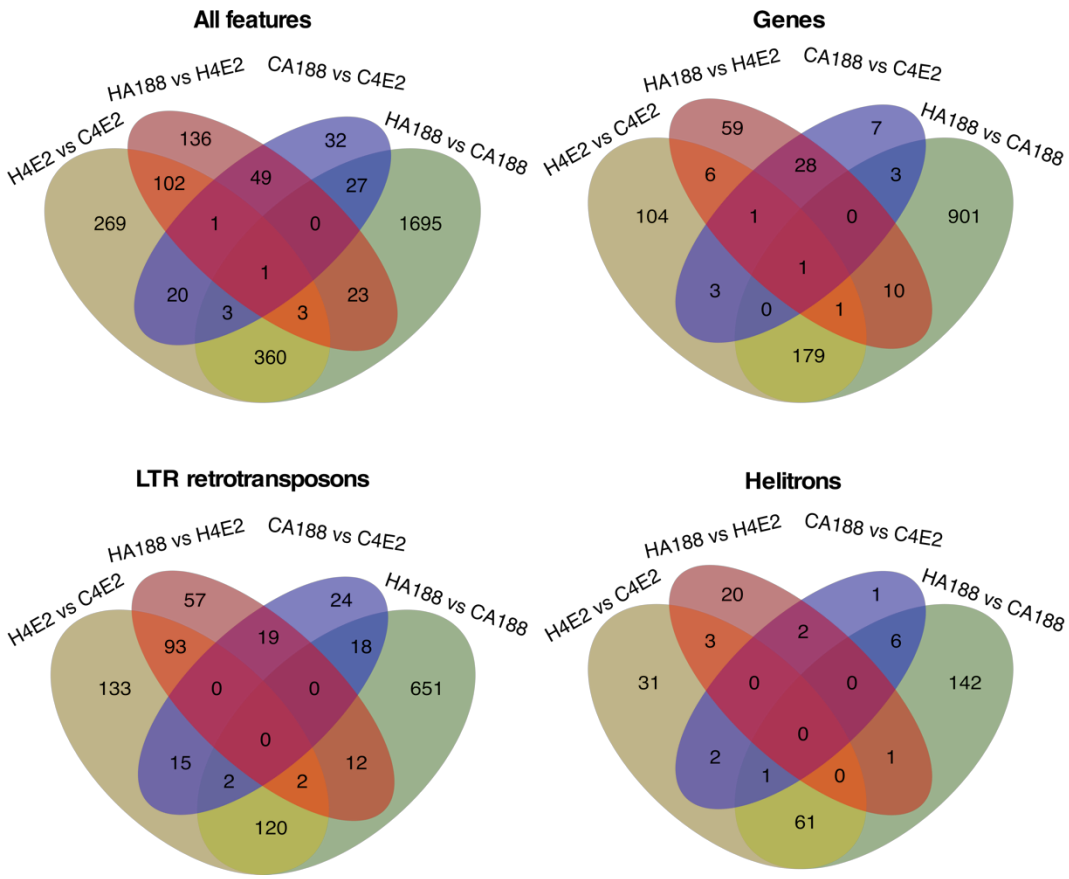

Figure 6.5: Pairwise differential expression analysis between wild type and MAGO downregulated lines after heat treatment. Differentially expressed features (top left), Genes (top right), LTR retrotransposons (bottom left) and Helitrons (bottom right). CA188, wild type control conditions; C4E2, RNAi control conditions; HA188, wild type heat stress conditions; H4E2, RNAi heat stress conditions. LTR retrotransposons upregulated in RNAi (blue box), LTR retrotransposons up regulated in RNAi heat stress conditions (FDR < 0.01 and fold change cut-off of 2).

greatly contributes to changes in gene expression. When we compared wild type and *MAGO* RNAi expression after heat stress we detected 106 genes that were differentially expressed, 105 of which were upregulated in *MAGO* RNAi which also suggests that *MAGO* may negatively regulate gene expression during meiosis (Figure 6.6A). Surprisingly, we found that LTR retrotransposons had the most differentially expressed transcripts within the transposon class when comparing expression under heat conditions (Total 183; 112 Upregulated, 71 Downregulated) (Figure 6.6B). Furthermore, we found that LTR retrotransposon expression was largely affected by genotype and by stress treatment displaying either downregulation or upregulation (Figure 6.6A). Although helitrons represent a significant proportion of the maize transposon repertoire, only 270 were differentially expressed and the majority were mainly affected by heat stress and not by genotype. These results suggest an interaction between MAGO and the regulation of LTRs after heat stress.

To better understand the role of MAGO proteins in regulating heat responsive genes, we looked for overlap in differentially expressed features between *MAGO1/2* RNAi and wild type plants under heat stress. We identified 914 genes differentially expressed in wild type anthers after heat stress that were not altered in RNAi anthers under the same conditions. We preformed gene ontology enrichment analysis on these genes to identify conserved biological processes that may be implicated (FDR adjusted $p \leq 0.05$). Go enrichment analysis revealed that most genes affected were associated with nucleosome assembly and chromatin organisation. These finding suggest that MAGO may be involved in heat induced chromatin remodelling responses in pre-meiotic anthers (Figure 6.7). These DEGs include several chromatin related proteins including SWI/SNF complex subunit SWI3A, Elongator complex protein 3, DNA methyl transferase 5,

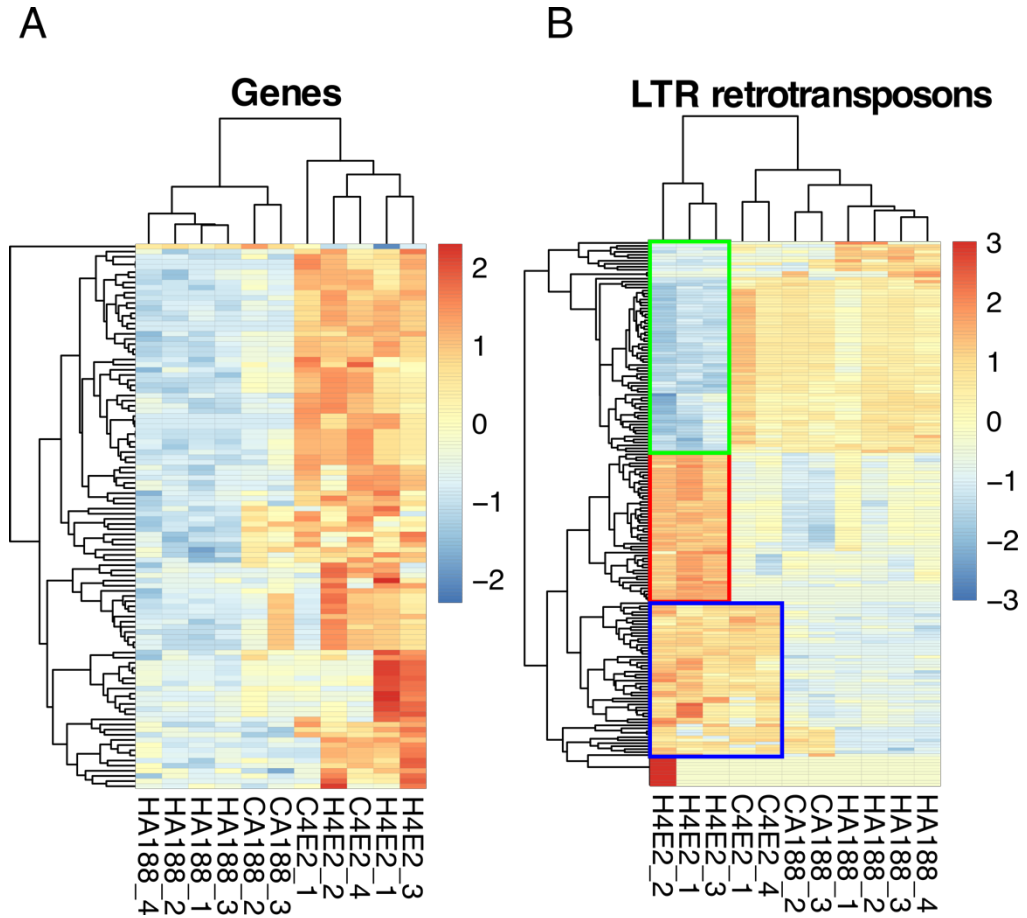

Figure 6.6: Heatmaps of differentially expressed features of wild type and RNAi after heat treatment. Scaled expression of (A) Genes and (B) LTR retrotransposons. CA188, wild type control conditions; C4E2, RNAi control conditions; HA188, wild type heat stress conditions; H4E2, RNAi heat stress conditions. LTR retrotransposons upregulated in RNAi (blue box), LTR retrotransposons up regulated in RNAi by heat stress conditions (red box) and LTR retrotransposons downregulated in RNAi by heat stress (FDR < 0.01 and fold change cut-off of log2(4)).

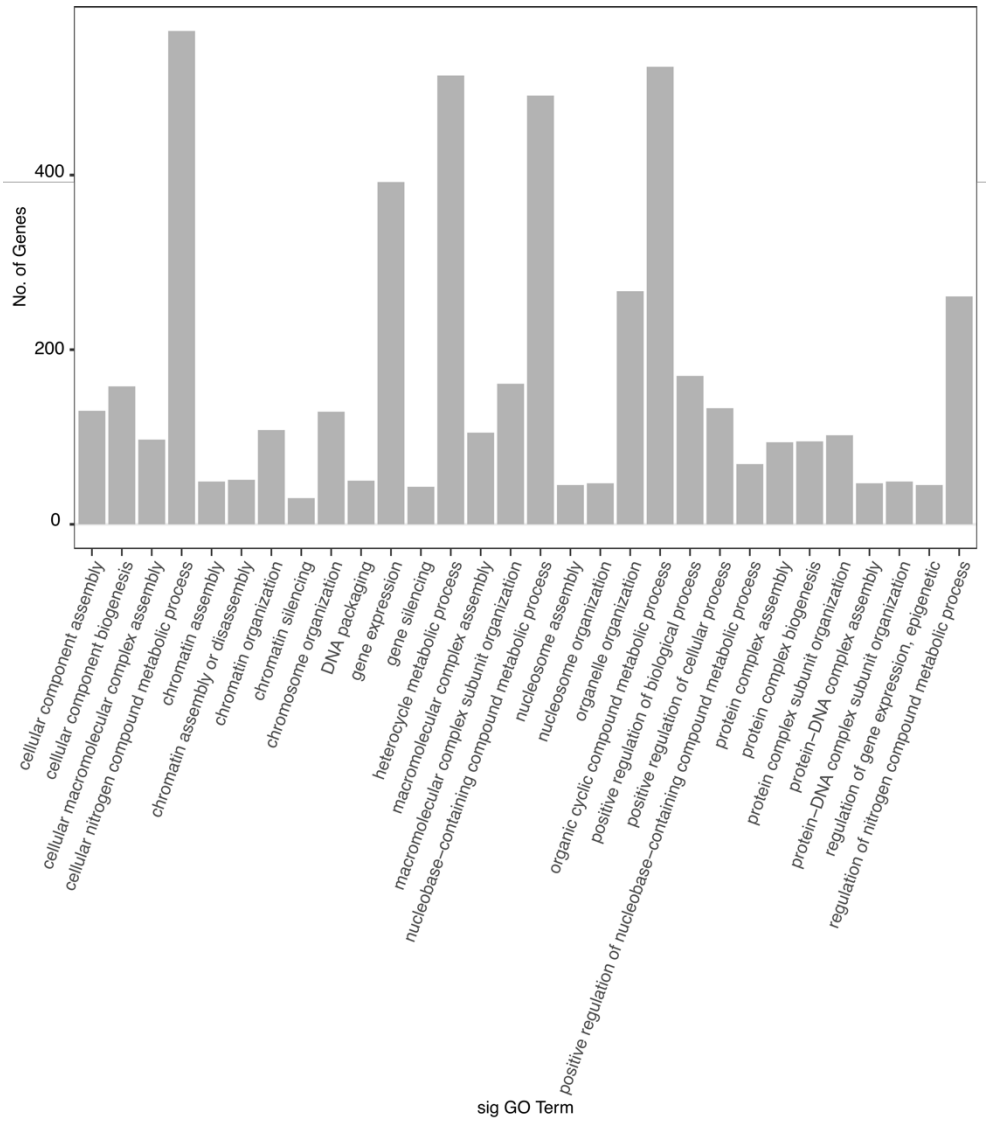

Figure 6.7: Gene ontology (GO) enrichment analysis for DEGs in in *MAGO* RNAi under heat stress. The top 30 GO terms enriched between wild type and *MAGO* RNAi under heat stress (FDR<0.05)

Increased DNA methylation 1 and histone H1-3 (Table 8.5). Additionally, we also detected the differential expression of the meiosis associated genes *Protein CHROMOSOME TRANSMISSION FIDELITY 7* and *Condensin-2* complex subunit H2, as well as genes associated with the oxidative stress responses such as *Protein DJ-1 homolog D* and *alternative oxidase2*. We also detected the upregulation of *SUPPRESSOR OF GENE SILENCING 3* which is essential for the production of trans-acting siRNAs (tasi-RNAs) (Appendix).

6.2.4 impact of heat stress on MAGO dependent sRNAs

Small RNAs are generated from many distinct loci during development and are known to be an amplification product of RNA slicing by Argonautes. To identify differentially regulated sRNA loci, we conducted pairwise comparisons between sRNA clusters in different genotypes and treatments (Figure 6.8). Most differentially expressed sRNA clusters were a result of heat treatment with 2136 in wild type and 2406 in RNAi lines (FDR adjusted < 0.001). Differences in genotype accounted for 231 sRNA clusters under control conditions and 72 under heat stress conditions (FDR adjusted p < 0.05) (Figure 6.8). To better understand the interaction between treatment and genotype, we performed pairwise comparisons between each sample group. We identified 87 sRNA clusters affected by the interaction of temperature stress and *MAGO* downregulation (FDR adjusted p<0.05) (Appendix). Only 7 overlapped with protein coding genes including the *MAGO* genes *MAGO1* (*ZmAGO5b*) and (*ZmAGO5c*) *MAGO2*. Heat shock protein 90-2, shows preferential sRNA accumulation only in heat treated wild type plants (Table 6.1). Thirty clusters overlap with LTR retrotransposons and 8 overlap with helitrons and is consistent with the transcriptome analysis (Figure 6.5). Surprisingly, 23 differentially regulated

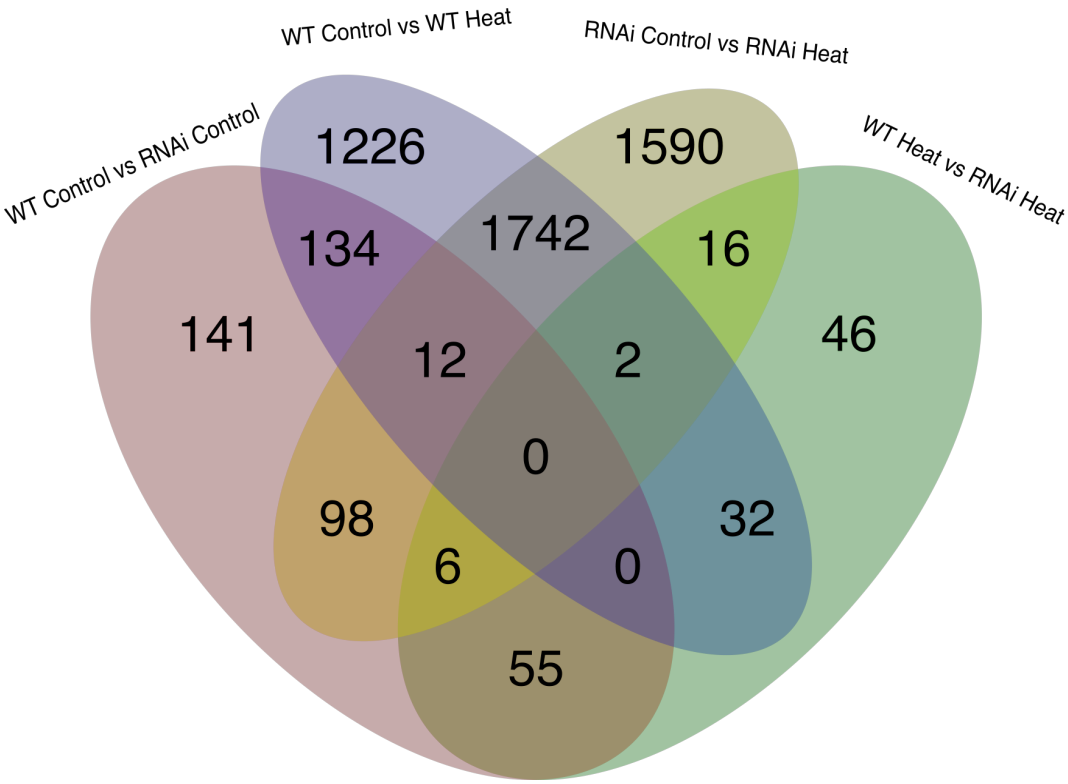

Figure 6.8: Differentially expressed sRNAs in *MAGO* RNAi under stress. Pairwise comparisons between wild type and *MAGO* RNAi under control (28°C) and Heat stress (35°C) conditions. FDR < 0.05.

Table 6.1. Differentially accumulated sRNA clusters for MAGO and Heat interaction. WT C , wild type control treatment; RNAi C, *MAGO* RNAi control treatment; WT H , wild type heat treatment; RNAi C, *MAGO* RNAi heat treatment; padj, adjusted p value. ($P < 0.05$).

			Control (28ºC)		Heat (35ºC)	
ID	Locus	Feature	Wild type	*MAGO* RNAi	Wild type	*MAGO* RNAi
Cluster_58253	Chr10:75740955..75741256	LTR	37.87	134.49	181.76	128.23
Cluster_45011	Chr7:135844980..135846806	Heat shock protein 90-2	53.65	109.91	611.62	130.05
Cluster_30373	Chr5:4113607..4113901	ZmAGO5c	18.28	1514.25	18.58	9607.86
Cluster_19973	Chr3:157124504..157124539	BTB/POZ domain-containing protein	1.89	10.39	147.77	82.33
Cluster_45010	Chr7:135843572..135843998	Heat shock protein 90-2	7.97	23.87	129.08	25.87
Cluster_5891	Chr1:217692750..217693301	L10-interacting MYB domain-containing protein	21.86	64.29	93.13	61.77
Cluster_16300	Chr2:239623413..239623566	ZmAGO5b	7.82	722.82	6.84	3917.12
Cluster_30372	Chr5:4113361..4113528	ZmAGO5c	8.53	629.10	6.81	2917.56
Cluster_55756	Chr9:140010406..140010513	LTR, tRNA	3406.45	1342.21	4419.06	11228.88

sRNA clusters overlapped with tRNA loci which are involved in transposons silencing and the plant stress response (Appendix). These results indicate that MAGO proteins may be involved in the silencing of LTR retrotransposons and, in addition to binding tRNA derived fragments, they may be required for tRF biogenesis. Additionally, one of the differentially accumulated tRNA loci generates the 5'-tRNA fragment previously shown to bind to MAGO (Results 3.2.5) (Table 6.1).

6.2.5 The 21-nt phasiRNAs are induced by heat

We have found that both the epidermal sRNAs and MAGO proteins are critical for pre-meiotic anther development and necessary for heat stress responses. We have also found that MAGO proteins can bind to the 21-nt phasiRNAs, a class of epidermally accumulating sRNAs required. However, it is not clear whether MAGO is necessary for 21-nt phasiRNA biogenesis. To determine the 21-nt phasiRNA expression dynamics in wild type and downregulated *MAGO1/2* RNAi lines grown in control or heat stress conditions, we used sRNA sequencing. sRNA reads were mapped to the 463 previously identified maize 21-nt *PHAS* loci to determine differential expression between samples (Zhai, Zhang et al. 2015). We found that in wild type plants 95 *PHAS* loci were differentially expressed between control and heat stress conditions and 128 *PHAS* loci were differentially expressed in *MAGO1/2* downregulated lines ($p < 0.01$) (Figure 6.9A). Seven *PHAS* loci were differentially expressed control wild type vs RNAi under control conditions and 29 *PHAS* loci were differentially expressed under heat conditions. The results indicate that a large proportion of the 21-nt phasiRNAs were differentially regulated by heat. To determine the effect of heat stress on total 21-nt phasiRNA abundance we compared read abundances of 21-nt phasiRNAs between samples. Total 21-nt phasiRNA

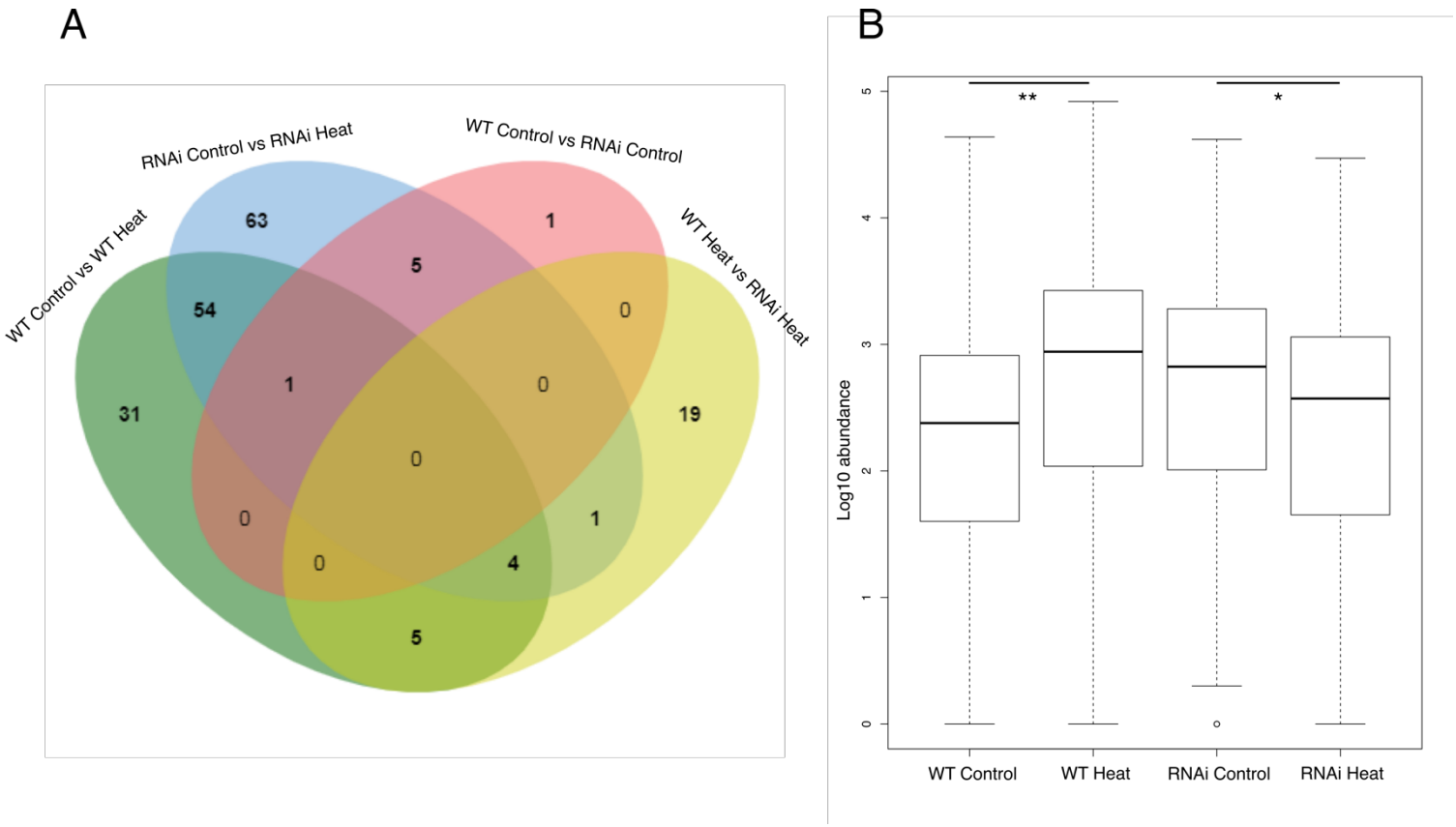

Figure 6.9: Comparison of 21-nt phasiRNA abundance between WT and RNAi after heat treatment. (A) DESeq2 pairwise differential accumulation of sRNAs mapped to the 463 previously identified maze 21PHAS loci (Zhai, Zhang et al. 2015). $p < 0.01$. (B) Log10 total mapped 21-nt phasiRNA abundances. Significance determined by Welch's t test *P = 5.637e-05, ** P = 3.26e-12.

abundance was significantly increased in wild type heat (469.62) compared to wild type control (157.15) ($p < 0.001$). However, 21-nt phasiRNA abundance in RNAi lines was significantly decreased in RNAi heat (204.03) compared to control conditions (378.98) ($p < 0.001$) (Figure 6.9B). To determine which *PHAS* loci were contributing to the increase in phasiRNA expression, we compared the accumulation of 21-nt phasiRNAs across all known PHAS loci. We found that a subset of the 21 *PHAS* loci are upregulated under heat stress conditions that are not responding in *MAGO* downregulated plants (Figure 6.10). To determine the spatial localization of these Heat induced 21-nt phasiRNAs (HphasiRNA) in developing anthers, we used RNA *in situ* hybridization. We identified 10 distinct unique 21-nt HphasiRNAs that were selected based on consistent accumulation patterns across each replicate and each experimental group. We found that HphasiRNAs accumulated in the anther epidermis, overlapping with miR2118 expression under control conditions though, the HphasiRNA expression levels are almost not detectable by meiosis (Figure 6.11). However, HphasiRNAs accumulate in the anther during meiosis after heat treatment. Not only is this expression higher than in control conditions, but also the HphasiRNAs appear to persist much longer in the developing anther. The HphasiRNAs are still abundant at meiosis and accumulate in the tapetum and meiocytes, consistent with MAGO1 accumulation in developing anthers (Figure 6.11 & Figure 3.5). Although HphasiRNAs accumulate after heat stress, miR2118 levels appeared unaffected.

It is thought that 21-nt small RNAs direct the RNA silencing activity of argonaute proteins though complementarity with the target transcripts (Axtell and Bowman 2008). It is likely that phasiRNAs may also direct MAGO proteins to target sequences through the same sequence specific manner.

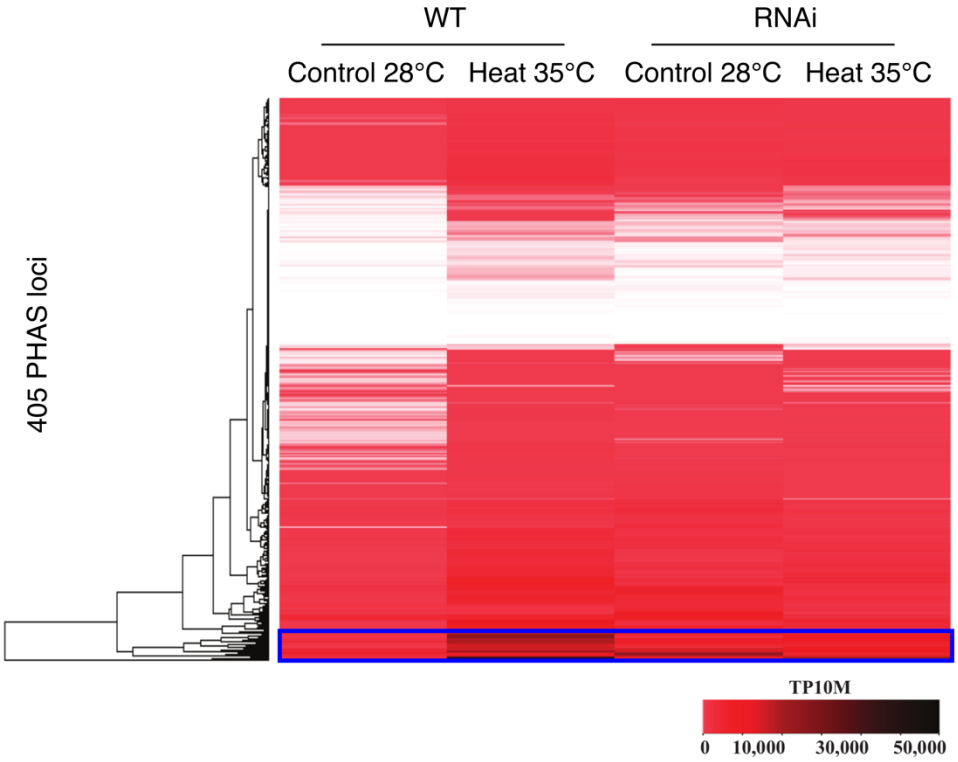

Figure 6.10: Abundance of reads mapping to the previously identified 21PHAS loci after pre-meiotic heat treatment (Zhai, Zhang et al. 2015). A subclass of the PHAS lncRNA loci are generating more sRNAs after pre-meiotic heat-stress in wild type samples and unaffected by heat in MAGO1/2 downregulated lines (blue box) (hit normalized).

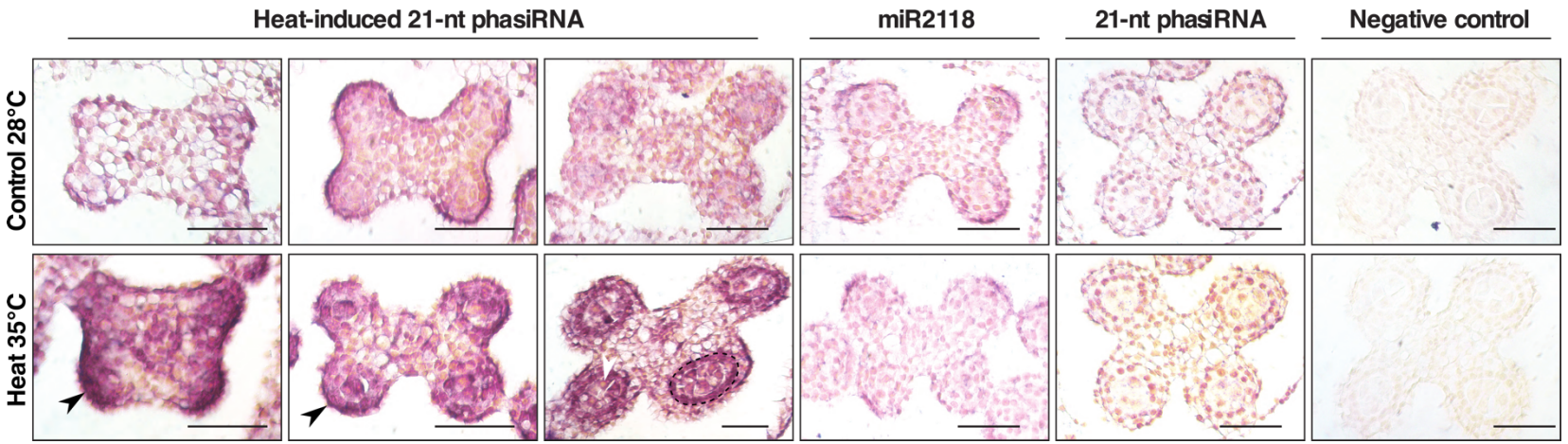

Figure 6.11: RNA *in situ* hybridisation for the heat-induced 21-nt phasiRNAs. heat-induced 21-nt phasiRNAs (first to third panels), miR2118 (fourth panels) and 21-nt phasiRNA (fifth panels) in developing anthers of WT under control (28°C)(top panels) and heat (35°C)(bottom panels) conditions. Scrambled RNA (sixth panels) was used as a negative control. Heat induced phasiRNAs are generated in the epidermis (black arrow) and accumulate the tapetum (dotted line) and meiocytes (white arrow). Scale bars, 50 µm.

Therefore, it could be possible to predict targets of the phasiRNAs *in silico* with this assumption. We identified 10 PHAS loci which are induced by heat, and selected all abundant (>100 reads) 21-nt and 24-nt sRNAs reads from these loci to carry out sRNA target prediction (psRNAtarget) (Dai, Zhuang et al. 2018). We found that HphasiRNA gene targets appear to be distributed equally across all 10 maize chromosomes (Figure 6.12A). To determine if the HphasiRNAs were preferentially targeting genes or transposable elements, target prediction was performed against predicted transposon transcripts in the maize genome. This analysis revealed a enrichment of 21-nt HphasiRNAs targeting transposons (0.0555 HphasiRNA binding sites per kb) compared with genes (0.0315 HphasiRNA binding sites per kb). 24-nt RNAs originating from the same loci as the 21-nt HphasiRNAs consistently had fewer predicted target sites for each group, although they were also enriched for TEs (0.00712 TE and 0.00498 gene binding sites per kb) (Figure 6.10B). Because many LTR retrotransposons are activated in *MAGO1/2* RNAi upon heat stress (Figure 6.6), we investigated if the phasiRNAs may be responsible for MAGO targeting to LTR retrotransposons. We found that the 21-nt HphasiRNAs predicted targets do not fit the expected distribution X^2 (5) = 191.593, $p < .001$ (Figure 6.12C). The majority of the predicted targets were LTR retrotransposons (80.9%) and these targets were distributed throughout the LTR retrotransposon transcript, with particular emphasis to the 5' region (data not shown). However, based on the number of LTR retrotransposons in the maize genome and because of their average length, we would expect many transposon targets (83.6%). Helitrons also represented a significant proportion of the predicted HphasiRNA targets (18.0%) which was enriched compared to the expected distribution (15.0%).

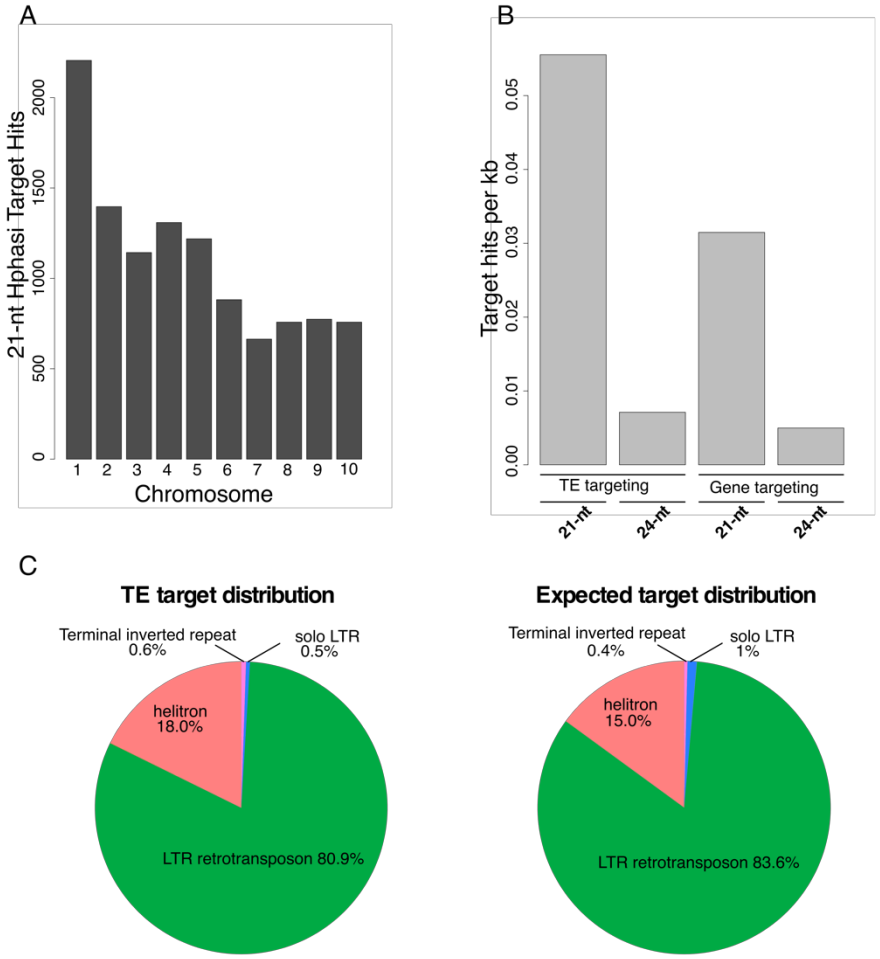

Figure 6.12: 21-nt HphasiRNA TE target prediction. (A) 21-nt HphasiRNA predicted targets are distributed on all maize chromosomes and are proportionally similar to chromosome size. (B) 21-nt HphasiRNA are predicted to preferentially target TEs with more hits per kb feature length. (C) Distribution of 21-nt HphasiRNA targets against annotated TE families. Significant deviation from the expected distribution was found X^2 (5) = 191.593, p < .001.

Argonautes target both genes and transposons for RNA silencing. Although HphasiRNAs appear to preferentially target transposons, genic targets may be functionally significant. To uncover the potential function of sequences targeted by these sRNAs we conducted a GO analysis (Tian, Liu et al. 2017). We found that genes targeted by HphasiRNAs displayed significantly enhanced terms for molecular function, including: RNA binding (p = 5.62e-5), nucleotide binding (p = 0.000675) and histone acetyl-transferase (p = 0.0342). Additionally, we found several biological process enriched, including: mitotic cell cycle (p = 4.36e-6), covalent chromatin modification (p = 0.00348), regulation of cellular component organization (p = 7.59e-6) and catabolic processes including; organic cyclic compound, heterocyclic, aromatic compound and cellular nitrogen compound catabolic processes (p = 1.26e-6) (Figure 6.13).

6.2.6 MAGO is required to silence LTR retrotransposons under heat stress

RNA sequencing revealed that many LTR retrotransposons are upregulated in *MAGO1/2* RNAi plants and this upregulation was enhanced by heat stress (Figure 6.6). Additionally, sRNA sequencing revealed 87 MAGO dependent sRNA clusters and most of them originating from LTR retrotransposons and induced by heat stress. This data suggests that MAGO proteins may be required for the regulation of LTR retrotransposons upon heat stress. To test this hypothesis, we investigated the expression profile of *Hek* ('Hek' nuclear in Korean)- a MAGO dependent LTR retrotransposon induced by heat. The expression of *Hek* was low under control conditions in anthers and meiocytes from wild type and RNAi lines (Figure 6.14A). Under heat stress conditions, the relative expression of the *Hek* was moderately upregulated in anthers of wild type plants but highly increased in anthers and dissected meiocytes of *MAGO* downregulated plants (76-fold increase)

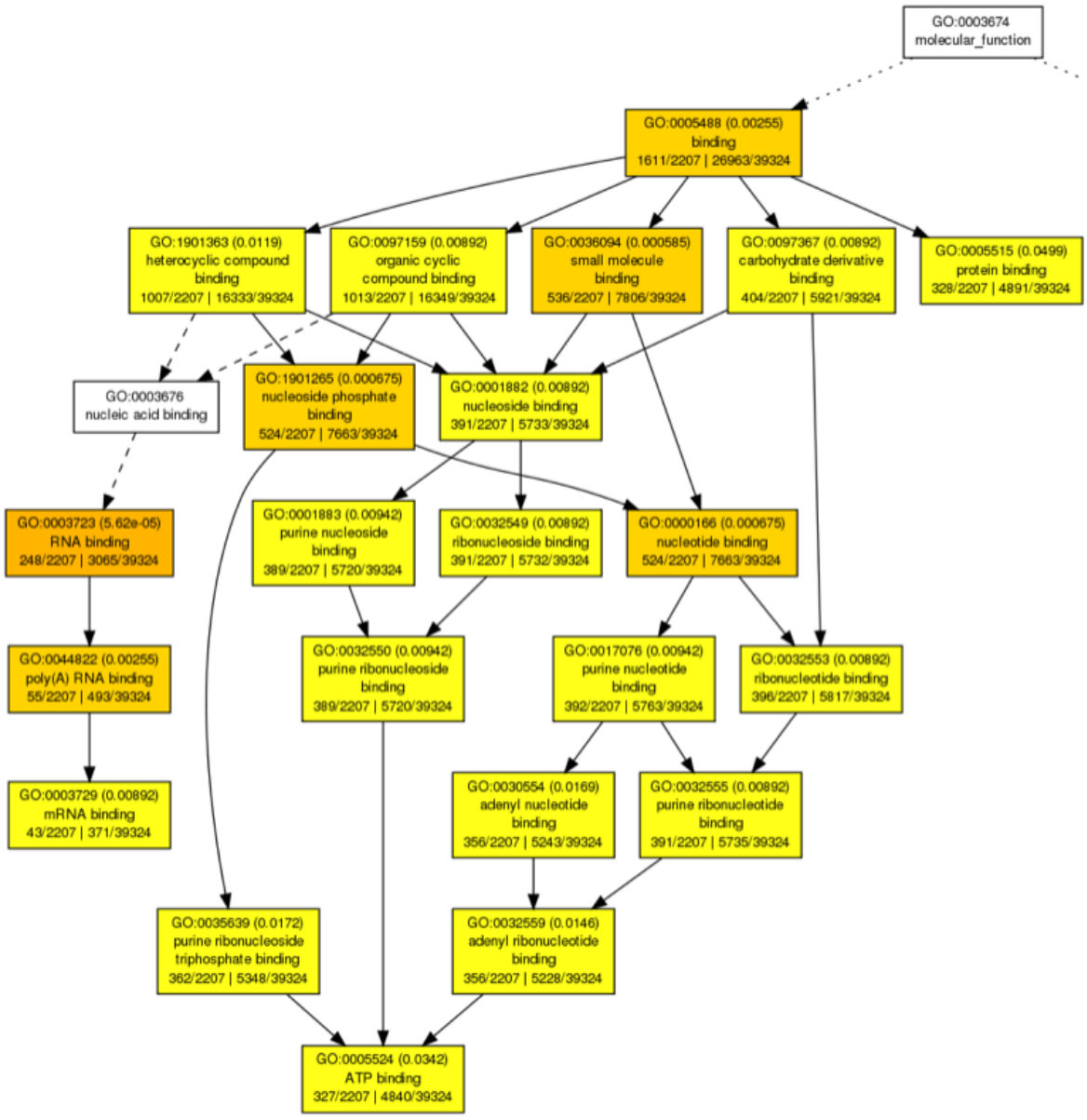

Figure 6.13: GO enrichment analysis of the predicted 21-nt HphasiRNA targets. Targets were predicted from the heat induced 21-nt phasiRNAs and the gene list analyzed for GO term enrichment (n=2207) ($P < 0.05$).

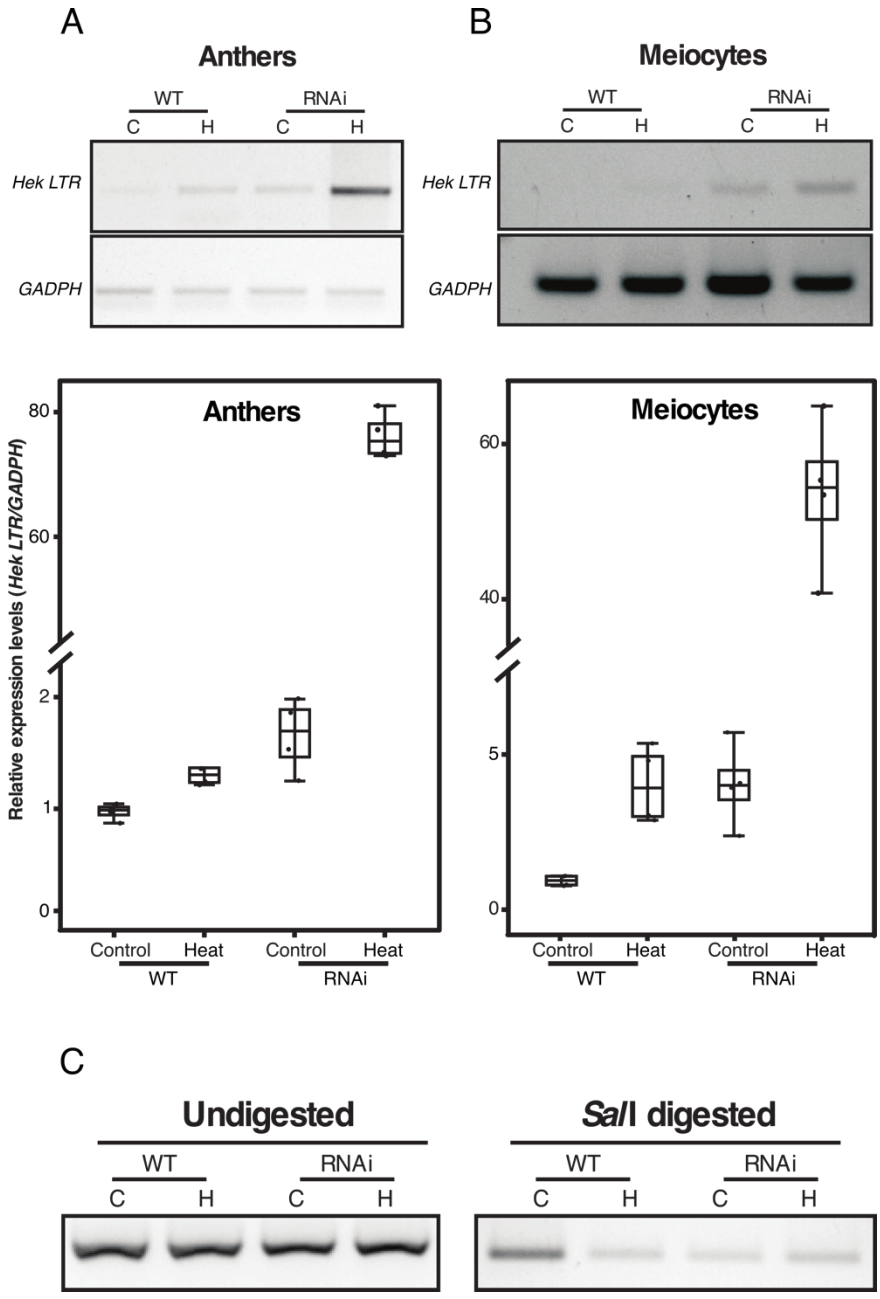

Figure 6.14: MAGO proteins are required for silencing transposable elements under heat conditions. (A) Expression levels of long terminal repeat (LTR) retrotransposon *Hek LTR* in WT and RNAi anthers (left) under control or heat conditions. (B) Comparison of LTR transcripts in WT and RNAi meiocytes (right) under control or heat conditions. *GAPDH* served as RNA loading control. (C) Comparison of DNA methylation of *Hek LTR*. Chop-PCR analyses of LTR region cut by *Sal*I in WT and RNAi under control and heat conditions (right). Undigested genomic DNAs served as loading controls (right). C, control; H, heat.

(Figure 6.14B). This data is in line with the low abundance of sRNAs from this region in wild type anthers under control conditions and their accumulation after heat stress (Appendix). The transcriptional activity of *Hek* may be regulated Epigenetically by sRNA directed RdDM (Lee, Gurazada et al. 2012, Marí-Ordóñez, Marchais et al. 2013). To test this hypothesis, we treated DNA isolated from developing anthers with methylation sensitive enzyme followed by PCR (Chop-PCR) (Zhang, Tang et al. 2014). Consistent with *Hek* expression, we found the highest level of DNA methylation in the wild type anthers under control conditions. Under heat stress conditions, Hek was hypomethylated, which correlates with its transcriptional activation (Figure 6.12C). However, *Hek* expression only moderately increased in wild type anthers indicating that activity may be regulated post-transcriptionally. In RNAi lines, *Hek* is consistently hypomethylated regardless of treatment, which is consistent with *Hek* transcriptional activation in *MAGO* downregulated plants (Figure 6.14C). These results further support that MAGO proteins may be required for the RNA silencing of LTR retrotransposons.

Summary

Pollen viability defects in *MAGO1/2* RNAi are enhanced after pre-meiotic heat stress. We found that MAGO proteins associate with the 21 and 24-nt phasiRNAs which we predict primarily target transposons. We detected significant transcriptional changes in meiotic anthers in *MAGO* RNAi lines. While few genes appear to be regulated by MAGO activity, many LTR retrotransposons are transcriptionally activated in *MAGO* RNAi lines. We hypothesise that MAGO may be silencing these retroelements at the transcriptional and post-transcriptional level.

6.3 Discussion

Temperature stress reveals *MAGO* RNAi fertility defects

Argonautes are essential for sRNA mediated silencing in plants, such as the silencing genes and transposable elements (Kapoor, Arora et al. 2008, Zhang, Xia et al. 2015, Liu, Xin et al. 2018). We found that, male sterility observed in *MAGO1/2* RNAi anthers is significantly enhanced after pre-meiotic heat stress (Figure 6.2). The pollen viability of RNAi lines is lowered significantly after heat stress while wild type plants appear unaffected. We also detected morphological defects in heat stressed RNAi lines that contributes to the male fertility defects (Figure 6.4). These resemble premature tapetal programmed cell death, which is common among heat sensitive male sterile mutants and is often attributed to the disruption of ROS homeostasis (Ahmed, Hall et al. 1992, Jung, Han et al. 2005, Nan, Zhai et al. 2016).

The tapetum is particularly sensitive to ROS, and early degeneration is catastrophic for meiocyte development, often resulting in complete male sterility. *MAGO1* is expressed in the anther epidermis during development and moves to the tapetum later in development coinciding with the accumulation of the 21-nt phasiRNAs (Figure 3.5 & 6.10). MAGO1 may therefore protect the tapetum from premature programmed cell death during stress.

Several genes involved in the oxidative stress response were differentially expressed by heat stress dependent on MAGO proteins such as *Peroxidase 3, Protein DJ-1 homolog D* and *alternative oxidase 2* that have been linked to tapetum maintenance during anther wall development (Table 8.4 & Table 8.5) (Jacobowitz and Weng 2018, Yang, Wu et al. 2018). This would suggest that MAGO may be necessary to regulate ROS homeostasis and signalling during stress in developing anthers. We detected many genes that respond

to the plant hormone Abscisic acid (ABA). ABA regulates many aspects of development including floral induction and the response to environmental stress including heat stress, and is linked to ROS signalling (Suzuki and Katano 2018). Furthermore, ABA signalling has been linked to heat induced infertility in anthers, as well as tapetal gene expression and programmed tapetal cell death (Saini, Sedgley et al. 1984, Parish, Phan et al. 2012). *ABSCISIC ACID-INSENSITIVE 5-like protein 5* (*ABI5*) is upregulated under heat stress in wild type anthers but not in *MAGO1/2* RNAi (Table 8.4). ABI5 is a bZIP transcription factor induced by ABA and in rice, suppression of ABI5 leads to reduced fertility but increased stress tolerance (Zou, Guan et al. 2008). These results strongly suggest that downregulation of MAGO1/2 in early anthers compromises ROS signalling, possibly due to disruption in the ABA response genes, leading to tapetal defects linked to the programmed tapetal cell death.

MAGO1/2 downregulation also results in the production of viable and non-viable pollen grains. Here, meiocytes escape the tapetal defects, though succumb to meiotic defects previously observed in non-stressed RNAi and reminiscent of wheat reproductive heat sensitivity (Saini, Sedgley et al. 1983). In wheat, developing meiocytes become disorientated in relation to the tapetum and as a consequence are perturbed in their ability to take up nutrients and developmental signals. In *MAGO* RNAi lines male fertility defects could therefore originate in the tapetum as observed in some male sterile mutants (Walbot and Egger 2016).

The appearance of meiotic defects in the *MAGO* RNAi germline coincide with *MAGO2* expression in the meiocyte nuclear compartment (Figure 3.5 & Figure 4.5). We found that chromatin assembly gene ontology terms were significantly enriched during heat stress in wild type anthers (Figure 6.13). Many differentially expressed genes were identified for chromatin

components, chromatin interacting proteins, and chromatin and DNA modifying enzymes, in addition to meiosis associated genes. This could indicate that *MAGO* RNAi and temperature stress impact the chromatin landscape in the male germline. During meiosis, chromatin compaction and pairing takes place and this process is known to be perturbed by heat stress (Probst and Scheid 2015). *Condensin-2 complex subunit H2* is significant downregulated by heat in wild type plants (Table 8.5). This protein is essential for meiotic and mitotic chromosome compaction. In *Arabidopsis* loss of Condensin II results in extensive crossover events, though downregulation is also associated with reduced crossover formation (Smith, Osman et al. 2014). This indicates that MAGO2 is associated with chromosome compaction and synapsis of sister chromatids during stress. Additionally, germline epigenetic pathways are necessary to silence of transposons and disruption of these pathways often leads to infertility (Kalmykova, Klenov et al. 2005, Oliver, Santos et al. 2016). Perhaps, the expression of these chromatin silencing components is required to maintain the silencing of genes and stress induced transposons such as LTR retrotransposons in the germline.

MAGO regulates the activity of heat induced transposons in the germline

MAGO proteins are essential for male germline development during heat stress. A subset of 21-nt phasiRNAs are induced upon heat stress in wild type plants, but this induction is MAGO dependent. We detected significant upregulation of *SUPPRESSOR OF GENE SILENCING 3*, a component of the tasiRNA biogenesis pathway, in wild type anthers after heat stress (Peragine, Yoshikawa et al. 2004). Like the tasiRNAs, phasiRNAs are secondary sRNAs generated by a conserved pathway, suggesting that MAGO may impact HphasiRNA induction by regulating the biogenesis pathway components

(Yang, Seo et al. 2007). These Heat induced phasiRNAs (HphasiRNAs) are highly enriched in the tapetum and meiocytes prior to meiosis and they are predicted to target TEs preferentially, specifically LTR retrotransposons and helitrons (Figure 6.11 & Figure 6.12). Interesting, small RNAs derived from LTR retrotransposon and helitron were also highly induced by heat stress and are MAGO dependent (Table 8.7). The generation of transcripts from these loci indicates they are activated by heat stress but controlled by post transcriptional silencing and generating siRNAs (Table 6.1 & Figure 6.5). TE derived siRNAs could then activate the RdDM pathway leading to TE transcriptional silencing in a MAGO dependent manor, though this could be both direct or indirect. This is clearly demonstrated with *Hek* LTR, which is methylated under control conditions and this methylation is lost under heat stress (Figure 6.13). Methylation is depleted at this locus in RNAi anthers, indicating MAGO may be required to maintain this epigenetic mark. Silencing of TEs by MAGO appears to be global phenomenon as many LTR retrotransposons and helitrons are activated by heat stress in MAGO downregulated plants.

The control of TEs by MAGO is remarkably similar to the PIWI silencing of transposons in the mammalian germline whereby piRNAs are generated in the male germline in somatic companion cells and migrate to the germ cells (Houwing, Kamminga et al. 2007). Such non-cell autonomous siRNA pathways are known to occur during pollen development in which transposons become active in the vegetative cell and generate 24-nt siRNAs that migrate to the sperm cells to maintain TE silencing (Slotkin, Vaughn et al. 2009). Similar mechanisms occur in *Arabidopsis* ovules where AGO9 Is necessary to silence LTR retrotransposons in pericentromeric regions. Perhaps MAGO represents a further level of transposon control during

microgametogenesis. One which mirrors female gamete development where transposons are silenced before meiosis by AGO9.

MAGO proteins bind to tRNA derived fragments

MAGO proteins clearly bind to a specific 5'-tRF prior to meiosis. We have found that many tRFs are also generated during the heat shock response and this biogenesis is dependent on functional *MAGO* expression (Table 8.7). tRFs are stress induced and are important for germline development (Hsieh, Lin et al. 2009, Thompson and Parker 2009, Molla-Herman, Vallés et al. 2015, Alves, Vicentini et al. 2017). tRFs are associated with the suppression of TE activation and are thought to interfere with transposition (Martinez, Choudury et al. 2017, Schorn, Gutbrod et al. 2017). MAGO could directly generate tRFs via phasiRNA directed cleavage of the precursor tRNAs that might regulate the silencing of transposable elements in the germline. Alternatively, downregulation of MAGO1/2 could result in derepression of the TEs during germline development. Stress signals resulting from this derepressed state may then induce tRNA biogenesis. tRFs have been found to be generated in a DCL1 dependent fashion, however DCL1 could act upstream of a MAGO dependent pathway of tRF biogenesis (Cole, Sobala et al. 2009, Alves, Vicentini et al. 2017). tRFs are a relatively cryptic class of sRNAs whose importance is currently not fully known. These elements represent an exciting area of further study.

7.0 General discussion

This thesis has greatly contributed to the understanding of the reproductive phasiRNAs and meiosis associated argonautes (MAGOs). We have uncovered clear evidence of phasiRNA movement which is critical for their role in male but not female reproductive development. Furthermore, we have discovered that the phasiRNAs are upregulated by heat stress, they bind to MAGO proteins, and this is essential to regulate heat-activated retroelements in the male germline. The implications of these findings are largely covered in their relevant discussion sections and here I will focus largely on the movement and targets of the reproductive phasiRNAs. The rationale behind this emphasis is that despite: years of research, their conservation in the grass lineages and their restricted but abundant accumulation in the male germline, the function of the reproductive phasiRNAs has remained elusive. We can now finally begin to understand their purpose and speculate as to their role in safeguarding the male germline from heat induced transposon assault.

The reproductive phasiRNAs are a small mobile signal necessary for pollen development

The reproductive phasiRNAs are a class of secondary small interfering RNAs that accumulate in the developing male inflorescences of monocots (Johnson, Kasprzewska et al. 2009, Komiya, Ohyanagi et al. 2014, Zhai, Zhang et al. 2015). The 21-nt phasiRNAs are generated from the anther epidermis, the location of precursor lncRNA and miRNA trigger accumulation (Komiya, Ohyanagi et al. 2014, Zhai, Zhang et al. 2015). As anthers mature these sRNAs appear to accumulate throughout the anther without accumulation of precursor molecules, suggesting they move. Although they accumulate specifically during anther development, it is not clear if they are strictly necessary for the production of pollen nor if they act non-cell autonomously.

Demonstrating sRNA movement is challenging and is often achieved through grafting experiments which are not feasible in maize anthers. By expressing the gene silencing suppressor HCPro we were able to specifically disrupt the movement of the 21-nt phasiRNAs only from the anther epidermis. We have obtained strong evidence that the 21-nt phasiRNAs are indeed critical for pollen production and that they must move from the anther epidermis to the inner anther cell layers and meiocytes. The importance of this movement is not clear; however, it seems to be a conserved strategy in plants and animals during reproductive development. Frequently, *Drosophila* PIWI interacting small RNAs (piRNAs) originate from transposon-like sequences in somatic cells before moving to testes or ovary (Malone, Brennecke et al. 2009, Ross, Weiner et al. 2014). Furthermore, PIWI proteins are predominantly expressed in the somatic cells encapsulating the germline in arthropods: where they bind to noncoding, repeat-associated siRNAs that silence transposons (Lewis, Quarles et al. 2018). Notably in plants, *Arabidopsis* AGO5 and AGO9 in are required for specification of the egg cell in the primordial ovule, though they are expressed in the epidermis (Olmedo-Monfil, Durán-Figueroa et al. 2010, Tucker, Okada et al. 2012). AGO9 is also thought to direct the silencing of transposable elements in pericentromeric regions of female germ cells (Durán-Figueroa and Vielle-Calzada 2010). Perhaps generating this signal in the somatic cells is a conserved strategy to remove the metabolic burden from the developing germ cells which already rely heavily on the tapetum for nourishment. Furthermore, this could more tightly regulate the deployment of this signal by relying on diffusion of sRNAs from neighbouring cells rather than relying on transcription and RNA processing in germ cells attempting to condense their chromatin ready for meiosis. By sequestering the sRNAs in the outer

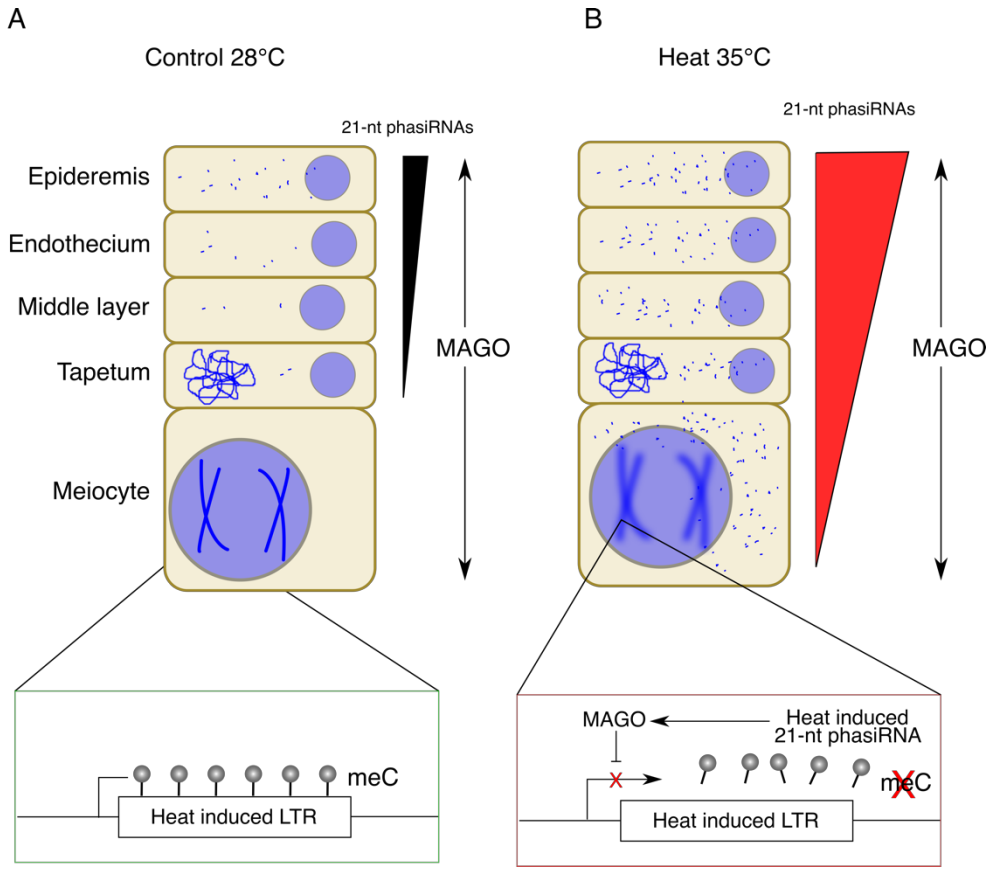

Figure 7.1: Hypothetical model of MAGO function in the developing anther. Under control conditions somatic siRNAs accumulate at low levels at the epidermis and move in-ward through the somatic anther cell layers. Under control condition, LTR retrotransposons remain transcriptionally silent. (B) Under heat stress many LTR retrotransposons such as *Hek* become active. Some somatic siRNAs also respond to the heat stress and accumulate at higher levels. these Heat induced 21-nt phasiRNAs are mobile and target the heat induced LTR retrotransposons for post transcriptional gene silencing by MAGO.

somatic cell layers of the developing anthers, we have shown the reproductive phasiRNAs act non-cell autonomously in the germ cells and are necessary for the development of the male gamete (Figure 7.1A).

LTR retroelements are the primary targets of the reproductive phasiRNAs

Many mutants have been studied in the phasiRNA pathways and argonaute proteins that bind to the phasiRNAs in rice anthers have been identified (Nonomura, Morohoshi et al. 2007, Komiya, Ohyanagi et al. 2014, Fan, Yang et al. 2016, Ono, Liu et al. 2018). Despite their clear requirement for the production of normal pollen, little progress has been made in identifying the precise role of the reproductive phasiRNAs (Johnson, Kasprzewska et al. 2009, Zhai, Zhang et al. 2015). The major aims of this thesis were to identify the targets of the phasiRNAs and therefore determine their importance in anther development. Rather than targeting the many miRNA triggers of phasiRNA biogenesis, or the 463 precursor lncRNAs, we opted for disrupting the expression of two meiosis associated argonaute proteins that we named MAGO1 and MAGO2. MAGOs displayed clear spatiotemporal accumulation resembling that of the reproductive phasiRNAs suggesting they may be loaded into these argonautes (Chapter 1). Indeed, our findings with sRNA immunoprecipitation of MAGO proteins and published work on the MAGO homologue MEL1 in rice supports this claim (Komiya, Ohyanagi et al. 2014). This provides clear evidence supporting the loading of both the 21-nt and 24-nt reproductive phasiRNAs into MAGO proteins. With this in mind, we could analyse the function and of the reproduction phasiRNA in anther development by investigating the transcriptional changes associated with MAGO downregulation.

Until now, the targets of the phasiRNAs have remained elusive. Previous work focused on gene expression changes to the anther transcriptome

during phasiRNA disruption (Johnson, Kasprzewska et al. 2009, Zhai, Zhang et al. 2015). However, we have found that LTR retrotransposons are the primary targets of the reproductive phasiRNAs (Chapter 6). Specifically, we identified the accumulation of cinful-zeon transcripts, a family of high copy gypsy LTR retrotransposons, especially after heat stress in the male germline. We suspect that these retroelements are also able to reintegrate into the genome, a phenomenon already known to occur in pollen in some maize mutants (Dooner, Wang et al. 2019). Furthermore, we hypothesise that other retroelements may also be transposing in *MAGO RNAi* lines, though their low copy number and low mapping efficiency may hinder their detection by conventional means. The next challenge will be to identify novel transposon insertions in these lines. This raises the question of how faithfully the male germline is transmitted, especially in environmentally stressed lines. It is clear that transposition events occur in the male germline at relatively high frequency in non-stressed maize ($2–4 \times 10^{-5}$ (Dooner, Wang et al. 2019).

Many transposons, especially LTR retrotransposons, are activated by stress with the potential to create new genetic variability (Gbadegesin 2012, Ito, Yoshida et al. 2013, Lisch 2013). This activation requires a combination of factors, including stress-induced global demethylation and stress response elements which are usually found in transposon sequences (Cavrak, Lettner et al. 2014, Dubin, Scheid et al. 2018). In animals, heat stress can lead to the activation of copia-like mobile elements and SINE elements and is known to lead to novel insertions (Ratner, Zabanov et al. 1992, Liu, Chu et al. 1995, Li, Spearow et al. 1999). In plants, several TEs are activated by stress, especially mediated by significant variation in temperature (Rehman and Nautiyal 2002, Hashida, Uchiyama et al. 2006, Dowen, Pelizzola et al. 2012).

Reproductive development is especially sensitive to stress, and the activation of transposons is known to account for stress induced sterility (Aravin, Hannon et al. 2007). In animals the disruption of the PIWI pathway increases stress infertility and in plants the disruption of RNA silencing pathways often results fertility defects (Kuramochi-Miyagawa, Watanabe et al. 2008, Mirouze, Reinders et al. 2009, Oliver, Santos et al. 2016). Because plants are sessile organisms, they are highly susceptible to stress-mediated infertility. Plants are thought to overcome this limitation by inducing rapid epigenetic changes in response to stress, in particular to control the activity of activated transposons. This protective role is particularly important in plant species like maize where almost 85% of the genome is accounted by transposon sequences (Schnable, Ware et al. 2009, Li, Guo et al. 2017). Preventing the opportunistic activity of stress-mediated transposons at early stages of sporogenesis will be of great importance in these plant species.

We hypothesise that MAGO may have been recruited in grass lineages to mediate a reproductive transposon 'immunity' in response to stress. Interestingly, we found that a small number of the 21-ntphasiRNAs appear to be induced by temperature stress in the male germline. This coincides with the stress activation of specific classes of LTR retroelements in the anthers of *MAGO RNAi* lines. It appears that by responding to stress in this way, the 21-nt phasiRNAs can sense the environment in the anther epidermis and migrate to the meiocytes in order to silence corresponding retroelements. It is not yet clear whether this response is limited to heat stress nor if it is limited to one specific family retroelements. Perhaps other abiotic stresses or even biotic stress during male germline development could trigger the accumulation of unique phasiRNAs. Furthermore, these unique phasiRNAs may be required repress a corresponding family of unique stress induced transposons.

This work demonstrates a novel strategy for understanding the relationship between argonautes and sRNAs in reproductive tissues under stress. For both animals and plants, it is now apparent that for many argonautes, stress can reveal phenotype and novel molecular functions. The function of several PIWI class argonautes in *C. elegans* are now being uncovered through the growth of mutants at elevated temperature (Batista, Ruby et al. 2008, Conine, Batista et al. 2010, Heestand, Simon et al. 2018). Surprisingly, a great number of argonaute mutants negatively impact the male, but not female germline in *C. elegans* which may suggest the male germline is particularly sensitive to epigenetic derepression, perhaps through the activation of transposable elements. In plants, there are numerous examples where the molecular functions of argonautes is only revealed after stress. These can range from altered sRNA binding preferences to altered protein subcellular localisation (Li, Henderson et al. 2008, Dolata, Bajczyk et al. 2016, Jullien, Grob et al. 2018, Liu, Xin et al. 2018, Teng, Zhang et al. 2018). It is clear that argonautes are highly responsive to environmental stimuli and may protect developmental programming under such conditions by finetuning gene expression and maintaining genomic stability.

This work highlights the way plants have expanded their argonaute repertoire to handle many diverse roles throughout development, especially during reproductive development. In summary, we have identified targets of the reproductive phasiRNAs, which until now were unknown. Furthermore, we have uncovered their role in reproductive development, acting as environmental stress sensors to safeguard the development of the male germline (Figure 7.1).

8.0 Appendix

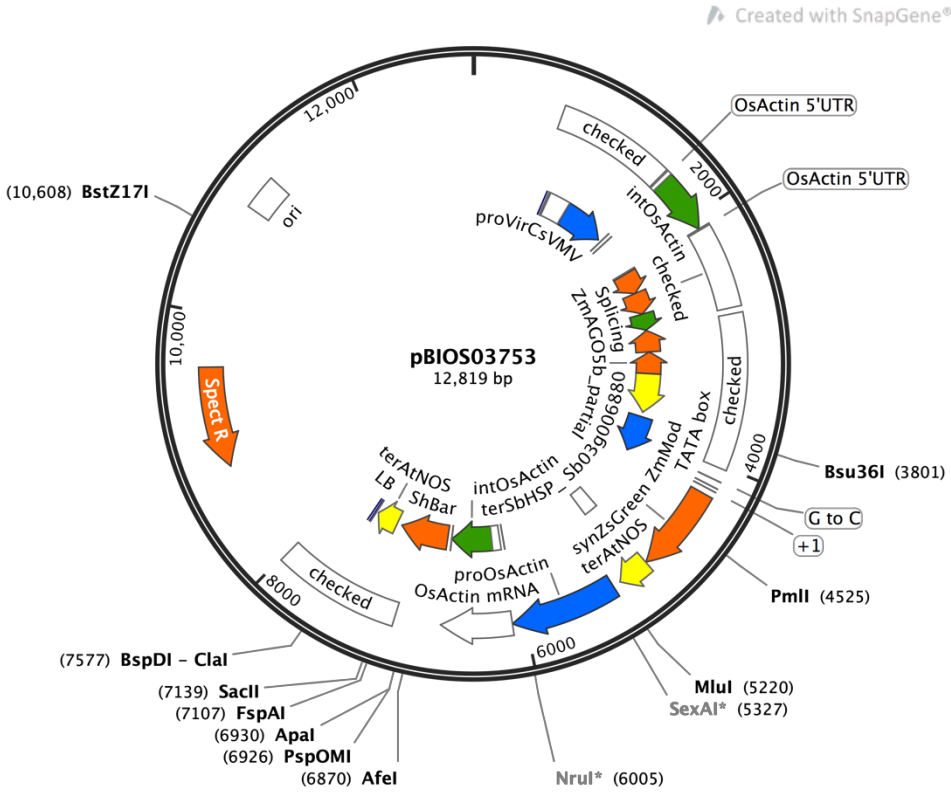

Figure 8.1: Vector map of pBIOS03753 for simultaneous downregulation of the MAGO genes in maize.

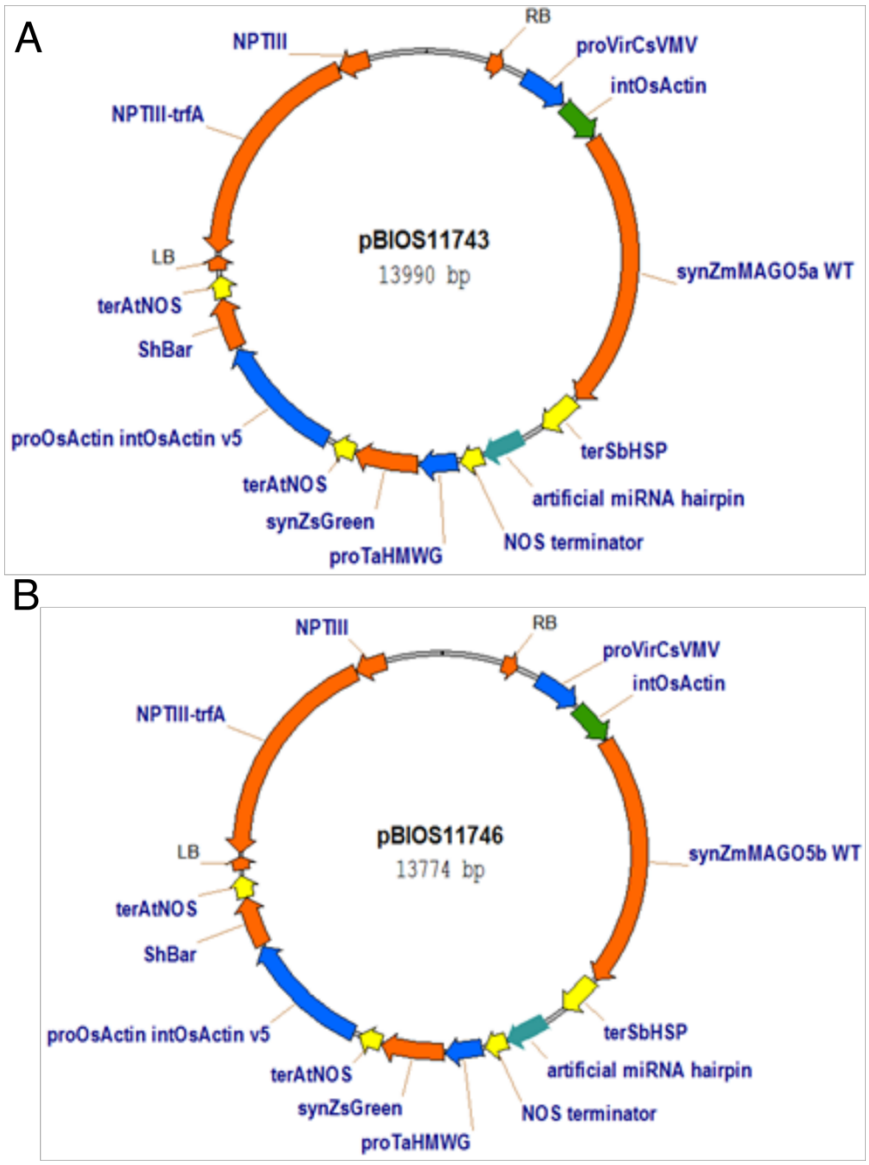

Figure 8.2: Vector map for simultaneous expression of MAGO and amiR2118 genes in *N. benthamiana*. (A) Vector map for pBIOS11743. (B) Vector map for pBIOS11746.

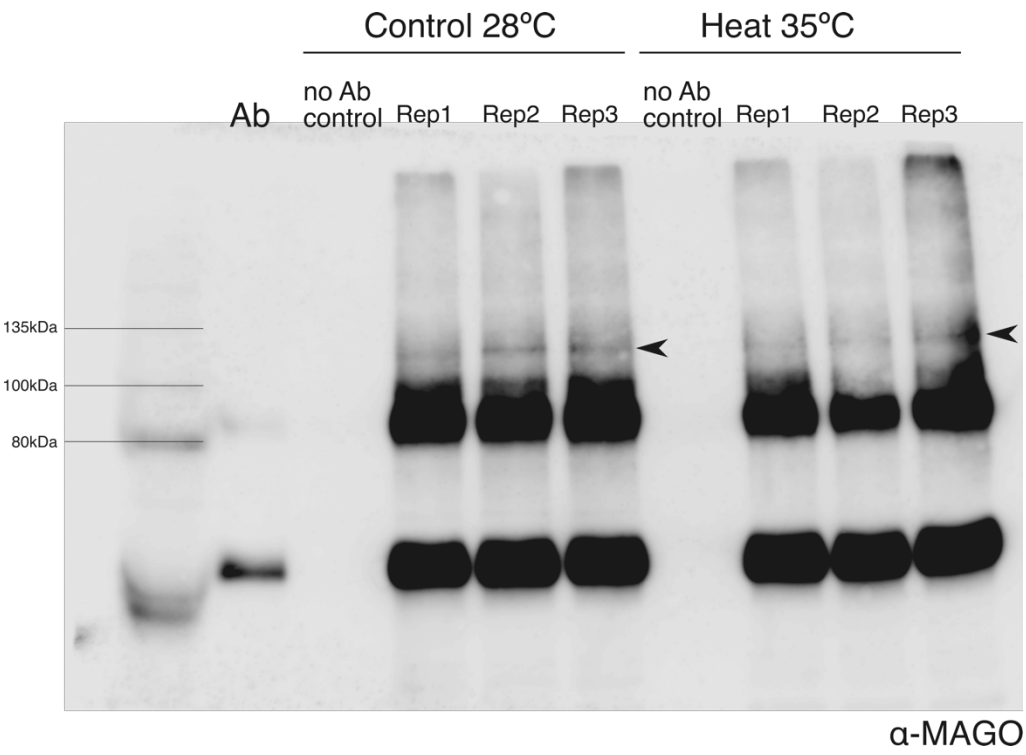

Figure 8.3: MAGO western blot following immunoprecipitation. MAGO protein was immunoprecipitated from total protein extracts of maize anthers grown under control and heat stress conditions. Immunoprecipitates were run on a 7.5% SDS-page gel before transfer and detected by both MAGO1 and MAGO2 antibodies simultaneously. Bands are detected at the approximate predicted size of full length MAGO protein (~110 kDa). Ab: Antibody control; No AB: no antibody immunoprecipitation controls.

Table 8.1: proportion of total sRNA and immunoprecipitation sRNA sequencing librarys mapping to distinct genomic features.

	control_Wt	control_Wt	control_Wt	control_RNAi	control_RNAi	control_RNAi	Heat_Wt	Heat_Wt	Heat_Wt	Heat_RNAi	Heat_RNAi	Heat_RNAi	MAGOIP_early	MAGOIP_late	negative	HCPROIP_rep1	HCPROIP_rep2
tRNA	0.108	0.130	0.116	0.118	0.023	0.076	0.056	0.072	0.044	0.117	0.107	0.070	0.157	0.266	0.020	0.008	0.019
rRNA	0.012	0.012	0.015	0.007	0.010	0.010	0.016	0.026	0.017	0.020	0.020	0.026	0.010	0.007	0.019	0.026	0.010
miRNA	0.005	0.001	0.001	0.007	0.002	0.004	0.007	0.001	0.006	0.004	0.004	0.002	0.002	0.001	0.039	0.020	0.030
snRNA	0.002	0.002	0.001	0.002	0.001	0.002	0.004	0.002	0.004	0.007	0.001	0.004	0.003	0.002	0.009	0.002	0.002
21PHAS	0.017	0.009	0.009	0.027	0.026	0.029	0.031	0.018	0.056	0.004	0.026	0.021	0.015	0.006	0.019	0.043	0.026
24PHAS	0.001	0.000	0.002	0.000	0.000	0.000	0.000	0.000	0.000	0.000	0.000	0.000	0.232	0.149	0.187	0.329	0.330
LTR derived	0.225	0.250	0.267	0.190	0.254	0.236	0.223	0.326	0.240	0.187	0.223	0.206	0.253	0.168	0.258	0.329	0.297
helitron derived	0.135	0.123	0.102	0.130	0.145	0.135	0.115	0.086	0.115	0.105	0.081	0.067	0.113	0.097	0.113	0.102	0.116
exon	0.188	0.194	0.162	0.196	0.090	0.152	0.156	0.139	0.150	0.229	0.171	0.142	0.215	0.306	0.335	0.142	0.171

Table 8.2: Selected MAGO RNAi lines. MAGO RNAi lines were selected containing a single T-DNA and segregating GFP reporter. Three lines with strong fertility defects (Bold)

Tissue culture code	Tissue culture event code	Event	Seedlot Code	Plant Code	Kernel number	T-DNA copy nb	Genotype	Segregation ratio (GFP+/GFP-) %
CM-08910D	CM-08910D-1	T02878_002	B0098963-01	B0098963	105	1	GFP+	56
CM-08910D	CM-08910D-1	T02878_002	B0098963-01	B0098963	83	1	GFP-	
CM-08902P	CM-08902P-1	T02878_003	B0098961-01	B0098961	36	1	GFP+	38
CM-08902P	CM-08902P-1	T02878_003	B0098961-01	B0098961	58	1	GFP-	
CM-08901O	**CM-08901O-1**	**T02878_006**	**B0098956-01**	**B0098956**	**73**	**1**	**GFP+**	**43**
CM-08901O	CM-08901O-1	T02878_006	B0098956-01	B0098956	97	1	GFP-	
CM-08901N	CM-08901N-1	T02878_007	B0098690-01	B0098690	135	1	GFP+	47
CM-08901N	CM-08901N-1	T02878_007	B0098690-01	B0098690	150	1	GFP-	
CM-08901M	CM-08901M-1	T02878_008	B0098689-01	B0098689	57	1	GFP+	46
CM-08901M	CM-08901M-1	T02878_008	B0098689-01	B0098689	66	1	GFP-	
CM-08901K	CM-08901K-1	T02878_009	B0098687-01	B0098687	104	1	GFP+ tri difficile	68
CM-08901K	CM-08901K-1	T02878_009	B0098687-01	B0098687	49	1	GFP-	
CM-08902L	CM-08902L-1	T02878_012	B0098701-01	B0098701	37	1	GFP+	59
CM-08902L	CM-08902L-1	T02878_012	B0098701-01	B0098701	26	1	GFP-	
CM-08902J	CM-08902J-1	T02878_014	B0098699-01	B0098699	86	1	GFP+	54
CM-08902J	CM-08902J-1	T02878_014	B0098699-01	B0098699	74	1	GFP-	
CM-08902A	CM-08902A-1	T02878_021	B0098691-01	B0098691	63	1	GFP+ tri difficile	77
CM-08902A	CM-08902A-1	T02878_021	B0098691-01	B0098691	19	1	GFP-	
CM-08901I	CM-08901I-1	T02878_023	B0098685-01	B0098685	76	1	GFP+	45
CM-08901I	CM-08901I-1	T02878_023	B0098685-01	B0098685	94	1	GFP-	
CM-08901F	CM-08901F-1	T02878_025	B0098683-01	B0098683	109	1	GFP+	54
CM-08901F	CM-08901F-1	T02878_025	B0098683-01	B0098683	94	1	GFP-	
CM-08901E	CM-08901E-1	T02878_026	B0098682-01	B0098682	161	1	GFP+ tri difficile	81
CM-08901E	CM-08901E-1	T02878_026	B0098682-01	B0098682	39	1	GFP-	
CM-08901B	CM-08901B-1	T02878_029	B0098679-01	B0098679	111	1	GFP+ tri difficile	79
CM-08901B	CM-08901B-1	T02878_029	B0098679-01	B0098679	30	1	GFP-	
CM-08903M	CM-08903M-1	T02878_030	B0098716-01	B0098716	74	1	GFP+	48
CM-08903M	CM-08903M-1	T02878_030	B0098716-01	B0098716	80	1	GFP-	
CM-08903H	CM-08903H-1	T02878_034	B0098711-01	B0098711	18	1	GFP-	0
CM-08903E	CM-08903E-1	T02878_037	B0098708-01	B0098708	69	1	GFP+	58
CM-08903E	CM-08903E-1	T02878_037	B0098708-01	B0098708	50	1	GFP-	
CM-08904E	**CM-08904E-1**	**T02878_040**	**B0098721-01**	**B0098721**	**125**	**1**	**GFP+**	**51**
CM-08904E	CM-08904E-1	T02878_040	B0098721-01	B0098721	119	1	GFP-	
CM-08902H	**CM-08902H-1**	**T02878_016**	**B0098959-01**	**B0098959**	**51**	**Truncated**	**GFP+**	**41**
CM-08902H	CM-08902H-1	T02878_016	B0098959-01	B0098959	74	Truncated	GFP-	

Table 8.3: Staging of anther meiosis in wild type (A188) and *MAGO* RNAi lines. Anther length was measured and pollen stage determined by carmine red staining of chromosomes.

A188 (mm)	Leptotene	Zygotene	Pachytene	Diplotene	Diakinesis	Metaphase I	Anaphase I	Telophase I
0.9-1.1 mm	3.07	96.01	0.92					
1.2-1.4 mm	5.45	84.41	10.15					
1.5-1.7 mm		37.76	44.29	2.04	9.59	4.29	2.04	
1.8-2.0 mm					1.04	18.58	13.19	67.19
>2.1 mm								
MAGO RNAi	Leptotene	Zygotene	Pachytene	Diplotene	Diakinesis	Metaphase I	Anaphase I	Telophase I
0.9-1.1 mm	57.76	42.24						
1.2-1.4 mm	33.97	56.80	9.22					
1.5-1.7 mm	0.30	35.90	63.80					
1.8-2.0 mm		3.60	74.19	4.84	17.37			
>2.1 mm						33.97	3.21	62.82

Table 8.4: Heat upregulated genes in dependent on *MAGO1/2* RNAi. (padj, FDR adjusted p value)

maizegdb	description	log2FoldChange	padj
Zm00001d017949	Endoglucanase 8	6.90747949	0.00056884
Zm00001d018266		5.252807	0.00058801
Zm00001d052019	Putative RING zinc finger domain superfamily protein	4.94288449	0.00924741
Zm00001d032265	WRKY69-superfamily of TFs having WRKY and zinc finger domains	4.66818254	0.00259943
Zm00001d033744	ubiquitin conjugating enzyme5	4.42528543	0.0030653
Zm00001d043444	plant-specific domain TIGR01615 family protein expressed	4.19005342	0.00576242
Zm00001d036033	Storage protein	4.17661212	0.00375675
Zm00001d014467	Peroxidase 3	3.88403559	0.00026783
Zm00001d051242	RNA polymerase II C-terminal domain phosphatase-like 1	3.64374148	0.00873814
Zm00001d026249	Villin-4	3.53119505	0.00138888
Zm00001d021703	oxygen evolving complex2	3.52691386	0.00101601
Zm00001d035818	Protein kinase superfamily protein with octicosapeptide/Phox/Bem1p domain	3.37271817	0.00365948
Zm00001d035455	Zinc finger CCCH domain-containing protein 29	3.2597282	0.00356399
Zm00001d027789		3.20181481	0.00155809
Zm00001d035669	Rab5-interacting family protein	3.19334573	0.00363958
Zm00001d041788	Protein SUPPRESSOR OF GENE SILENCING 3	3.15892614	0.00509748
Zm00001d028250	RNI-like superfamily protein	3.13920578	0.00160998
Zm00001d045192	Ribonucleoside-diphosphate reductase large subunit	3.02947308	0.00629037
Zm00001d025316	OsFBX59 - F-box domain containing protein expressed	2.89494869	0.00132829
Zm00001d020506	26S proteasome non-ATPase regulatory subunit 9	2.87675068	0.00082007
Zm00001d054107	FAM10 family protein	2.74128803	0.00996761
Zm00001d047392	Transducin/WD40 repeat-like superfamily protein	2.65608413	0.00671738
Zm00001d038616	ER6 protein	2.65566502	0.00438288
Zm00001d038022	Pentatricopeptide repeat-containing protein chloroplastic	2.34208499	0.0043067
Zm00001d010905		2.32957109	8.42E-05
Zm00001d050018	ABSCISIC ACID-INSENSITIVE 5-like protein 5	2.209053	0.00811846
Zm00001d049331	Nudix hydrolase 15 mitochondrial	2.20768231	0.00780316
Zm00001d039933	16.9 kDa class I heat shock protein 1	2.18003928	0.00479119
Zm00001d028187	Heparanase-like protein 1	2.11729443	0.00160363
Zm00001d044015	protein phosphatase homolog8	2.07565242	0.00596593
Zm00001d032166	Protein ENHANCED DISEASE RESISTANCE 2	2.02471693	0.00249052
Zm00001d034715	rubisco accumulation factor2	2.00959097	0.00341348
Zm00001d040383	Whole genome shotgun sequence of line PN40024 scaffold_123.assembly12x (Fragment)	1.93194846	0.00485907
Zm00001d033159	DEK domain-containing chromatin associated protein	1.89711489	0.00274488
Zm00001d019809	UTP:RNA uridylyltransferase 1	1.81998121	0.00074972
Zm00001d053376	AAA-type ATPase family protein / ankyrin repeat family protein	1.74625643	0.00965638
Zm00001d014742	F-box protein SKIP31	1.73215856	0.00029691
Zm00001d040666	alpha/beta-Hydrolases superfamily protein	1.7175827	0.00491114
Zm00001d014727	Carboxylesterase-like protein	1.6798895	0.00029571

Table 8.5: Top 100 heat downregulated genes in dependent on *MAGO1/2* RNAi. (padj, FDR adjusted p value)

maizegdb	description	log2FoldChange	padj
Zm00001d001953	Protein IQ-DOMAIN 32	-24.44504062	1.39E-12
Zm00001d023461	Expressed protein; protein	-7.516252535	0.00114809
Zm00001d006112	Arabinogalactan protein	-6.822464125	4.19E-06
Zm00001d008620	Metallothionein-like protein 2A	-6.625634034	3.03E-05
Zm00001d006918	histone acetyl transferase MYST family 101	-6.20318464	1.04E-05
Zm00001d007085	Haloacid dehalogenase-like hydrolase (HAD) superfamily protein	-6.202483179	1.18E-05
Zm00001d007912	Calcium-dependent protein kinase 20	-6.111672612	2.17E-05
Zm00001d002436	alternative oxidase2	-6.103472545	1.82E-09
Zm00001d023650	Protein yippee-like%3B Protein yippee-like protein isoform 1%3B Protein yippee-like protein isoform 2	-5.924301898	0.00117511
Zm00001d034172	Protein FATTY ACID EXPORT 3 chloroplastic	-5.456414114	0.00320169
Zm00001d002026	Protein kinase superfamily protein	-5.452734228	7.32E-12
Zm00001d009707	Protein ABIL1	-5.275070053	4.47E-05
Zm00001d013546	Ubiquitin-conjugating enzyme 15	-5.106287015	0.00022324
Zm00001d010336	Peptide methionine sulfoxide reductase B3	-4.973600841	6.74E-05
Zm00001d034054	Cleavage stimulation factor subunit 50	-4.89286239	0.00314092
Zm00001d042059		-4.882624334	0.0051092
Zm00001d002726	Pectinesterase	-4.655986656	9.09E-08
Zm00001d004669	mRNA capping enzyme family protein	-4.619055	8.91E-07
Zm00001d021635	Condensin-2 complex subunit H2	-4.595254874	0.00100952
Zm00001d002817	Kinesin-like protein KIN-7G	-4.423827645	9.09E-08
Zm00001d029975	Serine/threonine-protein kinase SRK2C	-4.205745965	0.00201319
Zm00001d002711	Serine racemase	-4.204147231	5.19E-08
Zm00001d003284	SWI/SNF complex subunit SWI3A	-4.15797884	2.62E-07
Zm00001d017100	Vacuolar protein sorting-associated protein 20 homolog 2	-4.111900831	0.00048758
Zm00001d006386	AP-3 complex subunit mu	-4.097086304	5.83E-06
Zm00001d003925	Serine/threonine-protein kinase PBS1	-4.054000263	6.04E-07
Zm00001d005359	ATP-dependent protease Clp ATPase subunit	-3.989988699	1.84E-06
Zm00001d006496	Polyadenylate-binding protein RBP45C	-3.985309451	6.43E-06
Zm00001d010780		-3.968287609	7.39E-05
Zm00001d006377	Asparagine--tRNA ligase chloroplastic/mitochondrial	-3.922586513	5.83E-06
Zm00001d008744	Transaminase/ transferase isoform 1%3B Transaminase/ transferase isoform 2%3B Transaminase/ transferase%2C transferring nitrogenous groups	-3.902514359	3.41E-05
Zm00001d007951	Casein kinase II subunit alpha	-3.810727625	2.22E-05
Zm00001d005866	Protein disulfide-isomerase like 2-2	-3.810338764	3.67E-06
Zm00001d010940		-3.801300929	8.45E-05
Zm00001d003216		-3.774925055	1.23E-07
Zm00001d006213	Probable histone H2A.4	-3.715440196	4.77E-06
Zm00001d042266	eukaryotic initiation factor 3 gamma subunit family protein	-3.687943624	0.00528366
Zm00001d033586		-3.494248387	0.00302996
Zm00001d004021	violaxanthin de-epoxidase1	-3.398195998	6.36E-07
Zm00001d013526	succinate dehydrogenase10	-3.378599275	0.00022224
Zm00001d005701	Ankyrin repeat-containing protein	-3.363083942	3.24E-06
Zm00001d005739		-3.326383826	3.45E-06
Zm00001d018489	Tumor-related protein	-3.316082378	0.00061303
Zm00001d009497	CDP-diacylglycerol--serine O-phosphatidyltransferase 1	-3.315318118	4.03E-05
Zm00001d045397	U-box domain-containing protein 35	-3.310272756	0.00632403
Zm00001d007012	Ribonucleoprotein A	-3.294561952	1.06E-05
Zm00001d015568	Nucleolin	-3.274121788	0.00040792
Zm00001d006705	ARM repeat superfamily protein	-3.255418689	8.64E-06
Zm00001d007277	Brassinosteroid LRR receptor kinase	-3.191238332	1.50E-05

Zm00001d029349		-3.154559318	0.00191125
Zm00001d034424	Folate-biopterin transporter 1 chloroplastic	-3.143722115	0.00329328
Zm00001d003715	Structural molecule	-3.130313838	5.08E-07
Zm00001d005407	myosin heavy chain-related	-3.118007813	1.98E-06
Zm00001d048483	THO complex subunit 7B	-3.116291095	0.00719222
Zm00001d008691	Autophagy-related protein 18c	-3.112070986	3.36E-05
Zm00001d014909	Acyl-CoA N-acyltransferase with RING/FYVE/PHD-type zinc finger domain	-3.106835961	0.00032774
Zm00001d035618	Histone H2A	-3.088802721	0.00361674
Zm00001d024094	Sister chromatid cohesion 1 protein 3	-3.08028749	0.0012281
Zm00001d025075		-3.073905366	0.00131701
Zm00001d010455		-3.07128458	6.79E-05
Zm00001d009776	Translation initiation factor IF-2	-3.058680009	4.70E-05
Zm00001d001896	Probable phytol kinase%2C chloroplastic	-3.028124989	8.84E-14
Zm00001d021300	Histone H2A	-2.967604997	0.00088196
Zm00001d016973	F-box protein GID2	-2.929180076	0.00048119
Zm00001d013131	Cell division protein FtsZ homolog 1 chloroplastic	-2.899836127	0.00019322
Zm00001d007677	Sister-chromatid cohesion protein 3	-2.88193848	1.95E-05
Zm00001d007778		-2.879687816	2.12E-05
Zm00001d022556	SH3 domain-containing protein 3	-2.859215292	0.00112662
Zm00001d052584	Protein kinase domain containing protein expressed	-2.829655903	0.0094302
Zm00001d005791	Histone H4	-2.826835537	3.46E-06
Zm00001d005547	Protein PHR1-LIKE 3	-2.824830697	3.14E-06
Zm00001d044239	RING/U-box superfamily protein	-2.820061652	0.00601994
Zm00001d012232		-2.815058167	0.00013018
Zm00001d008747	SH3 domain-containing protein 3	-2.809385585	3.41E-05
Zm00001d036118	Putative homeobox DNA-binding and leucine zipper domain family protein	-2.807849137	0.00379137
Zm00001d005015		-2.791733197	1.73E-06
Zm00001d019538	RNA-binding KH domain-containing protein	-2.778879136	0.00074693
Zm00001d030034	glucose-inhibited division family A protein	-2.744949597	0.00202666
Zm00001d007502	carotene isomerase2	-2.739840113	1.80E-05
Zm00001d008222		-2.702321878	2.26E-05
Zm00001d014994	NAD(P)-binding Rossmann-fold superfamily protein	-2.699296374	0.00032984
Zm00001d033925	cystathionine beta synthase domain protein1	-2.696455584	0.0031062
Zm00001d010296	protein; Protein kinase domain containing protein	-2.693664244	6.22E-05
Zm00001d007328	ABC transporter I family member 11 chloroplastic	-2.685025136	1.54E-05
Zm00001d012659	TRAM LAG1 and CLN8 (TLC) lipid-sensing domain containing protein	-2.677210981	0.00013918
Zm00001d047994	Inositol-tetrakisphosphate 1-kinase 3	-2.668945459	0.00708342
Zm00001d011963	ATP-dependent RNA helicase DHX8	-2.66549533	0.00012407
Zm00001d012881	DPP6 N-terminal domain-like protein	-2.651732324	0.00015978
Zm00001d047382	plasmacytoma 326 homolog	-2.650812694	0.00671179
Zm00001d007090	RNA pseudouridine synthase 6 chloroplastic	-2.642646845	1.21E-05
Zm00001d043386	Dynein light chain LC6%2C flagellar outer arm	-2.64200034	0.00575101
Zm00001d006461	SH3 domain-containing protein 3	-2.640480824	6.31E-06
Zm00001d036571	Heat shock 70 kDa protein 16	-2.622864865	0.00393058
Zm00001d025202	Protein kinase superfamily protein	-2.592880087	0.00132128
Zm00001d011828	Serine/arginine-rich splicing factor SR45	-2.575552722	0.00011926
Zm00001d015037	Glutamate--tRNA ligase chloroplastic/mitochondrial	-2.573763236	0.00034927
Zm00001d047849	Sulfoquinovosyl transferase SQD2	-2.569546143	0.00698463
Zm00001d037364	Golgin candidate 2	-2.524569856	0.00398759
Zm00001d013013	Magnesium-chelatase subunit ChlD chloroplastic	-2.521655776	0.00017966
Zm00001d036540	mRNA-decapping enzyme subunit 2	-2.513141106	0.00392321

Table 8.6: Differentially accumulating sRNAs mapped to genes. DEseq2 normalized reads mapping to gene features. MAGO1 (ZmAGO5b) and MAGO2 (ZmAGO5c) (Bold)

ID	Locus	Feature	wild type	MAGO RNAi	wild type	MAGO RNAi
Cluster_45011	Chr7:135844980..135846806	Heat shock protein 90-2	53.65	109.91	611.62	130.05
Cluster_30373	**Chr5:4113607..4113901**	**ZmAGO5c**	**18.28**	**1514.25**	**18.58**	**9607.86**
Cluster_55219	Chr9:124179349..124179973	LTR, sucrose synthase 1	62.61	57.55	10.91	89.37
Cluster_19973	Chr3:157124504..157124539	BTB/POZ domain-containing protein	1.89	10.39	147.77	82.33
Cluster_45010	Chr7:135843572..135843998	Heat shock protein 90-2	7.97	23.87	129.08	25.87
Cluster_5891	Chr1:217692750..217693301	L10-interacting MYB domain-containing protein	21.86	64.29	93.13	61.77
Cluster_16300	**Chr2:239623413..239623566**	**ZmAGO5b**	**7.82**	**722.82**	**6.84**	**3917.12**
Cluster_6815	Chr1:245842918..245843058	Phosphatase 2A_intron	10.33	43.67	66.63	66.24
Cluster_30372	**Chr5:4113361..4113528**	**ZmAGO5c**	**8.53**	**629.10**	**6.81**	**2917.56**
Cluster_12577	Chr2:124639805..124640042	Sec23/Sec24 protein transport family protein_intron	251.03	723.45	729.25	709.31
Cluster_52921	Chr9:18789123..18790556	Helitron, Hydrolase-like protein family	9.00	1.01	63.57	162.16
Cluster_24523	Chr4:46608435..46608614	LTR, methylthioadenosine nucleosidase 1	23.39	65.23	216.92	209.98
Cluster_42943	Chr7:38304450..38304896	cesa7 - cellulose synthase7	140.73	96.94	68.92	253.33

Table 8.7: Differentially accumulating sRNAs mapped to LTR retrotrasposons. DEseq2 normalized reads mapping to TE features. *Hek* LTR (bold)

			Control (28ºC)		Heat (35ºC)	
main	locus	Feature	Wild type	MAGO RNAi	Wild type	MAGO RNAi
Cluster_42851	Chr7:32076444..32076546	LTR	44.79	116.19	88.30	25.67
Cluster_17173	Chr3:22501067..22501278	LTR	20.56	65.35	127.16	67.10
Cluster_7201	Chr1:256958608..256958969	LTR	44.59	156.81	209.67	141.07
Cluster_4344	Chr1:158421952..158422318	LTR	57.89	232.69	277.01	227.44
Cluster_58253	**Chr10:75740955..75741256**	**LTR**	**37.87**	**134.49**	**181.76**	**128.23**
Cluster_40891	Chr6:149120768..149120958	LTR	28.36	103.50	145.42	103.62
Cluster_58235	Chr10:74515352..74515934	LTR	135.59	9.70	1.41	50.46
Cluster_58238	Chr10:74790773..74791812	LTR	116.41	15.21	6.66	44.50
Cluster_27145	Chr4:162120163..162120183	LTR	45.70	69.84	55.01	11.20
Cluster_48212	Chr8:62043076..62043325	LTR	27.17	89.01	143.55	103.78
Cluster_28319	Chr4:194386876..194387074	LTR	112.67	141.72	100.35	23.39
Cluster_16108	Chr2:235736072..235736200	LTR	32.17	157.45	143.18	100.69
Cluster_50191	Chr8:131525840..131525889	LTR	28.64	105.61	133.92	99.56
Cluster_37720	Chr6:33411752..33412881	LTR	173.09	21.58	6.92	27.42
Cluster_33732	Chr5:117183207..117183550	LTR	115.59	33.94	165.74	360.86
Cluster_9116	Chr1:304737103..304737344	LTR	64.28	213.53	278.85	224.90
Cluster_37254	Chr6:13481344..13481383	LTR	17.00	2.16	40.24	217.19
Cluster_16099	Chr2:235668559..235669209	LTR	245.52	36.27	7.08	125.17
Cluster_53120	Chr9:23061902..23061993	LTR	19.94	77.03	72.01	52.32
Cluster_53073	Chr9:22491308..22491699	LTR	57.27	155.13	202.34	157.25
Cluster_33387	Chr5:96480013..96480116	LTR	152.03	234.88	173.39	53.78
Cluster_55528	Chr9:133088611..133089343	LTR	112.87	26.52	83.60	302.34
Cluster_5583	Chr1:206048232..206048277	LTR	13.06	51.96	74.60	80.33
Cluster_26749	Chr4:149854478..149854672	LTR	26.98	112.79	63.32	48.65
Cluster_23249	Chr4:7634110..7634453	LTR	113.78	25.81	3.56	40.94
Cluster_10137	Chr2:21515103..21515424	LTR	16.78	53.28	65.46	50.50
Cluster_37227	Chr6:12757350..12757405	LTR	37.58	5.48	71.01	230.27
Cluster_55412	Chr9:129551683..129551827	LTR	30.26	131.06	70.49	63.84
Cluster_12503	Chr2:120009254..120009408	LTR	8.56	18.77	97.74	54.51

Table 8.8: Differentially accumulating sRNAs mapped to tRNAs. DEseq2 normalized reads mapping to tRNA features. MAGO binding 5'tRF (bold)

			Control (28ºC)		Heat (35ºC)	
ID	locus	Feature	wild type	MAGO RNAi	wild type	MAGO RNAi
Cluster_25944	Chr4:115346200..115346453	tRNA	2543.37	972.11	4263.55	13807.30
Cluster_18976	Chr3:115652819..115653100	tRNA	2485.67	749.99	1720.59	3390.05
Cluster_19701	Chr3:146474141..146474232	tRNA	393.04	129.11	379.77	1606.78
Cluster_141	Chr1:2998699..2998778	tRNA	639.53	99.86	1011.35	2801.05
Cluster_30061	Chr4:244500639..244500886	tRNA	43.94	15.45	35.66	144.20
Cluster_2012	Chr1:57390540..57390614	tRNA	119.77	16.25	78.86	308.39
Cluster_41014	Chr6:151754055..151754135	tRNA	50.28	24.87	22.83	87.82
Cluster_14630	Chr2:199183495..199183573	tRNA	1957.21	304.97	3004.56	8464.56
Cluster_27641	Chr4:177830265..177830341	tRNA	534.53	191.68	230.63	443.55
Cluster_37000	Chr6:1586846..1586932	tRNA	89.70	42.93	108.77	330.78
Cluster_1438	Chr1:40102937..40103076	tRNA	537.64	124.60	1043.91	1834.35
Cluster_59258	Chr10:110851696..110851782	tRNA	418.66	99.27	771.79	1362.73
Cluster_4131	Chr1:149757244..149757415	tRNA	3356.99	804.76	6519.04	11487.60
Cluster_55839	Chr9:141471870..141471955	tRNA	314.71	116.37	345.29	802.37
Cluster_37863	Chr6:41676925..41677084	tRNA	59.90	26.71	66.32	185.61
Cluster_55235	Chr9:124807682..124807778	tRNA	5807.32	1906.18	4615.57	16255.17
Cluster_27744	Chr4:180318402..180318497	tRNA	252.82	87.73	204.41	689.10
Cluster_46017	Chr7:162862426..162862506	tRNA	412.65	99.53	777.92	1356.31
Cluster_56157	Chr9:149323181..149323261	tRNA	135.06	30.59	261.28	435.74
Cluster_1674	Chr1:45719399..45719503	tRNA	3806.60	1486.45	4863.45	12475.78
Cluster_16473	Chr2:244404193..244404361	tRNA	92.37	35.18	107.97	192.26
Cluster_32177	Chr5:53093537..53093628	tRNA	8061.61	1713.69	4494.62	7664.61
Cluster_55756	**Chr9:140010406..140010513**	**LTR, tRNA**	3406.45	1342.21	4419.06	11228.88

References

Aarts, M. G., W. G. Dirkse, W. J. Stiekema and A. Pereira (1993). "Transposon tagging of a male sterility gene in Arabidopsis." Nature **363**(6431): 715.

Aarts, M. G., R. Hodge, K. Kalantidis, D. Florack, Z. A. Wilson, B. J. Mulligan, W. J. Stiekema, R. Scott and A. Pereira (1997). "The Arabidopsis MALE STERILITY 2 protein shares similarity with reductases in elongation/condensation complexes." The Plant Journal **12**(3): 615-623.

Abe, H., T. Urao, T. Ito, M. Seki, K. Shinozaki and K. Yamaguchi-Shinozaki (2003). "Arabidopsis AtMYC2 (bHLH) and AtMYB2 (MYB) function as transcriptional activators in abscisic acid signaling." The Plant Cell **15**(1): 63-78.

Adenot, X., T. Elmayan, D. Lauressergues, S. Boutet, N. Bouché, V. Gasciolli and H. Vaucheret (2006). "DRB4-dependent TAS3 trans-acting siRNAs control leaf morphology through AGO7." Current Biology **16**(9): 927-932.

Agashe, B., C. K. Prasad and I. Siddiqi (2002). "Identification and analysis of DYAD: a gene required for meiotic chromosome organisation and female meiotic progression in Arabidopsis." Development **129**(16): 3935-3943.

Agius, F., A. Kapoor and J.-K. Zhu (2006). "Role of the Arabidopsis DNA glycosylase/lyase ROS1 in active DNA demethylation." Proceedings of the National Academy of Sciences **103**(31): 11796-11801.

Ahmed, F. E., A. E. Hall and D. A. DeMason (1992). "Heat injury during floral development in cowpea (Vigna unguiculata, Fabaceae)." American Journal of Botany **79**(7): 784-791.

Aigner, A. (2006). "Gene silencing through RNA interference (RNAi) in vivo: strategies based on the direct application of siRNAs." Journal of biotechnology **124**(1): 12-25.

Alleman, M. and J. Doctor (2000). "Genomic imprinting in plants: observations and evolutionary implications." Plant molecular biology **43**(2-3): 147-161.

Allen, E., Z. Xie, A. M. Gustafson and J. C. Carrington (2005). "microRNA-directed phasing during trans-acting siRNA biogenesis in plants." Cell **121**(2): 207-221.

Alves, C. S., R. Vicentini, G. T. Duarte, V. F. Pinoti, M. Vincentz and F. T. Nogueira (2017). "Genome-wide identification and characterization of tRNA-derived RNA fragments in land plants." Plant molecular biology **93**(1-2): 35-48.

Ameyar-Zazoua, M., C. Rachez, M. Souidi, P. Robin, L. Fritsch, R. Young, N. Morozova, R. Fenouil, N. Descostes and J.-C. Andrau (2012). "Argonaute

proteins couple chromatin silencing to alternative splicing." Nature structural & molecular biology **19**(10): 998.
Anandalakshmi, R., G. J. Pruss, X. Ge, R. Marathe, A. C. Mallory, T. H. Smith and V. B. Vance (1998). "A viral suppressor of gene silencing in plants." Proceedings of the National Academy of Sciences **95**(22): 13079-13084.
Aravin, A. A., G. J. Hannon and J. Brennecke (2007). "The Piwi-piRNA pathway provides an adaptive defense in the transposon arms race." science **318**(5851): 761-764.
Aravin, A. A., N. M. Naumova, A. V. Tulin, V. V. Vagin, Y. M. Rozovsky and V. A. Gvozdev (2001). "Double-stranded RNA-mediated silencing of genomic tandem repeats and transposable elements in the D. melanogaster germline." Current Biology **11**(13): 1017-1027.
Aravin, A. A., R. Sachidanandam, A. Girard, K. Fejes-Toth and G. J. Hannon (2007). "Developmentally regulated piRNA clusters implicate MILI in transposon control." Science **316**(5825): 744-747.
Arita, K., M. Ariyoshi, H. Tochio, Y. Nakamura and M. Shirakawa (2008). "Recognition of hemi-methylated DNA by the SRA protein UHRF1 by a base-flipping mechanism." Nature **455**(7214): 818-821.
Armstrong, S. J., A. P. Caryl, G. H. Jones and F. C. H. Franklin (2002). "Asy1, a protein required for meiotic chromosome synapsis, localizes to axis-associated chromatin in Arabidopsis and Brassica." Journal of cell science **115**(18): 3645-3655.
Armstrong, S. J., F. C. H. Franklin and G. H. Jones (2001). "Nucleolus-associated telomere clustering and pairing precede meiotic chromosome synapsis in Arabidopsis thaliana." Journal of Cell Science **114**(23): 4207-4217.
Arteaga-Vazquez, M. A. and V. L. Chandler (2010). "Paramutation in maize: RNA mediated trans-generational gene silencing." Current opinion in genetics & development **20**(2): 156-163.
Atreya, C. D. and T. P. Pirone (1993). "Mutational analysis of the helper component-proteinase gene of a potyvirus: effects of amino acid substitutions, deletions, and gene replacement on virulence and aphid transmissibility." Proceedings of the National Academy of Sciences **90**(24): 11919-11923.
Aufsatz, W., T. Stoiber, B. Rakic and K. Naumann (2007). "Arabidopsis histone deacetylase 6: a green link to RNA silencing." Oncogene **26**(37): 5477.
Axtell, M. J. (2013). "Classification and comparison of small RNAs from plants." Annual review of plant biology **64**: 137-159.
Axtell, M. J. and J. L. Bowman (2008). "Evolution of plant microRNAs and their targets." Trends in plant science **13**(7): 343-349.

Bartee, L., F. Malagnac and J. Bender (2001). "Arabidopsis cmt3 chromomethylase mutations block non-CG methylation and silencing of an endogenous gene." Genes & development **15**(14): 1753-1758.
Batista, P. J., J. G. Ruby, J. M. Claycomb, R. Chiang, N. Fahlgren, K. D. Kasschau, D. A. Chaves, W. Gu, J. J. Vasale and S. Duan (2008). "PRG-1 and 21U-RNAs interact to form the piRNA complex required for fertility in C. elegans." Molecular cell **31**(1): 67-78.
Baumberger, N. and D. Baulcombe (2005). "Arabidopsis ARGONAUTE1 is an RNA Slicer that selectively recruits microRNAs and short interfering RNAs." Proceedings of the National Academy of Sciences **102**(33): 11928-11933.
Baute, J. and A. Depicker (2008). "Base excision repair and its role in maintaining genome stability." Critical Reviews in Biochemistry and Molecular Biology **43**(4): 239-276.
Baxter, A., R. Mittler and N. Suzuki (2013). "ROS as key players in plant stress signalling." Journal of experimental botany **65**(5): 1229-1240.
Bedinger, P. A. and J. E. Fowler (2009). The maize male gametophyte. Handbook of maize: Its biology, Springer**:** 57-77.
Belmonte, M. F., R. C. Kirkbride, S. L. Stone, J. M. Pelletier, A. Q. Bui, E. C. Yeung, M. Hashimoto, J. Fei, C. M. Harada and M. D. Munoz (2013). "Comprehensive developmental profiles of gene activity in regions and subregions of the Arabidopsis seed." Proceedings of the National Academy of Sciences **110**(5): E435-E444.
Benlloch-González, M., R. Sánchez-Lucas, M. Benlloch and F.-E. Ricardo (2018). "An approach to global warming effects on flowering and fruit set of olive trees growing under field conditions." Scientia Horticulturae **240**: 405-410.
Berger, F. and D. Twell (2011). "Germline specification and function in plants." Annual review of plant biology **62**: 461-484.
Berger, S. L. (2007). "The complex language of chromatin regulation during transcription." Nature **447**(7143): 407-412.
Bewick, A. J., L. Ji, C. E. Niederhuth, E.-M. Willing, B. T. Hofmeister, X. Shi, L. Wang, Z. Lu, N. A. Rohr and B. Hartwig (2016). "On the origin and evolutionary consequences of gene body DNA methylation." Proceedings of the National Academy of Sciences **113**(32): 9111-9116.
Bita, C. E., S. Zenoni, W. H. Vriezen, C. Mariani, M. Pezzotti and T. Gerats (2011). "Temperature stress differentially modulates transcription in meiotic anthers of heat-tolerant and heat-sensitive tomato plants." BMC genomics **12**(1): 384.
Blum, A., N. Klueva and H. Nguyen (2001). "Wheat cellular thermotolerance is related to yield under heat stress." Euphytica **117**(2): 117-123.

Boavida, L., J. D. Becker and J. A. Feijo (2005). "The making of gametes in higher plants." International Journal of Development Biology: 595-614.
Bohmert, K., I. Camus, C. Bellini, D. Bouchez, M. Caboche and C. Benning (1998). "AGO1 defines a novel locus of Arabidopsis controlling leaf development." The EMBO journal **17**(1): 170-180.
Bolger, A. M., M. Lohse and B. Usadel (2014). "Trimmomatic: a flexible trimmer for Illumina sequence data." Bioinformatics **30**(15): 2114-2120.
Bologna, N. G., R. Iselin, L. A. Abriata, A. Sarazin, N. Pumplin, F. Jay, T. Grentzinger, M. Dal Peraro and O. Voinnet (2018). "Nucleo-cytosolic Shuttling of ARGONAUTE1 Prompts a Revised Model of the Plant MicroRNA Pathway." Molecular cell **69**(4): 709-719. e705.
Borg, M., L. Brownfield and D. Twell (2009). "Male gametophyte development: a molecular perspective." Journal of experimental botany **60**(5): 1465-1478.
Borges, F. and R. A. Martienssen (2015). "The expanding world of small RNAs in plants." Nature reviews Molecular cell biology **16**(12): 727.
Bostick, M., J. K. Kim, P.-O. Estève, A. Clark, S. Pradhan and S. E. Jacobsen (2007). "UHRF1 plays a role in maintaining DNA methylation in mammalian cells." Science **317**(5845): 1760-1764.
Bowman, J. (2012). Arabidopsis: an atlas of morphology and development, Springer Science & Business Media.
Boyko, A. and I. Kovalchuk (2008). "Epigenetic control of plant stress response." Environmental and molecular mutagenesis **49**(1): 61-72.
Brennecke, J., A. A. Aravin, A. Stark, M. Dus, M. Kellis, R. Sachidanandam and G. J. Hannon (2007). "Discrete small RNA-generating loci as master regulators of transposon activity in Drosophila." Cell **128**(6): 1089-1103.
Brigneti, G., O. Voinnet, W. X. Li, L. H. Ji, S. W. Ding and D. C. Baulcombe (1998). "Retracted: Viral pathogenicity determinants are suppressors of transgene silencing in Nicotiana benthamiana." The EMBO journal **17**(22): 6739-6746.
Brink, R. A. (1958). Paramutation at the R locus in maize. Cold Spring Harbor symposia on quantitative biology, Cold Spring Harbor Laboratory Press.
Brunkard, J. O. and P. C. Zambryski (2017). "Plasmodesmata enable multicellularity: new insights into their evolution, biogenesis, and functions in development and immunity." Current opinion in plant biology **35**: 76-83.
Buhtz, A., F. Springer, L. Chappell, D. C. Baulcombe and J. Kehr (2008). "Identification and characterization of small RNAs from the phloem of Brassica napus." The Plant Journal **53**(5): 739-749.
Bukau, B., J. Weissman and A. Horwich (2006). "Molecular chaperones and protein quality control." Cell **125**(3): 443-451.

Calarco, J. P., F. Borges, M. T. Donoghue, F. Van Ex, P. E. Jullien, T. Lopes, R. Gardner, F. Berger, J. A. Feijó and J. D. Becker (2012). "Reprogramming of DNA methylation in pollen guides epigenetic inheritance via small RNA." Cell **151**(1): 194-205.

Canales, C., A. M. Bhatt, R. Scott and H. Dickinson (2002). "EXS, a putative LRR receptor kinase, regulates male germline cell number and tapetal identity and promotes seed development in Arabidopsis." Current biology **12**(20): 1718-1727.

Canto-Pastor, A., B. A. Santos, A. A. Valli, W. Summers, S. Schornack and D. C. Baulcombe (2019). "Enhanced resistance to bacterial and oomycete pathogens by short tandem target mimic RNAs in tomato." Proceedings of the National Academy of Sciences **116**(7): 2755-2760.

Cao, X. and S. E. Jacobsen (2002). "Role of the Arabidopsis DRM methyltransferases in de novo DNA methylation and gene silencing." Current Biology **12**(13): 1138-1144.

Carlsbecker, A., J.-Y. Lee, C. J. Roberts, J. Dettmer, S. Lehesranta, J. Zhou, O. Lindgren, M. A. Moreno-Risueno, A. Vatén and S. Thitamadee (2010). "Cell signalling by microRNA165/6 directs gene dose-dependent root cell fate." Nature **465**(7296): 316.

Carlson, C. M., A. J. Dupuy, S. Fritz, K. J. Roberg-Perez, C. F. Fletcher and D. A. Largaespada (2003). "Transposon mutagenesis of the mouse germline." Genetics **165**(1): 243-256.

Carmell, M. A., A. Girard, H. J. van de Kant, D. Bourc'his, T. H. Bestor, D. G. de Rooij and G. J. Hannon (2007). "MIWI2 is essential for spermatogenesis and repression of transposons in the mouse male germline." Developmental cell **12**(4): 503-514.

Caryl, A. P., S. J. Armstrong, G. H. Jones and F. C. H. Franklin (2000). "A homologue of the yeast HOP1 gene is inactivated in the Arabidopsis meiotic mutant asy1." Chromosoma **109**(1-2): 62-71.

Caryl, A. P., G. H. Jones and F. C. H. Franklin (2003). "Dissecting plant meiosis using Arabidopsis thaliana mutants." Journal of Experimental Botany **54**(380): 25-38.

Cavrak, V. V., N. Lettner, S. Jamge, A. Kosarewicz, L. M. Bayer and O. M. Scheid (2014). "How a retrotransposon exploits the plant's heat stress response for its activation." PLoS Genetics **10**(1): e1004115.

Chapman, E. J., A. I. Prokhnevsky, K. Gopinath, V. V. Dolja and J. C. Carrington (2004). "Viral RNA silencing suppressors inhibit the microRNA pathway at an intermediate step." Genes & development **18**(10): 1179-1186.

Chaubal, R., J. R. Anderson, M. R. Trimnell, T. W. Fox, M. C. Albertsen and P. Bedinger (2003). "The transformation of anthers in the msca1 mutant of maize." Planta **216**(5): 778-788.

Chen, C., A. D. Farmer, R. J. Langley, J. Mudge, J. A. Crow, G. D. May, J. Huntley, A. G. Smith and E. F. Retzel (2010). "Meiosis-specific gene discovery in plants: RNA-Seq applied to isolated Arabidopsis male meiocytes." BMC plant biology **10**(1): 280.
Chen, C., A. Marcus, W. Li, Y. Hu, J.-P. V. Calzada, U. Grossniklaus, R. J. Cyr and H. Ma (2002). "The Arabidopsis ATK1 gene is required for spindle morphogenesis in male meiosis." Development **129**(10): 2401-2409.
Chen, Q., M. Yan, Z. Cao, X. Li, Y. Zhang, J. Shi, G.-h. Feng, H. Peng, X. Zhang and Y. Zhang (2016). "Sperm tsRNAs contribute to intergenerational inheritance of an acquired metabolic disorder." Science **351**(6271): 397-400.
Chen, X. (2009). "Small RNAs and their roles in plant development." Annual Review of Cell and Developmental **25**: 21-44.
Chen, Y., A. Pane and T. Schüpbach (2007). "Cutoff and aubergine mutations result in retrotransposon upregulation and checkpoint activation in Drosophila." Current Biology **17**(7): 637-642.
Chen, Z. J. and L. Tian (2007). "Roles of dynamic and reversible histone acetylation in plant development and polyploidy." Biochimica et Biophysica Acta (BBA)-Gene Structure and Expression **1769**(5-6): 295-307.
Cheng, C., K.-Y. Yun, H. W. Ressom, B. Mohanty, V. B. Bajic, Y. Jia, S. J. Yun and B. G. de los Reyes (2007). "An early response regulatory cluster induced by low temperature and hydrogen peroxide in seedlings of chilling-tolerant japonica rice." BMC genomics **8**(1): 175.
Cheng, P., R. Greyson and D. Walden (1983). "Organ initiation and the development of unisexual flowers in the tassel and ear of Zea mays." American Journal of Botany **70**(3): 450-462.
Cheng, X. (2014). "Structural and functional coordination of DNA and histone methylation." Cold Spring Harbor perspectives in biology **6**(8): a018747.
Chitwood, D. H., F. T. Nogueira, M. D. Howell, T. A. Montgomery, J. C. Carrington and M. C. Timmermans (2009). "Pattern formation via small RNA mobility." Genes & development **23**(5): 549-554.
Choi, Y., M. Gehring, L. Johnson, M. Hannon, J. J. Harada, R. B. Goldberg, S. E. Jacobsen and R. L. Fischer (2002). "DEMETER, a DNA glycosylase domain protein, is required for endosperm gene imprinting and seed viability in Arabidopsis." Cell **110**(1): 33-42.
Cognat, V., G. Morelle, C. Megel, S. Lalande, J. Molinier, T. Vincent, I. Small, A.-M. Duchêne and L. Maréchal-Drouard (2016). "The nuclear and organellar tRNA-derived RNA fragment population in Arabidopsis thaliana is highly dynamic." Nucleic acids research **45**(6): 3460-3472.
Cogoni, C., J. Irelan, M. Schumacher, T. Schmidhauser, E. Selker and G. Macino (1996). "Transgene silencing of the al-1 gene in vegetative cells of Neurospora is mediated by a cytoplasmic effector and does not depend on

DNA-DNA interactions or DNA methylation." The EMBO journal **15**(12): 3153-3163.
Cokus, S. J., S. Feng, X. Zhang, Z. Chen, B. Merriman, C. D. Haudenschild, S. Pradhan, S. F. Nelson, M. Pellegrini and S. E. Jacobsen (2008). "Shotgun bisulphite sequencing of the Arabidopsis genome reveals DNA methylation patterning." Nature **452**(7184): 215-219.
Cole, C., A. Sobala, C. Lu, S. R. Thatcher, A. Bowman, J. W. Brown, P. J. Green, G. J. Barton and G. Hutvagner (2009). "Filtering of deep sequencing data reveals the existence of abundant Dicer-dependent small RNAs derived from tRNAs." Rna.
Conine, C., F. Sun, L. Song, J. Rivera-Perez and O. Rando (2018). "Small RNAs gained during epididymal transit of sperm are essential for embryonic development in mice." bioRxiv: 311670.
Conine, C. C., P. J. Batista, W. Gu, J. M. Claycomb, D. A. Chaves, M. Shirayama and C. C. Mello (2010). "Argonautes ALG-3 and ALG-4 are required for spermatogenesis-specific 26G-RNAs and thermotolerant sperm in Caenorhabditis elegans." Proceedings of the National Academy of Sciences **107**(8): 3588-3593.
Couteau, F., F. Belzile, C. Horlow, O. Grandjean, D. Vezon and M.-P. Doutriaux (1999). "Random chromosome segregation without meiotic arrest in both male and female meiocytes of a dmc1 mutant of Arabidopsis." The Plant Cell **11**(9): 1623-1634.
Cox, D. N., A. Chao, J. Baker, L. Chang, D. Qiao and H. Lin (1998). "A novel class of evolutionarily conserved genes defined by piwi are essential for stem cell self-renewal." Genes & development **12**(23): 3715-3727.
Craft, J., M. Samalova, C. Baroux, H. Townley, A. Martinez, I. Jepson, M. Tsiantis and I. Moore (2005). "New pOp/LhG4 vectors for stringent glucocorticoid-dependent transgene expression in Arabidopsis." The Plant Journal **41**(6): 899-918.
Creasey, K. M., J. Zhai, F. Borges, F. Van Ex, M. Regulski, B. C. Meyers and R. A. Martienssen (2014). "miRNAs trigger widespread epigenetically activated siRNAs from transposons in Arabidopsis." Nature **508**(7496): 411.
Crevillén, P., H. Yang, X. Cui, C. Greeff, M. Trick, Q. Qiu, X. Cao and C. Dean (2014). "Epigenetic reprogramming that prevents transgenerational inheritance of the vernalized state." Nature **515**(7528): 587.
Crimi, M., A. Astegno, G. Zoccatelli and M. Degli Esposti (2006). "Pro-apoptotic effect of maize lipid transfer protein on mammalian mitochondria." Archives of biochemistry and biophysics **445**(1): 65-71.
Dai, X., Z. Zhuang and P. X. Zhao (2018). "psRNATarget: a plant small RNA target analysis server (2017 release)." Nucleic acids research.

Dawe, R. K. and M. Freeling (1990). "Clonal analysis of the cell lineages in the male flower of maize." Developmental biology **142**(1): 233-245.
Dawe, R. K. and M. Freeling (1992). "The role of initial cells in maize anther morphogenesis." Development **116**(4): 1077-1085.
Dawson, J., Z. Wilson, M. Aarts, A. Braithwaite, L. Briarty and B. Mulligan (1993). "Microspore and pollen development in six male-sterile mutants of Arabidopsis thaliana." Canadian Journal of Botany **71**(4): 629-638.
Deng, Y., R. Srivastava, T. D. Quilichini, H. Dong, Y. Bao, H. T. Horner and S. H. Howell (2016). "IRE 1, a component of the unfolded protein response signaling pathway, protects pollen development in Arabidopsis from heat stress." The Plant Journal **88**(2): 193-204.
Dewan, S., K. Vander Mijnsbrugge, P. De Frenne, M. Steenackers, B. Michiels and K. Verheyen (2018). "Maternal temperature during seed maturation affects seed germination and timing of bud set in seedlings of European black poplar." Forest Ecology and Management **410**: 126-135.
Doering-Saad, C., H. J. Newbury, J. S. Bale and J. Pritchard (2002). "Use of aphid stylectomy and RT-PCR for the detection of transporter mRNAs in sieve elements." Journal of Experimental Botany **53**(369): 631-637.
Dolata, J., M. Bajczyk, D. Bielewicz, K. Niedojadlo, J. Niedojadlo, H. Pietrykowska, W. Walczak, Z. Szweykowska-Kulinska and A. Jarmolowski (2016). "Salt stress reveals a new role for ARGONAUTE 1 in miRNA biogenesis at the transcriptional and post-transcriptional levels." Plant physiology: pp. 00830.02016.
Dong, Z., M.-H. Han and N. Fedoroff (2008). "The RNA-binding proteins HYL1 and SE promote accurate in vitro processing of pri-miRNA by DCL1." Proceedings of the National Academy of Sciences **105**(29): 9970-9975.
Dooner, H. K., Q. Wang, J. T. Huang, Y. Li, L. He, W. Xiong and C. Du (2019). "Spontaneous mutations in maize pollen are frequent in some lines and arise mainly from retrotranspositions and deletions." Proceedings of the National Academy of Sciences **116**(22): 10734-10743.
Dowen, R. H., M. Pelizzola, R. J. Schmitz, R. Lister, J. M. Dowen, J. R. Nery, J. E. Dixon and J. R. Ecker (2012). "Widespread dynamic DNA methylation in response to biotic stress." Proc Natl Acad Sci USA **109**.
Driedonks, N., J. Xu, J. L. Peters, S. Park and I. Rieu (2015). "Multi-level interactions between heat shock factors, heat shock proteins, and the redox system regulate acclimation to heat." Frontiers in plant science **6**: 999.
Du, J., X. Zhong, Y. V. Bernatavichute, H. Stroud, S. Feng, E. Caro, A. A. Vashisht, J. Terragni, H. G. Chin, A. Tu, J. Hetzel, J. A. Wohlschlegel, S. Pradhan, D. J. Patel and S. E. Jacobsen (2012). "Dual binding of chromomethylase domains to H3K9me2-containing nucleosomes directs DNA methylation in plants." Cell **151**(1): 167-180.

Dubin, M. J., O. M. Scheid and C. Becker (2018). "Transposons: a blessing curse." Current opinion in plant biology **42**: 23-29.
Dukowic-Schulze, S., A. Sundararajan, T. Ramaraj, J. Mudge and C. Chen (2014). "Sequencing-based large-scale genomics approaches with small numbers of isolated maize meiocytes." Frontiers in plant science **5**.
Dunoyer, P., C. A. Brosnan, G. Schott, Y. Wang, F. Jay, A. Alioua, C. Himber and O. Voinnet (2010). "Retracted: An endogenous, systemic RNAi pathway in plants." The EMBO journal **29**(10): 1699-1712.
Dunoyer, P., C. Himber and O. Voinnet (2005). "DICER-LIKE 4 is required for RNA interference and produces the 21-nucleotide small interfering RNA component of the plant cell-to-cell silencing signal." Nature genetics **37**(12): 1356.
Dunoyer, P., C.-H. Lecellier, E. A. Parizotto, C. Himber and O. Voinnet (2004). "RETRACTED: Probing the MicroRNA and small interfering RNA pathways with virus-encoded suppressors of RNA silencing." The Plant Cell **16**(5): 1235-1250.
Dunoyer, P., G. Schott, C. Himber, D. Meyer, A. Takeda, J. C. Carrington and O. Voinnet (2010). "Small RNA duplexes function as mobile silencing signals between plant cells." Science: 1185880.
Durán-Figueroa, N. and J.-P. Vielle-Calzada (2010). "ARGONAUTE9-dependent silencing of transposable elements in pericentromeric regions of Arabidopsis." Plant signaling & behavior **5**(11): 1476-1479.
Durdevic, Z., R. S. Pillai and A. Ephrussi (2018). "Transposon silencing in the Drosophila female germline is essential for genome stability in progeny embryos." Life Science Alliance **1**(5): e201800179.
Earley, K. W., M. S. Shook, B. Brower-Toland, L. Hicks and C. S. Pikaard (2007). "In vitro specificities of Arabidopsis co-activator histone acetyltransferases: implications for histone hyperacetylation in gene activation." The Plant Journal **52**(4): 615-626.
Emery, J. F., S. K. Floyd, J. Alvarez, Y. Eshed, N. P. Hawker, A. Izhaki, S. F. Baum and J. L. Bowman (2003). "Radial patterning of Arabidopsis shoots by class III HD-ZIP and KANADI genes." Current Biology **13**(20): 1768-1774.
Erickson, A. and A. Markhart (2002). "Flower developmental stage and organ sensitivity of bell pepper (Capsicum annuum L.) to elevated temperature." Plant, Cell & Environment **25**(1): 123-130.
Fahlgren, N., T. A. Montgomery, M. D. Howell, E. Allen, S. K. Dvorak, A. L. Alexander and J. C. Carrington (2006). "Regulation of AUXIN RESPONSE FACTOR3 by TAS3 ta-siRNA affects developmental timing and patterning in Arabidopsis." Current biology **16**(9): 939-944.
Fan, Y., J. Yang, S. M. Mathioni, J. Yu, J. Shen, X. Yang, L. Wang, Q. Zhang, Z. Cai and C. Xu (2016). "PMS1T, producing phased small-interfering RNAs,

regulates photoperiod-sensitive male sterility in rice." Proceedings of the National Academy of Sciences **113**(52): 15144-15149.
Fei, Q., L. Yang, W. Liang, D. Zhang and B. C. Meyers (2016). "Dynamic changes of small RNAs in rice spikelet development reveal specialized reproductive phasiRNA pathways." Journal of experimental botany **67**(21): 6037-6049.
Felippes, F. F. and D. Weigel (2009). "Triggering the formation of tasiRNAs in Arabidopsis thaliana: the role of microRNA miR173." EMBO reports **10**(3): 264-270.
Feng, S., S. J. Cokus, X. Zhang, P.-Y. Chen, M. Bostick, M. G. Goll, J. Hetzel, J. Jain, S. H. Strauss and M. E. Halpern (2010). "Conservation and divergence of methylation patterning in plants and animals." Proceedings of the National Academy of Sciences **107**(19): 8689-8694.
Fernández Gómez, J. and Z. A. Wilson (2014). "A barley PHD finger transcription factor that confers male sterility by affecting tapetal development." Plant biotechnology journal **12**(6): 765-777.
Feschotte, C. (2008). "Transposable elements and the evolution of regulatory networks." Nature Reviews Genetics **9**(5): 397.
Fragkostefanakis, S., A. Mesihovic, Y. Hu and E. Schleiff (2016). "Unfolded protein response in pollen development and heat stress tolerance." Plant reproduction **29**(1-2): 81-91.
Frank, G., E. Pressman, R. Ophir, L. Althan, R. Shaked, M. Freedman, S. Shen and N. Firon (2009). "Transcriptional profiling of maturing tomato (Solanum lycopersicum L.) microspores reveals the involvement of heat shock proteins, ROS scavengers, hormones, and sugars in the heat stress response." Journal of experimental botany **60**(13): 3891-3908.
Fuchs, J., D. Demidov, A. Houben and I. Schubert (2006). "Chromosomal histone modification patterns--from conservation to diversity." Trends Plant Sci **11**(4): 199-208.
Garcia, D., S. A. Collier, M. E. Byrne and R. A. Martienssen (2006). "Specification of leaf polarity in Arabidopsis via the trans-acting siRNA pathway." Current Biology **16**(9): 933-938.
Garcia-Aguilar, M., C. Michaud, O. Leblanc and D. Grimanelli (2010). "Inactivation of a DNA methylation pathway in maize reproductive organs results in apomixis-like phenotypes." The Plant Cell **22**(10): 3249-3267.
Gasciolli, V., A. C. Mallory, D. P. Bartel and H. Vaucheret (2005). "Partially redundant functions of Arabidopsis DICER-like enzymes and a role for DCL4 in producing trans-acting siRNAs." Current Biology **15**(16): 1494-1500.
Gasior, S. L., T. P. Wakeman, B. Xu and P. L. Deininger (2006). "The human LINE-1 retrotransposon creates DNA double-strand breaks." Journal of molecular biology **357**(5): 1383-1393.

Gbadegesin, M. (2012). "Transposable elements in the genomes: parasites, junks or drivers of evolution?" African journal of medicine and medical sciences **41**: 13-25.
Gehring, M., K. L. Bubb and S. Henikoff (2009). "Extensive demethylation of repetitive elements during seed development underlies gene imprinting." Science **324**(5933): 1447-1451.
Gehring, M., J. H. Huh, T.-F. Hsieh, J. Penterman, Y. Choi, J. J. Harada, R. B. Goldberg and R. L. Fischer (2006). "DEMETER DNA glycosylase establishes MEDEA polycomb gene self-imprinting by allele-specific demethylation." cell **124**(3): 495-506.
Gehring, M., W. Reik and S. Henikoff (2009). "DNA demethylation by DNA repair." Trends in Genetics **25**(2): 82-90.
Goldberg, A. D., C. D. Allis and E. Bernstein (2007). "Epigenetics: a landscape takes shape." Cell **128**(4): 635-638.
Golubovskaya, I., Z. K. Grebennikova, N. A. Avalkina and W. Sheridan (1993). "The role of the ameiotic1 gene in the initiation of meiosis and in subsequent meiotic events in maize." Genetics **135**(4): 1151-1166.
Golubovskaya, I. N., O. Hamant, L. Timofejeva, C.-J. R. Wang, D. Braun, R. Meeley and W. Z. Cande (2006). "Alleles of afd1 dissect REC8 functions during meiotic prophase I." Journal of cell science **119**(16): 3306-3315.
Gong, Z., T. Morales-Ruiz, R. R. Ariza, T. Roldán-Arjona, L. David and J.-K. Zhu (2002). "ROS1, a repressor of transcriptional gene silencing in Arabidopsis, encodes a DNA glycosylase/lyase." cell **111**(6): 803-814.
Grant-Downton, R., S. Kourmpetli, S. Hafidh, H. Khatab, G. Le Trionnaire, H. Dickinson and D. Twell (2013). "Artificial microRNAs reveal cell-specific differences in small RNA activity in pollen." Current biology **23**(14): R599-R601.
Grelon, M., D. Vezon, G. Gendrot and G. Pelletier (2001). "AtSPO11-1 is necessary for efficient meiotic recombination in plants." The EMBO journal **20**(3): 589-600.
Gutierrez-Marcos, J. F. and H. G. Dickinson (2012). "Epigenetic reprogramming in plant reproductive lineages." Plant Cell Physiol **53**(5): 817-823.
Haag, J. R., T. S. Ream, M. Marasco, C. D. Nicora, A. D. Norbeck, L. Pasa-Tolic and C. S. Pikaard (2012). "In vitro transcription activities of Pol IV, Pol V, and RDR2 reveal coupling of Pol IV and RDR2 for dsRNA synthesis in plant RNA silencing." Molecular cell **48**(5): 811-818.
Hackenberg, M., P.-J. Huang, C.-Y. Huang, B.-J. Shi, P. Gustafson and P. Langridge (2012). "A comprehensive expression profile of microRNAs and other classes of non-coding small RNAs in barley under phosphorous-deficient and-sufficient conditions." DNA research **20**(2): 109-125.

Hajkova, P. (2011). "Epigenetic reprogramming in the germline: towards the ground state of the epigenome." Philosophical Transactions of the Royal Society of London B: Biological Sciences **366**(1575): 2266-2273.
Hall, A. E. (2018). Crop Responses to Environment: Adapting to Global Climate Change, CRC Press.
Hamant, O., H. Ma and W. Z. Cande (2006). "Genetics of meiotic prophase I in plants." Annu. Rev. Plant Biol. **57**: 267-302.
Hamera, S., X. Song, L. Su, X. Chen and R. Fang (2012). "Cucumber mosaic virus suppressor 2b binds to AGO4-related small RNAs and impairs AGO4 activities." The Plant Journal **69**(1): 104-115.
Hamilton, A. J. and D. C. Baulcombe (1999). "A species of small antisense RNA in posttranscriptional gene silencing in plants." Science **286**(5441): 950-952.
Hamilton, W. D. and D. C. Baulcombe (1989). "Infectious RNA produced by in vitro transcription of a full-length tobacco rattle virus RNA-1 cDNA." Journal of general virology **70**(4): 963-968.
Hartung, F. and H. Puchta (2001). "Molecular characterization of homologues of both subunits A (SPO11) and B of the archaebacterial topoisomerase 6 in plants." Gene **271**(1): 81-86.
Harvey, J. J., M. G. Lewsey, K. Patel, J. Westwood, S. Heimstädt, J. P. Carr and D. C. Baulcombe (2011). "An antiviral defense role of AGO2 in plants." PloS one **6**(1): e14639.
Hashida, S.-N., T. Uchiyama, C. Martin, Y. Kishima, Y. Sano and T. Mikami (2006). "The temperature-dependent change in methylation of the Antirrhinum transposon Tam3 is controlled by the activity of its transposase." The Plant Cell **18**(1): 104-118.
Havecker, E. R., L. M. Wallbridge, T. J. Hardcastle, M. S. Bush, K. A. Kelly, R. M. Dunn, F. Schwach, J. H. Doonan and D. C. Baulcombe (2010). "The Arabidopsis RNA-directed DNA methylation argonautes functionally diverge based on their expression and interaction with target loci." The Plant Cell **22**(2): 321-334.
Haywood, V., T. S. Yu, N. C. Huang and W. J. Lucas (2005). "Phloem long-distance trafficking of GIBBERELLIC ACID-INSENSITIVE RNA regulates leaf development." The Plant Journal **42**(1): 49-68.
He, C., U. Tirlapur, M. Cresti, M. Peja, D. E. Crone and J. P. Mascarenhas (1996). "An Arabidopsis mutant showing aberrations in male meiosis." Sexual Plant Reproduction **9**(1): 54-57.
Heestand, B., M. Simon, S. Frenk, D. Titov and S. Ahmed (2018). "Transgenerational sterility of piwi mutants represents a dynamic form of adult reproductive diapause." Cell reports **23**(1): 156-171.

Heyting, C. (1996). "Synaptonemal complexes: structure and function." Current opinion in cell biology **8**(3): 389-396.
Higgins, J. D. (2013). "Analyzing meiosis in barley." Plant Meiosis: Methods and Protocols: 135-144.
Higgins, J. D., E. Sanchez-Moran, S. J. Armstrong, G. H. Jones and F. C. H. Franklin (2005). "The Arabidopsis synaptonemal complex protein ZYP1 is required for chromosome synapsis and normal fidelity of crossing over." Genes & development **19**(20): 2488-2500.
Himber, C., P. Dunoyer, G. Moissiard, C. Ritzenthaler and O. Voinnet (2003). "Transitivity-dependent and-independent cell-to-cell movement of RNA silencing." The EMBO journal **22**(17): 4523-4533.
Honda, S., P. Loher, M. Shigematsu, J. P. Palazzo, R. Suzuki, I. Imoto, I. Rigoutsos and Y. Kirino (2015). "Sex hormone-dependent tRNA halves enhance cell proliferation in breast and prostate cancers." Proceedings of the National Academy of Sciences **112**(29): E3816-E3825.
Hong, J.-S. and H.-J. Ju (2017). "The plant cellular systems for plant virus movement." The plant pathology journal **33**(3): 213.
Hong, L., D. Tang, K. Zhu, K. Wang, M. Li and Z. Cheng (2012). "Somatic and reproductive cell development in rice anther is regulated by a putative glutaredoxin." The Plant Cell: tpc. 111.093740.
Honys, D. and D. Twell (2004). "Transcriptome analysis of haploid male gametophyte development in Arabidopsis." Genome biology **5**(11): R85.
Houwing, S., L. M. Kamminga, E. Berezikov, D. Cronembold, A. Girard, H. Van Den Elst, D. V. Filippov, H. Blaser, E. Raz and C. B. Moens (2007). "A role for Piwi and piRNAs in germ cell maintenance and transposon silencing in Zebrafish." Cell **129**(1): 69-82.
Hsieh, L.-C., S.-I. Lin, A. C.-C. Shih, J.-W. Chen, W.-Y. Lin, C.-Y. Tseng, W.-H. Li and T.-J. Chiou (2009). "Uncovering small RNA-mediated responses to phosphate deficiency in Arabidopsis by deep sequencing." Plant physiology **151**(4): 2120-2132.
Hsieh, T.-F., J. Shin, R. Uzawa, P. Silva, S. Cohen, M. J. Bauer, M. Hashimoto, R. C. Kirkbride, J. J. Harada and D. Zilberman (2011). "Regulation of imprinted gene expression in Arabidopsis endosperm." Proceedings of the National Academy of Sciences **108**(5): 1755-1762.
Hu, L., W. Liang, C. Yin, X. Cui, J. Zong, X. Wang, J. Hu and D. Zhang (2011). "Rice MADS3 regulates ROS homeostasis during late anther development." The Plant Cell: tpc. 110.074369.
Huh, J. H., M. J. Bauer, T.-F. Hsieh and R. L. Fischer (2008). "Cellular programming of plant gene imprinting." Cell **132**(5): 735-744.
Hutvagner, G. and M. J. Simard (2008). "Argonaute proteins: key players in RNA silencing." Nature reviews Molecular cell biology **9**(1): 22.

Ibarra, C. A., X. Feng, V. K. Schoft, T.-F. Hsieh, R. Uzawa, J. A. Rodrigues, A. Zemach, N. Chumak, A. Machlicova and T. Nishimura (2012). "Active DNA demethylation in plant companion cells reinforces transposon methylation in gametes." Science **337**(6100): 1360-1364.
Ikeda, Y. and T. Kinoshita (2009). "DNA demethylation: a lesson from the garden." Chromosoma **118**(1): 37-41.
Imlau, A., E. Truernit and N. Sauer (1999). "Cell-to-cell and long-distance trafficking of the green fluorescent protein in the phloem and symplastic unloading of the protein into sink tissues." The Plant Cell **11**(3): 309-322.
Ishida, Y., H. Saito, S. Ohta, Y. Hiei, T. Komari and T. Kumashiro (1996). "High efficiency transformation of maize (Zea mays L.) mediated by Agrobacterium tumefaciens." Nature biotechnology **14**(6): 745.
Ito, H., H. Gaubert, E. Bucher, M. Mirouze, I. Vaillant and J. Paszkowski (2011). "An siRNA pathway prevents transgenerational retrotransposition in plants subjected to stress." Nature **472**.
Ito, H., T. Yoshida, S. Tsukahara and A. Kawabe (2013). "Evolution of the ONSEN retrotransposon family activated upon heat stress in Brassicaceae." Gene **518**(2): 256-261.
Iwata, Y., N. V. Fedoroff and N. Koizumi (2008). "Arabidopsis bZIP60 is a proteolysis-activated transcription factor involved in the endoplasmic reticulum stress response." The Plant Cell **20**(11): 3107-3121.
Jacobowitz, J. and J.-K. Weng (2018). "PRX9 and PRX40 are extensin peroxidases essential for maintaining tapetum and microspore cell wall integrity during Arabidopsis anther development." bioRxiv: 319020.
Ji, L. and X. Chen (2012). "Regulation of small RNA stability: methylation and beyond." Cell research **22**(4): 624-636.
Jiao, Y., P. Peluso, J. Shi, T. Liang, M. C. Stitzer, B. Wang, M. S. Campbell, J. C. Stein, X. Wei and C.-S. Chin (2017). "Improved maize reference genome with single-molecule technologies." Nature **546**(7659): 524.
Jin, Y., O. H. Tam, E. Paniagua and M. Hammell (2015). "TEtranscripts: a package for including transposable elements in differential expression analysis of RNA-seq datasets." Bioinformatics **31**(22): 3593-3599.
Johnson, C., A. Kasprzewska, K. Tennessen, J. Fernandes, G.-L. Nan, V. Walbot, V. Sundaresan, V. Vance and L. H. Bowman (2009). "Clusters and superclusters of phased small RNAs in the developing inflorescence of rice." Genome research **19**(8): 1429-1440.
Johnson, N. R., J. M. Yeoh, C. Coruh and M. J. Axtell (2016). "Improved placement of multi-mapping small RNAs." G3: Genes, Genomes, Genetics: g3. 116.030452.
Jones, J. D., L. Shlumukov, F. Carland, J. English, S. Scofield, G. Bishop and K. Harrison (1992). "Effective vectors for transformation, expression of

heterologous genes, and assaying transposon excision in transgenic plants." Transgenic research **1**(6): 285-297.
Jones-Rhoades, M. W. and D. P. Bartel (2004). "Computational identification of plant microRNAs and their targets, including a stress-induced miRNA." Molecular cell **14**(6): 787-799.
Jullien, P. E., S. Grob, A. Marchais, N. Pumplin, C. Chevalier, C. Otto, G. Schott and O. Voinnet (2018). "Functional characterization of Arabidopsis ARGONAUTE 3 in reproductive tissue." bioRxiv: 500769.
Jullien, P. E., D. Susaki, R. Yelagandula, T. Higashiyama and F. Berger (2012). "DNA methylation dynamics during sexual reproduction in Arabidopsis thaliana." Curr Biol **22**(19): 1825-1830.
Jung, K.-H., M.-J. Han, Y.-S. Lee, Y.-W. Kim, I. Hwang, M.-J. Kim, Y.-K. Kim, B. H. Nahm and G. An (2005). "Rice Undeveloped Tapetum1 is a major regulator of early tapetum development." The Plant Cell **17**(10): 2705-2722.
Kakrana, A., S. M. Mathioni, K. Huang, R. Hammond, L. Vandivier, P. Patel, S. Arikit, O. Shevchenko, A. E. Harkess and B. Kingham (2018). "Plant 24-nt reproductive phasiRNAs from intramolecular duplex mRNAs in diverse monocots." Genome research **28**(9): 1333-1344.
Kalmykova, A. I., M. S. Klenov and V. A. Gvozdev (2005). "Argonaute protein PIWI controls mobilization of retrotransposons in the Drosophila male germline." Nucleic acids research **33**(6): 2052-2059.
Kapoor, M., R. Arora, T. Lama, A. Nijhawan, J. P. Khurana, A. K. Tyagi and S. Kapoor (2008). "Genome-wide identification, organization and phylogenetic analysis of Dicer-like, Argonaute and RNA-dependent RNA Polymerase gene families and their expression analysis during reproductive development and stress in rice." BMC genomics **9**(1): 451.
Kasschau, K. D., S. Cronin and J. C. Carrington (1997). "Genome amplification and long-distance movement functions associated with the central domain of tobacco etch potyvirus helper component–proteinase." Virology **228**(2): 251-262.
Kasschau, K. D., Z. Xie, E. Allen, C. Llave, E. J. Chapman, K. A. Krizan and J. C. Carrington (2003). "P1/HC-Pro, a viral suppressor of RNA silencing, interferes with Arabidopsis development and miRNA function." Developmental cell **4**(2): 205-217.
Kawanabe, T., T. Ariizumi, M. Kawai-Yamada, H. Uchimiya and K. Toriyama (2006). "Abolition of the tapetum suicide program ruins microsporogenesis." Plant and Cell Physiology **47**(6): 784-787.
Kawashima, T. and F. Berger (2014). "Epigenetic reprogramming in plant sexual reproduction." Nat Rev Genet **15**(9): 613-624.
Keeney, S. (2001). "Mechanism and control of meiotic recombination initiation."

Keller, M. and S. Simm (2018). "The coupling of transcriptome and proteome adaptation during development and heat stress response of tomato pollen." BMC genomics **19**(1): 447.
Kelliher, T. and V. Walbot (2011). "Emergence and patterning of the five cell types of the Zea mays anther locule." Developmental biology **350**(1): 32-49.
Kelliher, T. and V. Walbot (2012). "Hypoxia triggers meiotic fate acquisition in maize." Science **337**(6092): 345-348.
Kellogg, E. A. (2007). "Floral displays: genetic control of grass inflorescences." Current opinion in plant biology **10**(1): 26-31.
Keng, V. W., K. Yae, T. Hayakawa, S. Mizuno, Y. Uno, K. Yusa, C. Kokubu, T. Kinoshita, K. Akagi and N. A. Jenkins (2005). "Region-specific saturation germline mutagenesis in mice using the Sleeping Beauty transposon system." Nature Methods **2**(10): 763.
Kermicle, J. (1970). "Dependence of the R-mottled aleurone phenotype in maize on mode of sexual transmission." Genetics **66**(1): 69.
Kim, I. and P. C. Zambryski (2005). "Cell-to-cell communication via plasmodesmata during Arabidopsis embryogenesis." Current opinion in plant biology **8**(6): 593-599.
Kim, J.-M., T. K. To and M. Seki (2012). "An epigenetic integrator: new insights into genome regulation, environmental stress responses and developmental controls by histone deacetylase 6." Plant and Cell Physiology **53**(5): 794-800.
Kim, S. Y., C. B. Hong and I. Lee (2001). "Heat shock stress causes stage-specific male sterility in Arabidopsis thaliana." Journal of Plant Research **114**(3): 301-307.
Kinoshita, T., A. Miura, Y. Choi, Y. Kinoshita, X. Cao, S. E. Jacobsen, R. L. Fischer and T. Kakutani (2004). "One-way control of FWA imprinting in Arabidopsis endosperm by DNA methylation." Science **303**(5657): 521-523.
Klattenhoff, C., D. P. Bratu, N. McGinnis-Schultz, B. S. Koppetsch, H. A. Cook and W. E. Theurkauf (2007). "Drosophila rasiRNA pathway mutations disrupt embryonic axis specification through activation of an ATR/Chk2 DNA damage response." Developmental cell **12**(1): 45-55.
Kleckner, N. (2006). "Chiasma formation: chromatin/axis interplay and the role (s) of the synaptonemal complex." Chromosoma **115**(3): 175.
Knauer, S., A. L. Holt, I. Rubio-Somoza, E. J. Tucker, A. Hinze, M. Pisch, M. Javelle, M. C. Timmermans, M. R. Tucker and T. Laux (2013). "A protodermal miR394 signal defines a region of stem cell competence in the Arabidopsis shoot meristem." Developmental cell **24**(2): 125-132.
Komiya, R. (2017). "Biogenesis of diverse plant phasiRNAs involves an miRNA-trigger and Dicer-processing." Journal of plant research **130**(1): 17-23.

Komiya, R., H. Ohyanagi, M. Niihama, T. Watanabe, M. Nakano, N. Kurata and K. Nonomura (2014). "Rice germline-specific Argonaute MEL1 protein binds to phasiRNAs generated from more than 700 lincRNAs." Plant J **78**(3): 385-397.
Komiya, R., H. Ohyanagi, M. Niihama, T. Watanabe, M. Nakano, N. Kurata and K. I. Nonomura (2014). "Rice germline-specific Argonaute MEL1 protein binds to phasiRNAs generated from more than 700 lincRNAs." The Plant Journal **78**(3): 385-397.
Kotak, S., J. Larkindale, U. Lee, P. von Koskull-Döring, E. Vierling and K.-D. Scharf (2007). "Complexity of the heat stress response in plants." Current opinion in plant biology **10**(3): 310-316.
Kubo, T., M. Fujita, H. Takahashi, M. Nakazono, N. Tsutsumi and N. Kurata (2013). "Transcriptome analysis of developing ovules in rice isolated by laser microdissection." Plant and cell physiology **54**(5): 750-765.
Kumar, S., G. Stecher and K. Tamura (2016). "MEGA7: Molecular Evolutionary Genetics Analysis version 7.0 for bigger datasets." Molecular Biology and Evolution **33**: 1870-1874.
Kuramochi-Miyagawa, S., T. Watanabe, K. Gotoh, Y. Totoki, A. Toyoda, M. Ikawa, N. Asada, K. Kojima, Y. Yamaguchi and T. W. Ijiri (2008). "DNA methylation of retrotransposon genes is regulated by Piwi family members MILI and MIWI2 in murine fetal testes." Genes & development **22**(7): 908-917.
Kurihara, D., Y. Mizuta, Y. Sato and T. Higashiyama (2015). "ClearSee: a rapid optical clearing reagent for whole-plant fluorescence imaging." Development: dev. 127613.
Kurihara, Y. and Y. Watanabe (2004). "Arabidopsis micro-RNA biogenesis through Dicer-like 1 protein functions." Proceedings of the National Academy of Sciences of the United States of America **101**(34): 12753-12758.
Lakatos, L., G. Szittya, D. Silhavy and J. Burgyán (2004). "Molecular mechanism of RNA silencing suppression mediated by p19 protein of tombusviruses." The EMBO journal **23**(4): 876-884.
Laufs, P., A. Peaucelle, H. Morin and J. Traas (2004). "MicroRNA regulation of the CUC genes is required for boundary size control in Arabidopsis meristems." Development **131**(17): 4311-4322.
Law, J. A., I. Ausin, L. M. Johnson, A. A. Vashisht, J.-K. Zhu, J. A. Wohlschlegel and S. E. Jacobsen (2010). "A protein complex required for polymerase V transcripts and RNA-directed DNA methylation in Arabidopsis." Current Biology **20**(10): 951-956.
Law, J. A., J. Du, C. J. Hale, S. Feng, K. Krajewski, A. M. S. Palanca, B. D. Strahl, D. J. Patel and S. E. Jacobsen (2013). "Polymerase IV occupancy at RNA-directed DNA methylation sites requires SHH1." Nature **498**(7454): 385-389.

Law, J. A. and S. E. Jacobsen (2010). "Establishing, maintaining and modifying DNA methylation patterns in plants and animals." NATURE REVIEWS GENETICS **11**(3): 204-220.
Le Trionnaire, G., R. Grant-Downton, S. Kourmpetli, H. Dickinson and D. Twell (2010). "Small RNA activity and function in angiosperm gametophytes." Journal of experimental botany **62**(5): 1601-1610.
Lee, T.-f., S. G. R. Gurazada, J. Zhai, S. Li, S. A. Simon, M. A. Matzke, X. Chen and B. C. Meyers (2012). "RNA polymerase V-dependent small RNAs in Arabidopsis originate from small, intergenic loci including most SINE repeats." Epigenetics **7**(7): 781-795.
Leonhardt, H., A. W. Page, H.-U. Weier and T. H. Bestor (1992). "A targeting sequence directs DNA methyltransferase to sites of DNA replication in mammalian nuclei." Cell **71**(5): 865-873.
Lewis, S. H., K. A. Quarles, Y. Yang, M. Tanguy, L. Frézal, S. A. Smith, P. P. Sharma, R. Cordaux, C. Gilbert and I. Giraud (2018). "Pan-arthropod analysis reveals somatic piRNAs as an ancestral defence against transposable elements." Nature ecology & evolution **2**(1): 174.
Lewsey, M. G., T. J. Hardcastle, C. W. Melnyk, A. Molnar, A. Valli, M. A. Urich, J. R. Nery, D. C. Baulcombe and J. R. Ecker (2016). "Mobile small RNAs regulate genome-wide DNA methylation." Proceedings of the National Academy of Sciences **113**(6): E801-E810.
Li, C. F., I. R. Henderson, L. Song, N. Fedoroff, T. Lagrange and S. E. Jacobsen (2008). "Dynamic regulation of ARGONAUTE4 within multiple nuclear bodies in Arabidopsis thaliana." PLoS genetics **4**(2): e27.
Li, C. F., O. Pontes, M. El-Shami, I. R. Henderson, Y. V. Bernatavichute, S. W.-L. Chan, T. Lagrange, C. S. Pikaard and S. E. Jacobsen (2006). "An ARGONAUTE4-containing nuclear processing center colocalized with Cajal bodies in Arabidopsis thaliana." Cell **126**(1): 93-106.
Li, E. and Y. Zhang (2014). "DNA methylation in mammals." Cold Spring Harbor perspectives in biology **6**(5): a019133.
Li, J. and F. Berger (2012). "Endosperm: food for humankind and fodder for scientific discoveries." New Phytologist **195**(2): 290-305.
Li, S., B. Le, X. Ma, S. Li, C. You, Y. Yu, B. Zhang, L. Liu, L. Gao and T. Shi (2016). "Biogenesis of phased siRNAs on membrane-bound polysomes in Arabidopsis." Elife **5**: e22750.
Li, S., L. Liu, X. Zhuang, Y. Yu, X. Liu, X. Cui, L. Ji, Z. Pan, X. Cao and B. Mo (2013). "MicroRNAs inhibit the translation of target mRNAs on the endoplasmic reticulum in Arabidopsis." Cell **153**(3): 562-574.
Li, T.-H., J. Spearow, C. M. Rubin and C. W. Schmid (1999). "Physiological stresses increase mouse short interspersed element (SINE) RNA expression in vivo." Gene **239**(2): 367-372.

Li, X., K. Guo, X. Zhu, P. Chen, Y. Li, G. Xie, L. Wang, Y. Wang, S. Persson and L. Peng (2017). "Domestication of rice has reduced the occurrence of transposable elements within gene coding regions." BMC genomics **18**(1): 55.

Li, X., L. M. Lawas, R. Malo, U. Glaubitz, A. Erban, R. Mauleon, S. Heuer, E. Zuther, J. Kopka and D. K. Hincha (2015). "Metabolic and transcriptomic signatures of rice floral organs reveal sugar starvation as a factor in reproductive failure under heat and drought stress." Plant, cell & environment **38**(10): 2171-2192.

Liang, D., R. G. White and P. M. Waterhouse (2014). "Mobile gene silencing in Arabidopsis is regulated by hydrogen peroxide." PeerJ **2**: e701.

Liao, Y., G. K. Smyth and W. Shi (2013). "featureCounts: an efficient general purpose program for assigning sequence reads to genomic features." Bioinformatics **30**(7): 923-930.

Lin, J.-r. and J. Hu (2013). "SeqNLS: nuclear localization signal prediction based on frequent pattern mining and linear motif scoring." PloS one **8**(10): e76864.

Lin, M.-K., Y.-J. Lee, T. J. Lough, B. S. Phinney and W. J. Lucas (2009). "Analysis of the pumpkin phloem proteome provides insights into angiosperm sieve tube function." Molecular & Cellular Proteomics **8**(2): 343-356.

Lindroth, A. M., X. Cao, J. P. Jackson, D. Zilberman, C. M. McCallum, S. Henikoff and S. E. Jacobsen (2001). "Requirement of CHROMOMETHYLASE3 for maintenance of CpXpG methylation." Science **292**(5524): 2077-2080.

Lingel, A., B. Simon, E. Izaurralde and M. Sattler (2004). "Nucleic acid 3'-end recognition by the Argonaute2 PAZ domain." Nature Structural and Molecular Biology **11**(6): 576.

Lisch, D. (2009). "Epigenetic regulation of transposable elements in plants." Annual review of plant biology **60**: 43-66.

Lisch, D. (2013). "How important are transposons for plant evolution?" Nature Reviews Genetics **14**(1): 49.

Lisch, D. and J. L. Bennetzen (2011). "Transposable element origins of epigenetic gene regulation." Current opinion in plant biology **14**(2): 156-161.

Liu, C., F. Lu, X. Cui and X. Cao (2010). "Histone methylation in higher plants." Annual review of plant biology **61**: 395-420.

Liu, C., Y. Xin, L. Xu, Z. Cai, Y. Xue, Y. Liu, D. Xie, Y. Liu and Y. Qi (2018). "Arabidopsis ARGONAUTE 1 binds chromatin to promote gene transcription in response to hormones and stresses." Developmental cell **44**(3): 348-361. e347.

Liu, H. and K.-I. Nonomura (2016). "A wide reprogramming of histone H3 modifications during male meiosis I in rice is dependent on the Argonaute protein MEL1." J Cell Sci **129**(19): 3553-3561.

Liu, W.-M., W.-M. Chu, P. V. Choudary and C. W. Schmid (1995). "Cell stress and translational inhibitors transiently increase the abundance of mammalian SINE transcripts." Nucleic acids research **23**(10): 1758-1765.
Love, M. I., W. Huber and S. Anders (2014). "Moderated estimation of fold change and dispersion for RNA-seq data with DESeq2." Genome biology **15**(12): 550.
Luger, K., A. W. Mäder, R. K. Richmond, D. F. Sargent and T. J. Richmond (1997). "Crystal structure of the nucleosome core particle at 2.8 Å resolution." Nature **389**(6648): 251-260.
Luo, D., H. Xu, Z. Liu, J. Guo, H. Li, L. Chen, C. Fang, Q. Zhang, M. Bai and N. Yao (2013). "A detrimental mitochondrial-nuclear interaction causes cytoplasmic male sterility in rice." Nature genetics **45**(5): 573.
Luo, Q.-J., A. Mittal, F. Jia and C. D. Rock (2012). "An autoregulatory feedback loop involving PAP1 and TAS4 in response to sugars in Arabidopsis." Plant molecular biology **80**(1): 117-129.
Lusser, A., G. Brosch, A. Loidl, H. Haas and P. Loidl (1997). "Identification of maize histone deacetylase HD2 as an acidic nucleolar phosphoprotein." Science **277**(5322): 88-91.
Lusser, A., D. Kölle and P. Loidl (2001). "Histone acetylation: lessons from the plant kingdom." Trends in plant science **6**(2): 59-65.
Ma, J., D. S. Skibbe, J. Fernandes and V. Walbot (2008). "Male reproductive development: gene expression profiling of maize anther and pollen ontogeny." Genome biology **9**(12): R181.
Ma, J.-B., K. Ye and D. J. Patel (2004). "Structural basis for overhang-specific small interfering RNA recognition by the PAZ domain." nature **429**(6989): 318.
Ma, Y., L. Min, M. Wang, C. Wang, Y. Zhao, Y. Li, Q. Fang, Y. Wu, S. Xie and Y. Ding (2018). "Disrupted Genome Methylation in Response to High Temperature Has Distinct Affects on Microspore Abortion and Anther Indehiscence." The Plant Cell **30**(7): 1387-1403.
Mallory, A. and H. Vaucheret (2010). "Form, function, and regulation of ARGONAUTE proteins." The Plant Cell **22**(12): 3879-3889.
Malone, C. D., J. Brennecke, M. Dus, A. Stark, W. R. McCombie, R. Sachidanandam and G. J. Hannon (2009). "Specialized piRNA pathways act in germline and somatic tissues of the Drosophila ovary." Cell **137**(3): 522-535.
Manakov, S. A., D. Pezic, G. K. Marinov, W. A. Pastor, R. Sachidanandam and A. A. Aravin (2015). "MIWI2 and MILI have differential effects on piRNA biogenesis and DNA methylation." Cell reports **12**(8): 1234-1243.

Margis, R., A. F. Fusaro, N. A. Smith, S. J. Curtin, J. M. Watson, E. J. Finnegan and P. M. Waterhouse (2006). "The evolution and diversification of Dicers in plants." FEBS letters **580**(10): 2442-2450.

Marí-Ordóñez, A., A. Marchais, M. Etcheverry, A. Martin, V. Colot and O. Voinnet (2013). "Reconstructing de novo silencing of an active plant retrotransposon." Nature genetics **45**(9): 1029-1039.

Marin, E., V. Jouannet, A. Herz, A. S. Lokerse, D. Weijers, H. Vaucheret, L. Nussaume, M. D. Crespi and A. Maizel (2010). "miR390, Arabidopsis TAS3 tasiRNAs, and their AUXIN RESPONSE FACTOR targets define an autoregulatory network quantitatively regulating lateral root growth." The Plant Cell **22**(4): 1104-1117.

Marmorstein, R. and M.-M. Zhou (2014). "Writers and readers of histone acetylation: structure, mechanism, and inhibition." Cold Spring Harbor perspectives in biology **6**(7): a018762.

Martin, M. (2011). "Cutadapt removes adapter sequences from high-throughput sequencing reads." EMBnet. journal **17**(1): pp. 10-12.

Martinez, G., S. G. Choudury and R. K. Slotkin (2017). "tRNA-derived small RNAs target transposable element transcripts." Nucleic acids research **45**(9): 5142-5152.

Martínez, G., K. Panda, C. Köhler and R. K. Slotkin (2016). "Silencing in sperm cells is directed by RNA movement from the surrounding nurse cell." Nature plants **2**(4): 16030.

Matzke, M., T. Kanno, L. Daxinger, B. Huettel and A. J. Matzke (2009). "RNA-mediated chromatin-based silencing in plants." Curr Opin Cell Biol **21**(3): 367-376.

Maule, A. J. (2008). "Plasmodesmata: structure, function and biogenesis." Current opinion in plant biology **11**(6): 680-686.

McCarty, D. R., A. Mark Settles, M. Suzuki, B. C. Tan, S. Latshaw, T. Porch, K. Robin, J. Baier, W. Avigne and J. Lai (2005). "Steady-state transposon mutagenesis in inbred maize." The Plant Journal **44**(1): 52-61.

McClintock, B. (1946). "Maize genetics." Carnegie Inst Washington Year Book **45**: 176-186.

McCue, A. D., M. Cresti, J. A. Feijó and R. K. Slotkin (2011). "Cytoplasmic connection of sperm cells to the pollen vegetative cell nucleus: potential roles of the male germ unit revisited." Journal of experimental botany **62**(5): 1621-1631.

McCue, A. D., S. Nuthikattu, S. H. Reeder and R. K. Slotkin (2012). "Gene expression and stress response mediated by the epigenetic regulation of a transposable element small RNA." PLoS genetics **8**(2): e1002474.

McCue, A. D. and R. K. Slotkin (2012). "Transposable element small RNAs as regulators of gene expression." Trends in genetics **28**(12): 616-623.

Meister, G., M. Landthaler, A. Patkaniowska, Y. Dorsett, G. Teng and T. Tuschl (2004). "Human Argonaute2 mediates RNA cleavage targeted by miRNAs and siRNAs." Molecular cell **15**(2): 185-197.
Melnyk, C. W., A. Molnar and D. C. Baulcombe (2011). "Intercellular and systemic movement of RNA silencing signals." The EMBO journal **30**(17): 3553-3563.
Mérai, Z., Z. Kerényi, S. Kertész, M. Magna, L. Lakatos and D. Silhavy (2006). "Double-stranded RNA binding may be a general plant RNA viral strategy to suppress RNA silencing." Journal of Virology **80**(12): 5747-5756.
Mercier, R., D. Vezon, E. Bullier, J. C. Motamayor, A. Sellier, F. Lefèvre, G. Pelletier and C. Horlow (2001). "SWITCH1 (SWI1): a novel protein required for the establishment of sister chromatid cohesion and for bivalent formation at meiosis." Genes & development **15**(14): 1859-1871.
Mesihovic, A., R. Iannacone, N. Firon and S. Fragkostefanakis (2016). "Heat stress regimes for the investigation of pollen thermotolerance in crop plants." Plant reproduction **29**(1-2): 93-105.
Mi, S., T. Cai, Y. Hu, Y. Chen, E. Hodges, F. Ni, L. Wu, S. Li, H. Zhou and C. Long (2008). "Sorting of small RNAs into Arabidopsis argonaute complexes is directed by the 5′ terminal nucleotide." Cell **133**(1): 116-127.
Mirouze, M., J. Reinders, E. Bucher, T. Nishimura, K. Schneeberger, S. Ossowski, J. Cao, D. Weigel, J. Paszkowski and O. Mathieu (2009). "Selective epigenetic control of retrotransposition in Arabidopsis." Nature **461**(7262): 427.
Mittler, R., S. Vanderauwera, M. Gollery and F. Van Breusegem (2004). "Reactive oxygen gene network of plants." Trends in plant science **9**(10): 490-498.
Molla-Herman, A., A. M. Vallés, C. Ganem-Elbaz, C. Antoniewski and J. R. Huynh (2015). "tRNA processing defects induce replication stress and Chk2-dependent disruption of piRNA transcription." The EMBO journal: e201591006.
Molnar, A., C. W. Melnyk, A. Bassett, T. J. Hardcastle, R. Dunn and D. C. Baulcombe (2010). "Small silencing RNAs in plants are mobile and direct epigenetic modification in recipient cells." science **328**(5980): 872-875.
Montgomery, T. A., S. J. Yoo, N. Fahlgren, S. D. Gilbert, M. D. Howell, C. M. Sullivan, A. Alexander, G. Nguyen, E. Allen and J. H. Ahn (2008). "AGO1-miR173 complex initiates phased siRNA formation in plants." Proceedings of the National Academy of Sciences: pnas. 0810241105.
Moon, J., D. Skibbe, L. Timofejeva, C. J. R. Wang, T. Kelliher, K. Kremling, V. Walbot and W. Z. Cande (2013). "Regulation of cell divisions and differentiation by MALE STERILITY 32 is required for anther development in maize." The Plant Journal **76**(4): 592-602.

Morel, J.-B., C. Godon, P. Mourrain, C. Béclin, S. Boutet, F. Feuerbach, F. Proux and H. Vaucheret (2002). "Fertile hypomorphic ARGONAUTE (ago1) mutants impaired in post-transcriptional gene silencing and virus resistance." The Plant Cell **14**(3): 629-639.
Mosher, R. A., F. Schwach, D. Studholme and D. C. Baulcombe (2008). "PolIVb influences RNA-directed DNA methylation independently of its role in siRNA biogenesis." Proceedings of the National Academy of Sciences **105**(8): 3145-3150.
Nan, G.-L., J. Zhai, S. Arikit, D. Morrow, J. Fernandes, L. Mai, N. Nguyen, B. C. Meyers and V. Walbot (2016). "MS23, a master basic helix-loop-helix factor, regulates the specification and development of tapetum in maize." Development: dev. 140673.
Napoli, C., C. Lemieux and R. Jorgensen (1990). "Introduction of a chimeric chalcone synthase gene into petunia results in reversible co-suppression of homologous genes in trans." The plant cell **2**(4): 279-289.
Neale, M. J., J. Pan and S. Keeney (2005). "Endonucleolytic processing of covalent protein-linked DNA double-strand breaks." Nature **436**(7053): 1053.
Nelson, R. S. and V. Citovsky (2005). Plant viruses. Invaders of cells and pirates of cellular pathways, Am Soc Plant Biol.
Nishida, K. M., K. Saito, T. Mori, Y. Kawamura, T. Nagami-Okada, S. Inagaki, H. Siomi and M. C. Siomi (2007). "Gene silencing mechanisms mediated by Aubergine–piRNA complexes in Drosophila male gonad." Rna **13**(11): 1911-1922.
Niu, N., W. Liang, X. Yang, W. Jin, Z. A. Wilson, J. Hu and D. Zhang (2013). "EAT1 promotes tapetal cell death by regulating aspartic proteases during male reproductive development in rice." Nature communications **4**: 1445.
Nonomura, K., A. Morohoshi, M. Nakano, M. Eiguchi, A. Miyao, H. Hirochika and N. Kurata (2007). "A germ cell specific gene of the ARGONAUTE family is essential for the progression of premeiotic mitosis and meiosis during sporogenesis in rice." Plant Cell **19**(8): 2583-2594.
Nonomura, K.-I., A. Morohoshi, M. Nakano, M. Eiguchi, A. Miyao, H. Hirochika and N. Kurata (2007). "A germ cell–specific gene of the ARGONAUTE family is essential for the progression of premeiotic mitosis and meiosis during sporogenesis in rice." The Plant Cell **19**(8): 2583-2594.
Nowotny, M., S. A. Gaidamakov, R. J. Crouch and W. Yang (2005). "Crystal structures of RNase H bound to an RNA/DNA hybrid: substrate specificity and metal-dependent catalysis." Cell **121**(7): 1005-1016.
Nuthikattu, S., A. D. McCue, K. Panda, D. Fultz, C. DeFraia, E. N. Thomas and R. K. Slotkin (2013). "The initiation of epigenetic silencing of active

transposable elements is triggered by RDR6 and 21-22 nucleotide small interfering RNAs." Plant Physiology **162**(1): 116-131.
Nykänen, A., B. Haley and P. D. Zamore (2001). "ATP requirements and small interfering RNA structure in the RNA interference pathway." Cell **107**(3): 309-321.
Oliver, C., J. L. Santos and M. Pradillo (2016). "Accurate chromosome segregation at first meiotic division requires AGO4, a protein involved in RNA-dependent DNA methylation in Arabidopsis thaliana." Genetics: genetics. 116.189217.
Olmedo-Monfil, V., N. Durán-Figueroa, M. Arteaga-Vázquez, E. Demesa-Arévalo, D. Autran, D. Grimanelli, R. K. Slotkin, R. A. Martienssen and J.-P. Vielle-Calzada (2010). "Control of female gamete formation by a small RNA pathway in Arabidopsis." Nature **464**(7288): 628-632.
Ono, S., H. Liu, K. Tsuda, E. Fukai, K. Tanaka, T. Sasaki and K.-I. Nonomura (2018). "EAT1 transcription factor, a non-cell-autonomous regulator of pollen production, activates meiotic small RNA biogenesis in rice anther tapetum." PLoS genetics **14**(2): e1007238.
Ortega-Galisteo, A. P., T. Morales-Ruiz, R. R. Ariza and T. Roldán-Arjona (2008). "Arabidopsis DEMETER-LIKE proteins DML2 and DML3 are required for appropriate distribution of DNA methylation marks." Plant molecular biology **67**(6): 671-681.
Oshino, T., M. Abiko, R. Saito, E. Ichiishi, M. Endo, M. Kawagishi-Kobayashi and A. Higashitani (2007). "Premature progression of anther early developmental programs accompanied by comprehensive alterations in transcription during high-temperature injury in barley plants." Molecular Genetics and Genomics **278**(1): 31-42.
Otsuga, D., B. DeGuzman, M. J. Prigge, G. N. Drews and S. E. Clark (2001). "REVOLUTA regulates meristem initiation at lateral positions." The Plant Journal **25**(2): 223-236.
Palauqui, J. C., T. Elmayan, J. M. Pollien and H. Vaucheret (1997). "Systemic acquired silencing: transgene-specific post-transcriptional silencing is transmitted by grafting from silenced stocks to non-silenced scions." The EMBO journal **16**(15): 4738-4745.
Pant, B. D., A. Buhtz, J. Kehr and W. R. Scheible (2008). "MicroRNA399 is a long-distance signal for the regulation of plant phosphate homeostasis." The Plant Journal **53**(5): 731-738.
Parish, R. W., H. A. Phan, S. Iacuone and S. F. Li (2012). "Tapetal development and abiotic stress: a centre of vulnerability." Functional Plant Biology **39**(7): 553-559.
Parizotto, E. A., P. Dunoyer, N. Rahm, C. Himber and O. Voinnet (2004). "In vivo investigation of the transcription, processing, endonucleolytic activity,

and functional relevance of the spatial distribution of a plant miRNA." Genes & development **18**(18): 2237-2242.
Pecinka, A., H. Q. Dinh, T. Baubec, M. Rosa, N. Lettner and O. M. Scheid (2010). "Epigenetic regulation of repetitive elements is attenuated by prolonged heat stress in Arabidopsis." The Plant Cell: tpc. 110.078493.
Peet, M., S. Sato and R. Gardner (1998). "Comparing heat stress effects on male-fertile and male-sterile tomatoes." Plant, Cell & Environment **21**(2): 225-231.
Peragine, A., M. Yoshikawa, G. Wu, H. L. Albrecht and R. S. Poethig (2004). "SGS3 and SGS2/SDE1/RDR6 are required for juvenile development and the production of trans-acting siRNAs in Arabidopsis." Genes & development **18**(19): 2368-2379.
Peterson, R., J. P. Slovin and C. Chen (2010). "A simplified method for differential staining of aborted and non-aborted pollen grains." International Journal of Plant Biology **1**(2): 13.
Pikaard, C. S., J. R. Haag, T. Ream and A. T. Wierzbicki (2008). "Roles of RNA polymerase IV in gene silencing." Trends in plant science **13**(7): 390-397.
Pontvianne, F., T. Blevins and C. S. Pikaard (2010). Arabidopsis histone lysine methyltransferases. Advances in botanical research, Elsevier. **53:** 1-22.
Popova, O. V., H. Q. Dinh, W. Aufsatz and C. Jonak (2013). "The RdDM pathway is required for basal heat tolerance in Arabidopsis." Molecular plant **6**(2): 396-410.
Pradhan, S., A. Bacolla, R. D. Wells and R. J. Roberts (1999). "Recombinant human DNA (cytosine-5) methyltransferase I. Expression, purification, and comparison of de novo and maintenance methylation." Journal of Biological Chemistry **274**(46): 33002-33010.
Prasad, P. V. V., P. Q. Craufurd, V. G. Kakani, T. R. Wheeler and K. J. Boote (2001). "Influence of high temperature during pre-and post-anthesis stages of floral development on fruit-set and pollen germination in peanut." Functional Plant Biology **28**(3): 233-240.
Prieto, P., P. Shaw and G. Moore (2004). "Homologue recognition during meiosis is associated with a change in chromatin conformation." Nature cell biology **6**(9): 906.
Prigge, M. J., D. Otsuga, J. M. Alonso, J. R. Ecker, G. N. Drews and S. E. Clark (2005). "Class III homeodomain-leucine zipper gene family members have overlapping, antagonistic, and distinct roles in Arabidopsis development." The Plant Cell **17**(1): 61-76.
Probst, A. V. and O. M. Scheid (2015). "Stress-induced structural changes in plant chromatin." Current opinion in plant biology **27**: 8-16.
Qi, Y., A. M. Denli and G. J. Hannon (2005). "Biochemical specialization within Arabidopsis RNA silencing pathways." Molecular cell **19**(3): 421-428.

Qu, A.-L., Y.-F. Ding, Q. Jiang and C. Zhu (2013). "Molecular mechanisms of the plant heat stress response." Biochemical and biophysical research communications **432**(2): 203-207.
Raina, M. and M. Ibba (2014). "tRNAs as regulators of biological processes." Frontiers in genetics **5**: 171.
Rambaut, A. (2018). "FigTree."
Rang, Z., S. Jagadish, Q. Zhou, P. Craufurd and S. Heuer (2011). "Effect of high temperature and water stress on pollen germination and spikelet fertility in rice." Environmental and Experimental Botany **70**(1): 58-65.
Ratner, V. A., S. A. Zabanov, O. V. Kolesnikova and L. A. Vasilyeva (1992). "Induction of the mobile genetic element Dm-412 transpositions in the Drosophila genome by heat shock treatment." Proceedings of the National Academy of Sciences **89**(12): 5650-5654.
Regulski, M., Z. Lu, J. Kendall, M. T. Donoghue, J. Reinders, V. Llaca, S. Deschamps, A. Smith, D. Levy and W. R. McCombie (2013). "The maize methylome influences mRNA splice sites and reveals widespread paramutation-like switches guided by small RNA." Genome research: gr. 153510.153112.
Rehman, A. and C. S. Nautiyal (2002). "Effect of drought on the growth and survival of the stress-tolerant bacterium Rhizobium sp. NBRI2505 sesbania and its drought-sensitive transposon Tn5 mutant." Current microbiology **45**(5): 368-377.
Ren, J., L. Wen, X. Gao, C. Jin, Y. Xue and X. Yao (2009). "DOG 1.0: illustrator of protein domain structures." Cell research **19**(2): 271.
Rieu, I., D. Twell and N. Firon (2017). "Pollen development at high temperature: from acclimation to collapse." Plant physiology **173**(4): 1967-1976.
Rivas, F. V., N. H. Tolia, J.-J. Song, J. P. Aragon, J. Liu, G. J. Hannon and L. Joshua-Tor (2005). "Purified Argonaute2 and an siRNA form recombinant human RISC." Nature Structural and Molecular Biology **12**(4): 340.
Ross, K., P. Fransz, S. Armstrong, I. Vizir, B. Mulligan, F. Franklin and G. Jones (1997). "Cytological characterization of four meiotic mutants of Arabidopsis isolated from T-DNA-transformed lines." Chromosome Research **5**(8): 551-559.
Ross, K., P. Fransz and G. Jones (1996). "A light microscopic atlas of meiosis inArabidopsis thaliana." Chromosome research **4**(7): 507-516.
Ross, R. J., M. M. Weiner and H. Lin (2014). "PIWI proteins and PIWI-interacting RNAs in the soma." Nature **505**(7483): 353.
Rudich, J., E. Zamski and Y. Regev (1977). "Genotypic variation for sensitivity to high temperature in the tomato: pollination and fruit set." Botanical Gazette **138**(4): 448-452.

Saini, H., M. Sedgley and D. Aspinall (1983). "Effect of heat stress during floral development on pollen tube growth and ovary anatomy in wheat (Triticum aestivum L.)." Functional Plant Biology **10**(2): 137-144.
Saini, H., M. Sedgley and D. Aspinall (1984). "Development anatomy in wheat of male sterility induced by heat stress, water deficit or abscisic acid." Functional Plant Biology **11**(4): 243-253.
Sakata, T. and A. Higashitani (2008). "Male sterility accompanied with abnormal anther development in plants–genes and environmental stresses with special reference to high temperature injury." Int. J. Plant Dev. Biol **2**(4).
Samalova, M., B. Brzobohaty and I. Moore (2005). "pOp6/LhGR: a stringently regulated and highly responsive dexamethasone-inducible gene expression system for tobacco." The Plant Journal **41**(6): 919-935.
SanMiguel, P. and C. Vitte (2009). The LTR-Retrotransposons of Maize. Handbook of Maize: Genetics and Genomics. J. L. Bennetzen and S. Hake. New York, NY, Springer New York**:** 307-327.
Sato, S., M. Kamiyama, T. Iwata, N. Makita, H. Furukawa and H. Ikeda (2006). "Moderate increase of mean daily temperature adversely affects fruit set of Lycopersicon esculentum by disrupting specific physiological processes in male reproductive development." Annals of Botany **97**(5): 731-738.
Scharf, K.-D., T. Berberich, I. Ebersberger and L. Nover (2012). "The plant heat stress transcription factor (Hsf) family: structure, function and evolution." Biochimica et Biophysica Acta (BBA)-Gene Regulatory Mechanisms **1819**(2): 104-119.
Schnable, P. S., D. Ware, R. S. Fulton, J. C. Stein, F. Wei, S. Pasternak, C. Liang, J. Zhang, L. Fulton and T. A. Graves (2009). "The B73 maize genome: complexity, diversity, and dynamics." science **326**(5956): 1112-1115.
Schoft, V. K., N. Chumak, Y. Choi, M. Hannon, M. Garcia-Aguilar, A. Machlicova, L. Slusarz, M. Mosiolek, J.-S. Park and G. T. Park (2011). "Function of the DEMETER DNA glycosylase in the Arabidopsis thaliana male gametophyte." Proceedings of the National Academy of Sciences **108**(19): 8042-8047.
Schoft, V. K., N. Chumak, M. Mosiolek, L. Slusarz, V. Komnenovic, L. Brownfield, D. Twell, T. Kakutani and H. Tamaru (2009). "Induction of RNA-directed DNA methylation upon decondensation of constitutive heterochromatin." EMBO reports **10**(9): 1015-1021.
Schorn, A. J., M. J. Gutbrod, C. LeBlanc and R. Martienssen (2017). "LTR-retrotransposon control by tRNA-derived small RNAs." Cell **170**(1): 61-71. e11.
Servet, C., N. C. e Silva and D.-X. Zhou (2010). "Histone acetyltransferase AtGCN5/HAG1 is a versatile regulator of developmental and inducible gene expression in Arabidopsis." Molecular plant **3**(4): 670-677.

Sharma, U., C. C. Conine, J. M. Shea, A. Boskovic, A. G. Derr, X. Y. Bing, C. Belleannee, A. Kucukural, R. W. Serra and F. Sun (2016). "Biogenesis and function of tRNA fragments during sperm maturation and fertilization in mammals." Science **351**(6271): 391-396.
Sheridan, W. F., E. A. Golubeva, L. I. Abrhamova and I. N. Golubovskaya (1999). "The mac1 mutation alters the developmental fate of the hypodermal cells and their cellular progeny in the maize anther." Genetics **153**(2): 933-941.
Silhavy, D., A. Molnár, A. Lucioli, G. Szittya, C. Hornyik, M. Tavazza and J. Burgyán (2002). "A viral protein suppresses RNA silencing and binds silencing-generated, 21-to 25-nucleotide double-stranded RNAs." The EMBO journal **21**(12): 3070-3080.
Singh, M., S. Goel, R. B. Meeley, C. Dantec, H. Parrinello, C. Michaud, O. Leblanc and D. Grimanelli (2011). "Production of viable gametes without meiosis in maize deficient for an ARGONAUTE protein." The Plant Cell: tpc. 110.079020.
Slotkin, R. K., M. Vaughn, F. Borges, M. Tanurdzic, J. D. Becker, J. A. Feijo and R. A. Martienssen (2009). "Epigenetic reprogramming and small RNA silencing of transposable elements in pollen." Cell **136**(3): 461-472.
Slotkin, R. K., M. Vaughn, F. Borges, M. Tanurdžić, J. D. Becker, J. A. Feijó and R. A. Martienssen (2009). "Epigenetic reprogramming and small RNA silencing of transposable elements in pollen." Cell **136**(3): 461-472.
Smith, L. M., O. Pontes, I. Searle, N. Yelina, F. K. Yousafzai, A. J. Herr, C. S. Pikaard and D. C. Baulcombe (2007). "An SNF2 protein associated with nuclear RNA silencing and the spread of a silencing signal between cells in Arabidopsis." The Plant Cell **19**(5): 1507-1521.
Smith, S. J., K. Osman and F. C. H. Franklin (2014). "The condensin complexes play distinct roles to ensure normal chromosome morphogenesis during meiotic division in A rabidopsis." The Plant Journal **80**(2): 255-268.
Song, J.-J., J. Liu, N. H. Tolia, J. Schneiderman, S. K. Smith, R. A. Martienssen, G. J. Hannon and L. Joshua-Tor (2003). "The crystal structure of the Argonaute2 PAZ domain reveals an RNA binding motif in RNAi effector complexes." Nature Structural and Molecular Biology **10**(12): 1026.
Song, J.-J., S. K. Smith, G. J. Hannon and L. Joshua-Tor (2004). "Crystal structure of Argonaute and its implications for RISC slicer activity." science **305**(5689): 1434-1437.
Song, X., P. Li, J. Zhai, M. Zhou, L. Ma, B. Liu, D. H. Jeong, M. Nakano, S. Cao and C. Liu (2012). "Roles of DCL4 and DCL3b in rice phased small RNA biogenesis." The Plant Journal **69**(3): 462-474.
Stelpflug, S. C., R. S. Sekhon, B. Vaillancourt, C. N. Hirsch, C. R. Buell, N. de Leon and S. M. Kaeppler (2016). "An expanded maize gene expression atlas

based on RNA sequencing and its use to explore root development." The Plant Genome **9**(1).
Stonebloom, S., J. O. Brunkard, A. C. Cheung, K. Jiang, L. J. Feldman and P. C. Zambryski (2011). "Redox states of plastids and mitochondria differentially regulate intercellular transport via plasmodesmata." Plant Physiology: pp. 111.186130.
Stroud, H., M. V. Greenberg, S. Feng, Y. V. Bernatavichute and S. E. Jacobsen (2013). "Comprehensive analysis of silencing mutants reveals complex regulation of the Arabidopsis methylome." Cell **152**(1): 352-364.
Sunkar, R. and J.-K. Zhu (2004). "Novel and stress-regulated microRNAs and other small RNAs from Arabidopsis." The Plant Cell **16**(8): 2001-2019.
Suzuki, N. and K. Katano (2018). "Coordination between ROS regulatory systems and other pathways under heat stress and pathogen attack." Frontiers in plant science **9**: 490.
Svoboda, Y., M. K. Robson and J. A. Sved (1995). "P-element-induced male recombination can be produced in Drosophila melanogaster by combining end-deficient elements in trans." Genetics **139**(4): 1601-1610.
Szövényi, P., N. Devos, D. J. Weston, X. Yang, Z. Hock, J. A. Shaw, K. K. Shimizu, S. F. McDaniel and A. Wagner (2014). "Efficient purging of deleterious mutations in plants with haploid selfing." Genome biology and evolution **6**(5): 1238-1252.
Takebayashi, S.-i., T. Tamura, C. Matsuoka and M. Okano (2007). "Major and essential role for the DNA methylation mark in mouse embryogenesis and stable association of DNMT1 with newly replicated regions." Molecular and cellular biology **27**(23): 8243-8258.
Takeda, A., S. Iwasaki, T. Watanabe, M. Utsumi and Y. Watanabe (2008). "The mechanism selecting the guide strand from small RNA duplexes is different among argonaute proteins." Plant and cell physiology **49**(4): 493-500.
Tan, M., H. Luo, S. Lee, F. Jin, J. S. Yang, E. Montellier, T. Buchou, Z. Cheng, S. Rousseaux and N. Rajagopal (2011). "Identification of 67 histone marks and histone lysine crotonylation as a new type of histone modification." Cell **146**(6): 1016-1028.
Tang, G., J. Yan, Y. Gu, M. Qiao, R. Fan, Y. Mao and X. Tang (2012). "Construction of short tandem target mimic (STTM) to block the functions of plant and animal microRNAs." Methods **58**(2): 118-125.
Teng, C., H. Zhang, R. Hammond, K. Huang, B. Meyers and V. Walbot (2018). "Dicer-like 5 deficiency confers temperature-sensitive male sterility in maize." bioRxiv: 498410.

Thompson, D. M., C. Lu, P. J. Green and R. Parker (2008). "tRNA cleavage is a conserved response to oxidative stress in eukaryotes." Rna **14**(10): 2095-2103.
Thompson, D. M. and R. Parker (2009). "Stressing out over tRNA cleavage." Cell **138**(2): 215-219.
Tian, T., Y. Liu, H. Yan, Q. You, X. Yi, Z. Du, W. Xu and Z. Su (2017). "agriGO v2. 0: a GO analysis toolkit for the agricultural community, 2017 update." Nucleic acids research **45**(W1): W122-W129.
Tittel-Elmer, M., E. Bucher, L. Broger, O. Mathieu, J. Paszkowski and I. Vaillant (2010). "Stress-induced activation of heterochromatic transcription." PLoS genetics **6**(10): e1001175.
Tolia, N. H. and L. Joshua-Tor (2007). "Slicer and the argonautes." Nature chemical biology **3**(1): 36.
Trapnell, C., L. Pachter and S. L. Salzberg (2009). "TopHat: discovering splice junctions with RNA-Seq." Bioinformatics **25**.
Trinks, D., R. Rajeswaran, P. Shivaprasad, R. Akbergenov, E. J. Oakeley, K. Veluthambi, T. Hohn and M. M. Pooggin (2005). "Suppression of RNA silencing by a geminivirus nuclear protein, AC2, correlates with transactivation of host genes." Journal of Virology **79**(4): 2517-2527.
Tucker, M. R., T. Okada, Y. Hu, A. Scholefield, J. M. Taylor and A. M. Koltunow (2012). "Somatic small RNA pathways promote the mitotic events of megagametogenesis during female reproductive development in Arabidopsis." Development: dev. 075390.
Twell, D. (2011). "Male gametogenesis and germline specification in flowering plants." Sexual Plant Reproduction **24**(2): 149-160.
van Engelen, F. A., J. W. Molthoff, A. J. Conner, J.-P. Nap, A. Pereira and W. J. Stiekema (1995). "pBINPLUS: an improved plant transformation vector based on pBIN19." Transgenic research **4**(4): 288-290.
van Wezel, R., X. Dong, H. Liu, P. Tien, J. Stanley and Y. Hong (2002). "Mutation of three cysteine residues in Tomato yellow leaf curl virus-China C2 protein causes dysfunction in pathogenesis and posttranscriptional gene—silencing suppression." Molecular plant-microbe interactions **15**(3): 203-208.
Vaucheret, H. (2008). "Plant argonautes." Trends in plant science **13**(7): 350-358.
Vaucheret, H., F. Vazquez, P. Crété and D. P. Bartel (2004). "The action of ARGONAUTE1 in the miRNA pathway and its regulation by the miRNA pathway are crucial for plant development." Genes & development **18**(10): 1187-1197.
Vazquez, F., V. Gasciolli, P. Crété and H. Vaucheret (2004). "The nuclear dsRNA binding protein HYL1 is required for microRNA accumulation and

plant development, but not posttranscriptional transgene silencing." Current Biology **14**(4): 346-351.
Vazquez, F., H. Vaucheret, R. Rajagopalan, C. Lepers, V. Gasciolli, A. C. Mallory, J.-L. Hilbert, D. P. Bartel and P. Crété (2004). "Endogenous trans-acting siRNAs regulate the accumulation of Arabidopsis mRNAs." Molecular cell **16**(1): 69-79.
Veal, E. A., A. M. Day and B. A. Morgan (2007). "Hydrogen peroxide sensing and signaling." Molecular cell **26**(1): 1-14.
Vernoud, V., G. Laigle, F. Rozier, R. B. Meeley, P. Perez and P. M. Rogowsky (2009). "The HD-ZIP IV transcription factor OCL4 is necessary for trichome patterning and anther development in maize." The Plant Journal **59**(6): 883-894.
Villeneuve, A. M. and K. J. Hillers (2001). "Whence meiosis?" Cell **106**(6): 647-650.
Voinnet, O. (2005). "Induction and suppression of RNA silencing: insights from viral infections." Nature Reviews Genetics **6**(3): 206.
Voinnet, O. and D. C. Baulcombe (1997). "Systemic signalling in gene silencing." Nature **389**(6651): 553.
Voinnet, O., Y. M. Pinto and D. C. Baulcombe (1999). "Suppression of gene silencing: a general strategy used by diverse DNA and RNA viruses of plants." Proceedings of the National Academy of Sciences **96**(24): 14147-14152.
Voinnet, O., P. Vain, S. Angell and D. C. Baulcombe (1998). "Systemic spread of sequence-specific transgene RNA degradation in plants is initiated by localized introduction of ectopic promoterless DNA." Cell **95**(2): 177-187.
Volkov, R. A., I. I. Panchuk, P. M. Mullineaux and F. Schöffl (2006). "Heat stress-induced H 2 O 2 is required for effective expression of heat shock genes in Arabidopsis." Plant molecular biology **61**(4-5): 733-746.
Vongs, A., T. Kakutani, R. A. Martienssen and E. J. Richards (1993). "Arabidopsis thaliana DNA methylation mutants." Science **260**(5116): 1926-1928.
Waddington, C. H. (2012). "The epigenotype. 1942." Int J Epidemiol **41**(1): 10-13.
Walbot, V. and R. L. Egger (2016). "Pre-meiotic anther development: cell fate specification and differentiation." Annual review of plant biology **67**: 365-395.
Walbot, V. and M. M. Evans (2003). "Unique features of the plant life cycle and their consequences." Nature Reviews Genetics **4**(5): 369.
Walley, J. W., R. C. Sartor, Z. Shen, R. J. Schmitz, K. J. Wu, M. A. Urich, J. R. Nery, L. G. Smith, J. C. Schnable and J. R. Ecker (2016). "Integration of omic networks in a developmental atlas of maize." Science **353**(6301): 814-818.

Walsh, C. P., J. R. Chaillet and T. H. Bestor (1998). "Transcription of IAP endogenous retroviruses is constrained by cytosine methylation." Nature genetics **20**(2): 116.
Wang, C.-J. R., P. M. Carlton, I. N. Golubovskaya and W. Z. Cande (2009). "Interlock formation and coiling of meiotic chromosome axes during synapsis." Genetics.
Wang, C.-J. R., G.-L. Nan, T. Kelliher, L. Timofejeva, V. Vernoud, I. N. Golubovskaya, L. Harper, R. Egger, V. Walbot and W. Z. Cande (2012). "Maize multiple archesporial cells 1 (mac1), an ortholog of rice TDL1A, modulates cell proliferation and identity in early anther development." Development: dev. 077891.
Wang, H., X. Zhang, J. Liu, T. Kiba, J. Woo, T. Ojo, M. Hafner, T. Tuschl, N. H. Chua and X. J. Wang (2011). "Deep sequencing of small RNAs specifically associated with Arabidopsis AGO1 and AGO4 uncovers new AGO functions." THe plant journal **67**(2): 292-304.
Wang, X.-B., J. Jovel, P. Udomporn, Y. Wang, Q. Wu, W.-X. Li, V. Gasciolli, H. Vaucheret and S.-W. Ding (2011). "The 21-nucleotide, but not 22-nucleotide, viral secondary small interfering RNAs direct potent antiviral defense by two cooperative argonautes in Arabidopsis thaliana." The Plant Cell: tpc. 110.082305.
Ward, W. W. (2005). "Biochemical and physical properties of green fluorescent protein." Green fluorescent protein: properties, applications, and protocols **2**: 56.
Wei, L. Q., L. F. Yan and T. Wang (2011). "Deep sequencing on genome-wide scale reveals the unique composition and expression patterns of microRNAs in developing pollen of Oryza sativa." Genome biology **12**(6): R53.
Wei, W., Z. Ba, M. Gao, Y. Wu, Y. Ma, S. Amiard, C. I. White, J. M. R. Danielsen, Y.-G. Yang and Y. Qi (2012). "A role for small RNAs in DNA double-strand break repair." Cell **149**(1): 101-112.
Wierzbicki, A. T., J. R. Haag and C. S. Pikaard (2008). "Noncoding transcription by RNA polymerase Pol IVb/Pol V mediates transcriptional silencing of overlapping and adjacent genes." Cell **135**(4): 635-648.
Wilson, Z. A. and D.-B. Zhang (2009). "From Arabidopsis to rice: pathways in pollen development." Journal of experimental botany **60**(5): 1479-1492.
Wolffe, A. P. and D. Guschin (2000). "Chromatin structural features and targets that regulate transcription." Journal of structural biology **129**(2-3): 102-122.
Wollmann, H., H. Stroud, R. Yelagandula, Y. Tarutani, D. Jiang, L. Jing, B. Jamge, H. Takeuchi, S. Holec and X. Nie (2017). "The histone H3 variant H3. 3 regulates gene body DNA methylation in Arabidopsis thaliana." Genome biology **18**(1): 94.

Wu, J., Z. Yang, Y. Wang, L. Zheng, R. Ye, Y. Ji, S. Zhao, S. Ji, R. Liu and L. Xu (2015). "Viral-inducible Argonaute18 confers broad-spectrum virus resistance in rice by sequestering a host microRNA." Elife **4**: e05733.
Wu, L., Q. Zhang, H. Zhou, F. Ni, X. Wu and Y. Qi (2009). "Rice microRNA effector complexes and targets." The Plant Cell **21**(11): 3421-3435.
Wu-Scharf, D., B.-r. Jeong, C. Zhang and H. Cerutti (2000). "Transgene and transposon silencing in Chlamydomonas reinhardtii by a DEAH-box RNA helicase." Science **290**(5494): 1159-1162.
Xie, H.-T., Z.-Y. Wan, S. Li and Y. Zhang (2014). "Spatiotemporal production of reactive oxygen species by NADPH oxidase is critical for tapetal programmed cell death and pollen development in Arabidopsis." The Plant Cell: tpc. 114.125427.
Xie, Z., E. Allen, N. Fahlgren, A. Calamar, S. A. Givan and J. C. Carrington (2005). "Expression of Arabidopsis MIRNA genes." Plant physiology **138**(4): 2145-2154.
Xing, S. and S. Zachgo (2008). "ROXY1 and ROXY2, two Arabidopsis glutaredoxin genes, are required for anther development." The Plant Journal **53**(5): 790-801.
Yan, J., Y. Gu, X. Jia, W. Kang, S. Pan, X. Tang, X. Chen and G. Tang (2012). "Effective small RNA destruction by the expression of a short tandem target mimic in Arabidopsis." The Plant Cell **24**(2): 415-427.
Yang, H., P. Lu, Y. Wang and H. Ma (2011). "The transcriptome landscape of Arabidopsis male meiocytes from high-throughput sequencing: the complexity and evolution of the meiotic process." The Plant Journal **65**(4): 503-516.
Yang, J. H., H. H. Seo, S. J. Han, E. K. Yoon, M. S. Yang and W. S. Lee (2007). "Phytohormone abscisic acid control RNA-dependent RNA polymerase 6 gene expression and post-transcriptional gene silencing in rice cells." Nucleic acids research **36**(4): 1220-1226.
Yang, L., G. Wu and R. S. Poethig (2012). "Mutations in the GW-repeat protein SUO reveal a developmental function for microRNA-mediated translational repression in Arabidopsis." Proceedings of the national academy of sciences **109**(1): 315-320.
Yang, L., Y. Wu, M. Zhang, J. Zhang, J. M. Stewart, C. Xing, J. Wu and S. Jin (2018). "Transcriptome, cytological and biochemical analysis of cytoplasmic male sterility and maintainer line in CMS-D8 cotton." Plant molecular biology **97**(6): 537-551.
Yasuda, K., M. Ito, T. Sugita, T. Tsukiyama, H. Saito, K. Naito, M. Teraishi, T. Tanisaka and Y. Okumoto (2013). "Utilization of transposable element mPing as a novel genetic tool for modification of the stress response in rice." Molecular breeding **32**(3): 505-516.

Yi, J., S. Moon, Y.-S. Lee, L. Zhu, W. Liang, D. Zhang, K.-H. Jung and G. An (2016). "Defective Tapetum Cell Death 1 (DTC1) regulates ROS levels by binding to metallothionein during tapetum degeneration." Plant physiology: pp. 01561.02015.

Yigit, E., P. J. Batista, Y. Bei, K. M. Pang, C.-C. G. Chen, N. H. Tolia, L. Joshua-Tor, S. Mitani, M. J. Simard and C. C. Mello (2006). "Analysis of the C. elegans Argonaute family reveals that distinct Argonautes act sequentially during RNAi." Cell **127**(4): 747-757.

Yoo, B.-C., F. Kragler, E. Varkonyi-Gasic, V. Haywood, S. Archer-Evans, Y. M. Lee, T. J. Lough and W. J. Lucas (2004). "A systemic small RNA signaling system in plants." The Plant Cell **16**(8): 1979-2000.

Yoshikawa, M. (2013). "Biogenesis of trans-acting siRNAs, endogenous secondary siRNAs in plants." Genes & genetic systems **88**(2): 77-84.

Yoshikawa, M., A. Peragine, M. Y. Park and R. S. Poethig (2005). "A pathway for the biogenesis of trans-acting siRNAs in Arabidopsis." Genes & development **19**(18): 2164-2175.

Yu, B., Z. Yang, J. Li, S. Minakhina, M. Yang, R. W. Padgett, R. Steward and X. Chen (2005). "Methylation as a crucial step in plant microRNA biogenesis." Science **307**(5711): 932-935.

Yuan, Y.-R., Y. Pei, J.-B. Ma, V. Kuryavyi, M. Zhadina, G. Meister, H.-Y. Chen, Z. Dauter, T. Tuschl and D. J. Patel (2005). "Crystal structure of A. aeolicus argonaute, a site-specific DNA-guided endoribonuclease, provides insights into RISC-mediated mRNA cleavage." Molecular cell **19**(3): 405-419.

Zhai, J., H. Zhang, S. Arikit, K. Huang, G.-L. Nan, V. Walbot and B. C. Meyers (2015). "Spatiotemporally dynamic, cell-type–dependent premeiotic and meiotic phasiRNAs in maize anthers." Proceedings of the National Academy of Sciences **112**(10): 3146-3151.

Zhai, J., H. Zhang, S. Arikit, K. Huang, G. L. Nan, V. Walbot and B. C. Meyers (2015). "Spatiotemporally dynamic, cell-type-dependent premeiotic and meiotic phasiRNAs in maize anthers." Proc Natl Acad Sci U S A **112**(10): 3146-3151.

Zhai, L., W. Sun, K. Zhang, H. Jia, L. Liu, Z. Liu, F. Teng and Z. Zhang (2014). "Identification and characterization of Argonaute gene family and meiosis-enriched Argonaute during sporogenesis in maize." Journal of integrative plant biology **56**(11): 1042-1052.

Zhang, H., K. Tang, B. Wang, C.-G. Duan, Z. Lang and J.-K. Zhu (2014). "Protocol: a beginner's guide to the analysis of RNA-directed DNA methylation in plants." Plant methods **10**(1): 18.

Zhang, H., R. Xia, B. C. Meyers and V. Walbot (2015). "Evolution, functions, and mysteries of plant ARGONAUTE proteins." Current opinion in plant biology **27**: 84-90.

Zhang, X., J. Li, A. Liu, J. Zou, X. Zhou, J. Xiang, W. Rerksiri, Y. Peng, X. Xiong and X. Chen (2012). "Expression profile in rice panicle: insights into heat response mechanism at reproductive stage." Plos one **7**(11): e49652.

Zhang, X., J. Xia, Y. E. Lii, B. E. Barrera-Figueroa, X. Zhou, S. Gao, L. Lu, D. Niu, Z. Chen and C. Leung (2012). "Genome-wide analysis of plant nat-siRNAs reveals insights into their distribution, biogenesis and function." Genome biology **13**(3): R20.

Zhang, X., J. Yazaki, A. Sundaresan, S. Cokus, S. W.-L. Chan, H. Chen, I. R. Henderson, P. Shinn, M. Pellegrini and S. E. Jacobsen (2006). "Genome-wide high-resolution mapping and functional analysis of DNA methylation in Arabidopsis." Cell **126**(6): 1189-1201.

Zhang, X., Y.-R. Yuan, Y. Pei, S.-S. Lin, T. Tuschl, D. J. Patel and N.-H. Chua (2006). "Cucumber mosaic virus-encoded 2b suppressor inhibits Arabidopsis Argonaute1 cleavage activity to counter plant defense." Genes & development **20**(23): 3255-3268.

Zhang, X., H. Zhao, S. Gao, W.-C. Wang, S. Katiyar-Agarwal, H.-D. Huang, N. Raikhel and H. Jin (2011). "Arabidopsis Argonaute 2 regulates innate immunity via miRNA393∗-mediated silencing of a Golgi-localized SNARE gene, MEMB12." Molecular cell **42**(3): 356-366.

Zhang, Z., X. Liu, X. Guo, X.-J. Wang and X. Zhang (2016). "Arabidopsis AGO3 predominantly recruits 24-nt small RNAs to regulate epigenetic silencing." Nature plants **2**(5): 16049.

Zhu, J.-K. (2009). "Active DNA demethylation mediated by DNA glycosylases." Annual review of genetics **43**: 143-166.

Zickler, D. and N. Kleckner (1999). "Meiotic chromosomes: integrating structure and function." Annual review of genetics **33**(1): 603-754.

Zilberman, D., X. Cao and S. E. Jacobsen (2003). "ARGONAUTE4 control of locus-specific siRNA accumulation and DNA and histone methylation." Science **299**(5607): 716-719.

Zilberman, D., M. Gehring, R. K. Tran, T. Ballinger and S. Henikoff (2007). "Genome-wide analysis of Arabidopsis thaliana DNA methylation uncovers an interdependence between methylation and transcription." Nature genetics **39**(1): 61-69.

Zou, M., Y. Guan, H. Ren, F. Zhang and F. Chen (2008). "A bZIP transcription factor, OsABI5, is involved in rice fertility and stress tolerance." Plant molecular biology **66**(6): 675-683.